UCL

Genetic approaches to understanding pain mechanisms: Zfhx2 and peripheral sensory neuron ablation mouse transgenic models

PhD Thesis

Sonia Santana-Varela

Molecular Nociception Group
Division of Medicine - University College London
2022

Supervisors:
Prof. James Cox and Prof. John Wood

DECLARATION

I, Sonia Santana-Varela confirm that the work presented in this report is my own. The greater portion of the work described in the thesis has been undertaken subsequent to my registration for the higher degree part of which I am submitting for examination.

Where information, data, or work has been derived from other sources; I confirm that this has been appropriately acknowledged.

Sonia Santana-Varela

FUNDING

This project has received funding from:

PUBLICATIONS

First or joint first-author publications related to the work reported in this thesis:

Habib AM*, Matsuyama A*, Okorokov AL*, **Santana-Varela S***, Bras JT*, Aloisi AM*, Emery EC*, Bogdanov YD, Follenfant M, Gossage SJ, Gras M, Humphrey J, Kolesnikov A, Le Cann K, Li S, Minett MS, Pereira sV, Ponsolles C, Sikandar S, Torres JM, Yamaoka K, Zhao J, Komine Y, Yamamori T, Maniatis N, Panov KI, Houlden H, Ramirez JD, Bennett DLH, Marsili L, Bachiocco V, Wood JN, Cox JJ. A novel human pain insensitivity disorder caused by a point mutation in *ZFHX*2. Brain. 2018 Feb 1;141(2):365-376. DOI: 10.1093/brain/awx326.

Bangash MA*, Alles SRA*, **Santana-Varela S***, Millet Q*, Sikandar S*, de Clauser L*, Ter Heegde F*, Habib AM, Pereira V, Sexton JE, Emery EC, Li S, Luiz AP, Erdos J, Gossage SJ, Zhao J, Cox JJ, Wood JN. Distinct transcriptional responses of mouse sensory neurons in human chronic pain conditions models. Wellcome Open Res. 2018 Jun 25;3:78. DOI: 10.12688/wellcomeopenres.14641.1. eCollection 2018.

Santana-Varela S*, Bogdanov YD, Gossage SJ Andrei L. Okorokov, Shengnan Li, Larissa de Clauser, Marta Alves-Simoes, Jane E. Sexton, Federico Iseppon, Ana P. Luiz, Jing Zhao, John N. Wood, James J. Cox. Tools for analysis and conditional deletion of subsets of sensory neurons. Wellcome Open Res 2021, 6:250

Other relevant papers published during my PhD:

Ter Heegde F, Luiz AP, **Santana-Varela S**, Magnúsdóttir R, Hopkinson M, Chang Y, Poulet B, Fowkes RC, Wood JN, Chenu C. Osteoarthritis-related nociceptive behaviour following mechanical joint loading correlates with cartilage damage. Osteoarthritis Cartilage. 2020 Mar;28(3):383-395. DOI: 10.1016/j.joca.2019.12.004. Epub 2020 Jan 3. PMID: 31911151.

de Clauser L, Luiz AP, **Santana-Varela S**, Wood JN, Sikandar S. Sensitization of cutaneous primary afferents in bone cancer revealed by in vivo calcium imaging. Cancers (Basel). 2020 Nov 24;12(12):3491. DOI: 10.3390/cancers12123491. PMID: 33255209

de Clauser L, **Santana-Varela S**, Wood JN, Sikandar S. Physiologic osteoclasts are not sufficient to induce skeletal pain in mice. Eur J Pain. 2021 Jan;25(1):199-212. DOI: 10.1002/ejp.1662. Epub 2020 Oct 12. PMID: 32955748; PMCID: PMC8436750.

Alles SRA, Nascimento F, Luján R, Luiz AP, Millet Q, Bangash MA, **Santana-Varela S**, Zhou X, Cox JJ, Okorokov AL, Beato M, Zhao J, Wood JN. Sensory neuron-derived Nav1.7 contributes to dorsal horn neuron excitability. Sci Adv. 2020 Feb 19;6(8):eaax4568. doi: 10.1126/sciadv.aax4568. PMID: 32128393; PMCID: PMC7030926.

Luiz AP, MacDonald DI, **Santana-Varela S**, Millet Q, Sikandar S, Wood JN, Emery EC. Cold sensing by Nav1.8-positive and Nav1.8-negative sensory neurons. Proc Natl Acad Sci U S A. 2019 Feb 26;116(9):3811-3816. doi: 10.1073/pnas.1814545116. Epub 2019 Feb 12. PMID: 30755524; PMCID: PMC6397562.

Ter Heegde F, Luiz AP, **Santana-Varela S**, Chessell IP, Welsh F, Wood JN, Chenu C. Arthritis. Noninvasive mechanical joint loading as an alternative model for osteoarthritic pain. Rheumatol. 2019 Jul;71(7):1078-1088. DOI: 10.1002/art.40835. Epub 2019 May 17. PMID: 30638309.

Sikandar S, Minett MS, Millet Q, **Santana-Varela S**, Lau J, Wood JN, Zhao J. Brain-derived neurotrophic factor derived from sensory neurons plays a critical role in chronic pain. Brain. 2018 Apr 1;141(4):1028-1039. DOI: 10.1093/brain/awy009. PMID: 29394316; PMCID: PMC5888992.

Raouf R, Lolignier S, Sexton JE, Millet Q, **Santana-Varela S**, Biller A, Fuller AM, Pereira V, Choudhary JS, Collins MO, Moss SE, Lewis R, Tordo J, Henckaerts E, Linden M, Wood JN. Inhibition of somatosensory mechanotransduction by annexin A6. Sci Signal. 2018 Jun 19;11(535):eaao2060. DOI: 10.1126/scisignal.aao2060. PMID: 29921656; PMCID: PMC6485395.

This thesis is dedicated to my daughter Alanna,

"Because in your loving company bad things become good, sadness becomes joy and boredom do not exist"

ABSTRACT

Latest cutting-edge sequencing has allowed researchers to obtain a full array of differentially expressed neuronal genes within the peripheral nervous system. Understanding this heterogeneity and functional implication could unveil new therapeutic targets towards a more precise medicine.

Combining a novel reporter mouse with Cre recombinase strategies, I examined the spatial and functional organization of transcriptomically different subpopulations of neurons in the mouse DRG in pathological and non-pathological states. Results herein include: confirmation of Cre activity and specificity in all lines studied by RNA scope when compared to previous reports and transcriptomic analysis; significant upregulation of DRG gal expression after Complete Freund's Adjuvant (CFA) induced inflamation; normal weight and exploratory behaviour for all lines tested; motor activity assessed by Rotarod not significant, but further motor coordination tests on animals missing Th DRG neurons showed significant impairment; noxious mechanosensation reduced in animals lacking SCN10aCre and Tmem45b DRG; confirmation of CGRP-positive neurons role in heat and cold perception as well as in the formalin inflammatory model; Von Frey hypersensitivity on animals lacking CGRP; and lastly TrkB-positive neurons responsible for significant deficits in mechanical hypersensitivity in the partial sciatic nerve ligation neuropathic pain model whilst no effect in cancer induced bone pain model.

Parallelly, by reverse genetics approach, I explore the contribution of the Zfhx2 gene, whose mutation has been identified as responsible for the Marsili pain insensitivity syndrome, in two different animal models of nociception. Behavioural characterisation of bacterial artificial chromosome (BAC) transgenic mice bearing the orthologous murine mutation, as well as *Zfhx2* null mutant mice, shows significant deficits in pain sensitivity in thermal and mechanical tests respectively.

In summary, as well as validating several new useful transgenic mouse lines, this thesis provides insights into genes and neuronal subpopulations important in pain pathways and provides potential platforms for translational studies of pain syndromes.

IMPACT STATEMENT

"Supposing is good, but finding out is better." **Mark Twain**

Chronic pain is a highly complex biological phenomenon. It is considered a silent epidemic, with an increasing prevalence as the population ages. At the beginning of 2000, one-third of the British population have been reported to suffer from chronic pain (Breivik et al., 2006). The suffering, lasting for more than 12 weeks, is often accompanied by mood and behavioural changes referred to as "three I's: Interruption, Interference, and Impact on the patient's life. It represents one of the most frequent reasons for individuals to seek medical care, where both pain and its derived comorbidities can lead to severe physical and social disability with great derived societal costs.

A critical shortfall of new useful analgesic drugs is being reflected in the over-prescription of opioids, to an equivalent of 2,700 packs an hour in the UK in 2017 (Rhodes, 2018). Among the reasons for this failure is the high sophistication of the pain circuitry, where neuronal plasticity and mechanistic redundancy in pain phenotypes suggest that a magic single-reagent pill is unlikely to succeed. Instead, the revolution in genetics and the development of sequencing technologies are seeding the path towards the identification of pain-associated genes for a future tailored medicine identified as pharmacogenomics.

The work described in this thesis uses transgenic mouse models to mimic what has been seen in the clinic, with the aim to contribute towards a more precise medicine. It includes the characterisation of a novel diphtheria toxin A (DTA) carrier reporter line and the analysis of somatosensory deficits in the peripheral nervous system. The data obtained has provided background information of different neuronal subsets in mechanistically different pain perception frameworks that can be used as a platform for further pain studies.

In addition, this report has contributed to the study of a newly discovered pain insensitive mutation in humans. The *ZFHX2/Zfhx2* gene is a potential new

analgesic target in humans and mice and the validation of two mouse models will enable further preclinical translational studies of this gene.

The results generated in this thesis have been disseminated to the scientific community both through internal seminars and by two peer-reviewed publications in Wellcome Open Research (Bangash et al., 2018, Santana-Varela et al., 2021) and one in Brain (Habib et al., 2018a), which have been included in the appendix.

ACKNOWLEDGEMENTS

The completion of this doctoral thesis would not have been possible without the selfless cooperation of each and every person who I will quote below, who have been a very strong support in this difficult but highly rewarding journey.

I must start expressing my most sincere gratitude to both my supervisors. To Professor John Wood for giving me the opportunity to work in his lab and learn so much under his tutelage. Thank you for your inspirational mentoring and personal support over the last ten years. I am indebted to you for allowing me to carry out this doctoral thesis under your supervision and always providing me with sufficient means and finance backing to perform the work proposed during the development of this thesis.

My gratitude goes also to Professor James Cox, thank you for your encouragement, patience and crucial scientific guidance over my PhD and last years in the lab. Your support and trust in my work, and your ability to guide my ideas have been an invaluable contribution, not only in the development of this thesis, but also in my training as a researcher. Thank you for your professionalism, your kindness and your friendship in every step of the way. I am hoping that our paths will somehow join again in the future. Until then, remember that you have a friend "down south". Likewise, I would like to extend the last words to Dr Andrei Okorokov. Thank you for your helpful pragmatism and unmistakable style.

My sincere thanks go out to the past and current members of the Molecular Nociception Group who have been my support and company throughout the period of study and during my time at UCL. Thanks for giving me all the support, collaboration, fun times and above all, friendship.

Today and always, I thank my beloved friends and family for their affection and endless encouragement during the ups and downs of this journey. Within them, I would like to mention John. Thank you for the time you have granted me to do this, stolen from our little family moments. Without your love and support, this thesis would have never been written and for this reason, this work is also yours.

TABLE OF CONTENTS

LIST OF TABLES

LIST OF FIGURES

LIST OF ABBREVIATIONS

µl	Microlitres
µm	Micrometres
AAV	Adeno-associated virus
AIA	Adjuvant induced arthritis
AM	Ante Meridiem
ANOVA	Analysis of variance
Arg	Arginine
ASIC	Acid-sensing ion channel
ASC	Antisense control region
BAC	Bacterial artificial chromosome
BDNF	Brain-derived neurotrophic factor
BBC	British Broadcasting Corporation
Cav	Calcium voltage-gated channel
CCI	Chronic construction injury
Ceacam10	Carcinoembryonic antigen-related cell adhesion molecule
CFA	Complete Freund's adjuvant
CGRP	Calcitonin gene-related peptide
CIBP	Cancer-induced bone pain
CIP	Congenital insensitivity to pain
CNS	Central nervous system
CO_2	Carbon dioxide
Cre	Cyclization recombinase protein
Ct	Cycle threshold
Cysltr2	Cysteinyl leukotriene receptor 2
DH	Dorsal horn
DNA	Deoxyribonucleic acid
dNTPs	Deoxynucleotide triphosphates
DRGs	Dorsal root ganglia
DTA	Diphtheria toxin-subunit A
EDTA	Ethylenediaminetetraacetic acid
ERT2	Mutant estrogen ligand-binding domain

EtBr	Ethidium bromide
FAAH	Fatty-acid amide hydrolase
FF	Fresh frozen
FLEx	Flip-excision
g/GR	Grams
Gal	Galanin
GDNF	Glial cell-derived neurotrophic factor
GFP	Green fluorescent protein
GTEx	Genotype-tissue expression
H	Hours
HEK	Human embryonic kidney cells
Hox	Homeobox
HSAN	Hereditary sensory autonomic neuropathy
Htr1f	5-hydroxytryptamine receptor 1F
IL	Interleukin
i.p.	Intraperitoneal
KI	Knock-In
KO	Knock Out
LT	Low threshold
LTMR	Low threshold mechanoreceptor
Lys	Lysine
m	Metres
Min	Minutes
ml	Millilitres
mM	Millimolar
mRNA	Messenger RNA
Nav	Sodium voltage-gated channel
NCCs	Neural crest cells
NF/NEFH	Neurofilament heavy chain
NGF	Nerve growth factor
NGS	Next generation sequencing
NMDA	N-methyl-D-aspartate
NP	Non-peptidergic

NPPB	Natriuretic peptide type B
NPRS	Numeric pain rating scale
NSAID	Non-steroidal anti-inflammatory drug
NS	Nociceptive specific
NT	Neurotrophin
NTNG1	Netrin G1
NTRK2	Neurotrophic receptor tyrosine kinase 2
Nts	Neurotensin
OA	Osteoarthritis
OCT	Optimal cutting temperature
ORF	Open reading frame
Osmr	Oncostatin M receptor
PAG	Periaqueductal grey
P2X	Purinergic receptor
PBS	Phosphate buffered saline
PCR	Polymerase chain reaction
PEP	Peptidergic
PF	Perfused
PFA	Paraformaldehyde
PM	Latin post meridiem
PNS	Peripheral nervous system
PSNs	Primary sensory neurons
Pvalb	Parvalbumin
PWT	Paw withdrawal threshold
QST	Quantitative sensory test
RA	Rapidly adapting current
RNA	Ribonucleic acid
RPM	Rotations per minute
RT	Room temperature
RVM	Rostroventral medulla
S	Seconds
SA	Slowly adapting current
SEM	Standard error of the mean

SNI	Spared nerve injury
SNS	Sympathetic nervous system
SNT	Spinal nerve transection
SP	Substance P
Sst	Somatostatin
STZ	Streptozotocin
TAC1	Tachykinin precursor 1
TG	Trigeminal ganglia
TH	Tyrosine hydroxylase
TPP	Thermal plate preference
TRP	Transient receptor potential
Trk	Neurotrophic tyrosine kinase receptor
UCL	University College London
UK	United Kingdom
VGSC	Voltage-gated sodium channel
WDR	Wide dynamic range
WIBR	Wolfson Institute for Biomedical Research
WT	Wild type
*ZFHX*2	Zinc finger homeobox 2 gene

Chapter 1 - Introduction

1.1 Pain. Cognitive protection and disease

Initially considered as a "passion of the soul" by Aristotle, pain is a complex biopsychosocial phenomenon considered a major clinical, social, and economic problem in communities around the world. Since its first definition in 1979 by the International Association for the Study of Pain, the definition has recently been revised again as; "An unpleasant sensory and emotional experience associated with or resembling that associated with, actual or potential tissue damage" (Raja et al., 2020).

Decades of research have been drifting us away from an initial idea of pain as one phenomenon linked to one mechanism. Instead, strong evidence has identified this phenomenon as occurring from the crosstalk of multiple matrix circuits and suggesting that in reality, different types of pain can and do in fact take place (Basbaum et al., 2009b). Even when most of them will naturally drive our behaviour away from the source of possible harm, sometimes pain makes its appearance with no connection to a protective role. In such a case, it results in a destructive ongoing curse, as it affects the life of the person who suffers it in a great manner. It is precisely its duration and intensity that will establish the difference between acute or short-term pain and chronic or long-term pain.

Epidemiological surveys have documented that chronic pain, from moderate to severe intensity, occurs in 19% of adult Europeans (Breivik et al., 2006), or the equivalent of 1 in 5 people. It is defined as persisting for more than 6 months and with ≥5 pain intensity on an 11-point Numeric Pain Rating Scale (NPRS) (0 = no pain, 10 = worst pain imaginable). It represents the most common physical symptom in primary care and leads to massive societal health costs due to the associated negative impact on quality of life, work and social disability of the sufferer (British Pain Society. "*Pain: Less*" campaign 2018). However, despite being a global clinical problem that continues to grow as the population ages, little progress has been achieved in developing new useful pain management drugs. This failure is reflected by an over prescription of opioid medications, which has led to widespread misuse of these highly addictive compounds for pain relief. Opioids are considered very good analgesics for acute pain and pain at the end of life but there is no evidence to suggest that they are helpful for long-term pain.

Notwithstanding this, National healthcare data has reported the use of 24 million opioids during 2017, which is equivalent to 2,700 packs an hour in the UK (Rhodes, 2018). More recently, the University of Aberdeen has analysed the detrimental effect of the Covid-19 pandemic in surgery waiting lists and estimated that the use of preoperative opioids by patients in the UK has increased during 2020 by 40% compared to pre-pandemic levels (Farrow et al., 2021). To address one of the most severe crises in pharmacology, the scientific community widely agrees that it is essential to understand pain and how we perceive it to find more efficient alternatives. However, this still enigmatic phenomenon is intrinsically subjective and coloured by personal experiences and rooted beliefs, which constantly challenge its study and interpretation of results.

1.2   Neural circuits of pain

French philosopher Rene Descartes first attributed the sensation of pain to body features in 1664, by picturing a tube connecting an organ to the brain whilst comparing it to a cord attached to a bell (Figure 1). His analogy continues to state that once the cord is being pulled the bell will ring a signal of alarming pain in the brain (Descartes Dixit). This model was confirmed later in 1803 by Aldini and Galvani studies when, after applying electric current to human corpses, they managed to get their dead limbs to move. Those findings are considered today as the beginnings of electrophysiology.

Figure 1. The classic representation of pain by Descartes

1.2.1 Nociception

From Ramon y Cajal's anatomical studies (Ramón y Cajal, 1909), we know that the nervous system is comprised of distinct cell types on a map, with neurons as their fundamental unit. Within them, primary sensory neurons (PSNs) are the first-order neurons of the somatosensory system which allow an individual to detect and discriminate between a wide range of sensory information, such as temperature, touch, sense of movement (proprioception), itch and pain. The type of sensory neurons that detect signals from damage or potentially damaging insults are called nociceptors. They are the initial players in the pain mechanism, allowing the detection of potentially painful stimuli in the periphery of the nervous system by the process of nociception.

Nociception (from the Latin *nocere*, "to harm") is a term first introduced by Sherrington in 1910, used to describe the neural process of encoding and processing noxious stimuli. It occurs in evolved animals as it requires conscious awareness, to whom the perception of pain serves as an alarm to defend the organism against any potential danger (Wall and Melzac. 2000). Its functionality has been divided into at least three purposes: 1) to warn the individual of the existence of real tissue damage; 2) to warn the individual of the probability that tissue damage is about to occur by realizing that a stimulus has the potential to cause such damage; and 3) to warn a social group of danger as soon as it exists for any of its members (Le Bars et al., 2001).

Discovered back in 1967 (Perl, 2011), nociceptors are a type of specialised sensory afferent neurons that rely on a diverse array of modality-specific membrane receptors which represent the signature of functionally different subpopulations (see chapter 3.2.1). The somas of nociceptors are located within two different types of specialized peripheral ganglia. The trigeminal ganglia (TG), detecting sensory stimuli perceived at the facial level, and the dorsal root ganglia (DRG), detecting stimuli at the body level. In mammals, they can be further divided depending on the location of the distal process into two main groups (Kandel, 1991):

- External nociceptors, which have their terminals in tissues such as the skin (cutaneous nociceptors), the corneas (corneal nociceptors), and the mucosa (mucosal nociceptors).

- Internal nociceptors, which innervate a variety of organs, such as the muscles, bones, joints (articular nociceptors), the bladder, the gut and the digestive tract (visceral nociceptors).

1.2.2   From pain transmission to pain perception

Nociceptor activity itself does not equal pain perception. To sense pain, the peripheral information must reach higher centres. This occurs by a complex physiological circuitry composed of four processes: transduction, transmission, modulation, and finally perception.

Transduction is the process by which a noxious stimulus is transformed into an electrical signal. Once a nociceptor is excited, membrane voltage-gated ion channels (VGC) will change conformation leading to a shift in the electric charge distribution ("depolarization") of the nerve membrane. Located along the axon and synapse, VGCs are key in action potential generation and propagation ("transmission"). They have been extensively investigated, and mutations in their coding genes have been identified as responsible for several inherited human pain disorders (see chapter 1.6 about *SCN9A* coding for the $Na_v1.7$ sodium channel).

One of the hallmarks of sensory neurons as a component of the initial perception route is that they are anatomically unique in structure. They are pseudo-unipolar, where a single axon exits the soma and divides into two branches in a T junction structure. One reaches out to the periphery and the other one to the spinal cord. This peculiar structure allows for the transmission of an action potential initiated in the terminal of the distal process to a presynaptic terminal in the spinal cord and CNS regions without passing through the main cell body.

When the depolarization produced by the stimulus is enough to overtake the action potential threshold of the neuron, it is called a "generator potential" and

represents the starting point of the ascending pathway. The sensory information digitally encoded in the form of action potentials will be transmitted from central terminals of primary afferents that terminate in the dorsal horn (DH) of the spinal cord projecting to different laminae, corresponding to specific afferent termination (or motor efferent, in the ventral horn) (Todd, 2010). Aβ fibres terminate in lamina III, synapsing with interneurons whilst Aδ fibres terminate superficially in lamina I or deeper in lamina IV / V and C fibres in lamina II. There, second-order neurons are either activated by neurotransmitter release (such as glutamate), or by transmission of neuropeptides (such as substance P (SP) and Calcitonin Gene-Related Peptide (CGRP) (Raouf et al., 2010). Glutamate and substance P released into the synaptic cleft will bind to NMDA and AMPA calcium and sodium receptors respectively, and CGRP activate neurokinin 1 (NK1) receptors which will lead to NMDA activation via protein kinase C (PKC). The ultimate influx of calcium and sodium into the cell produces neuronal depolarisation but also triggers signalling secondary messenger cascades (such as mitogen-activated protein (MAP) kinase pathway).

Ultimately, the relay of nociceptive information from the spinal cord to the brain is achieved by specialized neurons called projection neurons, neurochemically defined mainly by their NK1 receptor as identity marker (Wercberger and Basbaum, 2019). They ascend to the nucleus of the solitary tract (NTS), the medial brainstem reticular formation, the caudal ventrolateral medulla (CVLM), the lateral parabrachial nucleus (LPb), the midbrain periaqueductal gray (PAG) and the thalamus and hypothalamus where third-order neurons will carry the impulse into the area of the cortex related to the area of injury (Figure 2).

Furthermore, glial cells have recently been identified as involved in the initiation and maintenance of neuronal activation, by glutamate regulation, production of cyclo-oxygenase (COX) receptors in response to cytokine release and brain-derived neurotropic factor (BDNF). Neuroinmune interactions or the communication between the nervous and immune systems is now considered to be involved in the development of chronic pain (Torsney, 2019).
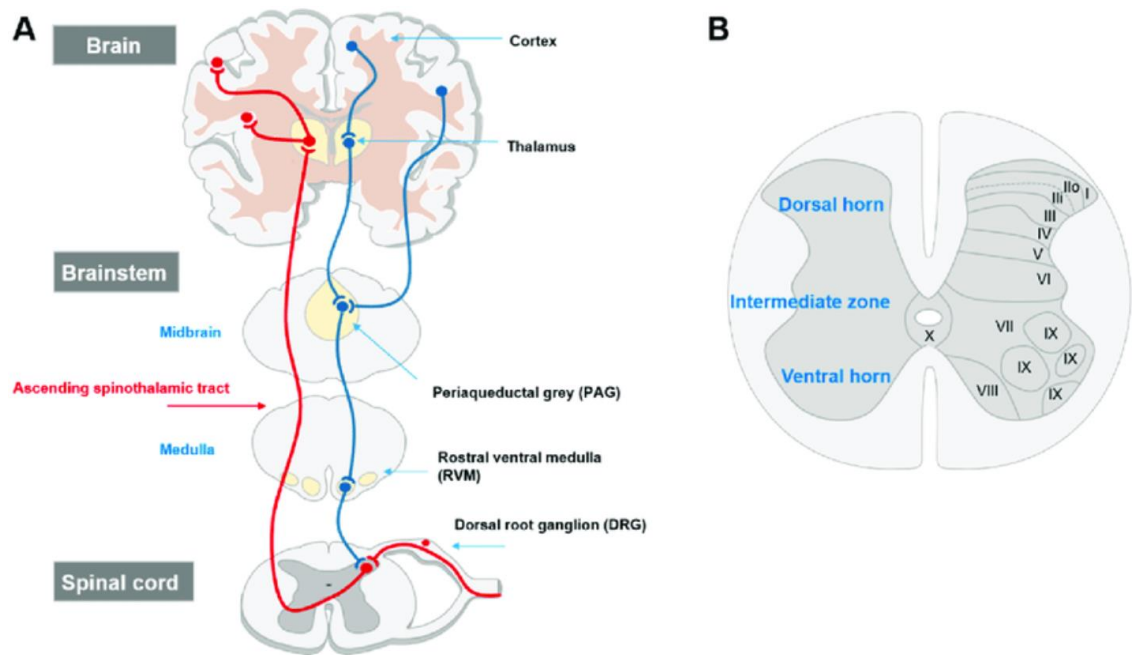
Figure 2. A; ascending and descending pain signalling pathways. (B) The Rexed laminae of the spinal cord grey matter (Cioffi, 2018).
Ascending pain pathway in red; modulatory descending tracts in blue. Afferent nociceptive input enters the spinal cord via DRG. Secondary order projection neurons ascend in the contralateral spinothalamic and spino-reticular tracts that relay the signal to cortical centres. Descending pathways projecting from the PAG in the midbrain and the RVM to the DH to modulate pain transmission.

It is important to mention that the sense of perception is a function of the higher levels of the nervous system, so activity in pathways that exist in their entirety within the spinal cord are not accompanied by any sensation. This is the case of spinal reflexes, with an afferent pathway from the sensory receptor and an efferent which will connect to a muscle or, sometimes gland. On the other hand supraspinal pain processing includes a highly dynamic and plastic central network.

In the brain, the periaqueductal grey matter (PAG), integrated by the amygdala, hypothalamus, and frontal lobe, will receive the ascending nociceptive input from the dorsal horn (DH) (Figure 2). From here, the neuronal axons descend through the rostral ventral medulla (RVM), which serves as a relay centre, towards the dorsal horn of the spinal cord. There, it will modulate the communication between

first and second-order neurons of the ascending pathway via releasing serotonin and noradrenaline and thus help control pain signalling. It is widely accepted that the effect of the descending system can be either inhibitory or facilitatory and in fact the imbalance or malfunction in their pathway has been reported to contribute to the development of neuropathic pain (Basbaum et al., 2009a).

Fundamentally, pain transmission is strictly dependent on the balance of the excitatory and inhibitory influences that act on the neuron where the ascending pathway is responsible for transmitting the pain signal up to the brain and the descending pathway is responsible for controlling and modulating it. On that note, one of the most important findings of the neurobiology mechanism underlying the modulation of pain is the discovery of enkephalin and opioid receptors. Along with glycine and GABA (γ-aminobutyric acid), they are the main inhibitory neurotransmitters dorsal horn. The ability of this endogenous opioid to inhibit pre and postsynaptic neurons and stop the continuation of the impulse up to the thalamus, led to a revolution in the pain drug market. Its role was discovered through electrical stimulation and injection of opioids into the PAG, showing specific suppression of pain both in animals and humans which was reversed by the opioid antagonist naloxone (Lewis and Gebhart, 1977).

Interestingly, neuronal somas enriched with Na and K channels are known as key modulators in action potential conduction into and from the CNS (Wolff et al., 1998) and pain insensitivity of mice and humans lacking $Na_v1.7$ (sodium channel) has been associated with opioid signalling (Minett et al., 2015, MacDonald et al., 2021). Furthermore, recent studies in $Na_v1.7$ mouse knockouts have found that a critical site of analgesia is at the central terminals of the primary afferents, where there is opioid-mediated suppression of neurotransmitter release (MacDonald et al., 2021). These findings correlate with the failure of peripherally restricted $Na_v1.7$ inhibitors as analgesics and highlight the importance of a deeper understanding of the biological processes underlying somatosensory processing for improved drug design.

1.3 Classification of primary afferents

The nervous system is composed of an array of distinct types of sensory neurons specialized in detecting various sensorial modalities. They include innocuous stimuli detection (such as light touch or warmth and cooling), or noxious insults.

Historically, DRG primary afferents, located along both sides of the spinal cord, have been categorized according to their neurophysiological features and conduction velocities with associated specific functions (Table 1). Nerve conduction velocity (CV) is the speed at which an electrochemical impulse is propagated within the neural pathway. Conduction velocities are affected by a wide array of factors which include age, sex, and various medical conditions. However, the most important one is the outside diameter of the nerve fibre and has formed the basis for classifying mammalian nerve fibres into groups in order of decreasing diameter and decreasing conduction velocity:

-A-fibres (Aα and Aβ) corresponding to neuronal cells with large diameter axons, with heavy to moderate myelinization and a conduction velocity of 70 to 120 m/sec. They are classically linked with the detection of non-noxious stimuli and have been associated with light touch and proprioceptive information processing (May et al., 2017)

-Aδ-fibres represent a group of thinly myelinated neurons, with a medium axon diameter and a conduction velocity of 2 to 70m/sec. They may detect both non-noxious and noxious or nociceptive stimuli. When sensitized, they mediate the so-called first pain, characterised by a fast and well localized pinprick sensation.

-C-fibres are characterized by small-diameter unmyelinated neuronal axons which are the slowest to conduct sensory information (between 0.5 and 2 m/sec). They are mostly (70%) involved in detecting noxious stimuli in a longer-lasting, more delayed pain sensation often described as duller and burning (Dubin and Patapoutian, 2010). However, within this group there is also a specific subset called silent nociceptors that remain inactive in basal conditions but that can become activated if sensitized after tissue injury (Schmidt et al., 1995).

Classification	Nerve fiber type	Nerve fiber subtype	Example	Relative diameter/Myelination	Relative conduction velocity
Sensory and Motor	A	α	α motorneurons	Large, heavily myelinated	Fast
		β	Touch, pressure	Medium, heavily myelinated	Moderate
		γ	Intrafusal fibers	Medium, heavily myelinated	Moderate
		δ	Touch, pressure, temperature, fast pain	Small, heavily myelinated	Moderate
	B		Preganglionic autonomic nerves	Small, lightly myelinated	Moderate
	C		Slow pain, postganglionic autonomic nerves, olfaction	Small, unmyelinated	Slow
Sensory only	I	a	Muscle spindle afferents	Large, myelinated	Fast
		b	Golgi tendon organ afferents	Large, myelinated	Fast
	II		Secondary afferents of muscle spindles; touch, pressure	Medium, myelinated	Moderate
	III		Touch, pressure, fast pain, temperature	Small, myelinated	Moderate
	IV		Pain, temperature, olfaction	Small, unmyelinated	Slow

Table 1. Nerve fibre types.

(Ludwig PE, Reddy V, Varacallo M. Neuroanatomy, Neurons. StatPearls Publishing; 2020 Jan)

In addition, all the above subsets of sensory neurons have differential projection patterns to the spinal cord and terminals in skin and muscle with direct functionality impact. Generally speaking, proprioceptive Aβ neurons project to lamina III-IV whilst nociceptive Aδ and C fibres project to lamina I-II (Lallemend and Ernfors, 2012). A third type, wide dynamic range neurons (WDR) that code for stimulus intensity are also present in the DH and form synapses with all three classes of primary afferents.

Given the heterogeneity of the different fibre responses to both innocuous and noxious input included in each subgroup, a further way to identify sensory neurons must be considered when trying to predict neuronal function (Wood, 2020). On that line, it was initially believed that all nociceptors were reacting preferentially to only one specific stimulus. However, recordings from multiple nerve fibres demonstrated the existence of neurons activated by many harmful or potentially harmful high threshold stimuli. They are the polymodal nociceptors, characterised by their ability to discriminate between different sensory modalities

(Mason, 2007). Therefore, to understand the sensory process system, it has been key to identify specialized DRG molecular sensors that convert a stimulus into an action potential within the neuron. These sensors have been found to rely their *modus operandi* on a diverse array of modality-specific membrane receptors, such as the triplet of ion channels TRP vanilloid TRPV1 channel, TRP ankyrin TRPA1 and TRPM3. These belong to the transient receptor potential cation family (TRP), and are critical for noxious heat sensation (Vriens and Voets, 2019).

In terms of mechanical sensory processing, several mechanoreceptors have been linked to generation of mechanically activated (MA) currents. There are three different types of MA current based on the rate of adaptation and pharmacological profiles. Small to medium diameter neurons can display all three types of current after noxious stimuli sensitization, whilst large-diameter neurons display mainly rapidly adapting MA currents and are responsible for touch and proprioception. Within the most studied mechano-transducer candidates, it is worth mentioning Piezo2 (Coste et al., 2010), to date considered critical for rapidly adapting currents in DRG neurons (Wood and Eijkelkamp, 2012).

In summary, there are neurons that respond to specific stimuli only, neurons that are capable to respond to more than one but specific type of a stimulus and neurons that are not specialised but serve as a dormant polymodal neuron that will join in to respond when stimuli reach a certain level threshold that exceeds normal house-keeping mode(s). The complexity in sensory modalities highlights that a classification of DRG primary afferents is crucial to determine their function in basal sensation and chronic pain states (Wood, 2020).

1.3.1 Classification of primary afferents based on neurochemistry

As already mentioned, the nervous system is composed of a diverse group of peripheral nerve endings specialized in the detection of various sensory modalities. These modalities comprise the detection of both innocuous and noxious stimuli, and provide information about the position of your body in space. The ability to discriminate between the diverse types of stimuli is reflected by the existence of functional and morphologically specialised sensory neurons. This

neuronal diversity depends not only on morphological differences but also on the expression of a diverse array of molecular markers which can potentially be associated with a particular function. Different marker genes often encode cell surface molecules, calcium-binding proteins and neuropeptides. They can be subdivided into two groups:

-*Peptidergic neurons*. They release neuropeptides such substance P (SP encoded by *Tac1* gene) and calcitonin gene-related peptide (CGRP encoded by *Calca*) or somatostatin (Som encoded by *Sst*). Among these are C-fibres and Aδ-fibres. Most of these neurons express neurotrophic tyrosine kinase receptor type 1 (TrkA, encoded by *Ntrk1*), which is the receptor for nerve growth factor (NGF), and some also express neuropeptide Y2 receptor (Npy2r) (Brumovsky et al., 2005).

-*Non-peptidergic damage sensing neurons*. They are neurons expressing the tyrosine kinase glial cell-derived neurotrophic factor receptor Ret, C fibre type based on conduction velocity (McCarthy and Lawson, 1990). The majority express G-protein coupled receptors of the Mrg purinergic family, which defines the binding to IB4 (plant *Griffonia simplicifolia* I-B4) and Ret-expressing non-peptidergic neurons (Snider and McMahon, 1998). Embedded among the C fibres are also some cooling nociceptors, expressing cold dependant ion channel TrpM8, as well as C-LTMRs responding to pinprick, soft and pleasant touch. The latter correspond to a special non-peptidergic Ret+ group expressing thyroxin hydroxylase (Th) and Vglut3 but not IB4 binding (Wood, 2020, McCarthy and Lawson, 1990).

This broad classification of biochemically distinguishable nociceptors has been successfully linked with functional changes via ablation studies of peptidergic (marked by TrpV1 expression) or non-peptidergic (marked by MrgprD expression) subpopulations, translating into thermal and mechanical response deficits respectively (Zhang et al., 2013). More recently, further conditional targeted manipulation of specific genes has been used to identify stimuli-specific transducer molecules involved in nociception and pain and have provided invaluable information about neuronal specialization and their underlying mechanisms in different pain models (Minett et al., 2014b).

Such is the case in the use of diphtheria toxin subunit A (DTA) tool mice to ablate $Na_v1.8$ positive neurons in DRG (Abrahamsen et al., 2008), and its effect on mechanical and cold pain. Or the identification of MrgA3 positive neurons as the subpopulation of nociceptors responsible for itch (Han et al., 2013b). Or most recently, the identification of the already mentioned triplet of ion channels (TRPV1, TRPA1, and TRPM3) involved in heat sensing (Vriens and Voets, 2019, Vandewauw et al., 2018). All are good examples to emphasise that dorsal root ganglia (DRG) consist of a functionally heterogeneous population of neurons.

The already mentioned anatomical and functional attributes of nociceptors have proved highly useful but have limitations in defining overlapping subpopulations, so it is essential to consider other ways to classify them. One way is the classification made when studying neuronal diversity in development (Figure 3) (Lallemend and Ernfors, 2012).
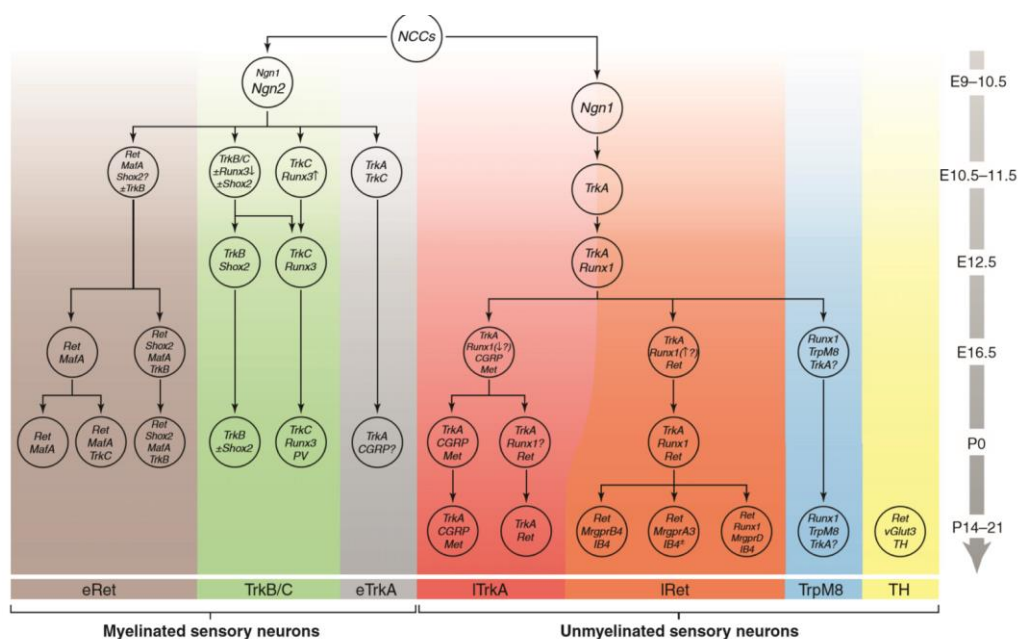
Figure 3. Changes in gene expression during development of DRG neurons from common neural crest cells (NCCs).

The far-right column refers to development stages in mice (E= embryonic P= postnatal stages). Within the myelinated and unmyelinated populations, colours represent different expression markers (Lallemend & Ernfors).

This starts by understanding that all neurons are derived from neural crest stem cells (NCS) that differentiate into neurons initially expressing different types of tyrosine kinase receptors (Trk). From there, changes in gene expression during development show shifts in the receptor expression, translated into different sensory modalities that would generate the different identities of subpopulations of DRG neurons in adulthood.

However it was not till the appearance of advances in single-cell transcriptional profiling when we have managed to further refine the classification into a more modern version (see 1.3.2) (Usoskin et al., 2015b, Zeisel et al., 2018b).

1.3.2 Transcriptome based classification of sensory neurons

Since the late nineteenth century, physiological studies have provided information about the properties of skin sensory afferents and later studies, consisting of applying thin probes to human skin have revealed spots of sensitivity for touch, heat and cold (Perl, 2011). The multifactorial element of pain perception evidenced already at its anatomical level has also been widely investigated via electrophysiological and calcium imaging studies. In 2016, *in vivo* calcium imaging showed that >85% of DRG neurons that responded to noxious stimulation were modality-specific, responding either to noxious mechanical, cold or heat stimuli (Emery et al., 2016). Further than their response profile, more work is needed to determine the importance of specific populations of neurons in one or several painful conditions, where advances in genetics and bioinformatics, are providing invaluable experiment designing tools to comprehend and differentiate their action mechanism.

The discovery of the first DNA sequencing technique (Sanger et al., 1977), the sequencing of both the human genome and also other evolutionary distant species, have represented seminal events in recent developments in pain research. Sequencing genomes and identifying mutations in genes for different diseases is a powerful high throughput technique that has sparked a revolution in the current scientific scenario. With pain management being still suboptimal, the genomics era is aiming to diminish the inter-individual variability in pain

sensitivity and response to analgesia. By finally obtaining "precise medicine" and developing pharmacogenomics we would be allowed to select treatments as personalized as our own DNA (Guigo and de Hoon, 2018).

Next-generation sequencing (NGS) is an improved sequencing method that allows to parallel sequence a large number of samples. It constitutes a very attractive tool for functional genomics, whose goal is to correspond genome regions with their biological function. The generation of a quantitative transcriptional profile of the genome (transcriptome), requires cDNA (formed with coding regions) derived from RNA (via RNA seq), where different transcribed information leads to anatomical and functional differences between cells. Its study, combined with *in situ* hybridization and histology, is called genotype-tissue expression (GTEx) and provides a resource to correlate tissue-specific gene expression and regulation to a function or an anatomical characteristic.

At present, when animal models are widely used to replicate human disease, comparative genome-wide scale studies have analysed transcriptional responses inter and intraspecies and fuelled the creation of gene databases which help to extrapolate lab studies into healthcare (Justice and Dhillon, 2016).

In 2015, Patrick Ernfors and his team undertook an ambitious transcriptome analysis of more than 600 single mouse DRG neurons by using single-cell RNA analysis (Usoskin et al., 2015a). Their findings have allowed the identification of both common and rare populations of neurons within the pool of analysed cells (Hwang et al., 2018). Based on the transcriptional profile of the PNS (peripheral nervous system) neurons, they unbiasedly identified eleven major clusters:

-one PEP1 or unmyelinated Peptidergic C-fibre neuron

-one PEP2 or lightly myelinated Aδ-nociceptor population

-five types of neurofilament (Nefh) expressing A-fibre neurons. NF1, NF2, NF3 as LTMRs and NF4 and NF5 as proprioceptive.

-Three types of nonpeptidergic neurons were identified called NP1, NP2, and NP3.

-One C-LTMR neuron type called Th population, expressing Vglut3 and Th.

Further sequencing (Zeisel et al., 2018b) revealed certain variability within the groups which lead to the identification of subclusters (Table 2). PEP1 subclusters are PEP1, NP1 and NP2; NP1 into NP1.1 and NP1.2; NP2 into NP2.1 and NP2.2. Additionally, they have newly identified the TRPM8 expressing group, with Trpm8.1, Trpm8.2 and Trpm8.3 as subclusters. All of them are comparable to electrophysiological and neurochemically based classical classifications (Usoskin et al., 2015). However, LTMRs have been studied more in depth in the Usoskin et al. studies, therefore, the most comprehensive classification is the one merging both.

Furthermore, the reported conserved interspecies organization (Kupari et al., 2021), as well as their associated molecular sensors, is likely to provide the base for functional prediction in modality-specific neurons (see chapter 3.2.1). Furthermore, recent microarray studies of the transcriptomic changes in different chronic mouse pain models have revealed a unique set of altered transcripts per model, implying that distinct cellular responses correspond to different painful stimuli (Bangash et al., 2018). These findings confirm what has already been evidenced in previous ion channel knockout studies, where $Na_v1.7$, $Na_v1.3$, $Na_v1.8$ and $Na_v1.9$ have been revealed to be critical in modality-specific responses (Minett et al., 2012b). This mechanistic redundancy within the nervous system has obstructed pain drug discovery both in industry and academia, where the understanding of somatosensory diversity and their function at baseline and under pathological conditions has been proven essential.

Both the new transcriptomic based classification of neurons and the transcriptomic changes in different pain models can allow us to interrogate the function of neuronal subsets and have seeded the grounds for the design of chapters 3 and 4 of this thesis.

	PSPEP6 TrpM8.1	PSPEP7 TrpM8.2	PSPEP8 TRPM8.3	PSPEP5 PEP1.1	PSPEP2 PEP1.2	PSPEP4 PEP1.3	PSPEP3 PEP1.4	PSPEP1 PEP2	PSNF1 NF1	PSNF2 NF2	PSNF2 NF3	PSNF3 NF4	PSNP1 TH	PSNP3 NP1.1	PSNP2 NP1.2	PSNP4 NP2.1	PSNP5 NP2.2	PSNP6 NP3
Calca				■	■	■	■	■								■	■	
Th													■					
Pvalb												■						
Scn10a				■	■	■	■	■						■	■	■	■	■
Tmem45b													■	■	■	■	■	■
Tmem233						■	■							■	■	■	■	■
Ntng1									■	■	■							
Ntrk2				■					■	■								
Avil	■	■	■	■	■	■	■	■	■	■	■	■	■	■	■	■	■	■

Table 2. Classification of DRG neuron types with selected marker genes, based on their expression profile.

The first row refers to the nomenclature presented (Zeisel et al., 2018b). The second row refers to the classification presented by Usoskin (Usoskin *et al.*, 2015)

1.4   Neuronal plasticity

Epigenetics (epi-"over, outside" genetics) is the study of changes in gene expression regulation without affecting the genetic code sequence. Such reprogramming may result from external or environmental challenges or be part of normal development (see Figure 3). The application of this discipline of study to neurobiology has revealed a sophisticated interconnection between genetic predetermination and environmental influences called neuronal plasticity (Lugaro 1906) that can profoundly change the activity and organization of its circuits. As per definition, it occurs continuously throughout life, every time a body is under the influence of a stimulus, applied with enough repetition and intensity to change or re-wire brain function. It is evidently expressed in adaptive behaviours and mediates gene-environment interactions, which are essential for the development, adaptation, and survival of the organism not only during immature stages but also in adulthood (Karpova et al., 2017, Ramachandran and Rogers-Ramachandran, 2000).

One representative example of this phenomenon is what has been reported in limb amputees' studies. At basal conditions, the intensity of sensation perceived by the brain is heterogeneous within the body, regardless of the type of stimulus. This is due, not only to the number of nociceptors, but also to the proportion of each of them in different tissues and organs. Electric shock studies in the 1940s have allowed Dr Penfield to represent the mapping of body space in the somatosensory area of the brain via the "*Homunculus*" (Figure 4).

After a member amputation, the sensory pathways do not disappear entirely and, interestingly, the representation of the limb in the brain persists. The phantom limb phenomenon occurs when somatosensory neurons in the cortex are still functional even when deprived of sensory input and might react to surrounding signalling. This way, an input to an amputee's face might "invade" a hand area (close in the homunculus representation) which leads to the particular illusion of feeling fingers (Ramachandran and Rogers-Ramachandran, 2000).
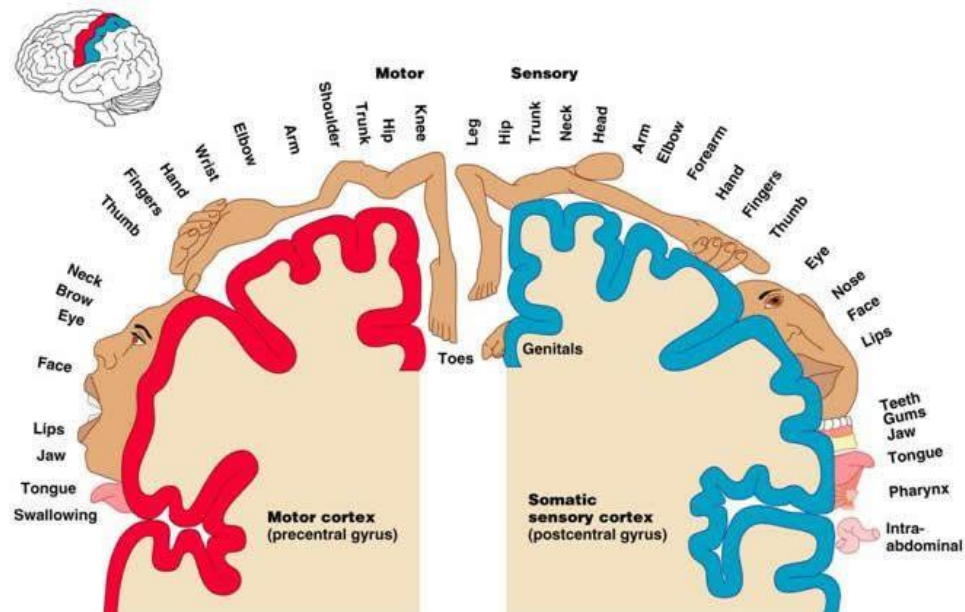
Figure 4. *"Homunculus" (*Wilder Penfield)

The first representation of a neurological topographic map of the human body, where the areas and its size are proportional to the sensitivity of the cerebral cortex in processing motor functions, or sensory functions.

In the clinic, current neurological rehabilitation units follow neuroplasticity-based paradigms. They introduce specific sensory information with repetition, to mimic what occurs naturally in our nervous system, improving, therefore, the functionality of inefficient brain networks. This controlled long-lasting protocols of neuronal stimulation cascades into specific neurotransmitter release which can induce gene expression or posttranscriptional regulation at the nuclear level to modify neuronal circuits (Leslie and Nedivi, 2011).

In any case, not only the existence but the intensity of the stimulus can derive from changes in the pain circuitry. Hypersensitivity is an alteration in the perception mechanism that occurs when pain persists after the noxious stimuli have been removed, therefore lacking the warning causality. This pain is believed to continue until the afferent gets "exhausted", which occurs when stimulation is maintained for more than 20-30 seconds (Schouenborg and Sjölund, 1983). It can be primary and restricted to the area of injury; or secondary, if the pain perception increases in the region surrounding the affected area.

Another important concept to mention refers to the progressively increased response of nociceptors to a repeated stimulus, called sensitization. *Peripheral sensitization* refers to reduction in the threshold (allodynia) and/or an increase in magnitude of responsiveness (primary hyperalgesia) at the peripheral ends of sensory nerve fibres that occurs after injury and/or inflammation. Like peripheral sensitization, *central sensitization* also involves an increased response to nociceptors, although in this case, these are in the spine and brain, when the nervous system goes through a process called wind-up and gets regulated in a persistent state of high reactivity. Central nervous system neurons might become hypersensitive to stimuli, over-reactive to innocuous stimuli or even produce a pain response with no stimulus. Unlike peripheral, the latter can affect other senses and cognitive functions such as memory and concentration. Phenotypically, if this enhanced peripheral or central sensitivity is to a noxious stimulus, it is called hyperalgesia; but if referring to normally innocuous stimuli, it is called allodynia.

Less commonly, central sensitization can lead to heightened sensitivities across all senses. One classical example is a migraine episode, which derives in light and smell sensitivity, photophobia and even motion sickness (Schwedt, 2013). Migraine sufferers are unable to recalibrate their normal pain scale mainly due to this associated comorbidity that generally takes place. The restless amplified pain *status quo* in these patients obstructs their medical diagnosis due to their inaccuracy when quantifying their own pain which has a negative impact on their improvement rate.

In research, peripheral excitability is considered a key determinant of pain chronification due to the relatively novel neuronal plasticity discovered in nociceptors. This paradigm has promoted the design of priming models of hyperalgesia for the study of the transition from acute to chronic (see 1.5.2), based on the ability of an insult or injury to produce an acute pain episode but also prime pain pathways to produce prolonged and latent hypersensitivity. One classic example is based on the injections of a low dose of prostaglandin E2 (PGE2), an inflammatory mediator first established by Levine et al. (Ferrari et al., 2015). After insult, the signalling travels back from the periphery to the terminal of the nociceptor mediating a long-lasting PGE2 induced hyperalgesia. The

transition from that initial peripheral nociceptor activity into central sensitization is the most important characteristic of this model, widely used for the study of the mechanisms of chronification (Reichling and Levine, 2009).

Analogously activity-regulated gene expression or transcriptional and post-transcriptional plasticity has been also linked to long or short term structural and physiological adaptations that take place during development. In which case, altered neural connectivity is affected by mechanisms such as DNA methylation and demethylation, histone modifications, chromatin-remodelling enzymes, transposons, and non-coding RNAs (Reichling and Levine, 2009, Karpova et al., 2017).

Plasticity based strategies and the study of its impairment (like in imprinting disorders), opens the door for the identification of new pain related genes and has helped to identify molecules such as the brain derived neurotrophic factor (BDNF), as a major player in mediating the transition from acute to chronic pain (Sikandar et al., 2018). In a clinical context, they could generate gene therapy pathway-centred approaches, on a specific individual, at a specific time, under a specific environmental condition.

1.5   Animal models of nociception

Every organism, in order to survive and propagate, relies on its fundamental ability to effectively perceive and gather information from the outside, as well as to be able to react to it. Their interaction with the outside facilitates its survival by helping it to find energy resources, to mate and reproduce, or defend itself from potentially harmful situations.

While the concept of nociception might be just a molecular mechanism (see Neural circuits of pain 1.2), its translation into human pain perception is constantly being adjusted by the influence of individual factors (Melzack and Wall, 1965), making its study and diagnosis a rather difficult task, often limited by ethical considerations. Furthermore, the complexity of pain studies gets escalated along with evolution, due to its multidimensional nature and its intricate system, folding in a maze of different processes within the nervous system that cannot be

simulated in scaled-down cell culture preparations. All these limitations highlight the importance of the development of animal models, as a fundamental way to mimic human experiences, for a better understanding of the mechanisms underlying each condition and/or to facilitate potential analgesic drug screening.

One of the major issues that animal research has faced over the years, is the inability of animals to communicate which obstructs the measure of pain and analgesia. However, since the late 19th century, researchers have been working on what is called animal models of nociception instead. Here, the presumably unpleasant emotional experience of pain is inferred from pain-like behaviours which can include; the withdrawal of a body part from a stimulus, reduced ambulation, agitation, an increase in grooming of the affected area, and vocalizations upon sensory stimulation (Deuis et al., 2017). Monitoring these spontaneous and evoked behaviours and thresholds, when performed under adapted quantification methodology (Mogil, 2009), has and is still generating specific, sensitive, validated, reliable and reproducible results.

It is well accepted that nociceptive pain is caused by the ongoing activation of $A\delta$ and C-fibres, during which the nature of the input or stimuli applied both in humans and animals play a key role in the study design (Mogil, 2009). Increasing progress on electrical recording techniques have facilitated the analysis of the nervous system at the level of nerve endings first and, more recently single neurons. They have identified modality-specific spots for sensation occurring in the skin with one or several sensory neurons responding to a range of painful stimuli (Perl, 2011). This is the case for transient receptor potential channels, as a prototypical molecular sensor for different activators (Figure 5).
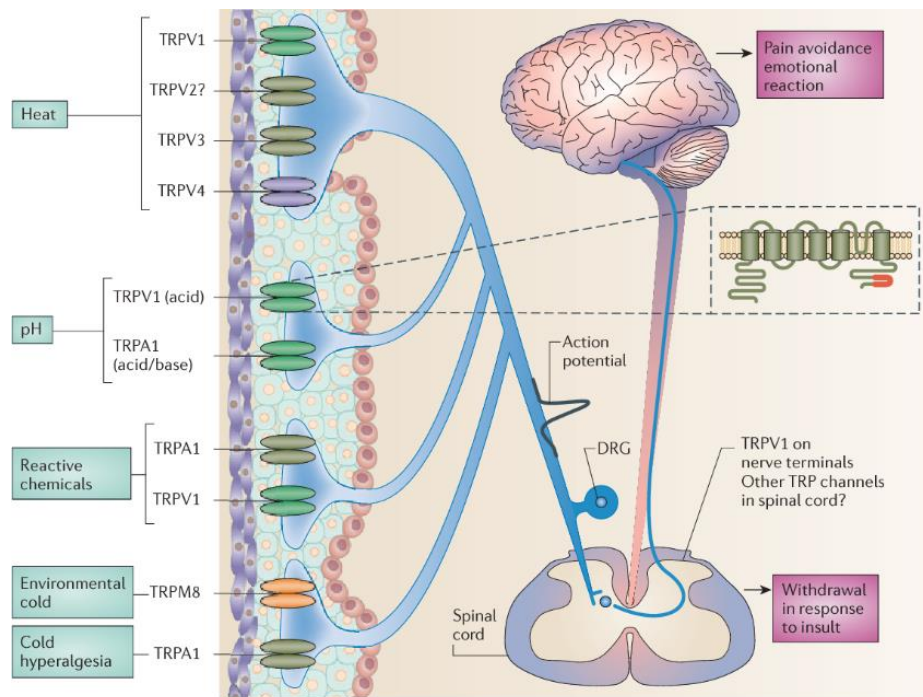
Figure 5. Transient receptor potential (TRP) channels as nociceptors.

TRP cation channel subfamily V; TRPV1, TRPV3 and TRPV4 responding to warming temperatures. Noxious heat activates TRPV2, but with unclear physiological relevance. Acids are robust activators of TRPV1, and bases have emerged as activators of cation channel chemoreceptor TRPA1. At higher concentrations, chemicals also activate TRPV1. TRP cation channel subfamily M, member 8 (TRPM8) serves as the key receptor for environmental cold, although TRPA1 also has a role in cold hyperalgesia (Macmillan Publishers Ltd).

Decades of neurobiology studies have continuously undergone refinement adapted to the discovery of new nociceptive targets, markers and pathways. Measures of reflexive behaviours, such as withdrawal thresholds to noxious stimuli are being widely used and, despite its human to mouse translational discrepancies, they have been proven to be highly useful in drug discovery. In fact, over the last years, a broad spectrum of analgesics has been found consistently reducing reflexive responses in rodents corresponding to human analgesia (Gregory et al., 2013).

Accepting that sex, strain and age are important modulating factors in pain experience and behaviour in both mice and humans when designing animal nociceptive models (Mogil and Chanda, 2005), there is a very simplistic assumption that the biological mechanisms underlying pain processing in animal

models can be extrapolated to what we see in human chronic pain patients. Even with the already significant improvement of the use of older subjects and the inclusion of both sexes and different strains, the lack of translational progress in the pain field continues to be present both in academia and industry.

Nevertheless, advances in genome engineering during the current so-called - Omics era are catapulting the development of tools for the replacement of mouse genomic regions with their human orthologs to target this forward translation" (from mouse to human). These genomically humanised mouse models will potentially improve largely the study of human disorders and drug therapy (Zhu et al., 2019), bringing finally the bench to the hospital bed closer in a not so distant future.

1.5.1 Pain assays

Since the ancient Greeks, animals have been successfully used as models to mimic different human diseases, both for the study of underlying pathophysiological mechanisms and the identification of potential drug targets. Historically mice have been the most validated species in biomedicine due to their breeding advantages and highly conserved genetic homology with us, although their predictive clinical efficacy of novel analgesics is still controversial (Berge, 2011).

The already mentioned nociceptive or nocio-perceptive assays detect and quantify "pain-like" behaviours of the animal (usually a rodent) under study. They can be divided into reflexive or non-reflexive stimulus independent.

Stimulus evoked or reflexive pain tests involve applying a noxious stimulus at or near threshold intensity. It leads to a measurable nocifensive response via withdrawal, licking, immobility and vocalization, which will describe:

Normo-reaction, allodynia (under-threshold stimuli response), hyperalgesia (enhanced supra-threshold stimuli response), or, in cases of sensory dysfunction, hypoalgesia (decreased sensitivity to painful stimuli) (Figure 6).
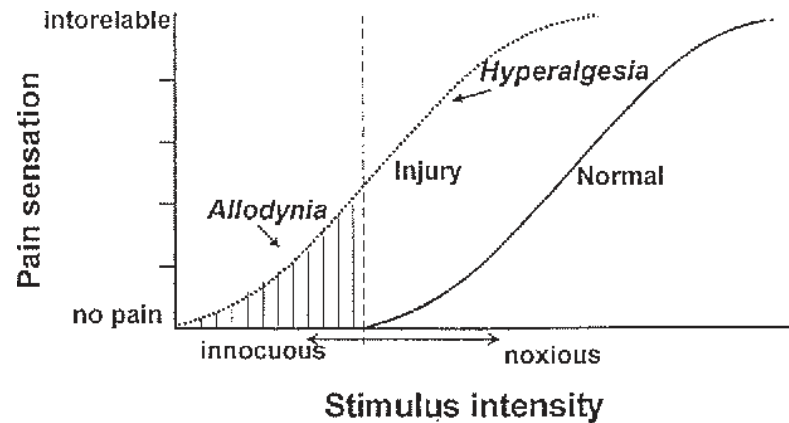
Figure 6. Relationship between stimulus intensity and pain sensation in normal and pain states (Mizumura, 1997).

Hyperalgesia is increased pain sensitivity or response to a suprathreshold stimulus. Allodynia is pain that occurs in response to a non-noxious or under-threshold stimulus normally incapable of activating nociceptors.

This stimulus evoked pain like behaviour can be further subdivided by stimulus modality into mechanical (such as manual or electronic von Frey and Randall-Selitto), chemical (capsaicin, CFA or formalin test) or thermal (Hargreaves', hot plate, tail-flick or cold plate, cold plantar assay and acetone evaporation test) (see chapter 2). Over the years, these assays have been proved essential in understanding the basis of sensation identifying some of their players (Basbaum et al., 2009a), and proven sensitive in some analgesic studies (Berge, 2011), whilst failed in others (Hill, 2000). On that line, the lack of translation into the clinic has led to the development of improved *non-reflexive* or stimulus independent pain measures (Mogil, 2009). They are indirect methods to quantify and analyse pain-like behaviours with minimal physical restriction which is likely to affect pain sensitivity (Huang et al., 2019b). They can be subdivided into; spontaneous measures, such as open field, limb score or weight bearing; or avoidance of evoked stimuli such as place preference involving decision making as a consequence of pain, all of them benefiting from less interaction from the researcher.

These new phenotyping techniques are strongly overtaking the old evoked measures (Wood, 2020) for providing improved clinic predictability. As an example worth mentioning, recent transgenic studies have identified TRPV1 expressing nociceptors as essential in orofacial pain, reflected by results on non-

reflexive measures such as facial grimacing or face-wiping. Whilst, data obtained from stimulus-evoked behaviours report them as TRPV1 independent (Wang et al., 2019).

Interestingly, while under normal conditions there is a direct correlation between rodent pain perception and stimuli existence and intensity (May et al., 2017), changes in input intensity and duration, could completely turn around the panel of activation. Over-sensitization of the central or peripheral nervous system results in the release of pronociceptive mediators which could create new interconnections between systems before apparently independent (see chapter 1.4). These plastic changes potentially translate into new different phenotypic responses depending on the type, intensity and duration of the stimulus, as well as the mechanisms cascaded from the subsequent injury (Minett et al., 2014b, Basbaum et al., 2009b).

As such, the diversity and adaptability within the nervous system are under constant investigation, where animal models provide invaluable platforms to untangle the mechanisms behind acute and chronic pain phenotypes.

1.5.2 Animal models of disease

Chronic pain is not just a prolonged form of acute pain, but the consequence of changes during peripheral and central sensitization, as well as in the brain where the signal is processed.

The so-called *chronic pain assays* are based on the longer lasting behavioural response and abnormal sensitivity to inflammatory pain, neuropathic and painful disease assays. They contain reflexive and non-reflexive responses involving supraspinal processing (Table 3) and are therefore more complex than the withdrawal mechanisms measured in acute assays.

Studies using hyperalgesic priming models (see 1.4) have suggested that neuronal plasticity is one of the key mechanisms for chronicity (Ferrari et al., 2015), and they have contributed to the novel identification of non neuronal cells (such as microglia and astrocytes) as important transition modulators (Wood, 2020).

	Inflammatory	Neuropathic	Arthritic	Muscle	Cancer	Incision
Reflexive tests						
Thermal						
Hot plate	✔	✔	✔	✔		
Hargreaves	✔	✔	✔	✔		
Cold	✔	✔	✔			
Tail flick						
Acetone	✔	✔	✔			
Mechanical						
Von Frey	✔	✔	✔	✔	✔	✔
Pressure	✔	✔	✔	✔	✔	✔
Electrical						
Nonreflexive tests						
Spontaneous						
Paw-elevation/licking	✔					
Evoked						
CPP	✔	✔				✔
CPA	✔					
Escape/avoidance	✔	✔		✔		
Quality of life/function	✔	✔	✔	✔	✔	

Table 3. Overview of Reflexive and Nonreflexive Tests in Different Animal Models of Pain (Gregory et al., 2013)

Chronic pain assays can be classified into:

-*Inflammation assays*. If a noxious insult is strong enough to induce tissue damage, it will produce a response where inflammatory modulators are released activating and sensitising surrounded sensory neurons leading to allodynia and hyperalgesia.

In rodent models, it is often induced locally in the paw via intradermal injection of irritable agents such as formalin, complete Freund's adjuvant, capsaicin or pro-inflammatory cytokines. It manifests as thermal and primary mechanical hyperalgesia if local; and/or secondary if distal from the injured area. Neurotransmitters and non neuronal proinflammatory mediators are discharged by nociceptors as a consequence of the tissue damage (Torsney, 2019). They will activate second messenger cascades that will result in pain, redness, heat, swelling and loss of sensory function (Hanesch et al., 1993).

Inflammatory assays have identified new peripheral pain modulators of pain such as the neurotrophins. These are a group of proteins that induce survival,

differentiation and neuronal growth and apoptosis. Within their family, the Nerve growth factor (NGF) binds to the TrkA receptor and regulates the expression of several pro-inflammatory mediators such as substance P and Calcitonin gene-related peptide (CGRP), as well as brain-derived neurotrophic factor (BDNF). NGF appears upregulated in a wide variety of inflammatory conditions suggesting an important involvement in inflammatory nociception. Due to this, antibodies that inhibit the function of NGF and its receptors have been developed and screened in clinical trials, proving the efficacy of NGF inhibition as a form of analgesia in chronic pain states including inflammatory osteoarthritis and chronic low back pain (Wise et al., 2021).

-*Neuropathic assays*. Pain perception associated with primary lesions or dysfunction in the nervous system is defined as neuropathic pain (Finnerup et al., 2016). It results in the development of spontaneous and abnormal activity in injured and uninjured afferent neurons which translates into burning and electric shock-like pain.

The mechanism underlying neuropathic pain involves ectopic activity in the pain pathways, peripheral and central sensitisation (Vardeh et al., 2016). This neuronal hyperexcitability has been linked to modulation of sodium and calcium channels, downregulation of potassium channels as well as phosphorylation of glutamate receptors. However, they are not the only players. The newly identified role of non neuronal immune cells such as astrocytes, microglia and macrophages and pro-inflammatory cytokine release in these types of syndromes, has evidenced the complexity of its mechanism (Coull et al., 2005). Improvements in the diagnosis of the cause of the syndrome are therefore considered essential to treat the pain more effectively (Wood, 2020).

For this matter, in 2019, the World Health Organization (WHO) has proposed a new classification of neuropathic pain into peripheral and central, each subdivided into several pain diagnosis entities (Scholz et al., 2019) (Figure 7). Its application in the clinic can aid to more specialised pain management, with

refined targeted drug delivery, neurosurgery, or neuromodulation according to the causality of the syndrome.
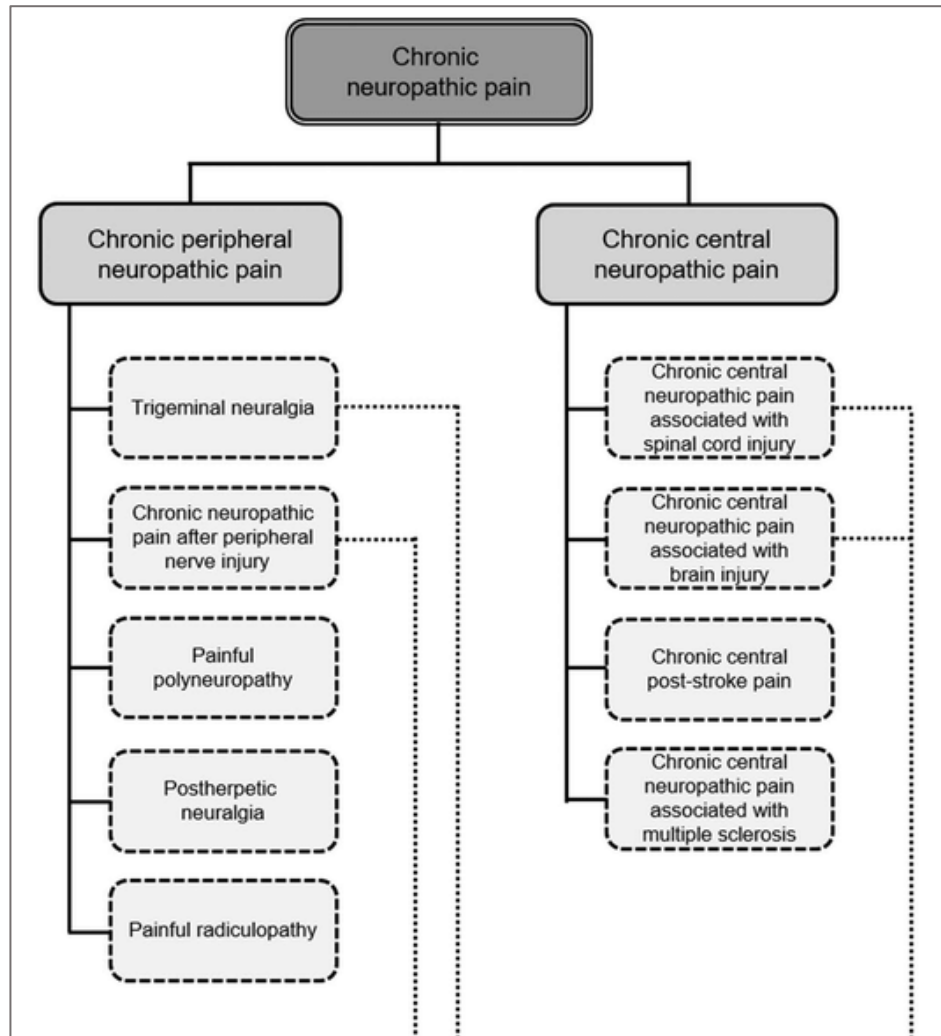
Figure 7. Classification of chronic neuropathic pain in ICD-11
In dark grey level 1 of diagnoses, mild grey level 2 and specific entities of chronic neuropathic pain at the next level (Scholz et al., 2019).

The classic neuropathic models are typically evaluated in a stimulus-response setting after different surgical interventions. This includes from complete nerve transections (SNT) to partial sciatic nerve ligation (PSL) (Berge, 2011). They can progress with thermal and or mechanical hyperalgesia as well as spontaneous place preference, and even motor activity impairment (Minett et al., 2012b). In neuropathic conditions, neuronal damage will lead to impaired neurotransmitter

trafficking which will cause enhanced firing activity. This subsequent mediator release into the surrounding areas can sensitize both injured and also intact neighbouring neurons, producing secondary hyperalgesia (Ji and Strichartz, 2004).

Initially developed to better understand the contribution of neuronal lesions to pain after a trauma, neuropathic assays are nowadays widening their causality spectrum. As such, models like diabetes derived neuropathy, neuropathy following ischemia or oxaliplatin injections are now also well acknowledged models for the study of neuropathic pain.

-*Cancer models.* Being one of the main causes of mortality, cancer research has been focusing on, not only continue increasing life expectancy but on rehabilitating the patient's quality of life.

Even though the bone is not a common site for primary tumours, it is very often a preferred place for metastases to develop. Consequently, patients suffer from dull pain episodes increasing over time and often evoked by limb use. Yet, the type of relief is limited to the severity of the metastases and is frequently associated with severe side effects (Mercadante et al., 2004).

In the late 90s, Schwei et al. described a model for localized cancer-induced bone pain CIBP (Schwei et al., 1999) which is now widely used and has been adapted to different mouse strains (Minett et al., 2014a, de Clauser et al., 2020). This model involves mechanisms that are characteristic of inflammation, neuropathy, nerve compression and ischaemia (Falk and Dickenson, 2014). It causes an increased osteoclast activity, deriving in surrounding acidosis which has been reported to specifically activate receptors TRPV1 and ASIC (Lipton and Balakumaran, 2012).

On account of a still very superficial understanding of the model, its limitations in translating it into the clinic have been evidenced for example in the studies on the receptor activator of the nuclear factor kappa-B ligand (RANKL). Produced by cancer cells, this osteoclast activity enhancer is associated with bone resorption, and the use of some of its inhibitors such as denosumab has proven to reduce bone loss and relieve pain in the clinic. Unfortunately, despite this, recent studies

have been reported that the administration of exogenous RANKL has not produced any changes in motor function or pain behaviours at both early and late time points (de Clauser et al., 2021) in mouse models.

Advances in science are continuously implemented in the study of the causality of carcinogenesis. Sophisticated human studies have identified for example downregulation in different noncoding miRNAs depending on the type of cancer (Volinia et al., 2006). In animal research context, similar results have been provided after DRG microarray of mice with bone cancer pain, suggesting post-transcriptional changes as a player in the CIBP mechanism (Bangash et al., 2018).

With neuronal contributions to peripheral sensitisation in bone cancer pain and the mechanisms involved still to be elucidated, the use of genetically labelled neurons of interest by using mouse reporter lines might provide a breakthrough towards the understanding of this type of disease (Santana-Varela et al., 2021). Conversely, the use of a now more affordable CRISPR/Cas 9 technology to produce transgenic mice and the increasing knowledge on tumour microenvironment with the use of humanized mouse models are providing the platform needed to start tailoring individual therapeutic pain relief in cancer patients.

- *Musculoskeletal pain assay*. This type of pain has been recently recognised by the World Health Organisation as the second largest contributor to global disability. It presents a complicated pathology with a transition from localised pain which will progress to a chronic state where it becomes widespread. It englobes patients with a whole range of heterogeneous diseases, from fibromyalgia to osteoarthritis, but all under the same or similar treatment protocol.

In order to mimic this syndrome, researchers have developed a model based on the injection of hypertonic saline or carrageenan into the gastrocnemius muscle in a long-term type of behavioural assay. The injections produce dose-dependent hyperalgesia to mechanical and heat stimuli ipsilaterally, lasting up to 7-8 weeks and that can spread to the contralateral side 1-2 weeks after injection according to K Sluka's findings (Radhakrishnan et al., 2003). These models, as well as other classic hyperalgesic priming models (Ferrari et al., 2015), are providing insights

not only into musculoskeletal pain processing but also the transition from acute to chronic pain, where plastic changes in the nervous system seem to be triggering the development of persistent pain (Sikandar et al., 2018).

- Another example of a chronic syndrome or disease-like pain assays is the *osteoarthritis OA joint pain model* via injection of an irritant such as monosodium acetate (MIA). This model has been recently improved by a novel non-invasive mechanical loading model (Ter Heegde et al., 2019) with promising results in the screening of new analgesic drugs.

All of the above, as well as other *visceral and migraine pain* models, might or might not have an inflammatory or a neuropathic component, but each of these assays has its role in illustrating the pathological pain system and, currently have still great use in basic pain research (Le Bars et al., 2001).

Interestingly, whether by causing inflammation, long-lasting injuries, and neuropathic or other aetiology lesions, they are all able to trigger brain mechanisms related to emotional and cognitive responses. One example is depression derived from the constant pain of the sufferer, between other comorbidities. The pain experience becomes then more than a sensory process and opens a consideration to the existence of different types of pain with different mechanisms (Wood, 2020), from acute to chronic and from defensive to neurologically diseased, all of which obstruct pain management protocols.

1.5.3 Mouse transgenic animals as a tool

The development of molecular cloning and genetic manipulation technology allows researchers to design studies with a reverse genetics approach, by analysing the phenotypic effects when a gene sequence is changed to elucidate its function (Gurumurthy and Lloyd, 2019). Both gain and loss of function models can be generated. In chapter five of this thesis I have used a BAC transgenic approach to model a mutation in the orthologous *Zfhx2* gene which is randomly inserted into the mouse genome (a gain of function model). I have also studied a model in which the *Zfhx2* gene is knocked out in every tissue (a global knockout).

In chapters 3 and 4 I study a variety of reporter lines in which the activity of the transgene is controlled temporally and spatially using Cre recombinase lines. The Cre recombinase system is based on the ability of the bacterial enzyme Cre recombinase to invert or excise a gene of interest that is flanked by loxP sites (Sauer, 1998). Expression of the Cre can be spatially or temporally regulated by the use of tissue-specific or inducible promoters respectively (Hans, Kaslin, Freudenreich, & Brand, 2009), cancelling the possibility of a false positive phenotype due to compensatory responses and being able to study the effect of a gene in different stages of development. More recent studies that use adenovirus and lentivirus vectors injected to infect cells have proven their efficacy in delivering Cre or FLP enzymes to target specific tissue or cells (Lee et al., 2017). In need of improvement, this method seems to present major challenges such as transient expression and vector immunogenicity that interfere in the transduction levels but the overall initial results have been promising.

Experiments using the Cre system in conditional transgenics have proven very effective and versatile in the study of pain, becoming, in some cases, indispensable. Such has been the case after the identification of *SCN9A* as a main player in congenital anaesthesia and pain pathways (Cox et al., 2006). The high expression of this gene in the olfactory bulb negatively affects pup survival due to the associated anosmia (Weiss et al., 2011). For this reason, initial knock out strategies have been refined towards the development of $Na_v1.7$ floxed transgenic animals, which along with conditional Cre lines crossing strategies, have represented a "*sine qua non*" way to continue understanding pain mechanisms (Nassar et al., 2004b). Behavioural studies on conditional $Na_v1.7$ KO mouse strains have shown that the expression of the gene in sensory and sympathetic neurons is important for noxious thermosensation and development of neuropathic pain respectively (Minett et al., 2012a).

In contrast, mice with a global knock-out of $Na_v1.8$ are viable but with attenuated sensitivity to noxious mechanical stimuli and prolonged extreme cold temperatures (Zimmermann et al., 2007, Luiz et al., 2019). And global KOs of $Na_v1.9$ show normal responses to mechanical and thermal noxious stimuli but reduced mechanical and thermal hypersensitivity in models of inflammatory pain (Lolignier et al., 2011).

Furthermore, recent transcriptomic analysis in rodents has identified sensory neuron subsets evolutionarily conserved in primates and therefore with great translational significance in humans (Usoskin et al., 2015a, Kupari et al., 2021). The existence of defined transcripts that distinguish particular sets of sensory neurons (1.3.2), provides an opportunity to analyse their function through conditional genetic ablation and this has been the basis of chapters three and four of this thesis.

1.5.4 Current approaches in animal research

Due to the ethical difficulties in working with human tissue and thanks to the advances in immunology, current research is racing to develop humanized mice. In these, the rodent has been xenotransplanted with human cells, tissue, genes, tumours, or a humanized immune system. One example is the widely available onco-HU mice in cancer research (Yao et al., 2016), a valuable method for immunotherapy screening as it recapitulates *in vivo* what would occur in the clinic.

In the context of neuroscience, UCI (University of California Irvine) has developed in 2019 a humanized mouse to study human brain cells in Alzheimer's disease (Hasselmann et al., 2019) to address the fact that rodent microglia fail to fully recapitulate the human condition. They successfully transplanted human microglia progenitors into immune-deficient mice, providing a tool for the study of human microglia in a controllable surrogate brain environment. Even with limitations, their use has been validated as a robust platform for the understanding of human processing and disease in several disciplines, with a much closer step to clinic proof of concept.

In parallel, several efforts are being made to complete a full comprehensive non-human primate comparison to the rodent. A catalogue of sensory neurons illustrating their diversity in primates, and their correlation to rodents will potentially establish a functional correlation of cell types in humans, from results obtained in mouse studies (Kupari et al., 2021).

Additionally, at the molecular level, the discovery of green fluorescence protein GFP has catapulted the development of calcium dependant fluorescent indicators

such as GCaMP. They allow us to *in vivo* and *in situ* visualize calcium-dependent neuronal activity and an important study reported that >85% of responsive dorsal root ganglion neurons are modality-specific, responding to either noxious mechanical, cold, or heat stimuli (Emery et al., 2016). From there, contributions to a good appreciation of the complexity of the mechanisms involved in pain, and advances in gene therapy techniques such as designer receptors exclusively activated by designer drugs (DREADDs), might represent a new era in animal experimentation with a quicker, less invasive and a reversible approach (Wood, 2020).

1.6   Pain variability

Over the years, pain studies have proven to be challenging to perform due to both biological and psychosocial variables (such as sex, ethnicity, or age). Each of them has the ability to shape the experience of pain in every individual at one specific time in a unique intricate manner. Understanding them and their interactions with each other is essential for the development of novel treatments towards more personalized pain care (Fillingim, 2017).

Idiosyncratic differences in pain responses have been widely reported over the years, although initially they were considered by researchers as merely disruption. Recent technical advances during the genomic revolution have turned this around, allowing us to unravel these individual discrepancies and decoding them into "pain genes". They are described as "a gene for which there are one or more polymorphisms that affect the expression or the functioning of its protein product in a way that affects pain response, both in sensitivity and susceptibility" (Wood, 2020).

1.6.1   Mendelian pain disorders

Mendelian disorders are human extreme phenotypes caused by one or two hereditary mutations, typically single-nucleotide changes in a single gene. They can result in painful disorders by causing aberrant neuronal activity which translates into excess pain. Syndromes such as primary erythromelalgia or small fibre neuropathy (affecting small diameter fibre density), are examples belonging

to this category. On the other hand, Mendelian pain disorders may have painless phenotypes. These are, in turn, further classified into; developmental, when there is a lack of nociceptors during early stages; or functional, if the nociceptors are present but are dysfunctional (Wood, 2020).

Pain loss disorders have been reported worldwide over the years, but their prevalence is still unknown due to both mis- and underdiagnosis. This is mainly due to the lack of awareness and understanding of the disease, and the impossibility to access genetic testing in certain areas. They can be classified as congenital insensitivity to pain (CIP) or hereditary sensory neuropathy (HSAN), both manifested through developmental defects of sensory nerve cells due to neurodegeneration or through altered excitability.

Hereditary sensory neuropathy (HSAN)

HSAN include several rare inherited degenerative disorders of the nervous system, normally occurring with loss of sensation in hands and feet due to small fibre sensory dysfunction, and its associated consequences of delayed healing (Axelrod and Gold-von Simson, 2007). There are up to 8 different types of HSAN neuropathies which are different phenotypically and associated with several inherited genes.

HSAN type I is the most common, caused by a mutation in the *SPTLC1* gene; HSAN type 2 by mutations in the *WNK1* gene and HSAN type 3 (RileyDay syndrome or familial dysautonomia) in the *IKBKAP* gene; HSAN type 4, also called congenital insensitivity to pain with anhidrosis (CIPA), is caused by mutations in the *NTRK1* gene and finally, HSAN type 5 in the *NGFB* gene (Axelrod and Gold-von Simson, 2007).

Congenital insensitivity to pain (CIP)

The inherited condition known as congenital insensitivity to pain (CIP) is a rare phenotype where lack of physical pain awareness and inability to perceive noxious stimuli leads, in the most extreme forms, to premature death due to the failure in learning pain-avoiding behaviours and accumulation of undetected health issues. Three homozygous nonsense mutations in the *SCN9A* gene encoding $Na_v1.7$ were first identified as responsible for this condition (Cox et al., 2006), with a proband described with a normal sural nerve biopsy and therefore considered separated from the HSAN disorders.

The *SCN9A* gene encodes the alpha subunit of the $Na_v1.7$ voltage-gated sodium channel (VGSC), which mediates voltage-dependent sodium ion permeability of excitable membranes. *SCN9A* is highly expressed in nociceptive DRG neurons and sympathetic ganglion neurons, and has been proven to be essential and a non-redundant requirement for nociception in humans. In a more recent study, a single point polymorphism in this gene has been suggested to explain variation in pain thresholds between individuals in the general population (Reimann et al., 2010).

Not only mutations in genes encoding sodium channels are responsible for both HSAN and CIP disorders. Instead, there are over twenty different pathogenic gene variants that have been identified over the years, resulting in developmental defects, neurodegeneration and/or altered neuronal excitability of peripheral sensing neurons (Table 4).

The surprisingly low number of genes that cause these disorders, especially when compared with for example congenital blindness, suggests a considerable redundancy within the pain-sensing and processing and the lack of complete understanding of the underlying mechanism (Wood, 2020).

One of the most recently discovered pain insensitivity conditions has been reported in a Scottish patient, as a result of a co-inheritance of a microdeletion in the fatty-acid amide hydrolase (*FAAH*) pseudogene together with a hypomorphic SNP in FAAH. The loss of function of the FAAH enzyme produces a significant

elevation in anandamide levels within the endogenous cannabinoid system, explaining the analgesic effect characteristic of this patient (Habib et al., 2019b).

Also present in the table, *the ZFHX*2 gene encodes a transcription factor highly expressed in nociceptors, and has been reported as the causal gene for the autosomal dominant form of a human pain insensitivity disorder called Marsili syndrome (Habib et al., 2018a). Six members of an Italian family are affected, where a heterozygous point mutation in this gene translates into diverse grades of hyposensitivity to noxious heat, and painless bone fractures (Habib et al., 2017, Spinsanti et al., 2008). The *Zfhx2* gene has been extensively analysed in this project with the aim to investigate its role in mouse pain processing (see Chapter 5 -).

Gene	Protein	Function	Inheritance	OMIM	Disorder	Onset	Pain	Additional	Motor	Skeletal	Autonomic	Other
GMPPA	GMPPA	Protein glycosylation	AR	615510	AAMR	Congenital	Loss of pain sensation	Neurological defects				Achalasia, alacrimia
KIF1A	KIF1A	Axonal transport	AR	614213	HSAN2	Childhood	Loss of pain sensation		Muscle weakness may occur	Ulcerations Mutilations	Autonomic involvement rare	
MADD	MADD	TNF-α signalling	AR	619004	DEEAH	Congenital	Reduced pain sensation		Psychomotor delay			Exocrine and endocrine dysfunction
NGF	NGF	Neurotrophin signalling	AR	608654	HSAN5	Congenital	Insensitivity to pain	Variable degree of intellectual disability		Painless fractures Osteomyelitis Corneal lesions	Anhidrosis Fever episodes	
NTRK1	TRKA	Neurotrophin signalling	AR	256800	HSAN4	Congenital	Insensitivity to pain	Variable degree of intellectual disability		Painless fractures Osteomyelitis Corneal lesions	Anhidrosis Fever episodes	
PRDM12	PRDM12	Epigenetic regulation	AR	616488	HSAN8	Congenital	Insensitivity to pain	Intellectual disability may occur (less common)		Facial injuries Corneal lesions	Hypohidrosis	
RAB7A	RAB7	Axonal transport	AD	600882	CMT2B	Adulthood	Reduced pain sensation		Strong motor involvement	Ulceration Osteomyelitis		Also classified as Charcot-Marie-Tooth (CMT2B)
RETREG1	RETREG1 / FAM134B	Selective autophagy of the ER (ER-Phagy), Golgi	AR	613115	HSAN2	Childhood	Loss of pain sensation	Spasticity	Muscle weakness may occur	Acral ulcerations Osteomyelitis	Hyperhidrosis	
SCN9A	NaV1.7	Voltage-gated sodium channel (neuron excitability)	AR	243000	CIP / HSAN2	Congenital	Insensitivity to pain	Anosmia		Ulcerations Fractures Mutilations		
SCN11A	NaV1.9	Voltage-gated sodium channel (neuron excitability)	AD	615548	CIP / HSAN7	Congenital	Insensitivity to pain	Pruritus	Delayed motor development	Joint hypermobility Skin ulcers (cervical region)	Intestinal dysmotility	
SPTLC1	SPTLC1	Sphingolipid-Metabolism	AD	162400	HSAN1	Adulthood	Loss of pain sensation (lancinating pain may occur)		Mild motor involvement (some cases more pronounced)	Ulcerations Mutilations Osteomyelitis Amputations	Autonomic involvement rare	
SPTLC2	SPTLC2	Sphingolipid-Metabolism	AD	613640	HSAN1	Adulthood	Loss of pain sensation (lancinating pain may occur)		Mild motor involvement (some cases more pronounced)	Ulcerations Mutilations Osteomyelitis Amputations	Autonomic involvement rare	
WNK1	WNK1	Kinase activity, ion transport	AR	201300	HSAN2	Childhood	Loss of pain sensation			Acral mutilations (severe)		
ZFHX2	ZFHX2	Transcription	AD	147430	CIP	Congenital	Reduced pain sensation			Painless injuries		

Table 4. Classification of Human pain insensitivity disorders based on their pathogenic causative gene.

AD= autosomal dominant; AR = autosomal recessive; GIT = gastrointestinal tract; N = normal (Wood, 2020)

1.6.2 Clinical Applications

Like Na$_v$1.7, mutations in the Na$_v$1.8 and Na$_v$1.9 VGSCs have also been implicated in rare human inherited pain disorders (Table 5). With great clinical relevance, these types of discoveries have triggered an outbreak in transgenic mouse research studies, in which the sodium channels are genetically deleted from specific neural populations, generating pain-free or hypersensitive mouse strains. These have been extensively validated as an efficient way to conduct standardized, sensitive, and reliable pre-clinical studies in rodents.

Protein	Gene	Loss of function phenotype	Gain of function phenotype
Na$_v$1.7	SCN9A	Channelopathy-associated insensitivity to pain [408, 409]	Primary erythromelalgia [410]
		Hereditary sensory and autonomic neuropathy type IID [411]	Paroxysmal extreme pain disorder [412]
			Small-fibre neuropathy [413]
Na$_v$1.8	SCN10A	None reported in humans	Painful small-fibre neuropathy [414, 415]
Na$_v$1.9	SCN11A	None reported in humans	Congenital inability to experience pain [416]
			Familial episodic pain [417]

Table 5. Classification of three main sodium pain channelopathies

These case examples and many other believed under-reported, have the capacity to contribute to a better understanding of the causes of congenital analgesia within the research community and have provided novel targets for the development of new treatments for chronic pain. One of them is the use of broad-spectrum sodium channel antagonists as nerve blocking local anaesthetics. Whilst they are still considered an efficient way to treat pain, the associated

inhibition of innocuous sensation makes them less attractive and impractical for most treatments. However, Na$_v$1.7 antagonists, due to their particular nature, could represent a more selective solution without the side effects (such as cardiotoxicity) associated with broad-spectrum sodium channel blockers (Minett et al., 2015).

In summary, with the discovery of more genes related to analgesia, researchers could potentially be able to unravel new possible pathways and neurons involved in the human response to pain, narrowing down the currently too wide spectrum approach on drug design, and helping the development of gene therapies for gene manipulation (Habib et al., 2018b, Habib et al., 2019a, Cox et al., 2010).

By looking at this approach, it is only fair to say that the current reality in neuroscience is sometimes coloured with irony, when the study of the painless, in congenital analgesia sufferers, can be essential to help people with the opposite problem: *too much pain*.

1.7   Aims of the project

One of the main reasons for the failure in finding new analgesic drugs is the intrinsic complexity of the pain system. To overcome this problem, the identification of key genes and cells for pain signalling has become essential. New advanced genetic tools in transgenics and the invaluable information obtained from transcriptomic neuronal profiling have allowed us to develop this project whose aims are:

-Firstly, to identify the spatial distribution of transcriptomically different subpopulations of neurons in the mouse DRG by RNAscope. Once cre activity and specificity is confirmed, I then aim to determine the role of each subpopulation in different types of pain, focusing on the peripheral nervous system by using an extensive array of behavioural tests. I used a Cre recombinase system driven by genes expressed across the different eighteen subpopulations identified by Zeisel et al. to conditionally ablate them in the DRG. This work involves the characterisation of a new *Advillin* driven DTA reporter line, four already available Cre lines (Cgrp^{CreER} (*Calca*), Th^{CreERT2}, *Scn10a*^{Cre} (Na$_v$1.8), , *Ntng1*^{Cre} and TrkB^{CreER} (*Ntrk2*).) and two newly generated Cre lines (*Tmem45b*^{Cre}, *Tmem233*^{Cre}).

-Secondly, I use some of these genetically defined neuronal subpopulations characterised in last chapter and explore their possible implication in chronic pain and disease-like models relevant to the pain clinic such as formalin induced inflammatory pain. I also interrogate the effect of TrkB positive neuron depletion after neuropathic pain and bone cancer pain, and analyse Galanin expression changes after complete a Freund's Adjuvant (CFA) inflammation model to assess potential plasticity in mouse DRG.

-Lastly, I took a different approach and studied the function of the novel *Zfhx2* gene, whose p.R1913K causal point mutation has been identified in the human pain insensitive Marsili syndrome. Using transgenics, I aim to validate two different mouse models, one with loss of function and one with an overexpression approach in order to better understand this novel pain insensitivity condition. For doing so, I include the acute behavioural characterisation of both transgenics under normal and pathological conditions such as neuropathic pain and CFA induced inflammatory pain.

Chapter 2 - Materials and methods

2.1   Animals

All transgenic strains used for this thesis (Table 6) were previously generated and imported to the UK from our collaborators, except for the *Zfhx2* R1907K BAC transgenic mouse which was generated by Cyagen with the mutation inserted into BAC RP23-248M20; *Tmem45b* and *Tmem233* Cre designed by J. Cox and *Advillin* Flox-tdTomato-Stop-diphtheria toxin (DTA) by Y. Bogdanov.

Mouse Strain	Repository	Paper
Advillin Flox-tdTomato-Stop-diphtheria toxin (DTA)	UCL	(Santana-Varela et al., 2021)
Rosa-CAG-flox-stop-tdTomato	Jax-007905	(Madisen et al., 2010)
Ntrk2 (TrkB) creERT2	Jax- 027214	(Rutlin et al., 2014a)
Gal-Cre	MGI:4367008	(Gong et al., 2003)
Th creERT2	Jax-025614	(Abraira et al., 2017)
CGRP CreER	MGI:5460801	(Song et al., 2012)
Tmem45B Cre	UCL	(Santana-Varela et al., 2021)
Tmem233 Cre	UCL	(Santana-Varela et al., 2021)
Ntng1 Cre	MGI:1934028	(Bolding et al., 2020)
Zfhx2 * BAC transgenic	UCL	(Habib et al., 2018a)
Global *Zfhx2* knockout	MGI:3626365	(Komine et al., 2013)

Table 6. Transgenic mouse strains used in this study

All males or females were housed in groups of a maximum of five, in individually ventilated cages and fed a Teckland 2018-C maintenance diet *ad libitum*. The environment was climate and light controlled; temperature 21°C (±2°C), humidity 50% (±10%) and lights on from 7 AM to 7 PM.

2.2 Genotyping

All genotyping required for this study was performed by Dr James Cox, Dr Abdella Habib and me at WIBR (UCL), from genomic DNA isolated from the ear. Tissue samples were collected by ear biopsy and digested in 30µl DNA lysis buffer (Table 7) + 0.075µl Proteinase K (19.7 mg/ml Roche 03 115n844), for 2 hours at 55°C, followed by 95°C for 5 minutes.

Component		Volume (ml)
10X GB buffer 1.5M Tris pH 8.8	4.47	3.60
1.0M Ammonium Sulphate	1.66	
1.0M Magnesium Chloride	0.67	
H_2O	3.20	
25% TritonX-100		0.72
β-mercaptoethanol		0.36
H_2O		31.32

Table 7: Ear lysis buffer

DNA from the digested tissue was used to check gene expression with appropriate primers for each gene of interest by using the Polymerase Chain Reactions (PCR). Reactions consisted of 1 µl of template DNA, 0.5-1 µl of each specific primer (for most reactions), 5 µl GoTaq buffer, 1-1.5 µl MgCl2 (25mM), 0.5 µl dNTPs (10mM), 0.1-0.3 µl GoTaq polymerase and 10-15 µl of DNA free water (Fermentas) in 0.2 ml tubes. A multiplex reaction was designed and performed when needed to make sure the sample had DNA and avoid false negatives. General PCR conditions were:

- Initial denaturing step: 94°C – 2 minutes
1) Cycling denaturing step: 94°C – 30 seconds

2) Cycling annealing step: Different depending on primer pair needs (Table 8) –
30 seconds

3) Cycling extension step: 72°C – 60 seconds

- Steps 1, 2 & 3 cycled 28-35 times (adjusted where necessary per primer combination)

- Final extension: 72°C – 2-5 minutes.

Mouse Strain	Gene insertion	Primer pair sequence (5'-3')	Annealing temperature	Band size
Advillin Flox-tdTomato-Stop-DTA	Transgene (BAC)	DTAqf-GCGTGGTCAAAGTGACGTAT DTAqr-AACTCTTCCGTTCCGACTTG WTfw-AAAGTCGCTCTGAGTTGTTAT WTrev-GGAGCGGGAGAAATGGATATG	54°C	mutant allele Size 133 bp wildtype allele Size 602bp
Flox-stop-flox-Tomato	KI	Mutant Forward-GGCATTAAAGCAGCGTATCC Mutant Reverse-CTGTTCCTGTACGGCATGG WTfwd-AAGGGAGCTGCAGTGGAGTA WTrev-	64°C	wildtype allele Size 297bp floxed allele Size 196bp
Ntrk2 *CreER* (TrkB)	KI ti	TrkBfwd-GACACGCACTCCGACTGACT TrkBrev-ACACCTGCCTGATTCCTGAG WTfwd-GACACGCACTCCGACTGACT WTrev-GCA TGAAGTGCAAGAACGTG	65°C	wildtype allele Size 302 bp mutant allele Size 500 bp
Gal *Cre*	Transgene (BAC)	GS-Gal F-CCAGACGTGTGCGTGTTGAGGT GS-Gal R1-CGGCAAACGGACAGAAGCATT	60°C	mutant allele Size 244 bp
Th *CreER*	Transgene (BAC) ti	Thfwd-ATGAGCTGCACACCCTGAC Threv-TGCTAGGAGCTATCATTGTGG WTrev-AGGCAAATTTTGGTGTACGG	65°C	mutant allele Size 150 bp wildtype allele Size 345bp
CGRP *CreER*	Transgene (BAC) ti	OPT-2695+2701-TCCTCCATCTTTAGGGCTAGATTCTTTCCAAA OPT-2262+2263-AGTGGTGAAAGCATTTTGTTAGTTAAAGGGCTA WTfwd-TCCAAACCGTATAGGCTACATGC WTrev-CCCTGAACATGTCCATCAGGTTC	57°C	wildtype allele Size 500bp mutant allele Size 300bp
TMEM45B *Cre*	Transgene (BAC)	Tmem45B GT b fwd-ATCATGCAAGCTGGTGGCTGGA Tmem45B GT b rev-GCAAACAGAGTCTTCACTGCAC	58°C	mutant allele Size 574 bp

TMEM233[^Cre]	KI	Tmem233 MUT fwd-CCTGCTGTCCATTCCTTATTCCAT Tmem233 MUT rev-GAGTCTGAGCGGGAAGCATACT Tmem233 WT fwd-TCATCTCCCTTGAGCCCGGAG	62°C	mutant allele Size 361 bp
Ntng1[^Cre]	KI	Ntng-AS-GGCTCTTACATACATCATAATGTCC Ntng-1S -TTTGGTTTTGGAATCTGCTTTGAG Cre AS3-TTCCGGTTATTCAACTTGCACCATG	60°C	wildtype allele Size 500bp mutant allele Size 300bp
*Zfhx*2 KO	KI	F11-CTACCATGGCTACCCTTAACTCA R11-ACTGTGCTGGTGTCCGGTACTTC GFP71A-GAGCTGGACGGCGACGTAAAC GFP671B-AACTCCAGCAGGACCATGTG	60°C	wildtype allele Size 913bp mutant allele Size 620bp
Zfhx2 p.R1907K BAC	Transgene (BAC)	Transgene PCR primer F-CTCATCAGTGACCGGGACA Transgene PCR primer R-CGCTTTCTGGAGACGCTTTA	65°C	Size 593bp for Sanger sequencing

Table 8: Primer sequences, annealing temperature and expected band sizes.

Reactions were carried out in a PCT-220 DNA Dyad (MJ research) machine and resolved via electrophoresis on a 1% agarose (Sigma) per 50ml 1X TAE buffer (40mM Tris-acetate, 1mM EDTA) gel with Ethidium bromide (EtBr) (0.5μg/ml). Individual samples were loaded when the gel was set, along with 5 μl of a specific molecular weight marker (ladder) and run for 45 minutes at 100-125 volts to separate bands per size, which were after visualised using a Biodoc System. Subsequent Sanger sequencing of the product was used to identify mice carrying the *Zfhx2* p.R1907K mutant transgene in the BAC transgenic line.

Strains designed in house required initial primer design (by J. Cox and me) and PCR gradient optimization to determine the optimum annealing conditions. In addition, different primers were designed targeting different areas in the sequence to confirm full insertion in each of the founders/chimaeras obtained. Products were sent for Sanger sequencing (Source Bioscience) and compared with the Cyagen report.

2.2.1 Copy number establishment

BAC transgenic strains generated by Cyagen required copy number establishment. Genomic DNA was used to determine how many copies of the transgene were present in each founder (performed by Dr A. Habib, UCL in *Zfhx2* p.R1907K BAC, and me for the *Advillin*-floxed-stop-floxed-DTA).

Genomic DNA was extracted from mouse ear biopsies and digested (as above) and then further purified using the DNeasy Blood and Tissue Kit (Qiagen), as per the manufacturer's protocol. Real-time PCR was carried out in each reaction mixture (20 µl) for each gene target with genomic DNA (20 ng) sample, final 1x concentration of Universal SYBR Green Supermix™ (Bio-Rad) and gene of interest primer set or the copy number reference Dicer1 primer pairs (Table 9).

The amplification of the selected genes from each sample was performed in triplicate on a 96-well reaction plate in 20 µl total volume using BioRad CFX with the following cycling conditions: denaturation 2 min at 95°C, 40 Cycles of 5 seconds denaturation at 95°C and annealing at 65°C.

Gene of interest	Primer pair sequence (5'-3')
Zfhx2	*Zfhx2*qpcr1- CTA CCA TGG CTA CCC TTA ACT CA *Zfhx2*qpcr1-GGC TCT CCA ATC TCC TTT GGT G
Dicer1	Dicerqpcr-CTG GTG GCT TGA GGA CAA GAC Dicerqpcr2-AGT GTA GCC TTA GCC ATT TGC
Advillin Flox-tdTomato-Stop-DTA	DTAqpcrf- TAAGGTTGCTGGTTAGGCTTTAC DTAqpcrr-ATGCCGCAGTAGACTGAAGCAG
Tmem45b^{Cre}	Tmem45bAf-GTGTGAACTGTTTCATGGACACTG Tmem45bAr-TTCATCTCTGAAGACTGAGATTGGTCTCAGATCC

Table 9: Primer sequence per gene of interest

The reference Dicer1 gene (two genomic copies) was measured on the same sample in parallel with the gene of interest, giving a CT or cycle threshold difference (ΔCT) for Dicer1 minus gene of interest. The ΔCT data was converted

to relative expression levels (2ˆΔCT) to give copy number per haploid genome and then multiplied by two to calculate diploid copy number. Whilst the copy number for Dicer is constant at two in both the wild-type and transgenic animals, the gene of interest copy number is two only for the wild-type littermates.

The resulting products were run on an agarose gel alongside a housekeeping gene control to ensure the PCR reaction worked. When needed, the band was excised and via Qiagen gel extraction kit protocol, DNA was eluted in 50µl elution buffer, and the concentration was measured using a Nanodrop spectrophotometer (Thermo Scientific). Samples were sent to Source Bioscience (Cambridge) for Sanger sequencing. Results were analysed using Snap-Gene viewer software and sequence alignments performed using NCBI nucleotide BLAST.

2.2.2 Primer design

Primer design was performed when needed using UCSC tools to determine pair sequence with melting temperature of around 68˚C (as per dicer) and 60% guanine-cytosine. The last step included an *in-silico* PCR genome assembly with the chosen primers to determine the product size, ideally around the 200bp dicer product.

2.3 Drug administration. Tamoxifen preparation and injection.

2mg of tamoxifen per animal was administrated intraperitoneally in strains for site and time specific gene targeting (Metzger and Chambon, 2001). The injections were performed over five consecutive days on the lines *Ntrk2* (TrkB) CreER, CGRP CreER and Th CreER, at least 15 days before testing or tissue collection. A mixture of 1g of tamoxifen (Sigma) in 15 ml of pure ethanol was dissolved in 100 ml of autoclaved sunflower oil the day of the injection.

2.4 Behaviour tests

2.4.1 Acute pain tests

Procedures and behavioural tests were conducted during the light phase of a day-night cycle between 8 AM and 6 PM. All experiments were carried out in compliance with the Animals (Scientific Procedures) Act (1986) and approved by the UK Home Office license and UCL ethics committee under a Home Office project license. Experiments were conducted using age and sex matching animals and tested when at least eight weeks old.

2.4.1.1 Mechanical Sensitivity

> Mechanical sensitivity was assessed by using the von Frey up-down method to obtain the 50% paw withdrawal threshold (PWT). Mice were placed in darkened enclosures with a wire mesh floor and left to habituate for at least 1h. A set of nylon von Frey microfilaments (Bioseb), with weights from 0.008g to 2g, were applied into the plantar surface of the hind paw of each animal. Starting always from the 0.4g filament, responses were recorded as positives or negatives. If the response was positive, a lower strength was used for the next stimulation, whilst if negative or no reaction, a filament with increased strength was applied. To determine the optimal threshold, flinching, biting or paw withdrawal during or immediately after the stimulation was considered positive nociceptive defensive behaviour. After the first change in responsiveness, five additional measures were taken to establish a pattern of response to calculate:

50% threshold = (10[χ+κδ])/10,000), where χ is the log of the final von Frey filament used, κ = tabular value for the pattern of responses and δ the mean difference between filaments (in log units) (Chaplan et al., 1994).

> Randall-Selitto test. Animals were restrained in a clear plastic tube with an acclimatisation period of approximately 1-2 minutes. A blunt probe was applied to the first third of the tail with increasing controlled pressure until the animal exhibited a painful like response. When struggling, withdrawal of tail, or vocalisation occurred, the pressure was removed from the animal,

and the weight in which the reaction occurred was noted. The average of three repeated threshold measures was multiplied by 20 to get the grams equivalent (Randall and Selitto, 1957).

2.4.1.2 Thermal sensitivity

➤ Hot plate. Each mouse was placed on a clean hot plate apparatus (Ugo Basile) with controllable floor temperature. During different experimental sessions for setups with 50°C and 55°C platform heat, the time until the animal showed a nociceptive response (lifting, shaking and licking) on the hind paw was assessed. Cut off was set at 60 seconds to prevent damage to the paw plantar surface (Eddy and Leimbach, 1953, Espejo and Mir, 1993).

➤ Hargreaves'. Supraspinal thermal nociceptive responses were tested after applying radiant heat light at a ramp of 1.5 °C per second on each hind paw while the animal was still but awake (idle and active intensity 2% and 20% respectively). Latency in seconds to licking, lifting or shaking the paw was taken three times from each paw, with 5-10 min break between them. Animals were placed in Plexiglass boxes on clean glass flooring and acclimatised for over 1 h before testing. Cut off was 30 seconds latency for the specific ramp (Hargreaves et al., 1988) or 60 seconds in a modified 0.75°C per second ramp setting.

➤ Dry ice-cold plantar assay. Using the same setting as for the Hargreaves' test explained above, animal response latency to temperatures up to 13 °C (Figure 8) was tested after applying a crushed dry ice pellet compressed on an opened 2 ml syringe. This was located contacting the glass surface (6 mm thickness) just below the chosen paw with a cut off of 30 seconds. The average of three measures was taken with a resting time of 15 min between stimulations (Brenner et al., 2012).
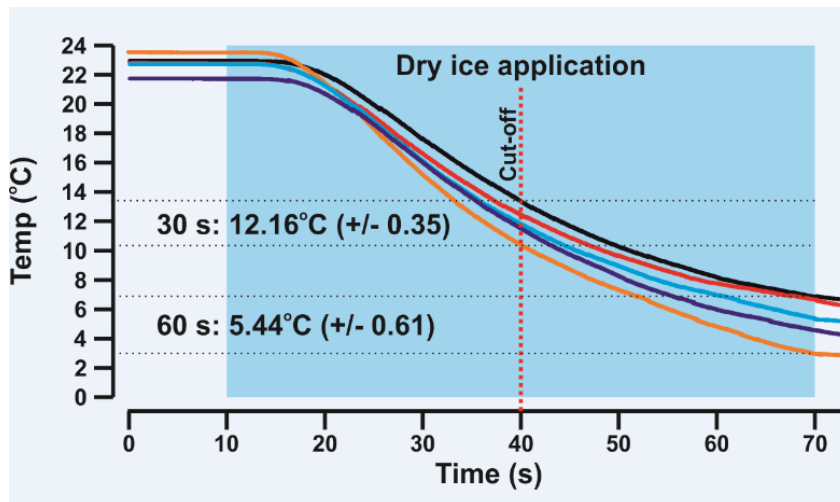
Figure 8: Cooling dynamics of the cold plantar assay (Dry ice).

The temperature of the glass platform used in the cold plantar test, before and during dry ice application (by Dr E. Emery).

➤ Acetone evaporation test. Animals were kept in a mesh bottomed darkened enclosure for a 2 hour acclimatization period, after which, a drop of acetone was gently applied to the back paw. Fluttering or paw licking response duration was timed for one min and repeated three times after resting intervals of 5-10 min (Choi et al., 1994).

2.4.1.3 Dynamic light touch: Cotton swab test

Mice were placed on an elevated platform with a mesh floor and habituated for at least 60 min. A standard cotton swab was manually "puffed-out" to about three times its original size. The hind paw of mice was then brushed using this cotton swab in a heel-to-toe direction. The frequency of responses was noted in each trial, repeated five times alternating between paws with an interval of one min between them (Garrison et al., 2012).

2.4.1.4 Motor coordination

➤ Accelerating Rotarod test (mouse-adapted apparatus; IITC). Mice were individually placed on a rod with an initial moving ramp of 4 revolutions per minute (rpm) which was increased steadily up to 40 rpm at 3 minutes and remained at 40 rpm for the last 2 minutes. Animals were trained to use the

machine for 2 days before testing. The duration (s) when the animals were able to stay on the rotarod was measured for three different cycles, as well as distance travelled (m) and maximum speed (rpm) reached (Jones and Roberts, 1968).

➢ Adapted walking beam. Animals were trained during three consecutive days to walk on a hand-made metal elevated beam (approximately 50cm above table surface) (Luong et al., 2011). Each subject was placed in one extreme of the elevated beam with a light source, and the time to walk to its home cage at the end of the beam was recorded. This was repeated three times for a 12 mm wide beam and three in a 6 mm wide beam (Figure 9).

The total walking time to complete the 80 cm established final point was measured, as well as the number of slips on performing the task.
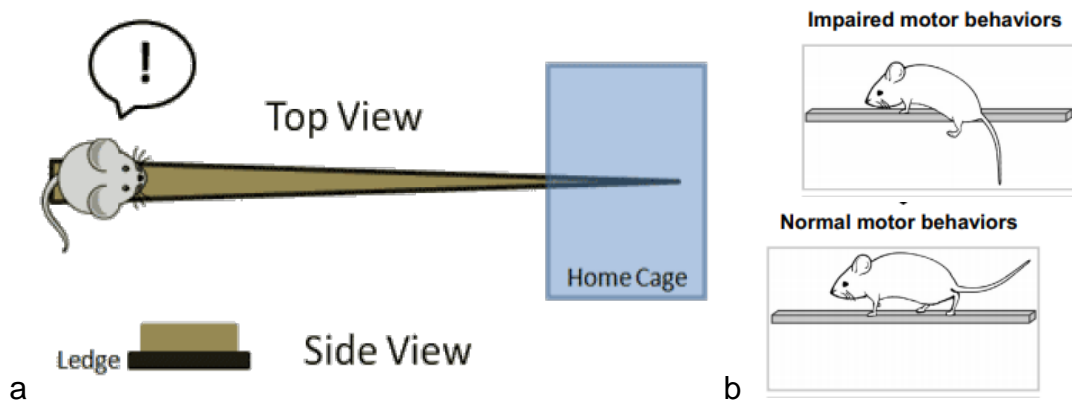
Figure 9. (a) Walking beam test representation (from Stanford Behavioural and functional neuroscience laboratory). (b) Walking beam test slips

➢ Adapted pole test. Previously trained, the mouse is placed on a vertical standing tube wrapped in a mesh material to facilitate the gripping head skyward oriented. The time that it takes him to turn around (T turn time) (Figure 10) and to climb down the length of the pole was counted and repeated three times (Matsuura et al., 1997).
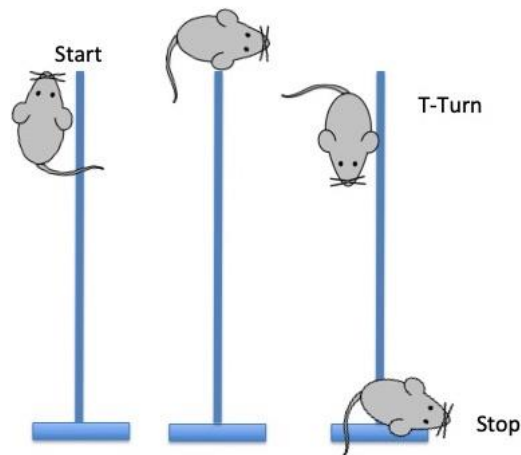
Figure 10. Pole test representation (Brenner et al., 2012)

2.4.1.5 Exploratory behaviour test by open field maze

A hand-made acrylic enclosure with white walls and flooring was made to allow the animal to walk freely over 5 min (72x72cm surface and 36cm high). The total floor surface was divided into 16 equidistant squares (18x18cm). Each animal was placed in the same corner square and total crossings were manually scored for a 5 minute test duration. Movement in the corners and the four middle squares (representing anxiety and depressive behaviours) were also counted. Each animal was tested only the first time that he touches the arena, and ethanol surface cleaning was performed after each test to avoid odour impregnation (Walsh and Cummins, 1976).

2.4.2 Inflammatory pain tests

2.4.2.1 Formalin

Animals were acclimatised to Hargreaves' type Plexiglass enclosures for at least 1 h before the test. They were injected with 20 µl of 5% Formalin into the plantar right hind paw and were video recorded for 60 min (Murray et al., 1988). Time spent licking, shaking or biting the affected paw was counted in five-minute blocks as classically described, and data were expressed in a time point graph or divided between an early acute phase (Phase I, 0-10min) and the latter inflammatory phase (Phase II, 10-60min) and analysed separately.

In chapter four, for formalin the video recordings were sampled for 10 sec at 1 min intervals using a Python script and scored for the presence or absence of nocifensive behaviours toward the injected hind paw (licking, biting, flinching). Data were processed by L De Clauser and expressed as a percentage of nocifensive responses out of all responses.

2.4.2.2 Complete Freund's adjuvant (CFA)

After the previous establishment of baselines, 20µl of CFA (SIGMA, F4258) was injected intraplantarly into the right hind paw of the mouse (Larson et al., 1986). The von Frey up-down method and Hargreaves' tests were performed at baseline and 1-, 3- and 7-days post-injection. At the end of the experiment, injected paws were collected and weighed to discard any oedema differences between the groups.

2.4.2.3 Capsaicin induced nociception test

Animals were acclimatised to individual transparent Plexiglas enclosures for at least 1 h before the test. 20µl of capsaicin (equivalent to 1.6 µg of capsaicin per paw) or vehicle (PBS) was injected ventrally under the skin of the hind paw (intraplantar) using an insulin syringe and immediately placed back into the chamber where the mouse was then recorded for 5 minutes. Time licking, biting and flicking of the affected paw was measured per minute in every animal of each group (Sakurada et al., 2003).

2.4.3 Neuropathic model.

Both mechanical and thermal baseline thresholds were recorded using von Frey and Hargreaves' tests. Animals were anaesthetised with isoflurane before an incision was made in the shaved skin in a parallel line with the left femur in an aseptic environment. The left sciatic nerve was exposed at mid-thigh level through blunt dissection.

2.4.3.1 Chronic constriction injury (CCI)

Three independent loose ligatures using 8-0 non-absorbable sutures (Ethicon) were made around the sciatic nerve with 3 knots in each (Figure 11) (Bennett & Xie, 1988).
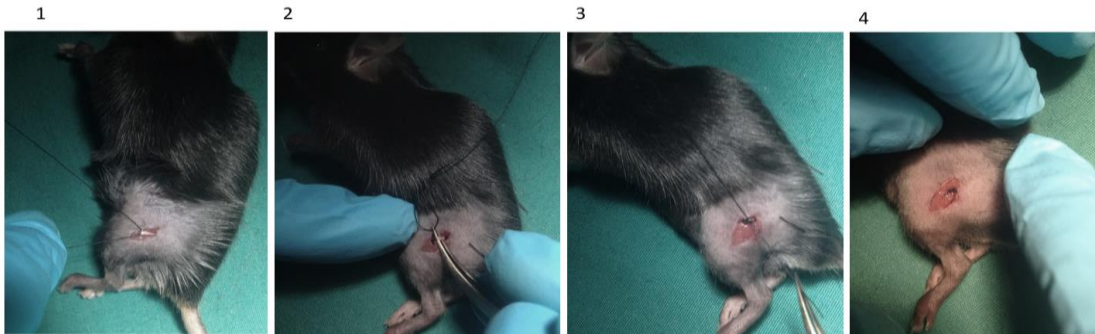
Figure 11. (1-4) Representation of CCI constriction
(By S. Santana, from *Zfhx2* global KO and littermates experiments. Drape removed temporarily for pictures)

The muscle edges were joined together with one absorbable suture stitch, and the skin was closed via modified internal suturing (Figure 12) in order to avoid reopening due to self-biting and to reduce post-surgical infections.
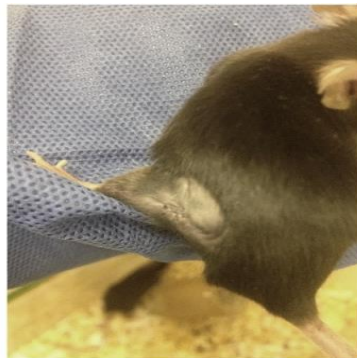
Figure 12. Representative animal with internal sutures 4 hours after CCI surgery.
(By S. Santana, from *Zfhx2* global KO and littermate experiments)

Animal wounds and general wellbeing were monitored daily, with thermal and mechanical thresholds being measured from 7 to 15 days post-surgery for all animals.

2.4.3.2 Partial nerve ligation (PSL or Seltzer model).

A tight ligature around approximately 1/3 to 1/2 the diameter of the sciatic nerve was tied using 6-0 non-absorbable sutures (Ethicon) (Malmberg and Basbaum, 1998). The muscle and skin were closed in layers as explained above, and thermal and mechanical thresholds were monitored from 7 to 21 days post-surgery.

2.4.4 Cancer model

2.4.4.1 Tissue culture

Lewis Lung carcinoma LL/2 cells (Sigma) were cultured in DMEM supplemented with 10% FBS and 1% Penicillin/Streptomycin for at least 2 weeks prior to surgery. 5 days before surgery, Penicillin/Streptomycin was avoided. Cells were split at 70-80% confluence two or one day before the procedure. On the day of surgery, cells were harvested and resuspended in DMEM at a final concentration of $2x10^7$ cells/ml and kept on ice till use. The viability and number of cells were counted pre and immediately after surgery.

2.4.4.2 Surgery

Animals were anaesthetised with isoflurane, before being shaved and sterile Lacri-Lube applied to their eyes. An incision was made in the shaved and clean skin of the left knee (Minett et al., 2014a), where the lateral retinaculum tendons were loosened to move the patella to the side and expose the distal femoral epiphysis. A 30 gauge needle was used to mechanically drill a hole till the medullary cavity was reached. 10 µl of the $2x10^7$ carcinoma cells were administered intrafemorally with a 0.3 ml disposable syringe ($2x10^5$ per animal). After a minute, the needle was removed, and the hole closed with warmed bone wax (Johnson&Johnson). The area was thoroughly washed out with sterile saline before tendons were moved back in place. The skin was sutured with 6-0 absorbable vicryl rapid (Ethicon) (see 2.4.3.1 internal sutures), and Lidocaine spray (Intubeaze, 20mg/ml, Dechra) applied to the wound. Animals were placed on a heated platform to ease up their recovery from the anaesthesia and were

given wet food for the 3 following days after surgery during which wound and general wellbeing were also monitored.

2.4.4.3 Dynamic weight bearing

Weight-bearing asymmetry was tested using an incapacitance meter (Bioseb) consisting of two scales. After several training sessions, mice were voluntarily introducing themselves into an inclined red plexiglass tube while hind paws were exposed and located one on each apparatus platform. Once animals were in rest, the weight distribution on each paw was taken by triplicate. The average weight-bearing was measured by sensors with pressure transducers in each independent floor, and the left-right ratio was calculated as the weight placed on the affected limb divided by the total weight on both contra and ipsilateral hind limbs (Quadros et al., 2015).

2.4.4.4 Limb use score

Using a transparent glass box (30x45 cm), animals were acclimatised 5-10 minutes before the test, when each individual was recorded for 5 minutes. The use of the affected limb was scored from 4 to 0 as follows:

4: Normal use of the limb, 3: slight limping, characterized by preferential use of the unaffected limb when rearing, 2: clear limping, 1: clear limping and partial lack of use of the limb, 0: lack of use of the affected limb during most of the observation time, after which the animal was culled and experiment ended (Falk et al., 2013).

2.4.4.5 Femur sample preparation

Immediately after sacrifice, both hind limbs were dissected and skin and soft tissues removed to expose the femur and tibia. Ankle joint and foot were left on the sample to facilitate identification and handling. Bones were placed in 4% paraformaldehyde and allowed to fix for 48 hours at 4°C. Subsequently, they were embedded in 70% ethanol and stored at 4°C until μCT scanning could be performed.

2.4.5 Statistics

Data on different groups were analysed using GraphPad Prism (GraphPad Software, Inc), and results are presented as mean ± SEM with n referring to the number of samples tested per group, as indicated in figure legends. Student's t-test (two-tailed) was performed to compare the distribution and one-way analysis of variance (ANOVA) with Bonferroni post hoc test for various groups.

Behavioural data group analysis over multiple time points was analysed using parametric two-way ANOVA followed by Bonferroni post hoc test where appropriate. Significant interaction effects between groups and over time (compared to within group baseline values) were presented with p-value (p) $*p < 0.05$, $**p < 0.01$, $***p < 0.001$ as statistically significant.

2.5   Post-mortem studies

2.5.1   Immunofluorescence

Depending on the antibody used, the animals were either perfused with 4% paraformaldehyde (PFA) before dissection, or fresh frozen tissue collected.

> ➢ PFA perfused tissue collection and preparation. After terminal anaesthesia via intraperitoneal (i.p.) injection of sodium pentobarbitone (150mg/kg) (Rhône Mérieux), animals were transcardially perfused with 10 ml heparinized saline (0.9%NaCl) into the left ventricle, followed by 25 ml of ice cold 4% paraformaldehyde in 0.1M phosphate-buffered saline pH 7.4. DRG were extracted from the lumbar area and post-fixed with the same fixative solution for at least 2 hours at 4°C, before being immersed in cryopreservative solution (30% w/v sucrose in 0.1 M PBS) overnight at 4°C.

> ➢ When freshly extracted DRG were required, animals were previously euthanized using standardized schedule 1 protocol of CO_2 overdose and subsequent cervical dislocation. Sections underwent a postfix in ice-cold 4% PFA for 5-10 minutes just before the first step of the immunostaining protocol.

Tissue samples were then embedded in optimal cutting temperature compound (OCT) blocks and snap frozen for posterior sectioning using a cryostat (Bright). 11 µm thick sections were mounted onto electrostatically charged Superfrost Plus slides (Fisher Scientific), allowed to dry overnight at RT, and then stored at −80 °C for a period no longer than three months. Tissue samples were sequentially defrosted from -80 °C to -20 °C and then 4 °C before starting the immuno protocol at room temperature (RT). They were permeabilized with 0.1% Triton X-100 in PBS three times for 5 min, before being blocked in 10% goat serum in PBS for 1hr RT. The primary antibody incubation was at different dilutions in blocking solution, and left overnight at 4°C in the dark. After washing in PBST, bound primary antibodies were detected by incubating with a corresponding secondary antibody (Table 10) at RT for two hours away from the light. The slides were then washed, dried, and finally mounted with Vectashield mounting medium and a coverslip before being sealed and stored in the dark.

ANTIBODY	DESCRIPTION	DILUTION
Primary		
Peripherin	IgG mouse monoclonal anti-peripherin (Sigma, P-5117)	1:1000 FF
N200	IgG rabbit anti-neurofilament 200 (Sigma, N4142)	1:200 FF
NeuN	IgG rabbit anti-NeuN (Abcam, Ab177487)	1:400 FF
Tyrosine Hydroxylase	Rabbit Anti-TH (Merck Millipore AB152)	1:100 PF
Secondary		
Alexa594	IgG goat monoclonal anti-rabbit (Invitrogen, 11037)	1:1000
Alexa488	IgG goat monoclonal anti-mouse (Invitrogen, A11017)	1:1000

Table 10. Antibodies (FF fresh frozen, PF perfused)

2.5.2 Fluorescent Nissl Stain

A standard histological method was used in combination with immunohistochemistry to identify neurons. Following the protocol as described by Thermofisher, after secondary antibody incubation, slides were further incubated in Nissl (Blue NeuroTrace™ N-21479) diluted in PBS (1:1000) for 20 min and mounted as normal before visualization and counting.

2.5.3 Cell counting

Tissue samples were visualised using a Leica SP5 confocal microscope, I obtained the images at 10x and 20x magnification with 4x averaging and exported as jpeg files with 7,200 pix on the longest side at 300 ppi. Fluorescence on the sample images were analysed using the cell counter plugin for ImageJ 1.47a using global adjustments for brightness and contrast. The number of cells per DRG was estimated by averaging cell counts from at least three animals per experimental group. For each animal ~10-15 section images (each separated by ~88μm) were counted.

2.5.4 Statistics

Data were analysed using GraphPad Prism (GraphPad Software, Inc), and results presented as mean ± SEM with n referring to the number of animals tested per group, as indicated in figure legends. Student's t-test (two-tailed) was performed to compare the distribution and one-way analysis of variance (ANOVA) with Bonferroni post hoc test for various groups.

2.6   In situ Hybridization (ISH) sample preparation and RNAScope

(For tissue collection and preparation see PFA perfused tissue, see chapter 2.5.1)

Two 11 µm thick sections were mounted onto each electrostatically charged slides Superfrost Plus (Fisher Scientific), allowed to freeze-dry overnight -80°C, and then stored at −80 °C for a period no longer than a month.

In situ Hybridization *(ISH)*, was performed using the RNAScope system (Advanced Cell Diagnostics). Following a preparation protocol for fresh-frozen samples (see 2.5.1) and 1h post-fixing with 4% PFA in PBS at 4 °C, the DRG sections were stepwise dehydrated with 50%, 70% and 100% Ethanol. Tissue pre-treatment consisted of hydrogen peroxide and Protease IV (10 and 20 min respectively) at RT after which a probe Hybridization and detection with the Multiplex Fluorescence Kit v2 were performed according to the manufacturer's protocol.

Probes included are: *Tmem233* (#519851), *Tmem45b* (#420461-c3), NEFH (#443671 or #443671-c4), Th (#317621-c4), CGRP (*Calca* #417961-c3), *Ntng1* (#488871-C2), *Ntrk2* (#423611-c3) and tdTomato (#317041-c4). Ribonucleic acid (RNA) localisation was detected with Alexa Fluor™ 488 Tyramide (Cat# B40953, green, for all target gene RNA products) and Opal 570 (Cat# FP1488001KT, red, when a probe against tdTomato was used) fluorochrome dyes (Perkin Elmer) compared to DAPI staining (nuclei) or TS-coumarin (TS405, blue, Cat# NEL703001KT, Perkin Elmer) used for neurofilament heavy chain (NEFH). ISH slides were mounted using Prolong Gold (ThermoFisher Scientific #P36930).

The last step consisted of fluorescence detection using Zeiss LSM 880 Airyscan microscope. Images were taken by A. Okorokov at 10x and 20x magnification with 4x averaging (typically stitched 16-20 tiles), air scan processed and exported as 16-bit uncompressed tiff files for further basic editing in Adobe Lightroom v6 (Adobe) on colour calibrated iMac retina monitor. Final images were exported as jpeg files with 7,200 pix on the longest side at 300 ppi.

2.7 RNA extraction and gene expression analysis

RNA was extracted from dissected mouse lumbar DRG, suspended in 1ml trizol solution (Ambion 15596018) homogenised for 3 x 10 seconds using a MINILYS benchtop homogeniser (Peqlab) and kept at -80°C until digestion. Total RNA was extracted using PureLink RNA Micro Kit (Invitrogen 12183-016), following the manufacturer's instructions.

1 μg of RNA was then transformed into cDNA by reverse transcriptase SuperScript III first strand cDNA synthesis kit (Invitrogen), where its components (Table 11) were incubated at 65°C for 5 minutes and placed on ice for at least 1 minute.

COMPONENT	AMOUNT
RNA	1-3μg
Random hexamers	1μl
10mM dNTP mix	1μl
DEPC-treated water	To 10μl

Table 11. cDNA synthesis mix

A master mix was prepared (Table 12) and added to the RNA mixture and incubated at 25°C for 10 minutes, 50°C for 50 minutes, followed by a reverse transcriptase heat inactivation step at 85°C for 5 minutes. 1μl of RNase-H was then added to each reaction tube and incubated at 37°C for 20 minutes. cDNA was stored at -20°C.

COMPONENT	AMOUNT
10X RT buffer	2µl
25mM MgCl$_2$	4µl
0.1M DTT	2µl
RNaseOUT (40 U/µl)	1µl
SuperScript III RT (200U/µl)	1µl

Table 12. cDNA master mix

Non-reverse transcriptase reactions were also included to discard possible contamination of genomic DNA in RNA samples.

2.7.1 Real-time qPCR

In order to detect levels of target gene expression in the tissue, quantitative RT-PCR Taqman (Thermo Fisher Scientific) reactions were performed according to the manufacturer's instructions. The PCR reaction mix consisted of first-strand cDNA template, primer pairs (Taqman probes for the gene of interest and actin (Actb) (Table 13) as well as TaqMan Universal Master Mix II (Thermo Fisher Scientific 4440038).

GENE OF INTEREST	TAQMAN CATALOGUE NUMBER
Zfhx2: (Mm01313868_m1)	4331182
Actb: Mm01205647_g1	4331182
Scn8a: Mm00488110_m1	4331182
Tmem45b: Mm00460733_m1	4331182

Table 13. Taqman probe and catalogue number per gene.

Amplification of the selected genes from each sample was performed in triplicate on a 96-well reaction plate in 20µl volume using BioRad CFX with the following protocol:

-Denaturation 2min at 50°C

-10min polymerase activation at 95°C

-40 Cycles of 15 sec denaturation at 95°C, 1min annealing at 60°C and 72°C extension for 30 seconds.

Relative expression of the target gene was calculated using the comparative 2ΔΔCT method (Livak and Schmittgen, 2001). Expression of the test gene was compared with that of b-Actin measured on the same sample, giving a cycle threshold difference (ΔCT) for b-Actin minus the test gene. The CT difference, ΔCT values of individual samples were compared to ΔCT of the control of WT clones, giving ΔΔCT values of each clone. The relative expression was calculated as 2-ΔΔCT from which mean, S.E.M. and statistics were calculated.

The resulting products were run on an agarose gel alongside a housekeeping gene control to ensure the cDNA sample and PCR reaction worked. When needed, the band was excised and via Qiagen, gel extraction kit protocol was then sent for sequencing.

2.7.2 Statistics

Statistical data analysis on different groups were analysed using GraphPad Prism (GraphPad Software, Inc), and results were presented as mean ± SEM with n referring to the number of samples tested per group, as indicated in figure legends. Student's t-test (two-tailed) was performed to compare distribution and one-way analysis of variance (ANOVA) with Bonferroni post hoc test for various groups, with $*p < 0.05$, $**p < 0.01$, $***p < 0.001$ as statistically significant.

Chapter 3 - Characterisation of sensory neuronal subsets using a conditional ablative DTA mouse model

3.1   Summary

One of the reasons for the recent failure in developing useful analgesic drugs, is due to the current lack of a full understanding of the pain system, its players and their interactions. However, major technical advances in sequencing and genetic analyses have allowed us to identify pain associated genes expressed in the peripheral nervous system which represent potential drug targets (see 1.3.2).

Transcriptome analysis of single sensory neurons by the Ernfors group has provided, by using comprehensive single-cell RNA seq, invaluable information with a reclassification of somatosensory mouse DRG neurons into at least eighteen subtypes (Usoskin et al., 2015b, Zeisel et al., 2018b). This technique is not viable to be performed in humans due to the rapid post-mortem time required to prepare samples and accurately profile sensory neurons. Therefore, in order to target mouse-human translational issues, parallel studies undertaken at the Karolinska Institute have generated a catalogue of primate sensory neurons which have then been correlated to the rodent data (Kupari et al., 2021). Their findings have shown overall cross-species conservation of somatosensory neurons between primate and mouse which increases substantially the translational value of mouse models.

This chapter aims to identify the role of transcriptomically different subpopulations of neurons in different types of pain, focusing on the peripheral nervous system. The work included herein uses the Cre recombinase system across the different subpopulations identified by Zeisel et al. (Zeisel et al., 2018a) and includes four already available Cre lines and two newly generated, with the aim to encompass the majority of DRG subpopulations.

-Firstly, I validated both new and already established Cre lines by crossing them to a tomato reporter line. Their expected DRG neuronal expression pattern was verified by DRG marker analysis via immunostaining or RNAscope.

-Secondly, I verified a newly generated *Advillin* Flox-tdTomato-Stop-diphtheria toxin (DTA) mouse line which depletes targeted sensory neurons at the DRG level when crossed with a selected Cre line.

- Lastly, I used behavioural studies to characterise genetically defined sensory neuron subsets in the peripheral nervous system, by studying a range of Cre lines crossed with the previously validated *Advillin* Flox-tdTomato-Stop-DTA BAC mouse. Tamoxifen induced Cre-ERT2 lines were used when DRG expression of Cre lines was reported as changing during development according to literature.

3.2   Introduction

3.2.1   Functional prediction of neuronal types

Although each somatosensory neuron can be responsible for several sensory modalities and intensities, they can be broadly defined by their physiological responses to heat, cold and noxious mechanical stimuli, with distinct signalling networks respectively. This neuronal reactivity is due to the existence of specific molecular sensors which provide characteristic peripheral innervation and functional sensitivity to specific stimuli. Several studies have analysed both these sensors and their encoding genes by the use of Cre mouse driven lines, with the aim to associate them with a function (Dhandapani et al., 2018, Vandewauw et al., 2018, Han et al., 2013a).

Results from these studies can be applied to the recent classification of somatosensory neurons, based on differential transcriptomic profiles (Zeisel et al., 2018b, Usoskin et al., 2015b). When doing so, we can potentially associate a distinctive transcriptomic profiling to a sensory phenotype (Figure 13), which constitutes the hypothesis of this thesis chapter.
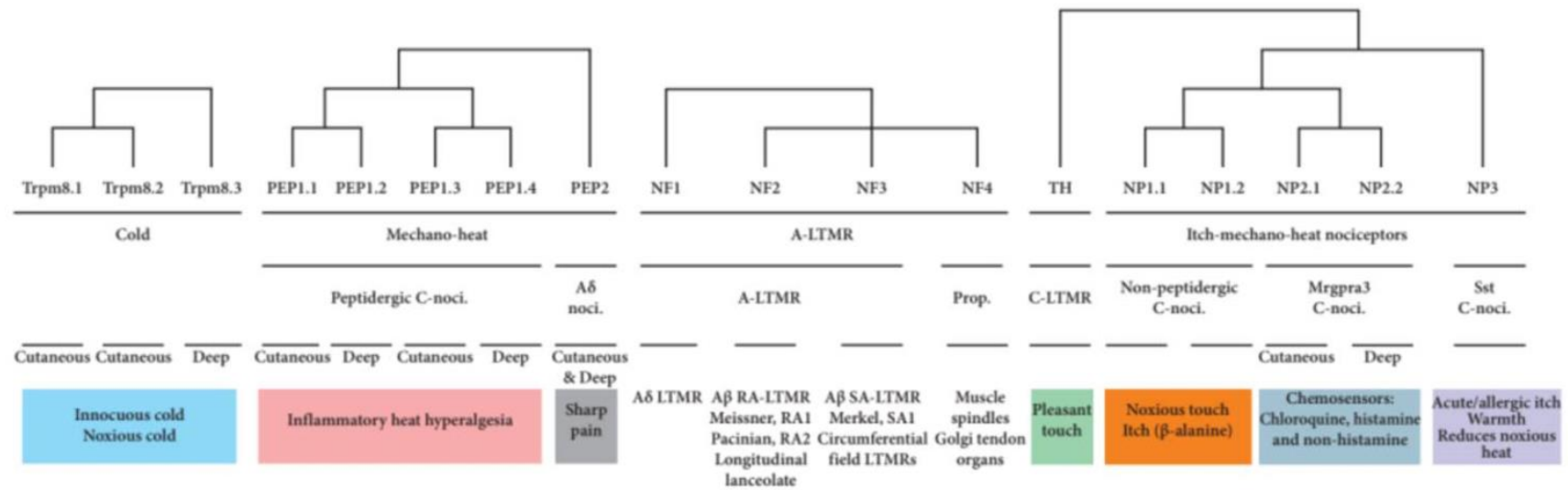
Figure 13. Taxonomy of somatosensory DRG neurons (Wood, 2020).

The first row represents the subpopulations of neurons based on their transcriptomic profile (Zeisel et al., 2018b), linked to their predictive function and association to classic classifications and tissue innervation.

The figure above includes a correlation between Zeisel's somatosensory neuron classification and their predictive function as well as their specific innervation. This functional prediction is based on the existence of the following pain markers/molecular sensors:

-*Cold sensing neurons: Trpm8.1, Trpm8.2, Trpm8.3*

Cold temperatures (0-20˚C) activate around 20% of all sensory neurons when stimulated *in vitro* (Hjerling-Leffler et al., 2007). As the temperature is reduced to below 0˚C the percentage of sensitivity increases significantly to even 100% (with insults below minus 18˚C). This global sensitization, however, is attributed to cold induced damage rather than specific cold sensitive transducers and therefore excluded for marker identification (Simone and Kajander, 1997).

The TrpM8 transducer is the main candidate for mediating cooling perceptions of temperatures below 26˚C (Bautista et al., 2007). Mouse studies in which this receptor was knocked out showed animals with a significant reduction in behavioural responses to cold temperatures, whilst responses to noxious cold (below 10˚C) were, albeit lessened, still present (Bautista et al., 2007). Interestingly, further studies where TrpM8 neurons were ablated showed more profound insensitivity to noxious cold temperatures (Knowlton et al., 2013). These results highlight not only the importance of this molecular sensor in cold sensation but also the existence of other cold transducers within TrpM8 positive neurons. Within them, the controversial TrpA1, as well as sodium channels $Na_v1.8$, and $Na_v1.9$, and some potassium channels have been associated with cold sensing processing (Lolignier et al., 2016).

-*Noxious mechano-heat sensing neurons: PEP1.1, PEP1.2, PEP1.3, PEP1.4, PEP2*

Peptidergic neurons (PEP) are characterised by the expression of Tac1 (encoding substance P or SP). Along with the NP3 cluster, they both represent the SP positive subpopulation of neurons, characterised by their reactivity to noxious mechanical and heat stimuli (Wood, 2020).

In 2018, the molecular sensors responsible for acute heat sensing in mice were identified within the transient receptor potential (TRP) family. They are TRPM3, TRPV1 and TRPA1 ion channels (Vandewauw et al., 2018). Both TRPV1 and TRPM3 are expressed in all PEP1 clusters (as well as in NP3, and NP1 respectively). On the other hand, TRPA1 is present in PEP1.1 and PEP1.4 (and again in NP1), suggesting potential combinatorial co-expression within the heat perception. These receptors can be activated by both endo- and exogenous substances such as capsaicin, acidosis derived protons, or proinflammatory neuropeptides which will lead to the so called "neurogenic inflammation" (Vriens and Voets, 2019, Wood, 2020). Recent transcriptomic classifications have suggested the NP subset and PEP subset should perhaps no longer be suitable for defining neuron types, because of their neuropeptide expression co-localization (Li et al., 2016), when proposing a new hierarchical clustering.

Another classic molecular marker for Peptidergic somatosensory neurons is the *Calc* gene (*Calca* subtype when expressed in DRG), encoding calcitonin gene-related peptide (CGRP) (Basbaum et al., 2009a). Ablation studies in mice have reported that CGRP positive DRG neurons are required to sense heat and itch (McCoy et al., 2013), as well as, unexpectedly cold thermoregulation.

-A-Low Threshold Mechano Receptors (LTMRs) and proprioceptive neurons NF1, NF2, NF3, NF4

NF1 is a subset of LTMRs characterised by expressing high levels of *Ntrk2*. This gene belongs to the neurotrophic tyrosine receptor kinase family along with Ntrk1 and Ntrk3, encoding for different tyrosine receptor kinase receptors (Trk). Abnormal Ntrk gene fusions have recently been identified as driving unregulated cell growth and proliferation in a range of cancer types. They serve not only as a biomarker in onco-diagnosis, but as cancer therapy by Trk inhibition (Lange and Lo, 2018, Vaishnavi et al., 2015).

TrkB protein, encoded by *Ntrk2*, is involved in neuronal differentiation and survival and has been reported as key in mechanical hypersensitivity processing after neuropathic nerve injury (Dhandapani et al., 2018). It acts as a receptor for neurotrophins such as neurotrophin-4 (NT-4), and neurotrophin-3 (NT-3) or brain-derived neurotrophic factor (BDNF). Each of them has been associated with

specific roles, for example, BDNF ablation in mice has been reported as critical in the transition from acute to chronic pain (Sikandar et al., 2018).

NF2 neurons respond to movement and vibration. They are rapidly adapting mechanoreceptive neurons expressing *Ret* and *Calb* as well as, in low levels, *Ntrk2*. On the contrary, NF3 are slowly adapting neurons expressing *Ntrk3* (Wood, 2020), believed to be involved in the survival of the NF4 neuronal subset during development. The NF4 cluster, corresponds to the proprioceptive neurons, expressing *Ntrk3* (encoding TrkC) and *Pvalb.* This latter gene encodes the calcium-binding protein Parvalbumin cutaneous molecular marker that is required for innocuous mechanical sensation including vibration sensing (Usoskin et al., 2015b, Ernfors et al., 1994).

-C-Low threshold mechanoreceptors (TH)

C fibre low threshold mechanoreceptors (C-LTMRs) innervate hairy skin and are associated with pleasant touch. The hedonic components of "liking" and "wanting" in human and animal touch are very complex. The first one refers to an immediate reaction to a stimulus whilst the second one refers to the reward driven consequences with a greater central processing component (Perini et al., 2015).

This discrete population of neurons expresses Tyrosine Hydroxylase (Th) and Ceacam10 (carcinoembryonic antigen-related cell adhesion molecule). Interestingly, mice where the $Na_v1.7$ sodium channel is knocked out contain significantly downregulated expression of the *Ceacam10* transcript (Minett et al., 2015). Considering that $Na_v1.7$ is one of the key players in pain sensation this makes Ceacam10 and, by association Th positive neurons, an interesting cluster for further pain studies.

-Itch-Mechano-Heat Neurons (NP1.1, NP1.2, NP2.1, NP2.2 and NP3 Neurons)

NP1 neurons are characterised by high levels of *MrgprD*, which mediates a specific B-Alanine induced itch (Liu and Dong, 2015). They are histamine independent itch-mechano-heat neurons also involved in mechanical sensitivity. The NP2 sub-cluster innervates the skin, and is the only subset containing the pruritogen receptor MrgprA3 which mediates Chloroquine dependent itch.

Transgenic ablation studies have associated these polymodal nociceptors with broad itch sensation (both histamine dependent and independent), as well as responding very slightly to noxious heat and mechanical stimuli (Han et al., 2012). As well as NP2, NP3 are also broad itch neurons, and present non-noxious heat sensitivity. They specifically mediate interleukin-31 induced itch and express markers such as: somatostatin (Sst), neurotensin (Nts), natriuretic peptide type B (NPPB), interleukin-31 receptor A (IL-31ra) and its co-receptor oncostatin M receptor (Osmr), the cysteinyl leukotriene receptor 2 (Cysltr2), 5-hydroxytryptamine receptor 1F (Htr1f), and Npy2r. They uniquely express the Trpm-2 ion channel, essential for the already mentioned non-noxious temperature sensing (Tan and McNaughton, 2016).

Analogously to the Ernfors/Zeisel functional association, studies by Li et al. have demonstrated that based on the current understanding of function and signalling processing, transcriptome data can indeed partially predict the function of neuron types (Li et al., 2016). They propose that a specific type of neuron has certain morphological properties, a unique transcriptome and transcriptome-derived signalling networks and markers, and an associated functional phenotype. They classified mouse DRG neurons into ten types and fourteen subordinate subtypes with distinct transcriptional patterns, molecular markers and predictive associated functions (Table 14). These results have been deposited in a public domain and provide a new system to catalogue somatosensory neurons, particularly for nociceptors, for the study of sensory and pain mechanisms.

	Temperature		Nociception
Thermoception	Trpv2	>52 °C	-
	Trpv1	>42 °C	T (heat, > 50 °C)
	Trpv4	28~42 °C	T (heat, 45 - 46 °C)
	Trpm8	15~28 °C	T (cold)
	Trpa1	<18 °C	T (cold), M, F
	Trpm3	25~40 °C	T (heat)
	Ano1	>25 °C	T (heat), F
	Mechanical stimulus		**Nociception**
Mechanoception	Mrgprb4	Massage-like stroking	-
	Trpc1	Light-touch	-
	Kcnk2	Mild mechanical stimulus	T (heat, cold), M
	Kcnk4	Mild mechanical stimulus	T (heat), M
	Trpc3/Trpc6	Innocuous mechanical stimulus	-
	Asic3	Candidate channel	T (heat, cold), M
	Piezo2	Candidate channel	-
	Chemical		**Nociception**
Chemoreception	P2rx2	ATP	F
	P2rx3	ATP	F
	P2ry1	ATP	T (heat, cold)
	Ptgdr	Prostaglandin D	F
	Ptger1	Prostaglandin E	T (heat)
	Ptger2	Prostaglandin E	T (heat), M, F
	Ptgfr	Prostaglandin F	T (heat)
	Ptgir	Prostaglandin I	T (heat)
	Adora1	Adenosine	T (heat)
	Pruritogen		**Nociception**
Pruriception	Nppb	Non-selective	-
	Il31ra	Il31	-
	F2rl1	Proteases	-
	Hrh1	Histamine	T (heat), M, F
	Mrgprc11	BAM8–22	-
	Mrgpra3	Chloroquine	-
	Mrgprd	β-alanine	T (cold, heat)
	Htr2a	Serotonin	-

Table 14 Correlation between neuron clusters (C1 to C10) and functional molecular markers.

The right table contains different markers and their involvement in thermoception T, mechanoreception M, chemoreception F and pruriception. The left table contains the level of expression of each marker per newly identified neuronal cluster. (Li et al., 2016)

3.2.2 Conditional ablation of DRG neurons in mice using Cre/loxP system

The use of transgenic mice, where a target gene or its level of expression is genetically modified, is one of the most valuable tools to assess the function of a novel gene, and potential drug screening. The complexity of the designs have been increasing over time, and we can now even artificially overexpress a pre-designed mutation using gain of function models, or conditionally control the ablation temporally and/or spatially in loss of function models (see chapter 1.5.3).

One of the most common methods for producing transgenic lines is based on the Cre/loxP recombination system. By using a gene specific promoter driven Cre it is possible to target specific subpopulations of neurons in the mouse DRG and manipulate expression of the target floxed gene. Two types of knockout mouse models are normally used: constitutive (when the target gene expression is

permanently inactivated in every cell of the organism) and conditional (when gene expression is time-controlled inactivated or inducible).

I have studied the function of different subpopulations of neurons that were defined on the basis of RNAseq data (Usoskin et al., 2015a) using conditional ablation of neurons through a novel *Advillin* Flox-tdTomato-Stop-DTA BAC tool mouse and a range of Cre lines (Santana-Varela et al., 2021). Our lab recruited existing Cre lines and generated others to represent different subpopulations of neurons within the transcriptome spectrum in the DRG (see Table 2) and with potential or previously confirmed implications in somatosensation. They are:

- TrkB^{CreER} (*Ntrk2*). Tyrosine Kinase Receptor B (TrkB), encoded by *Ntrk2* (Neurotrophic Receptor Tyrosine Kinase 2), is a receptor for brain-derived neurotrophic factor (BDNF). Involved in neuronal differentiation and survival, it has been identified as an anti-tumour target and is a key player in neuropathic pain after spared nerve injury (SNI) (Dhandapani et al., 2018).

- *Tmem45b*^{Cre}. Transmembrane protein 45b (*Tmem45b*) is a protein expressed in a subset of unmyelinated primary sensory neurons and has been recently reported as essential in inflammation and tissue injury-induced mechanical hyperalgesia (Tadashi et al., 2021). With similar distribution to *Scn10a*^{Cre} (Na$_v$1.8), both lines have been studied comparatively.

- Cgrp^{CreER} (*Calca*). Calcitonin gene-related peptide (CGRP) is a classic molecular marker of Peptidergic primary somatosensory neurons (Basbaum et al., 2009a). It is present in the form of two peptides: CGRPα and CGRPβ, encoded by *Calca* and *Calcb* respectively. The former is highly expressed in DRG neurons, where peptidergic CGRP positive neurons are both myelinated (A-fibres) or unmyelinated (C-fibres) and have been identified as responsible for migraine and vasodilatation, as well as encoding heat, itch and cold processes (McCoy et al., 2013).

Previous studies have shown that CGRP-positive neurons do not co-express TRPM8 (<1%) but do co-localise with *Tmem45b* (Tadashi et al., 2021), TRPV1

(heat and capsaicin sensitive nociceptive neurons) and other peptidergic neuron markers (Table 15) (McCoy et al., 2012).

Marker	% CGRPα-GFP$^{+/-}$/Marker$^+$	% Marker$^+$/CGRPα-GFP$^{+/-}$
CGRP	67.8±0.8	88.9±0.5
TRPV1	47.8±2.0	47.9±1.8
TRPM8	0.2±0.1	0.9±0.4
IB4	6.2±0.7	9.3±1.4
PAP	9.1±0.8	10.5±0.7
NF200	18.1±0.5	24.0±0.9
DTR	0	0

Table 15. Percentage of CGRP-GFP positive neurons co-labelled with different markers.
(McCoy et al., 2012)

- *Ntng1*[Cre]. Initially discovered in the 1990s as part of the laminin superfamily, the Netrin-G1 gene (*NTNG1*) encodes an axonal membrane adhesion protein which is attached to the plasma membrane surface by a glycosyl-phosphatidylinositol linkage. Whilst classic netrins are phylogenetically conserved, the G types have no invertebrate orthologs. In mammals, they are expressed in a highly conserved pattern over distinct neuronal subsets. Genetic deletion studies have linked them to the dissociation of neural circuits for the modulation of emotion-related behaviours (Zhang et al., 2016).

- *Tmem233*[Cre] : Transcriptome data shows transmembrane protein 233 (*Tmem233)* to be highly expressed in non-Peptidergic DRG neurons but its role is to date unknown.

- Th[CreERT2].The *Th* (tyrosine hydroxylase) gene encodes an enzyme that converts amino acid L-tyrosine to L-3,4-dihydroxyphenylalanine (L-DOPA), a precursor to the dopamine neurotransmitter in the CNS (Nagatsu et al., 1964). Outside the CNS, *Th* is also expressed in the gut, in peripheral sympathetic neurons and in mouse DRGs where they represent a small/medium-sized group of neurons essentially CGRP and IB4-negative (Brumovsky et al., 2006). Interestingly, ~15%

of adult lumbar DRG neurons have been reported to be immunoreactive to *Th* but its mRNA appears to be expressed in ~37% of L4–L6 mouse DRG neurons. Whether *Th* transcripts are translated into protein in all neurons remains to be established (Brumovsky, 2016).

Strategy

The expression pattern of each functional Cre was first examined by crossing every promoter driven (x) Cre positive mouse line with mice expressing a tomato fluorescent protein reporter (Rosa-CAG-flox-stop-tdTomato) strain. The genotype of every pup was confirmed using PCR of genomic DNA isolated from ear samples (see chapter 2.2). The resulting transgenic strain (x-CreTomato) has all x positive neurons labelled red (Madisen et al., 2010, Santana-Varela et al., 2021).

The reporter strain is a floxed-stop tdTomato with loxP sites flanking a transcriptional stop. ROSA26 locus is one of the most commonly used because genes inserted here are constitutively and stably expressed in all cells, and it does not contain any essential genes. The loxP-flanked STOP cassette prevents the transcription of the downstream red fluorescent protein variant (tdTomato). Recombination between LoxP sites is catalysed by Cre recombinase which will delete the fragment between them. By deleting the transcriptional stop, it allows the expression of tdTomato. The specificity is given by the promoter which drives the Cre, targeting then a specific neuronal subpopulation when expressed (Figure 14).

Promoter driven Cre line   **Rosa-CAG-flox-stop-tdTomato**
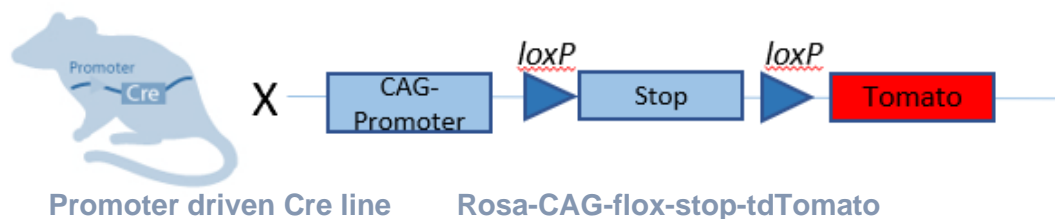
Figure 14 Representative figure of the transgenic design and its crossing with a Cre line. A global promoter will lead to the expression of downstream tomato in the presence of a Cre by excision of the lox P flanked Stop codon.

A second temporal control of Cre activity has been obtained in some strains by using a tamoxifen inducible element. Cre then, is substituted by the Cre ER (oestrogen receptor) variant and is only activated after tamoxifen administration in the adult mouse (post-development).

Dorsal root ganglion sensory neurons are molecularly defined by their mRNA-expression signatures and can be subclassified into Peptidergic, or non-Peptidergic nociceptors and large diameter mechanoreceptors that express neurofilament-200 (NF200) (see chapter 1.3). Although there is some overlap between these markers, their exclusivity as unique subpopulations in mouse DRG is widely recognized and it has been confirmed by single-cell RNA sequencing (Usoskin et al., 2015b, Zeisel et al., 2018b).

Lumbar spinal level L4, L5 & L6 DRG have been described as the ones innervating rodents hind paws (Kim et al., 1996; Thompson, 1970), therefore perfused DRG sections at this level were taken from each newly generated x-CreTomato mouse, generating a battery of red labelled populations of neurons, different depending on the promoter driving the Cre. Each experiment has generated a data figure with:

td Tomato, target gene, merged (td Tomato + Target gene), Nefh, merged (td Tomato + Nefh) and total merged.

Once every Cre was validated both in activity and specificity in the DRG, each promoter driven Cre was then crossed with a novel *Advillin* Flox-tdTomato-Stop-DTA BAC tool mouse under a sensory neuron specific promoter. This mouse contains a targeting construct with diphtheria toxin A (DTA), preceded by a floxed transcriptional stop signal (pA) and a tomato fluorescent protein which, in the absence of Cre, is expressed in all sensory neurons (Figure 15). Under normal conditions, the transcriptional stop prevents the transcription of the toxin from occurring. But, if the Cre enzyme is expressed, the tomato gene and transcriptional stop signal flanked by lox P sites will be excised, allowing the toxin to be expressed, ablating the neurons when and where this takes place.
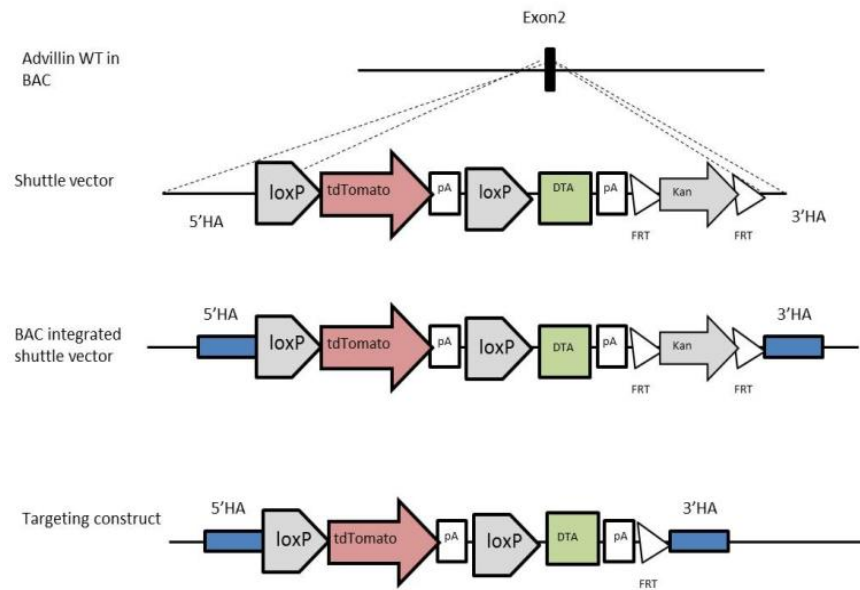
Figure 15 Construct design of Advillin Flox-tdTomato-Stop-DTA BAC
(by Dr Y. Bognanov) generated using a recombineering protocol (Copeland et al.,
2001) to clone exon 2 of the *Advillin* gene into a vector containing a floxTomatoDTA
and a Kanamycin cassette (flanked by flippase recognition target (FRT) sites later
removed). The BAC RPCI23-424F19 clone contains tdTomato sequence followed by
polyadenylation signals (pA) (STOP codons), flanked by the loxP sites, and fused with
a DTA sequence followed again by pA signals (Santana-Varela et al., 2021).

The resulting BAC containing the targeting cassette was sent to Cyagen for
pronucleus injection and founders bred with wild-type C57BL6/J mice to obtain
germline transmission. Newly generated animals crossed with the ablative tool
mouse were characterised by a battery of acute tests in order to assess how
behaviour was affected after deleting specific subpopulations of DRG neurons
(Table 16).

STRAIN		ACUTE BEHAVIOUR										PAIN MODELS			
		VonFrey	Cotton Swab	Hargreaves	Dry ice	hot plate	Randall Selitto tail	Rotorod	Randall Selitto Paw	open field	Balance beam/Pole	CFA	FORMALIN	PSL	BONE CANCER
Tmem233^{Cre}	cre alone														
Tmem233^{Cre}	+Avil FloxtdTomatoStopDTA	Paused, not breeding. Global KO generated but no phenotype.Only enough for formalin Subpopulation covered by tmem45b - Thcre											✓		
Ntrk2-^{CreRT2}	cre alone	✓	✓	✓	✓	✓	✓	✓	✓						
Ntrk2-^{CreRT2}	+Avil FloxtdTomatoStopDTA	✓	✓	✓	✓	✓	✓	✓	✓			✓		✓	✓
Tmem45b^{Cre}	cre alone	✓	✓	✓	✓	✓	✓	✓	✓	✓					
Tmem45b^{Cre}	+Avil FloxtdTomatoStopDTA	✓	✓	✓	✓	✓	✓	✓	✓	✓			✓		
Th^{CreERT2}	cre alone	✓	✓	✓	✓	✓	✓	✓	✓	✓	✓				
Th^{CreERT2}	+Avil FloxtdTomatoStopDTA	✓	✓	✓	✓	✓	✓	✓	✓	✓	✓		✓		
CGRP^{CreERT2}	cre alone	✓		✓	✓	✓	✓	✓	✓	✓					
CGRP^{CreERT2}	+Avil FloxtdTomatoStopDTA	✓		✓	✓	✓	✓	✓	✓	✓			✓		
Ntng1^{Cre}	cre alone	✓		✓	✓	✓	✓	✓	✓						
Ntng1^{Cre}	+Avil FloxtdTomatoStopDTA	✓		✓	✓	✓	✓	✓	✓				✓		
Na$_v$1.8^{Cre}	Published (xDTA)	✓		✓		✓	✓		✓			✓	✓	✓	✓
GalCre	cre alone											✓			

Table 16. Summary of behaviour tests performed for the characterisation of each Cre line

3.3   Results

3.3.1   RNAscope *in situ* hybridization analyses to confirm the expression pattern of Cre lines

Using four male adult mice per group, DRG tissue samples underwent multiplex RNAscope *in situ* hybridization to elucidate the expression pattern of each Cre line. By doing so, I checked if there was Cre expression in neuronal populations earlier in development, outside of the expected expression profile in adult mice. Along with Dr Okorocov, I used a probe specific to the endogenous mRNA which was detected with Alexa Fluor (AF) 488 (green) (ie for the *Tmem45b*[Cre] line I used a probe against *Tmem45b* mRNA). I then compared the mRNA expression for that endogenous gene with the Cre induced red fluorescence tomato protein. In general, I observed a large overlap between tdTomato expression and the target, indicating that Cre activity was consistent with the expression of the endogenous marker gene for all the mouse lines (Santana-Varela et al., 2021).

Secondly, I used in all strains a classic neurofilament marker *Nefh/Nfh* probe, detected with TS405 (blue). Its co-localization with tomato was observed to help us categorise the cellular population profile by a classic cell diameter distribution. This helped us to make a comparison with what has been predicted from single-cell RNAseq data (Usoskin et al., 2015b, Zeisel et al., 2018b).

3.3.1.1 TrkB-positive sensory neurons are confirmed in large NF200 positive neurons

I used *Ntrk2*[CreER] mice previously generated by the Ginty lab (Rutlin et al., 2014b) and crossed them with theRosa-CAG-flox-stop-tdTomato reporter following the strategy described above (see chapter 3.2.2). Following tamoxifen administration to activate the Cre in adult mice, I confirmed the presence of *Ntrk2* mRNA expressing neurons (in green) as well as the effectivity of the *Ntrk2* driven Cre (in red) (Figure 16) (Zeisel et al., 2018b).
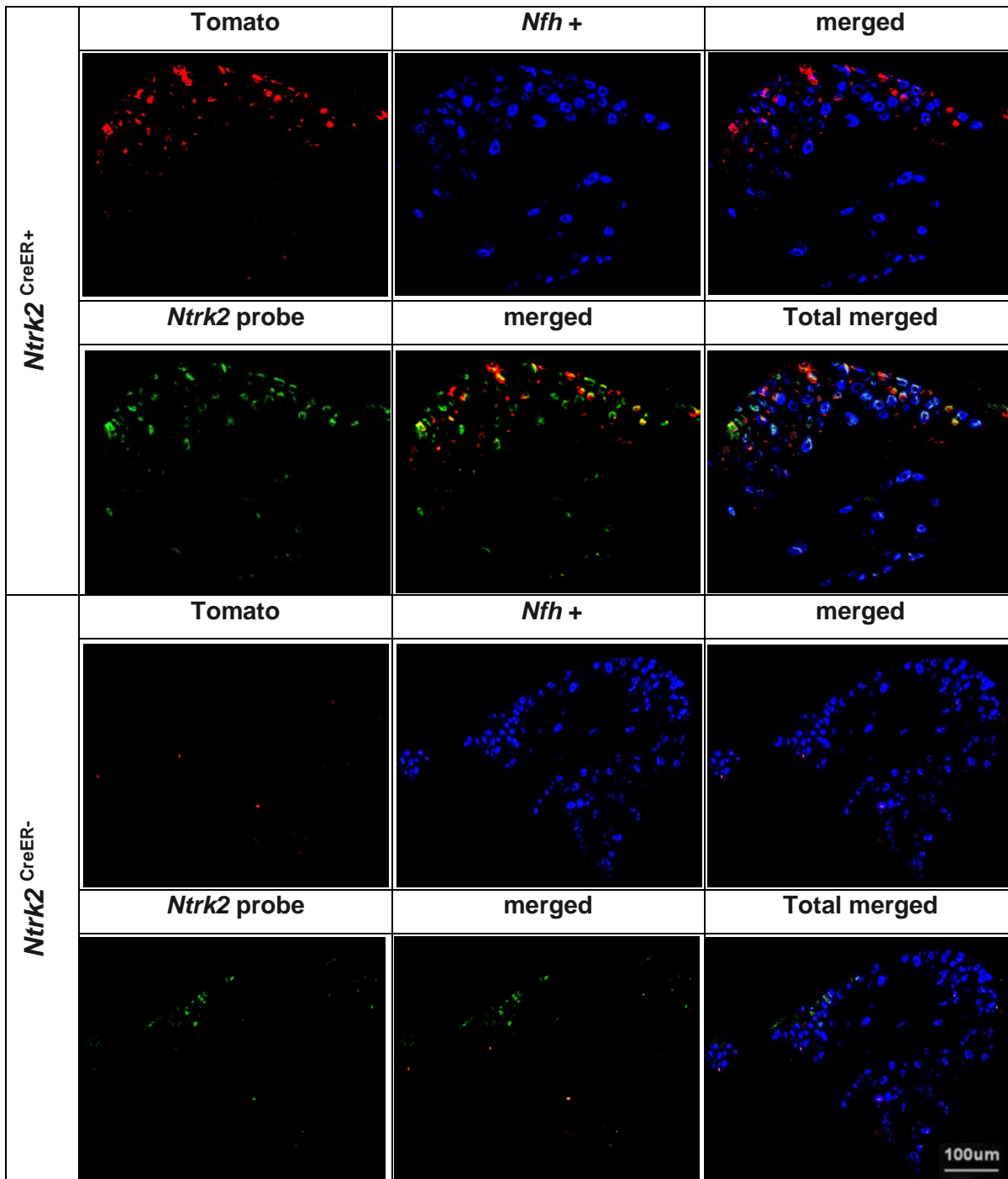
Figure 16. Representative images from *Ntrk2*^{CreER+} */Rosa-CAG-flox-stop-tdTomato* mice in lumbar DRGs.

RNAscope *in situ* hybridization: (1st row) large neurons *Nfh* positive (blue) in partial colocalization with TrkB positive (red). (2nd row) *Ntrk2* mRNA expressing cells (green) co-localise with Cre induced tomato red protein, confirming expected Cre activity. (3rd row). Cre negative reporter mice show no tomato red fluorescence protein expression.

3.3.1.2 Validation of a new Tmem45b^{Cre} line

The *Tmem45b*^{Cre} strain is a BAC transgenic designed in house and generated by Cyagen in a C57bl/6 background (Santana-Varela et al., 2021), from which three founders were initially generated (O, P and R). I designed two primers to confirm the presence of the specific Cre: A (Transgene PCR product size: 368 bp / FWD primer is before exon 2, REV primer is in Cre) and B (Transgene PCR product size: 574 bp / FWD primer is in Cre, REV primer in exon 2 after Cre insertion). Products from genotyping were Sanger sequenced to confirm the insertion (Figure 17).
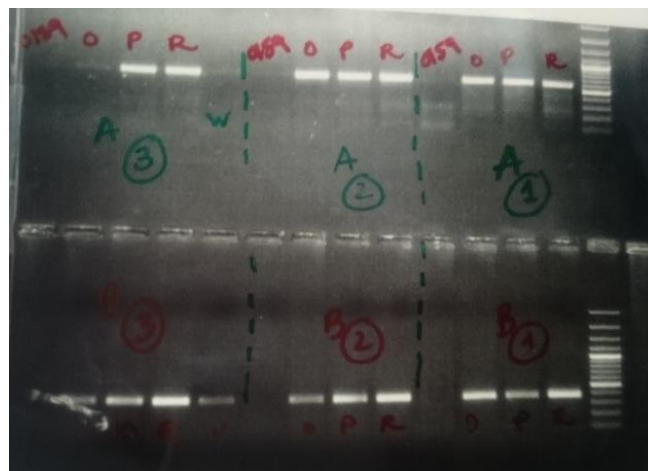
Figure 17. Genotyping gel from *Tmem45b*^{Cre+} for all founders with two primer sets. Number 1 represents an annealing temperature of 54.3 °C, 2 is 58.3 °C and 3 is 62 °C. All founders were positive for amplicons A and B.

Animals were initially crossed with the tomato reporter line following the strategy already explained (see 3.2.2), after which *in situ* hybridization images confirmed positive Cre activity, with a high level of co-localization with the endogenous *Tmem45b* mRNA (Figure 18.). With my findings, I report that *Tmem45b* is preferentially expressed in small-diameter unmyelinated sensory afferents, or *Nfh*-negative neurons. This pattern is similar to the voltage-gated sodium channel $Na_v1.8$ expression profile that has already been reported (Abrahamsen et al., 2008) (Tadashi et al., 2021) (Usoskin et al., 2015b, Zeisel et al., 2018b).

Figure 18. Representative images from the *Tmem45b*[Cre+] */Rosa-CAG-flox-stop-tdTomato* mice in lumbar DRGs.

RNAscope *in situ* hybridization. (1st row) *Tmem45*[Cre+] induced tomato fluorescence (red) does not colocalise with large *Nfh* positive neurons. (2nd row) *Tmem45b* mRNA expressing cells (green) colocalise with Cre induced tomato protein, confirming expected Cre activity. (3rd row) Cre negative reporter mice show no tomato red fluorescence protein expression.

3.3.1.3 Tmem45b Cre activity detected in some Th positive neurons

RNAscope data showed Tmem45b Cre activity in the majority of small diameter nociceptors. Recent data have located it in IB4-positive (non-peptidergic unmyelinated neurons), CGRP-positive (Peptidergic) and TRPV1-positive (heat and capsaicin sensitive) neurons (Tadashi et al., 2021). I observed, by performing further immunostaining, that *Tmem45b* Cre activity is also present in a subset of tyrosine hydroxylase (*TH*)-rich neurons (C-LTMRs) (Figure 19), which correlates with the data provided by single-cell RNA sequencing (Usoskin et al., 2015b, Zeisel et al., 2018b).
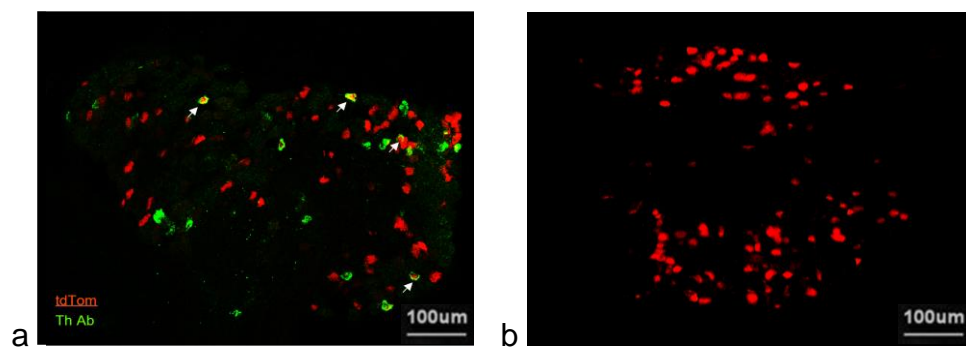
Figure 19. Representative immunofluorescence image of lumbar DRG sections of *Tmem45b*[cre+] */Rosa-CAG-flox-stop-tdTomato* with a *Th* antibody.
(a) Arrows indicate co-localization of *Tmem45b* Cre activity (red) and *Th* staining (green) (b) Negative control (no primary *Th* antibody)

3.3.1.4 Validation of new Tmem233[Cre] line

A Cre knockin was designed in the lab to be used as a Cre-driver strain (herein) as well as a *Tmem233* gene knockout when in the homozygous state (Santana-Varela et al., 2021) to interrogate this particular subpopulation of neurons. *Tmem233* Cre mice generated were crossed with the tomato reporter following the strategy explained at the beginning of this chapter.

In situ hybridization images confirmed positive Cre activity and a high level of colocalization with the *Tmem233* endogenous gene RNA (green) and tomato at protein level (red) (Figure 20). I found the *Tmem233* subpopulation to be preferentially small-diameter unmyelinated *Nfh*-negative sensory afferents, as predicted by published transcriptome data (Usoskin et al., 2015b, Zeisel et al., 2018b).
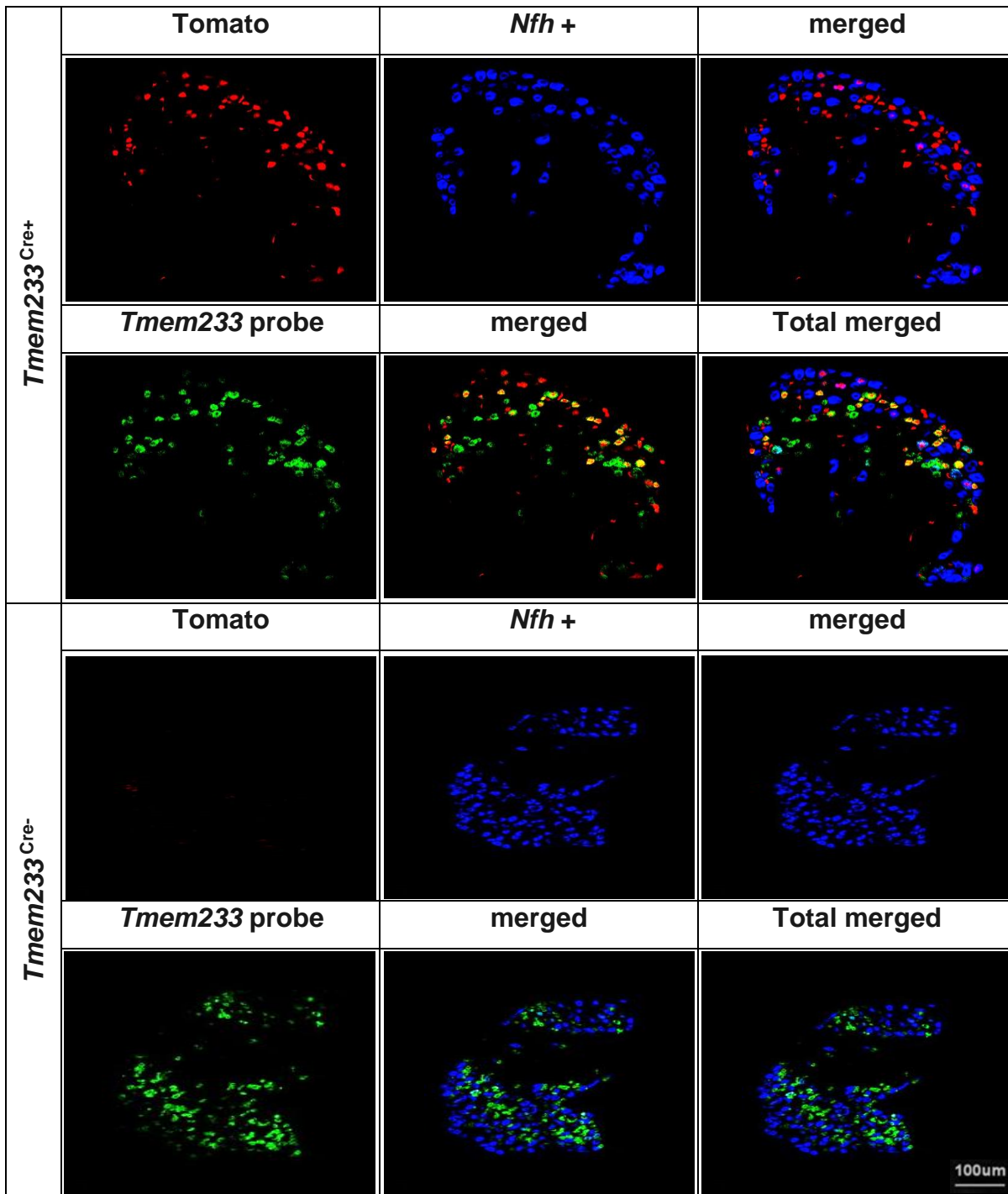
Figure 20. Representative images from the *Tmem233*^{Cre+} */Rosa-CAG-flox-stop-tdTomato* mice in lumbar DRGs.

(1st row) *Tmem233*^{Cre+} induced tomato fluorescence does not colocalise with large *Nfh* positive neurons. (2nd row) *Tmem233* mRNA expressing cells (green) and their colocalization with Cre induced tomato red protein, confirm expected Cre activity. (3rd row) Cre negative reporter mice show no tomato red fluorescence protein expression.

3.3.1.5 Cgrp CreER expression analysis in DRG

I used a CGRP[CreER] mouse line already reported (Song et al., 2012), and crossed it with the tomato reporter line following the strategy already described.
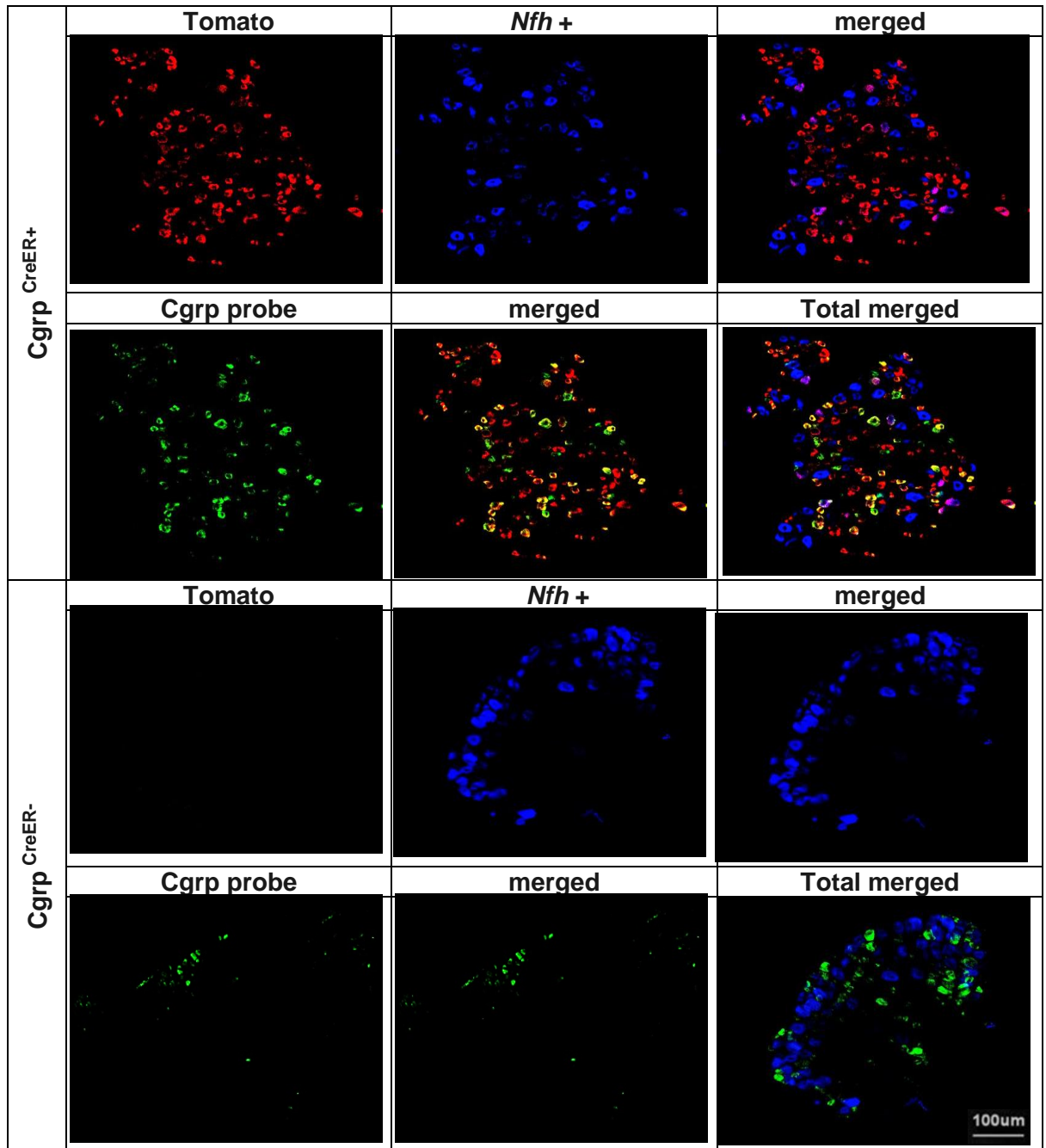
Figure 21. Representative images from the Cgrp[CreER+] */Rosa-CAG-flox-stop-tdTomato* (1st row) Large-diameter neurons *Nfh* positive in blue in partial colocalization with Cgrp positive neurons in red (merged). (2nd row) Cgrp mRNA expressing cells in green and their co-localization with Cre induced tomato red protein, confirming Cre activity. (3rd row) Cre negative reporter mice shows no tomato red fluorescence protein expression.

I confirmed the presence of *Calca* mRNA expressing neurons (in green) as well as the effectivity of the *Calca* driven Cre (in red) with good levels of co-expression (Figure 21). Neuronal distribution and co-localization with Nf200 positive neurons corroborate the pattern expected (Usoskin et al., 2015b, McCoy et al., 2012).

3.3.1.6 Ntng1 Cre expression analysis in DRG

The netrin G1-Cre knock-in mouse line (*Ntng1*^Cre) imported was initially generated using CRISPR technology with sequences encoding the Cre recombinase and a polyA inserted at the *Ntng1* start codon (Bolding et al., 2020). After crossing these mice with the tomato reporter, RNAscope studies confirmed that Cre activity was consistent with the expression of the endogenous marker gene, and as predicted from single-cell RNAseq data and when compared to Nefh (Figure 22. Representative images from the *Ntng1*^Cre+ /Rosa-CAG-flox-stop-tdTomato* mice in lumbar DRGs (Figure 22)
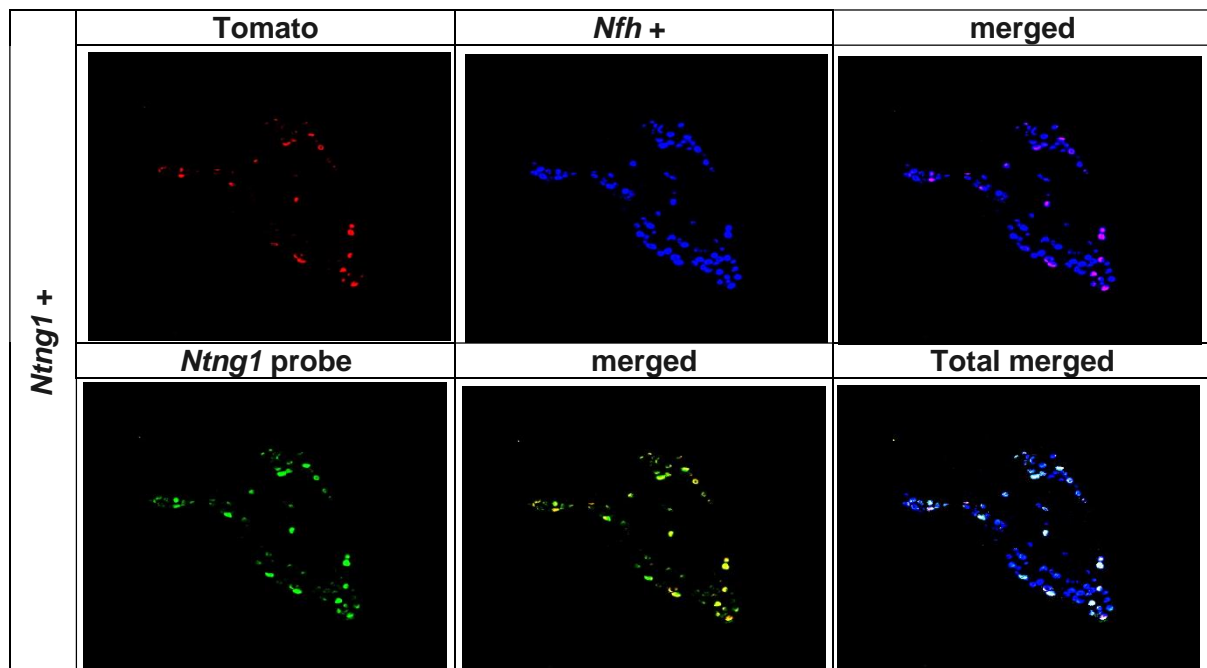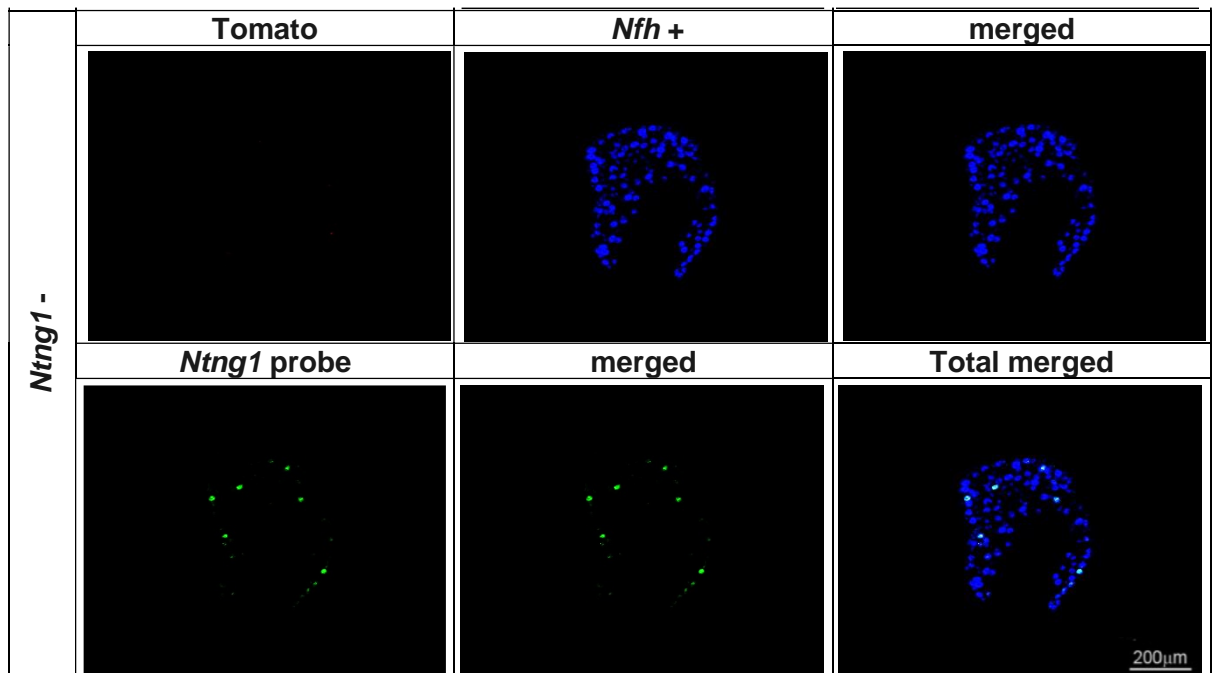
Figure 22. Representative images from the *Ntng1^Cre+* */Rosa-CAG-flox-stop-tdTomato* mice in lumbar DRGs

RNAscope *in situ* hybridization labelled *Ntng1* in green (2nd row) and *Nfh* in blue (1st row) confirming Cre activity. (3rd row) Cre negative reporter mice with no tomato protein expression.

3.3.1.7 Th CreERT2 expression analysis in DRG

I have used a *Th*^CreERT2 line previously generated by the Ginty lab (Abraira et al., 2017) which carries a tamoxifen inducible Cre-ERT2 sequence for temporal control of its activity. *In situ* hybridization images (Figure 23) confirm positive Cre activity of the strain (in red) with good, but not complete overlap with the *Th* endogenous RNA.
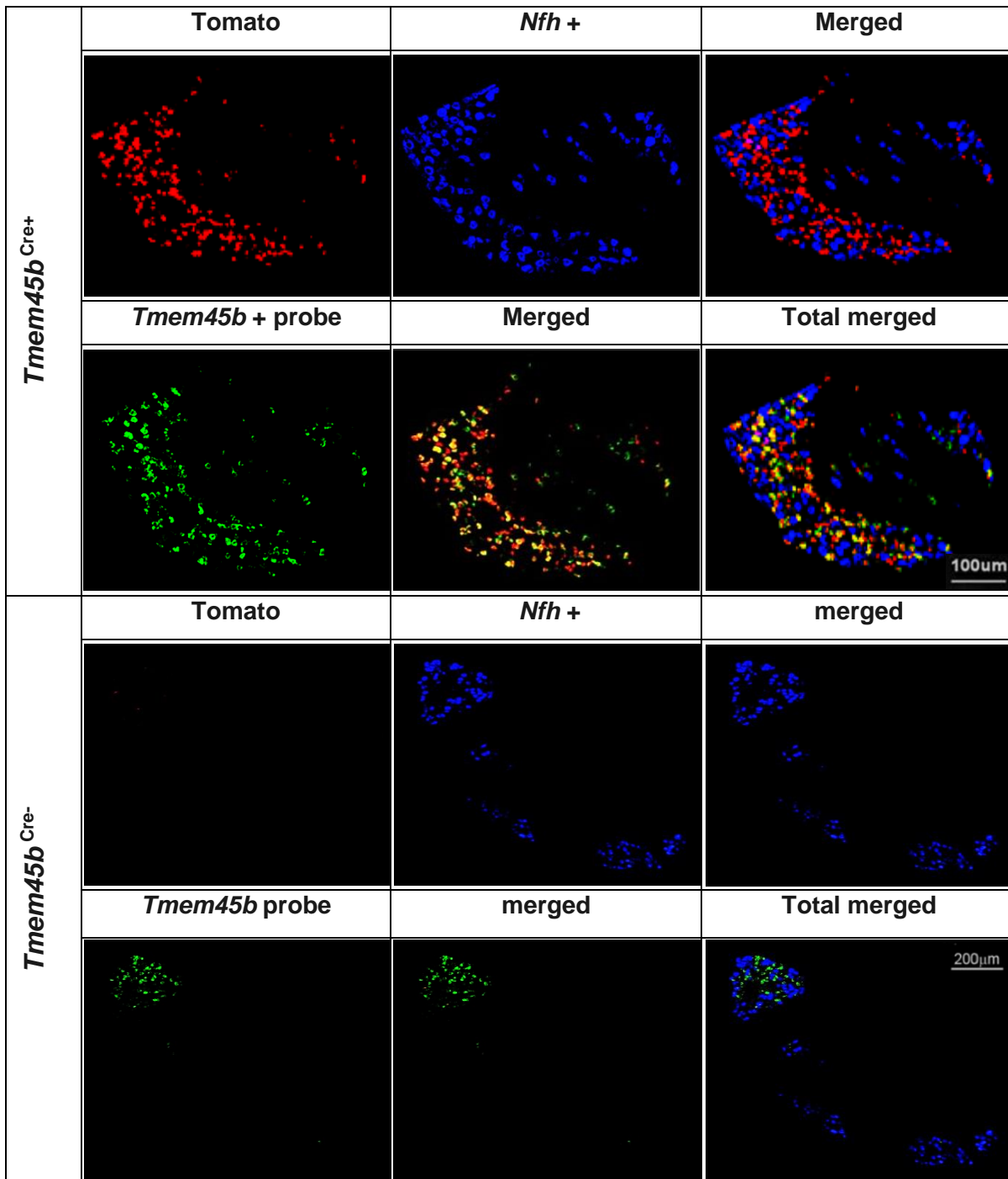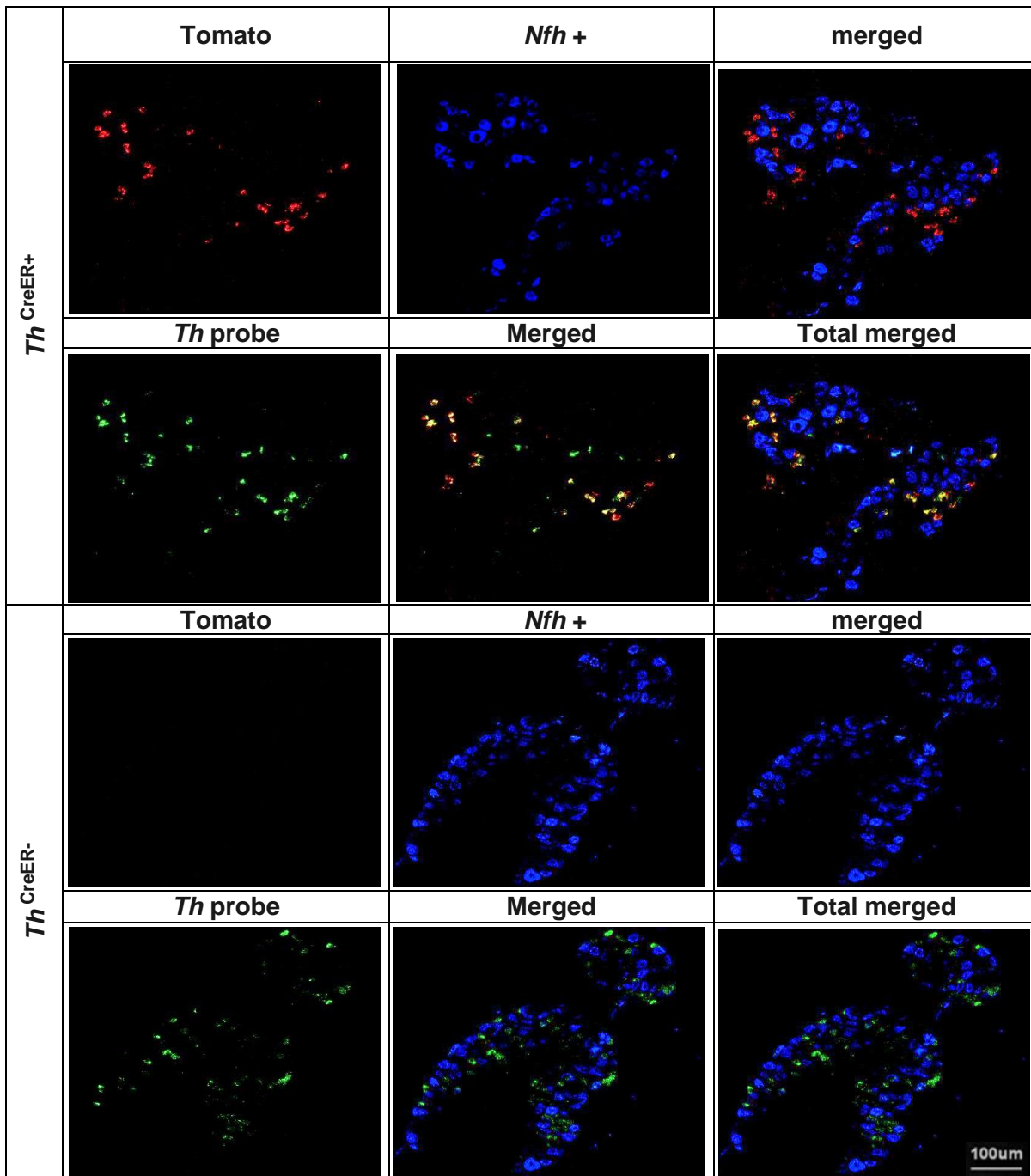
Figure 23. Representative images from the *Th* ^{CreERT2+} */Rosa-CAG-flox-stop-tdTomato* mice in lumbar DRGs.

(1st row) RNAscope *in situ* hybridization shows a discreet Cre activity (red) in small-medium diameter neurons which are *Nfh* (blue) negative, corroborating the pattern expected (Brumovsky et al., 2006, Usoskin et al., 2015b). (2nd row) *Th* mRNA expressing cells in green with some, but not complete, overlap with Cre induced tomato red protein. (3rd row) Cre negative reporter mice show no tomato red fluorescence protein expression.

Subsequently, I performed a series of DRG immunostaining experiments and observed clear co-localization between Cre-induced tomato expression (red) and *Th* endogenous protein (Figure 24) labelled in green with a specific Th antibody (Merck Millipore). With our results therefore, I confirm the Cre activity as specific.

	Tomato	*TH* Ab	Merged *Th*+tom
Th ^{CreER+}			
Th ^{CreER-}			100um
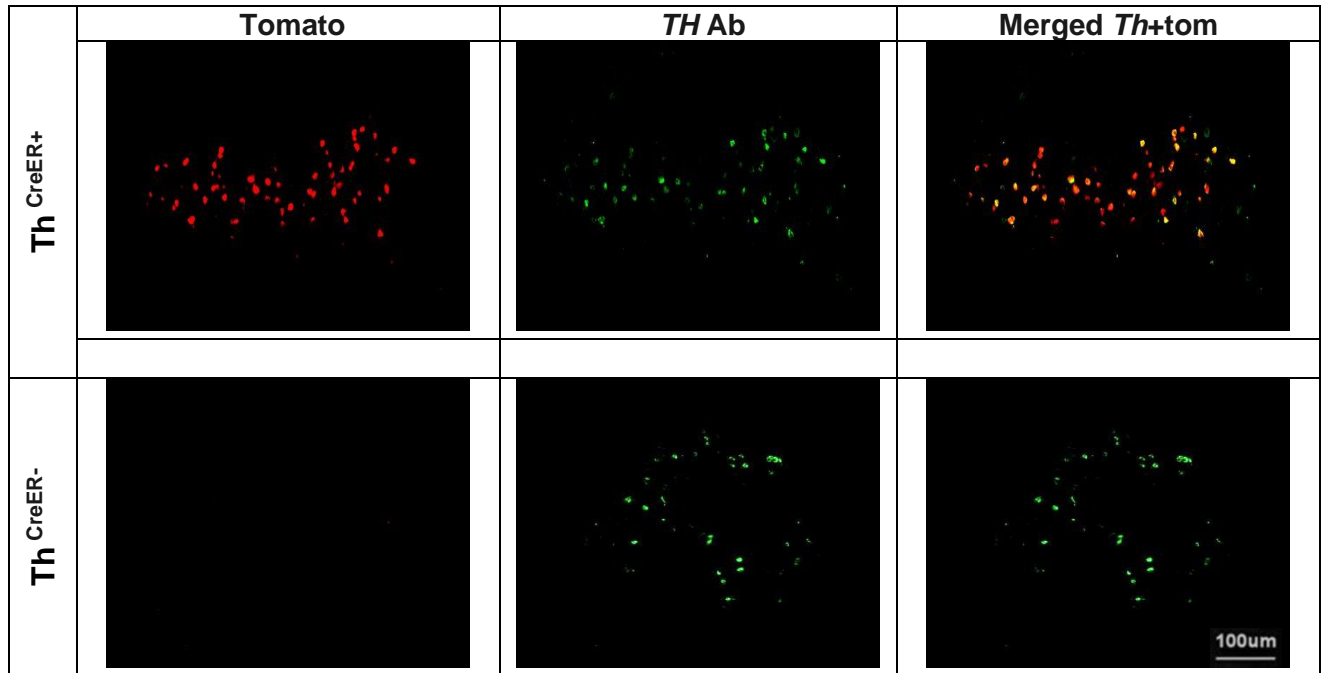
Figure 24. Representative images from the *Th* ^{CreERT2+} */Rosa-CAG-flox-stop-tdTomato* mice in lumbar DRGs after immuno labelling.

Th antibody (in green) shows good co-localization with tomato expression. The last row represents the Cre-negative sample control.

3.3.1.8 Th is partially co-expressed in parvalbumin positive DRG neurons

Following some unexpected phenotype in motor coordination behavioural tests when Th DRG subpopulation was ablated (revealed in chapter 3.3.2), I decided to interrogate the spatial colocalization of this subset of neurons with other probes. Along with Dr Okorocov, I performed further RNAscope experiments in the ThCreERT2+/ tomato line using first Carcinoembryonic antigen-related cell adhesion molecule 10 (Ceacam10) and Parvalbumin as probes (
Figure 25). As predicted from RNAseq data (Zeisel et al., 2018a, Usoskin et al., 2015a), there was strong overlap between Cre activity (in red) and Ceacam10 expression (which is present within the Th positive neuronal population). And,

interestingly, I also observed some Cre activity in some parvalbumin positive neurons, a classic proprioceptor marker (Ernfors et al., 1994).
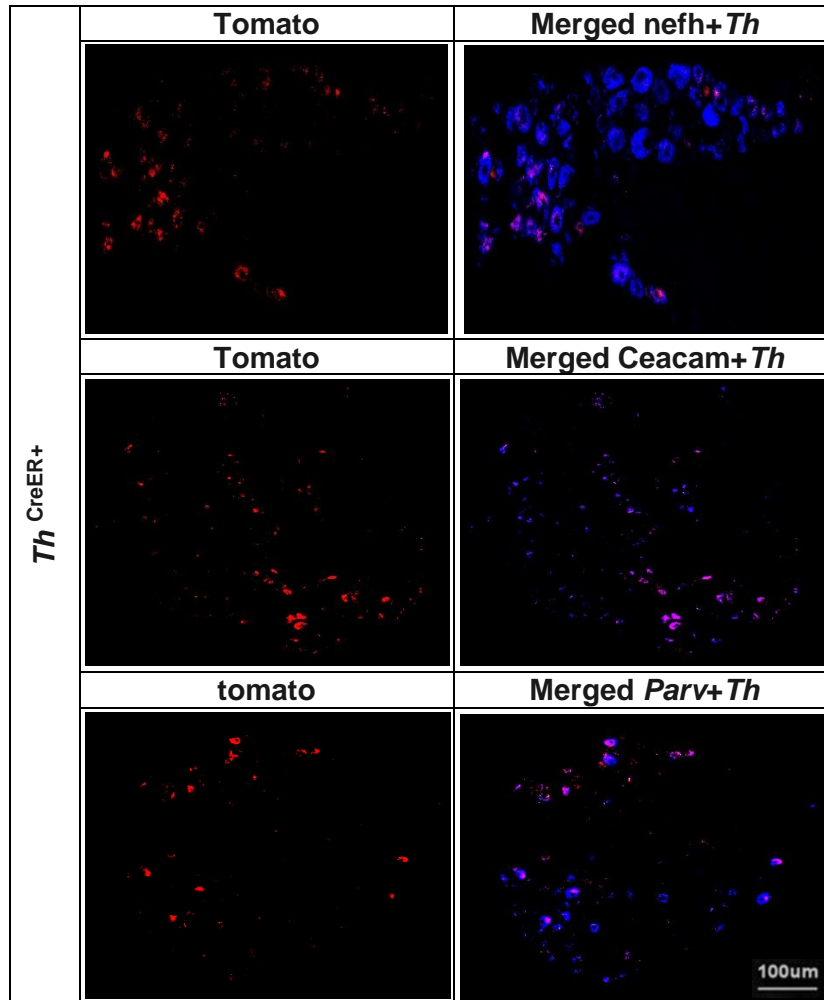
Figure 25. Representative images from the *Th* ^{CreERT2} */Rosa-CAG-flox-stop-tdTomato* mice in lumbar DRGs after Ceacam and Parv antibody labelling.
DRG neurons with tomato positive *Th* Cre activity (red) labelled with RNAscope *in situ* hybridization for (1st row) *Nfh* probe in blue. (2nd row) Ceacam10 probe (in blue). (3rd row) Parvalbumin probe. All of them are partially colocalising.

3.3.1.9 Summary
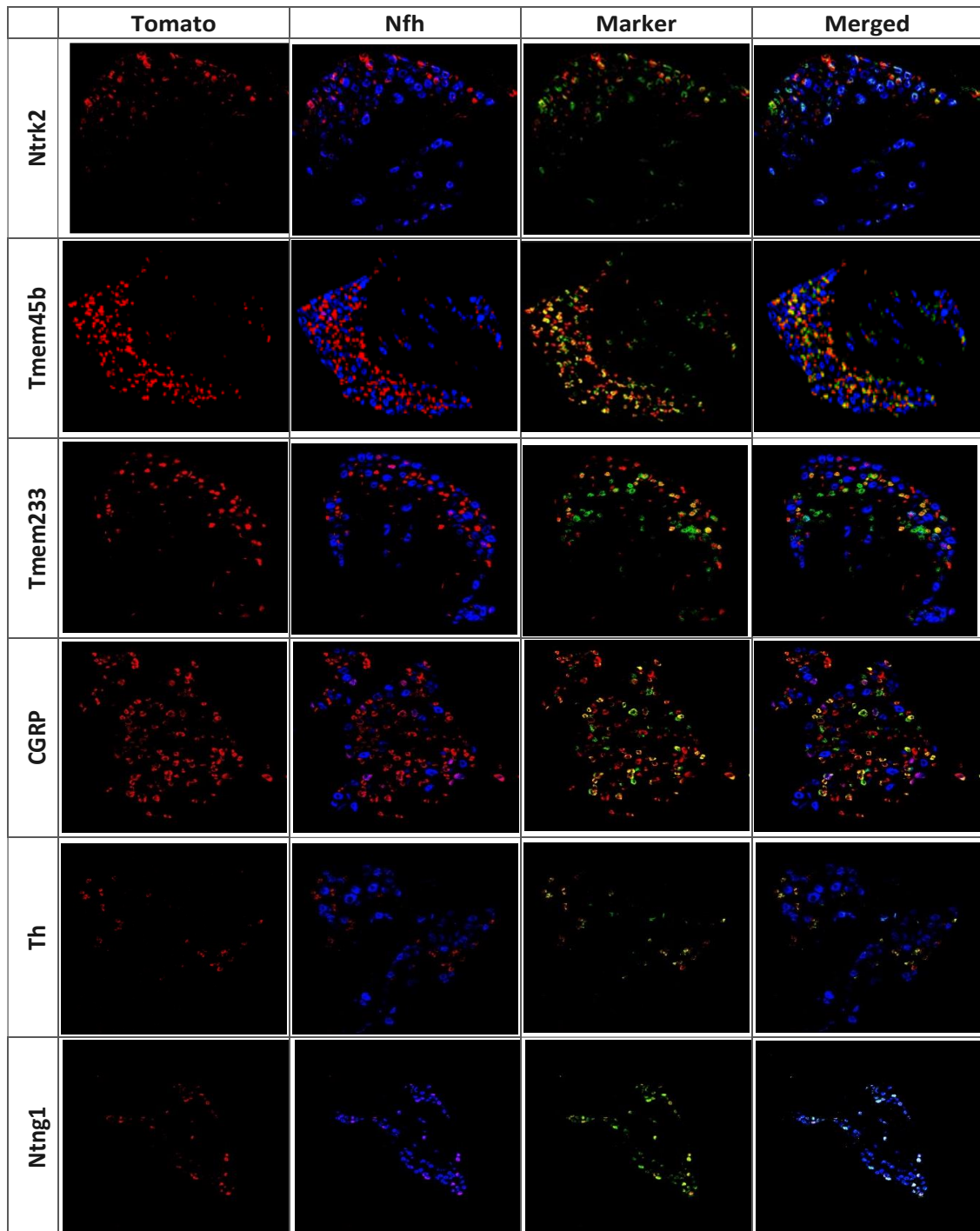
Figure 26. RNAscope analysis of Cre activity in dorsal root ganglia (DRG) neurons. Expression of tdTomato (red), Nefh RNA (blue) and target marker gene RNA (green). Cre lines: TrkB[CreER+] (*Ntrk2*), Tmem45b[Cre+], Th[CreERT2+], Tmem233[Cre+], Ntng1[Cre+], CGRP[CreER+] (*Calca*) (Santana-Varela et al., 2021).

Based on the above Figure, and in combination with Table 2 in regards to the transcriptome data analysis, I recapitulate my predicted and novel findings in order to appreciate subsequent ablation studies revealed in next chapter as follows:

- I confirm *Ntrk2* expression levels within the NF200 subpopulation of neurons as predicted.

- I found the *Tmem233* and *Tmem*45b neuronal subpopulation to be preferentially small-diameter unmyelinated *Nfh*-negative sensory afferents, with the latter also present in Th positive neurons, as predicted by published transcriptome data.

- As previously reported, I show *Calca* mRNA expressing neurons in around 18% of Nf200 positive neurons (see table 5).

- Ntng1 also follow predicted patterns of distribution and colocalization .

- Lastly, I report a discreet Th expression in small-medium diameter neurons which are Nfh (blue) negative, corroborating the pattern expected. However, Th mRNA expressing cells in green with some, but not complete, overlap with Cre induced tomato red protein. After further studies, we unexpectedly find Th expression within the Parvalbumin expressing DRG neurons.

3.3.2 Acute characterisation of different subsets of sensory neurons after conditional ablation

Having established the activity and specificity of each Cre recombinase line, I carried out a preliminary study of acute pain behaviour following ablation of subsets of sensory neurons after crossing to the *Advillin* Flox-tdTomato-Stop-DTA BAC line (Table 17).

STRAIN		VonFrey	Cotton Swab	Hargreaves	Dry ice	hot plate	Randall Selitto tail	Rotorod	Randall Selitto Paw	open field	Balance beam/Pole
Tmem233^{Cre}	cre alone										
Tmem233^{Cre}	+Avil FloxtdTomatoStopDT.	Paused, not breeding. Global KO generated but no phenotype.Only enough for formalin Subpopulation covered by tmem45b - Thcre									
Ntrk2-^{CreRT2}	cre alone	✓	✓	✓	✓	✓	✓	✓	✓		
Ntrk2-^{CreRT2}	+Avil FloxtdTomatoStopDT.	✓	✓	✓	✓	✓	✓	✓	✓		
Tmem45b^{Cre}	cre alone	✓	✓	✓	✓	✓	✓	✓	✓	✓	
Tmem45b^{Cre}	+Avil FloxtdTomatoStopDT.	✓	✓	✓	✓	✓	✓	✓	✓	✓	
Th^{CreERT2}	cre alone	✓	✓	✓	✓	✓	✓	✓	✓	✓	✓
Th^{CreERT2}	+Avil FloxtdTomatoStopDT.	✓	✓	✓	✓	✓	✓	✓	✓	✓	✓
CGRP^{CreERT2}	cre alone	✓		✓	✓	✓	✓	✓	✓	✓	
CGRP^{CreERT2}	+Avil FloxtdTomatoStopDT.	✓		✓	✓	✓	✓	✓	✓	✓	
Ntng1^{Cre}	cre alone	✓		✓	✓	✓	✓	✓	✓		
Ntng1^{Cre}	+Avil FloxtdTomatoStopDT.	✓		✓	✓	✓	✓	✓	✓		
Na$_v$1.8^{Cre}	Published (xDTA)	✓		✓		✓	✓	✓	✓		

Table 17. Summary of behaviour tests performed for the characterisation of each Cre line.

3.3.2.1 Na$_v$1.8^{Cre+}/ *Advillin* Flox-tdTomato-Stop-DTA immunostaining and behaviour tests report comparative results to the previously characterized Na$_v$1.8^{Cr+e}/ DTA

As a proof of concept, I crossed the *Advillin* Flox-tdTomato-Stop-DTA with the phenotypically well-established Na$_v$1.8^{Cre} line (Abrahamsen et al., 2008) in order to compare results. The construct of the novel tool mouse (see chapter 3.2.2) contains the required information to express red fluorescent protein in DRG neurons under the *Advillin* promoter (Figure 27).
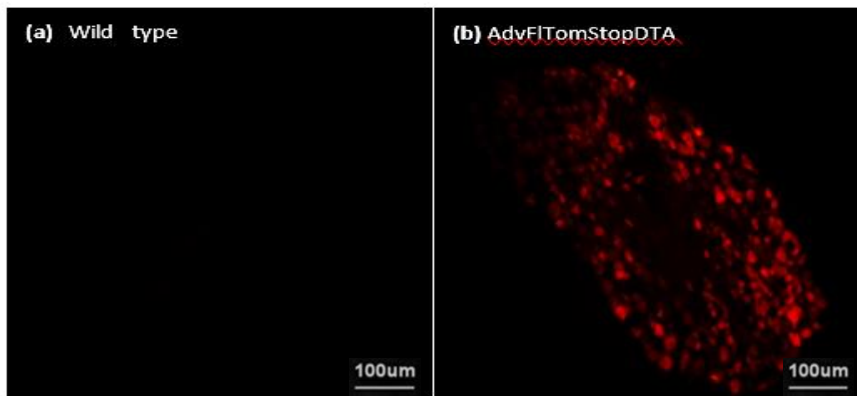
Figure 27. tdTomato expression is seen in sensory neurons of the DRG (L4) in mice expressing *Advillin* Flox-tdTomato-Stop-DTA transgene; (a) Wild type DRG; (b) *Advillin* Flox-tdTomato-Stop-DTA DRG

I performed immunostaining on DRG isolated from the newly generated transgenic strain ($Na_v1.8^{Cre+}$/*Advillin* Flox-tdTomato-Stop-DTA). As expected, tdTomato (red), whilst weak, was present in all sensory neurons except the $Na_v1.8$-positive ones which were ablated. Next, I used an anti-peripherin antibody (green) as a classic marker for small nociceptors, and report a significant reduction in the proportion of peripherin positive cells in Cre+/ *Advillin* Flox-tdTomato-Stop-DTA mice compared to their Cre negative littermates (

Figure 28).
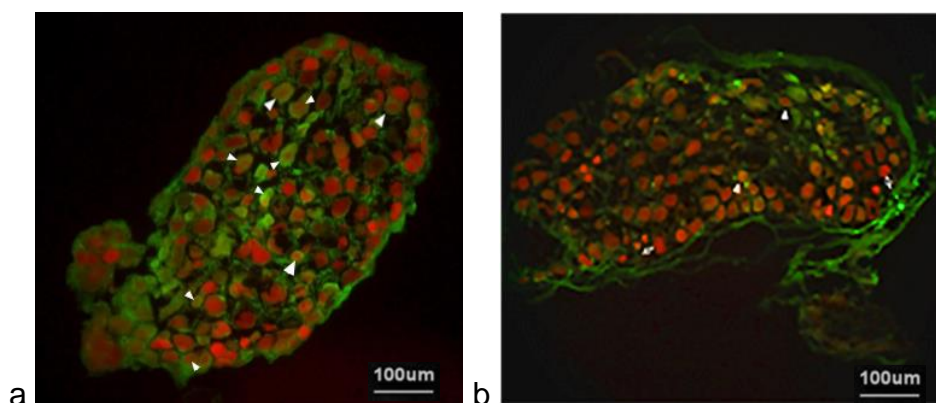
Figure 28. tdTomato (red) expression in lumbar DRG sensory neurons expressing *Advillin* Flox-tdTomato-Stop-DTA transgene.

Anti-peripherin (green) labels small diameter fibres where arrowheads show colabelled neurons. (a) $Na_v1.8^{Cre-}$x *Advillin* Flox-tdTomato-Stop-DTA (b) $Na_v1.8^{Cre+}$/ *Advillin* Flox-tdTomato-Stop-DTA.
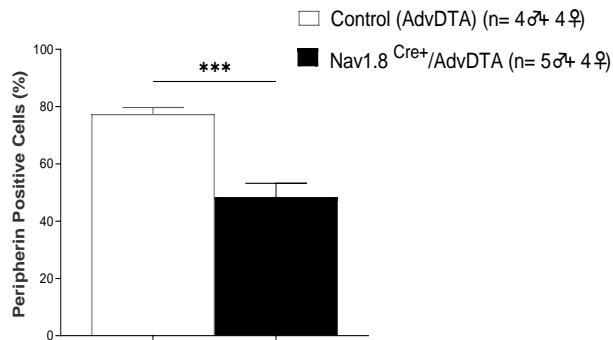
(c) Fewer co-labelled neurons are present in mice expressing $Na_v1.8^{Cre}$ at the L4 and L5 level P ≤ 0.001) than in control animals ($Na_v1.8^{Cre}$ negative). Mixed gender results are presented as mean ± S.E.M. and analysed by t-test

Phenotypically, $Na_v1.8^{Cre+}$/ *Advillin* Flox-tdTomato-Stop-DTA mice showed normal responses to noxious thermal stimuli in the Hargreaves' test (Figure 29) whilst presenting significantly impaired noxious mechanosensation in the Randall-Selitto (performed by Dr Sexton). To summarise, significant noxious mechanosensation deficits are observed in these $Na_v1.8^{Cre+}$/ *Advillin* Flox-tdTomato-Stop-DTA mice, which corroborates previous data by using a different DTA knockin line (Abrahamsen et al., 2008).
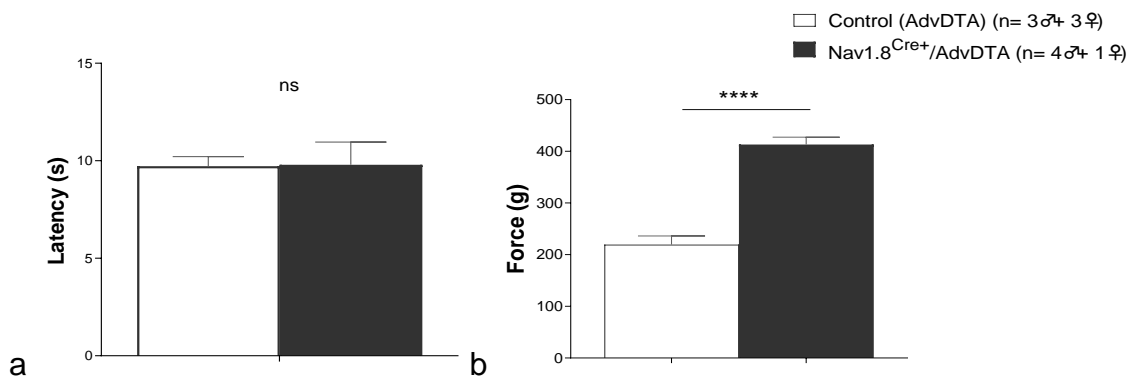
Figure 29. Characterisation of Na$_v$1.8 [Cre+]/ *Advillin* Flox-tdTomato-Stop-DTA mice.
Na$_v$1.8 [Cre+]/ AdvDTA mice develop a normal response to thermal stimuli by the
Hargreaves' test. (b) Randall Selitto test evidencing hypoalgesia to noxious mechanical
stimuli in AdvDTA+/Cre+ mice (P ≤ 0.0001). Mixed gender results are presented as
mean ± S.E.M. and analysed by t-test.

Furthermore, I performed quantitative RT-PCR analysis on adult DRG samples
and confirmed negligible levels of mRNA Na$_v$1.8 expression in Na$_v$1.8[Cre+] */Advillin*
Flox-tdTomato-Stop-DTA mice when compared to their littermate controls. This
corresponds again, to what has been reported by other DTA ablating tool models
(Abrahamsen et al., 2008) (Figure 30).
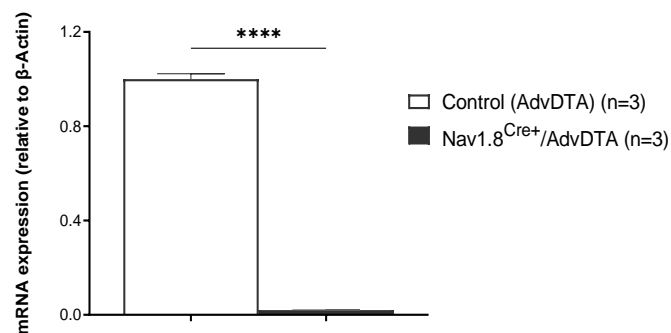
Figure 30. Real-time qRT-PCR analysis of Na$_v$1.8 mRNA expression in DRG
Na$_v$1.8[Cre+]/ *Advillin* Flox-tdTomato-Stop-DTA against their Cre negative controls shows
Na$_v$1.8 to be markedly down-regulated (P ≤ 0.0001). The mRNA level relative to β-Actin
was calculated using the comparative ΔΔCt (Ct) and shown as mean ± SEM mixed
gender and t-test analysis.

I used RT-PCR analysis to also validate the newly generated *Tmem45b*[Cre+]/ *Advillin* Flox-tdTomato-Stop-DTA mice. When doing so, the levels of *Tmem45b* mRNA were significantly down-regulated in comparison with the controls (Figure 31). This confirms the positive Cre activity in this novel line, which was already observed by qualitative RNA *in situ* hybridization studies. After this two last results, I considered *Advillin* Flox-tdTomato-Stop-DTA mice ablative activity sufficient and mRNA levels of rest of the lines crossings were assumed negligent, since we could compare our results with previous reports on the already described Cre lines.

Surprisingly, when looking deeper into the data, individual mRNA values within the control group appeared to be quite segregated. This variability should not be ignored and will be taken into consideration during the discussion (see chapter 3.4).
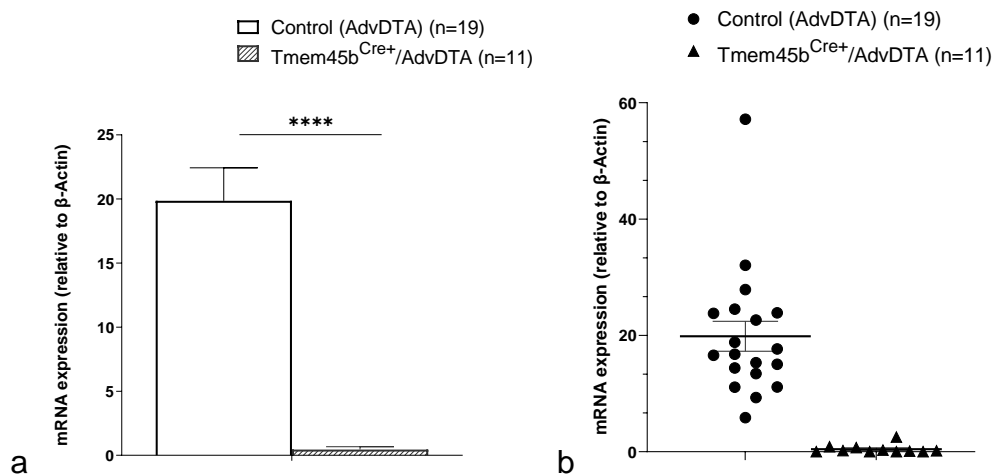
Figure 31. Real-time qRT-PCR analysis of mRNA expression in DRG of *Tmem45b*[Cre+]/ *Advillin* Flox-tdTomato-Stop-DTA against their DTA controls.
(a)The mRNA level relative to β-Actin was calculated using the comparative ΔΔCt (Ct) and shown as mean ± SEM mixed gender analysed by t-test. (b) Individual values plotted.

In summary, although the tomato expression in *Advillin* Flox-tdTomato-Stop-DTA was not strong enough to be used as a marker for post mortem immuno-studies, its ablation mechanism seemed to be effective. We continued therefore with the strategy initially designed, generating conditional transgenic Cre-DTA lines by

crossing male or female promoter-driven Cre mice with *Advillin* Flox-tdTomato-Stop-DTA mice. The offspring obtained were;

1- Advillin Flox-tdTomato-Stop-DTA +/ Promoter-cre +

2- Control *Advillin* Flox-tdTomato-Stop-DTA -/ Promoter-cre –

3- Control *Advillin* Flox-tdTomato-Stop-DTA -/ Promoter-cre +

4- Control *Advillin* Flox-tdTomato-Stop-DTA +/ Promoter-cre –

In order to study the phenotype after the promoter driven ablation, we had to assess also the potential effect of each Cre or DTA insertion site into the genome, to discard any potential repercussion when compared to their WT littermates.

I therefore included all genotype combinations in every experiment set, using mixed gender animals at a similar adult age. Since equipment capacity only allowed a maximum of 24 animals per set, two or three individual experiments sets were required to reach statistically enough n number per group.

Each comparative experiment was analysed individually per set, in order to discard noise difference per experimental day. After, data were plotted together against a common control: *Advillin* Flox-tdTomato-Stop-DTA for easier understanding. Data will be shown as mixed gender and ANOVA statistical analysis. Additional male and female graphs were added, but due to the low n number of males in some of the groups, statistical analysis was not possible. Trends on both sex groups were therefore considered, but no sex difference conclusions were drawn.

3.3.2.2 Weight analysis of Cre+ / Advillin Flox-tdTomato-Stop-DTA mice

Each group of transgenic mice, whether with gene insertions or deletions, were born in average litter sizes and exhibited largely normal health to adulthood. The only exception was the $Tmem233^{Cre+}$/ *Advillin* Flox-tdTomato-Stop-DTA mouse line where breeding was problematic and we were unable to obtain enough

individuals for acute behavioural experiments (formalin experiments on this line will be mentioned in chapter 4).

When reaching adulthood (circa eight weeks old), there was no significant difference in the mass of the animals (Figure 32) in comparison with their WT littermates, both in males and in females.
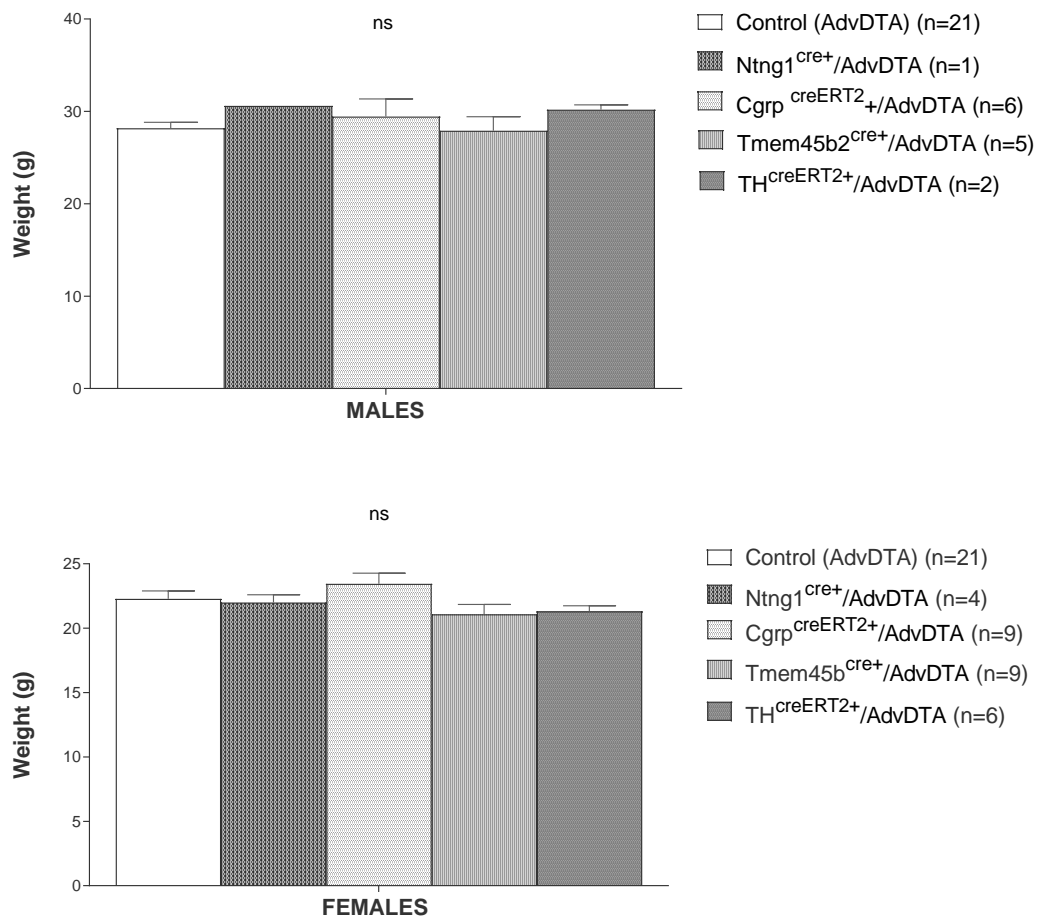
Figure 32. Weight of animals at 8 weeks old was not significantly different between groups. Data are shown as Mean±SEM with one-way ANOVA.

3.3.2.3 Exploratory behaviour, as assessed by the open field test, does not show any impairment in the Cre lines tested.

The open field activity monitoring system is a useful tool used in animal models of neuromuscular disease, and for screening of the efficacy of therapeutic drugs that may improve locomotion and/or muscle function. In addition, it can also

provide information about changes in individual exploratory behaviour and anxiety which will be evaluated herein.

By counting the number of total, corner and centre crossings in the maze (Figure 33), I found normal ambulatory activity and movement in all animals tested in comparison with their littermate controls.
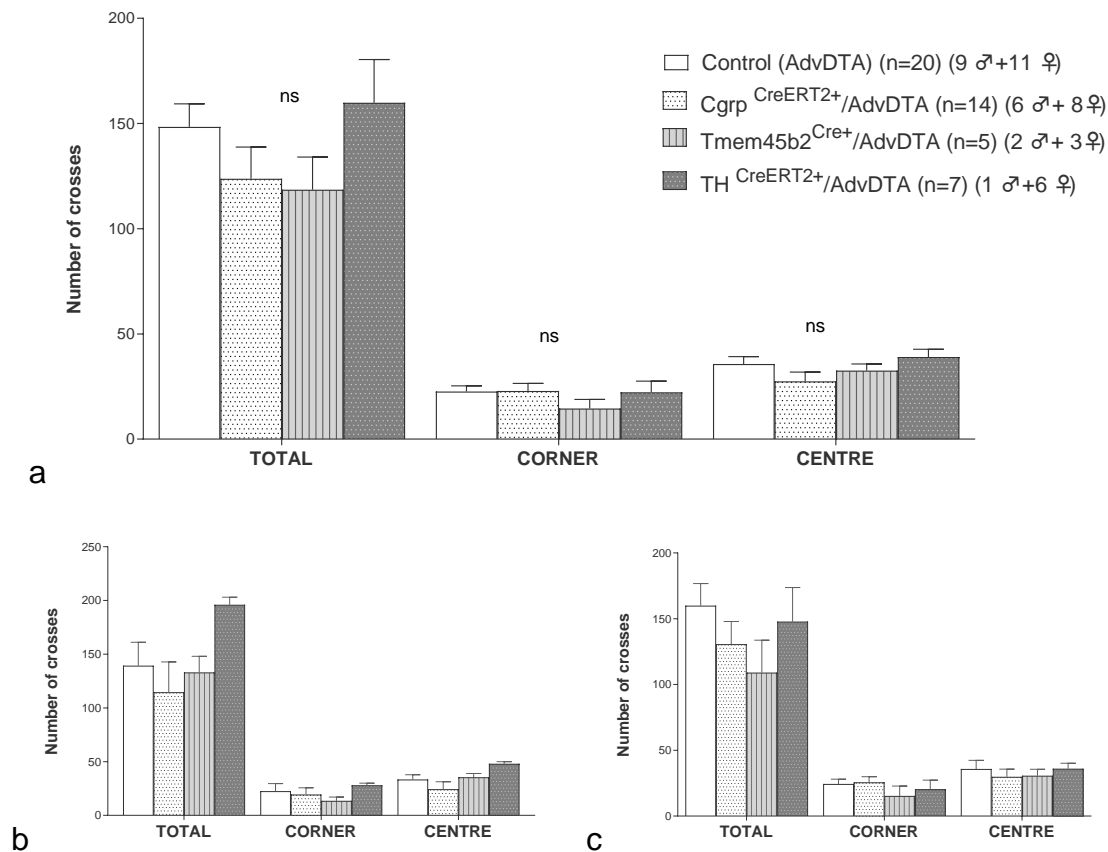
Figure 33. Total crosses travelled in the maze by age and gender matched groups shows no significant difference when compared against the control littermates. The same applied when analysing corner and centre areas crossings. (a) Mixed gender (b) Males (c) Females. Data are shown as Mean±SEM with one-way ANOVA for (a) and (c) graphs.

3.3.2.4 Motor coordination abilities, as assessed by the Rotarod, are normal for all Cre lines tested

Motor function was assessed using the Rotarod test at increasing speed. The time spent on the rotating rod was found not significantly different in any of the groups when compared to their littermate controls (Figure 34).
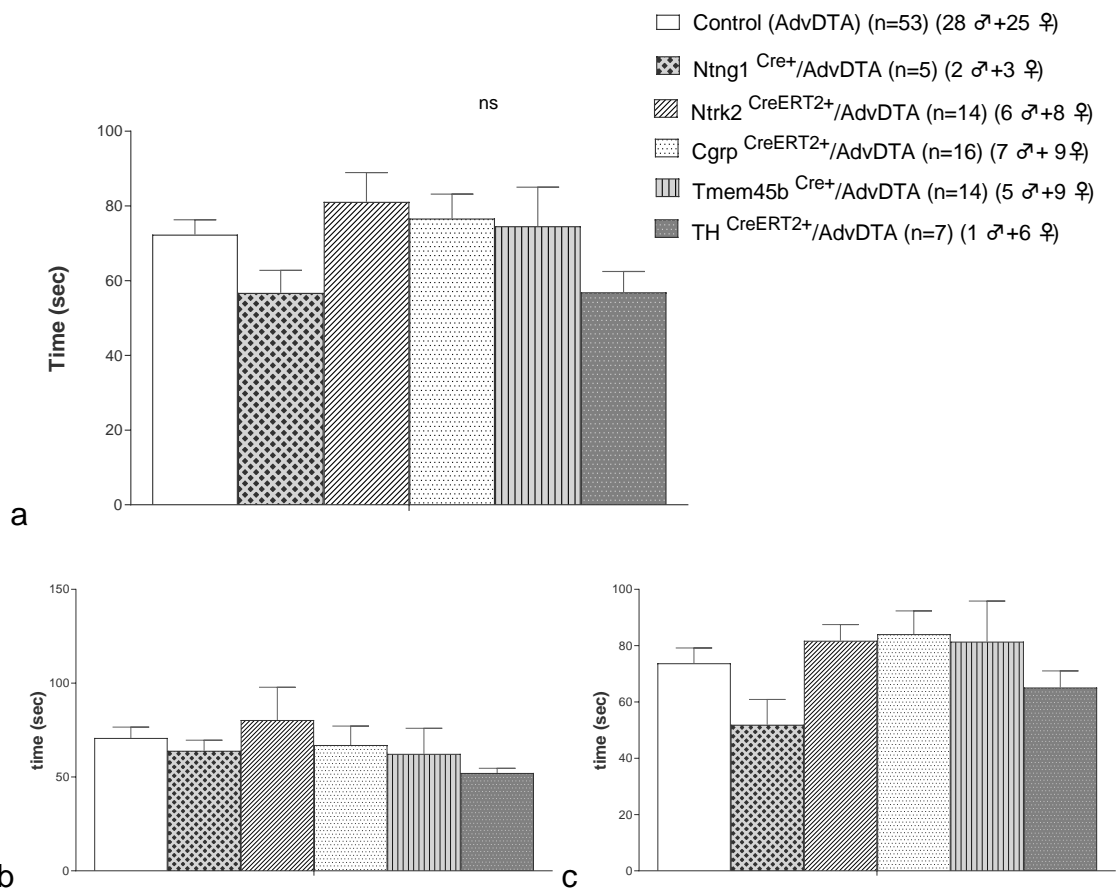
Figure 34. The duration mice were able to remain on the accelerating rotarod was not significantly different for the different Cre lines despite the gender

when compared with their littermate controls. (a) Mixed gender (b) Males (c) Females. Data are shown as Mean±SEM with one-way ANOVA for (a) and (c) graphs.

Interestingly, even though Th$^{CreERT2+}$ / *Advillin* Flox-tdTomato-Stop-DTA animals showed normal motor ability on the Rotarod test, I observed some coordination difficulties which we decided to investigate further. First, I tested the animals on a beam balance test, during which I observed significant motor coordination issues while walking on the suspended beam/platform when compared to their WT littermates control (Figure 35). Whilst the time spent to complete the course was not different (nor in the rotarod when compared to their controls), the way to perform the task was clearly abnormal and the number of hind paw slips observed was significantly higher. This effect was even more evident on a narrower platform.

Similarly, when the balance was assessed on a vertical surface instead of horizontal, Th$^{CreERT2+}$/AdvDTA individuals showed a significantly longer time and more difficulties when walking and turning on the pole (Figure 35).

a

b
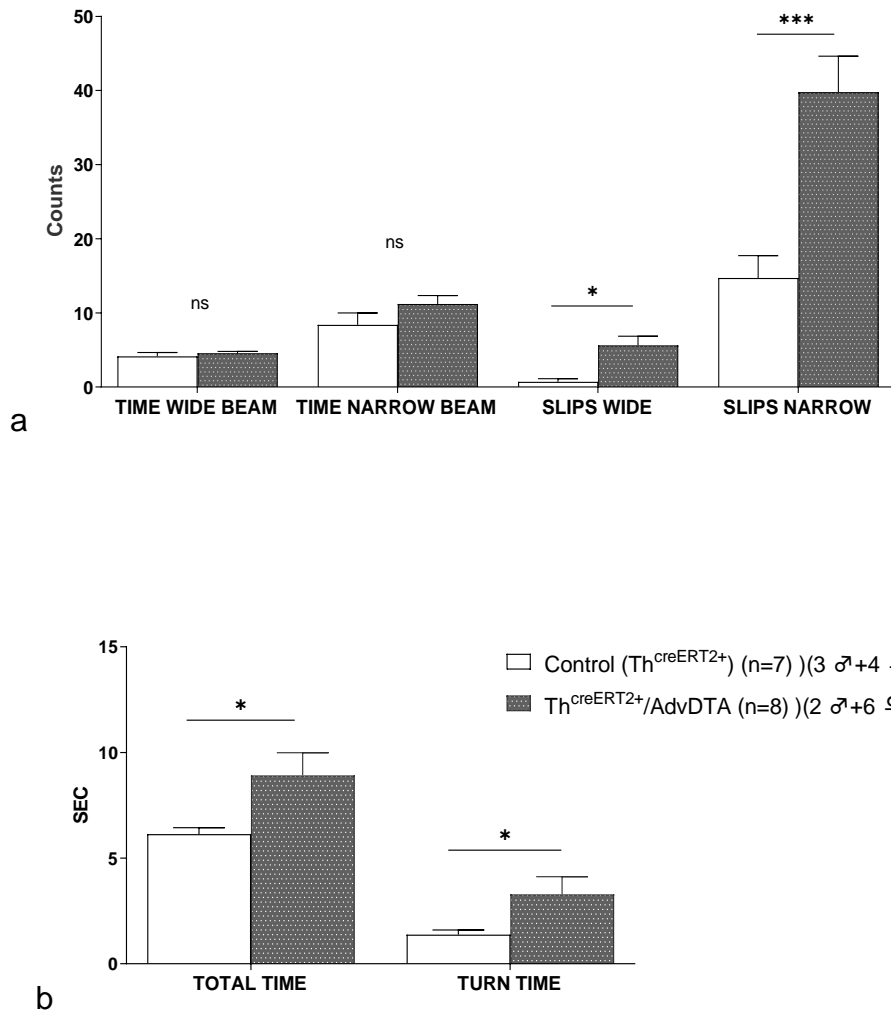
Figure 35. Th$^{CreERT2+}$/*Advillin* Flox-tdTomato-Stop-DTA motor coordination assessment. Whilst animals spend the same time to complete the course on a suspended platform, (a) individuals lacking *Th* neurons show a significantly higher number of hind paw slips along the way (P ≤ 0.05 and P ≤ 0.001). Similarly, they find more difficulties in walking and turning on a vertical pole (b) and need longer to complete the task (P ≤ 0.05). Data are shown as mixed gender Mean±SEM with one-way ANOVA.

3.3.2.5 Mice with conditional deletion of CGRP-positive DRG neurons have impaired mechanical sensitivity in the von Frey test

Most of the transgenic lines with ablated neuronal subpopulations showed normal reactivity to Von Frey mechanical stimuli tested using different weighted filaments in the glabrous skin of the paw (Figure 36). However surprisingly, I found paw withdrawal threshold (PWT) significantly lower in animals lacking the CGRP neuronal subpopulation when compared to their littermate DTA controls. When splitting the group by sex, I observed that the unexpected effect was following the same trend in male mice but not females. In addition, I found a significant difference in female $Ntrk2^{CreER+}$/ $Advillin$ Flox-tdTomato-Stop-DTA, but not male mice, which requires further investigation and an increase in n number.
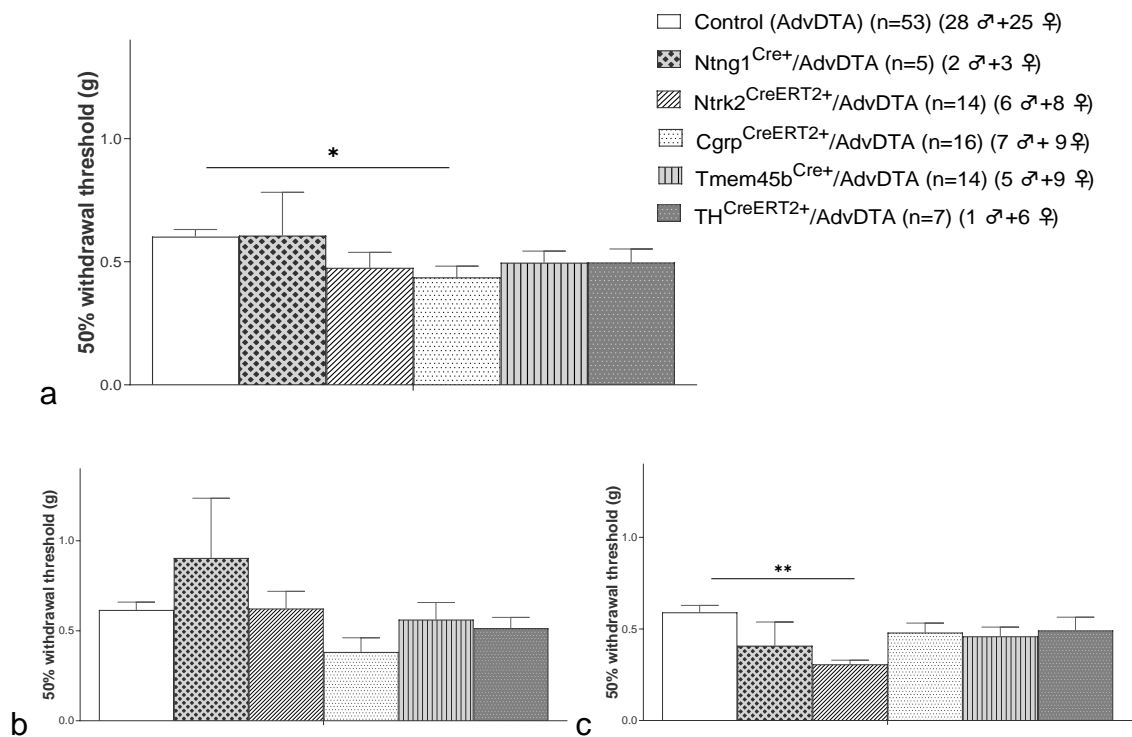
Figure 36. Innocuous mechanical sensitivity is impaired in mice with CGRP ablated DRG neurons

(a), demonstrated by a significant decrease in PWT on the glabrous skin of the paw. ($P \leq 0.05$) There is a trend for this impairment in males (b) but not in females (c). I found a significant decrease in von Frey mechanical sensitivity in females (without $Ntrk2$ DRG neurons ($P \leq 0.01$). Data are shown as Mean±SEM with one-way ANOVA for (a) and (c) graph.

3.3.2.6 Tmem45b^{Cre+}/ AdvDTA mice show reduced responses to noxious mechanical stimuli

Deleting Na$_v$1.8 from all DRG neurons using the *Advillin*-driven DTA tool mice (Na$_v$1.8^{Cre+}/*Adv*DTA) has previously been shown to specifically abolish responses to noxious mechanical stimuli, whilst leaving thermal responses unaffected (see Chapter 3.3.2.1). Figure 37 shows that deleting the *Tmem45b* subpopulation of neurons in mouse DRG recapitulates this pain phenotype, as expected from their similar neuronal distribution (Usoskin et al., 2015b). On the contrary, the other tested transgenic lines showed normal noxious Randall-Selitto nociceptive thresholds.
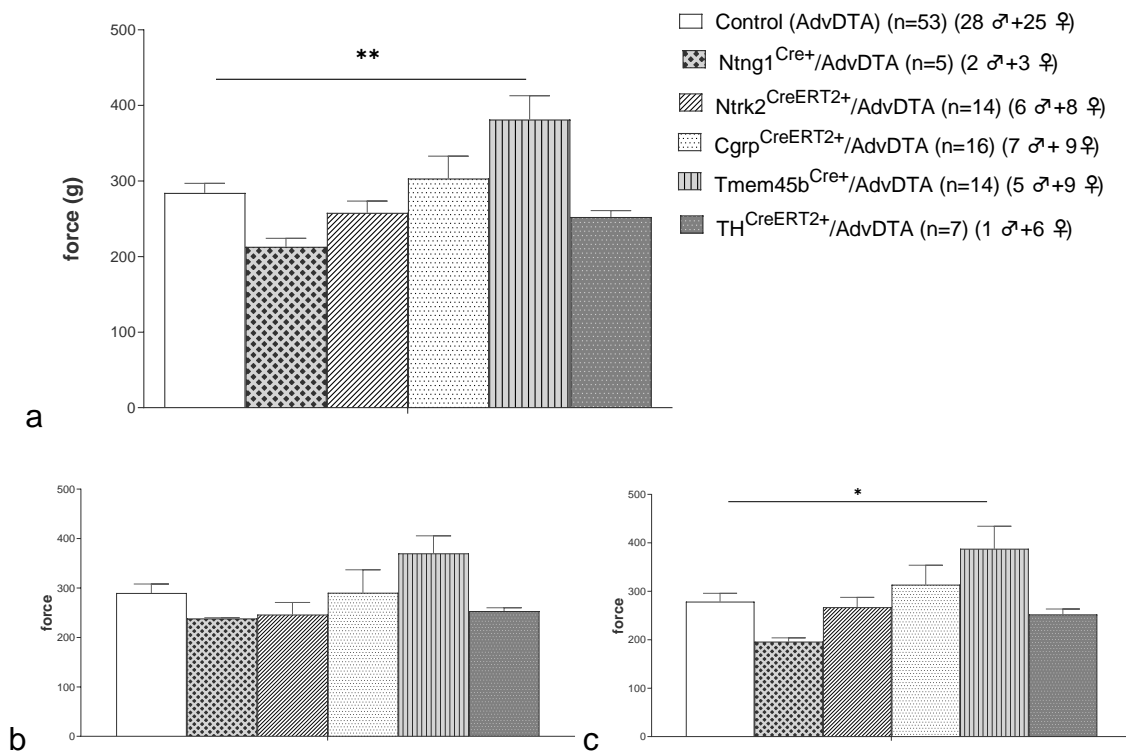
Figure 37. Noxious mechanical sensation (Randall-Selitto test) is impaired in mice with *Tmem45b* positive DRG neurons ablated (a) mixed gender.

This reaches statistical significance in female (c) but not male (b) mice. Data are shown as Mean±SEM with one-way ANOVA for (a) and (c) graph.

3.3.2.7 Cgrp[CreER+]/ Advillin Flox-tdTomato-Stop-DTA mice show reduced responses to noxious heat

Mice were exposed to an increasing radiant heat by the Hargreaves' test and a 50^0C hot plate test. I found no difference in heat sensitivity between the genotypes with one exception (Figure 38 and Figure 39). The ablation of CGRP+ neurons leads to increased latency in nocifensive responses in both the Hargreaves' spinal reflex test, and in the supraspinal hot plate test at 50°C. This confirms other studies that report CGRP+ neurons as partially expressed in the TRPV1+ subpopulation and linked to itch and heat (McCoy et al., 2013, McCoy et al., 2012).
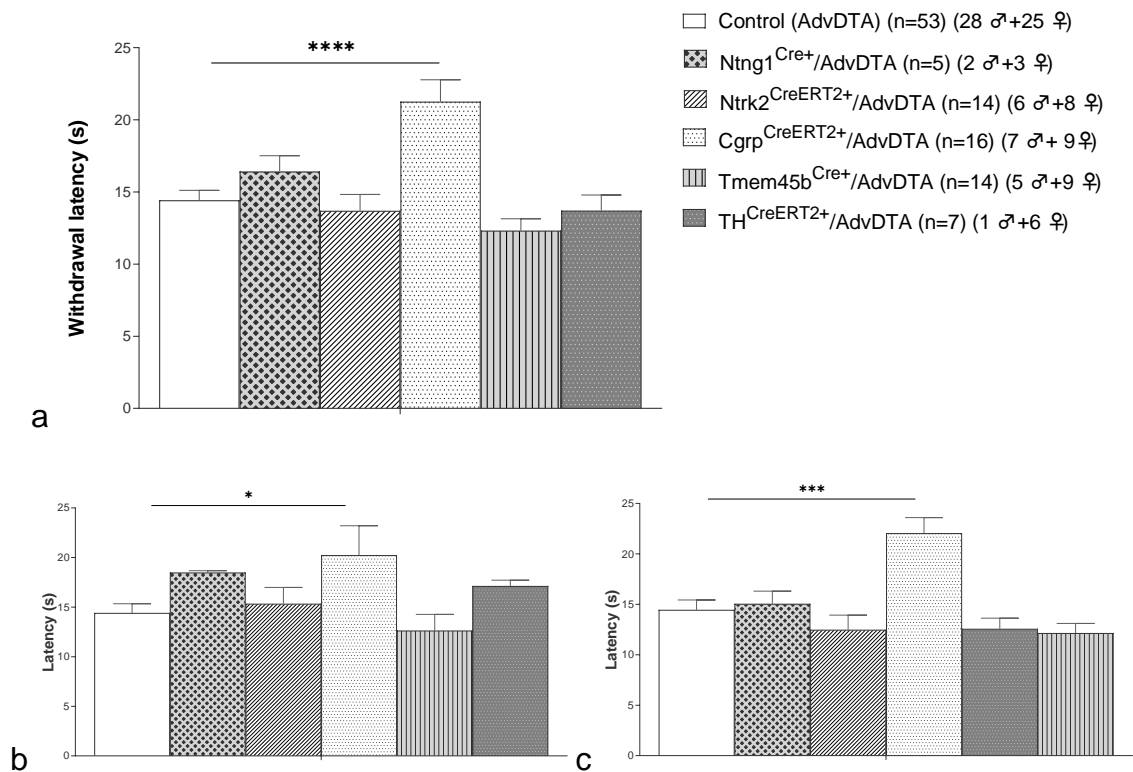
Figure 38. Behavioural responses to thermosensation by Hargreaves' test are unimpaired in all groups except for an increase in latency for the CGRP[CreERT2+]/AdvDTA animals

when compared to their AdvDTA controls (P ≤ 0.0001). (a) Represents mixed gender, (b) males and (c) females. Data are shown as Mean±SEM with one-way ANOVA for (a) and (c) graph
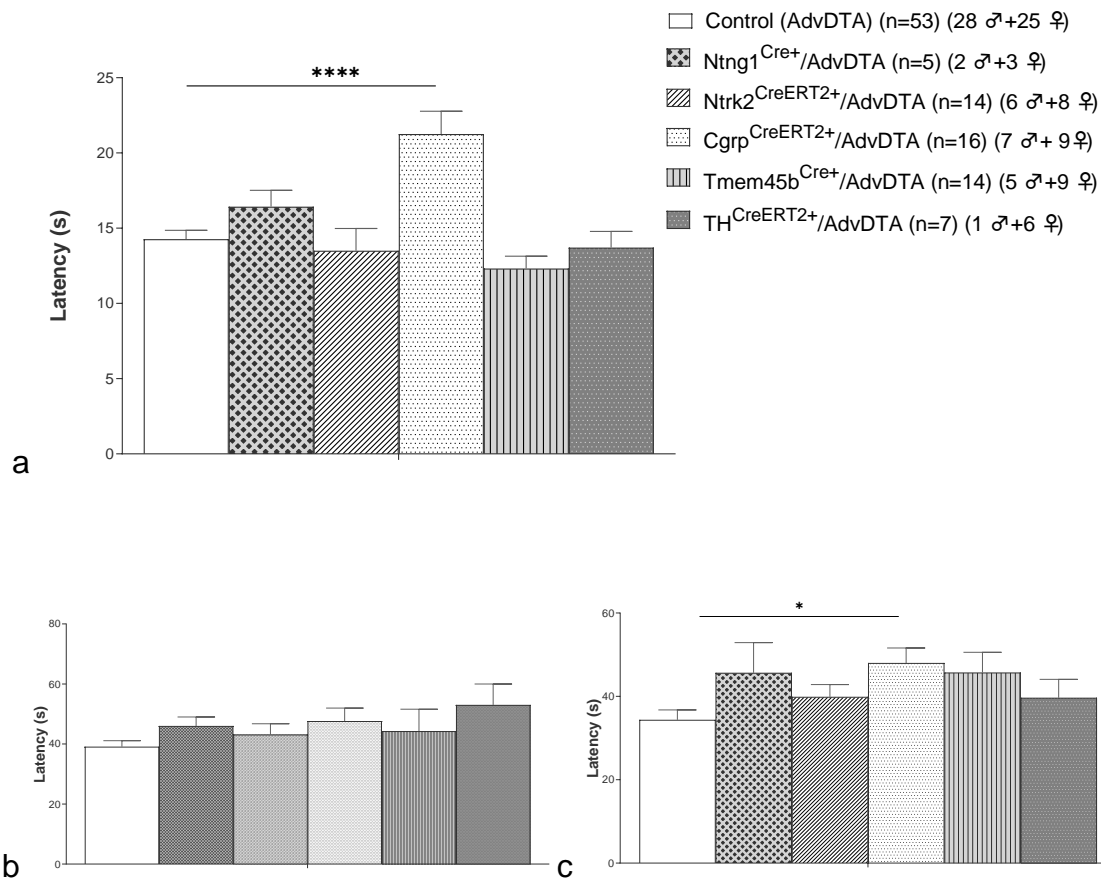
Figure 39. Behavioural responses to thermosensation by the hot plate test are unimpaired at 50°C in all groups except for an increase in latency for the CGRP[CreERT2+]/AdvDTA animals
when compared to their AdvDTA controls (P ≤ 0.0001). (a) Represents mixed gender, (b) males and (c) females. Data are shown as Mean±SEM with one-way ANOVA for (a) and (c) graph.

3.3.2.8 Normal innocuous cold sensation in all lines tested

To finalise the thermal function assessment, I performed a cold plantar assay by the dry ice test. I found no significant difference in sensitivities between the groups studied and report no phenotypic difference in response to innocuous cold by the ablation of the different subpopulations, regardless of sex (Figure 40).
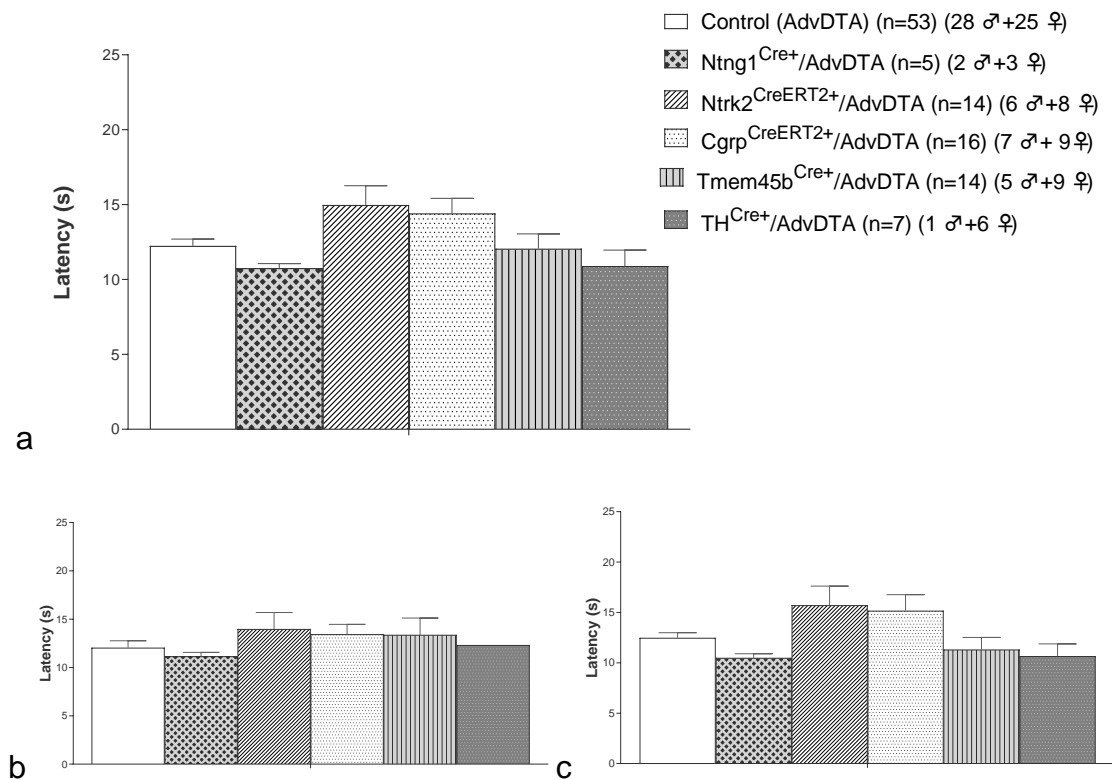
Figure 40. Behavioural responses to innocuous cold by dry ice test show no difference when compared to their AdvDTA controls.

(a) Represents mixed gender, (b) males and (c) females. Data are shown as Mean±SEM with one-way ANOVA for (a) and (c) graph.

After these last findings, we decided to investigate further the implication of *CGRP* expressing neurons in cold as per bibliography (McCoy et al., 2013), and performed a subsequent noxious cooling assay. By applying acetone onto the hind paw of the animals, I confirmed that CGRP positive neurons seem to be implicated in cold processing mechanisms when compared to their control littermates (Figure 41), and report that their ablation does inhibit the development of acetone induced cold allodynia.
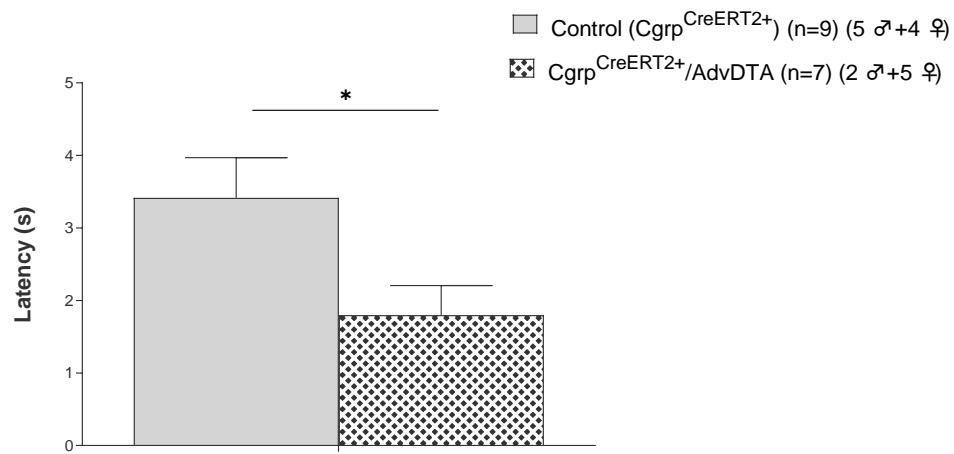
Figure 41. Behavioural response to noxious cooling of CGRP[CreER+]/ *Advillin* Flox-tdTomato-Stop-DTA against control littermates

Data are shown as Mean±SEM mixed gender with t-test analysis.

3.3.2.9 Summary

To sum up my behavioural findings:

STRAIN		ACUTE BEHAVIOUR								
		VonFrey	Cotton Swab	Hargreaves	Dry ice	hot plate	Randall Selitto tail	Rotorod	open field	Balance beam/Pole
Ntrk2^{CreRT2}	cre alone	N		N	N	N	N	N		
Ntrk2^{CreRT2}	+Avil FloxtdTomatoStopDTA	N	hypo*	N	N	N	N	N		
Tmem45b^{Cre}	cre alone	N		N	N	N	N	N	N	
Tmem45b^{Cre}	+Avil FloxtdTomatoStopDTA	N		N	N	N	hypo	N	N	
Th^{CreRT2}	cre alone	N		N	N	N	N	N	N	
Th^{CreRT2}	+Avil FloxtdTomatoStopDTA	N		N	N	N	N	N	N	Impaired
CGRP^{CreRT2}	cre alone	N		N	N	N	N	N	N	
CGRP^{CreRT2}	+Avil FloxtdTomatoStopDTA	hyper		hypo	N	hypo	N	N	N	
Ntng1^{Cre}	cre alone	N		N	N	N	N	N		
Ntng1^{Cre}	+Avil FloxtdTomatoStopDTA	N		N	N	N	N	N		
Na$_v$1.8^{Cre}	+Avil FloxtdTomatoStopDTA			N			hypo			

Table 18. Summary of behavioural findings for all lines studied per test.

N= normal, Hypo= Hyposensitive and Hyper=hypersensitive. In black results predicted or confirming already published data and novel or unpredicted in red. (* data shown on chapter 4)

3.4   Discussion

Major advances in genetic techniques for analysing and manipulating single sensory neurons during the current 'omics' era have highlighted the heterogeneity within the sensory neuron population and provided the tools for a novel taxonomy of somatosensory DRG neurons in the peripheral nervous system (fig 13). Using comprehensive single-cell RNAseq and bioinformatics, the findings from Usoskin et al. have been combined with a recent large-scale study by the Zeisel group to generate a more detailed census of mouse primary afferents (Usoskin et al., 2015b, Zeisel et al., 2018b) defined by their mRNA expression signatures. Each of the neuronal clusters, containing different sensitivity and innervation, have been grouped by developmental anatomical units and by the expression of neurotransmitters and neuropeptides. The primary afferent diversity is driven by encoding genes whose identification has provided a solid base for understanding the molecular architecture of the nervous system and enables genetic manipulation of specific cell types for functional studies. A more recent study has produced a slightly different somatosensory neuron taxonomy, based on the transcriptomic profile where 'NP subset" and "PEP subset" is being voided. This is because their neuropeptide expression profile (such as substance P and CGRP) is not unique to the group (Li et al., 2016).

The importance of this neuronal classification has reached higher clinical relevance after the publication of an extension of this study in primates (Kupari et al., 2021). The resulting catalogue of sensory neurons, until now missing, not only reiterates the diversity of sensory types but also correlates it to rodents. Historically, the use of transgenic mice has contributed to accelerating our understanding of the molecular mechanisms underlying pain, and have successfully identified several key players in peripheral pain processing and transmission, some of which have already been translated into promising analgesic targets (Wise et al., 2021, Doebele et al., 2020, MacDonald et al., 2021). The overall cross-species conservation of somatosensory primary afferents between one of the most used animals in research and primates has started to seed the path for a successful ''forward'' translation from rodents to the clinic.

The very initial aim of this study was to link single transcriptomically defined clusters of primary afferents to specific pain mechanisms. This was proven to be too ambitious, especially after analysing the expression changes in mouse DRG in different clinically relevant animal pain models (Bangash et al., 2018). Microarray data revealed known and to date unknown genes dysregulated, and no direct link between transcriptomically distinct sets of neurons and particular pain models, suggesting that distinct cell types may contribute to identical phenotypes.

To overcome this mechanistic redundancy, I tuned our project design according to these findings and opted for a wider approach where multiple subpopulations of neurons were ablated instead of focussing on just one unique subtype. Using transgenic Cre-loxP mouse strategies and labelling techniques described in this thesis (see chapter 3.2.2), I examined the contribution of different neuronal clusters to pain. I conducted an array of experiments (Table 16) on a comprehensive set of currently available Cre recombinase lines driven by genes differentially expressed across the whole spectrum of the transcriptome profile (as per the Usoskin et al. dataset). They are $Na_v1.8^{Cre}$ (*Scn10a*), $Ntng1^{Cre}$, and three tamoxifen-induced lines $TrkB^{CreER}$ (*Ntrk2*), $Cgrp^{CreER}$ (*Calca*) and $Th^{CreERT2}$ (Table 6). The widely used temporal control Cre^{ER} tool allows the mice to develop normally until the Cre activity is switched on using tamoxifen administration in adulthood, avoiding any potential developmental defects caused by early ablation. Such is the case of the gene encoding tyrosine hydroxylase *(Th)* whose regulation during development jumps from inducing *Th* expression at the early embryonic stage to its reactivation during the post-natal development in the brain (Matsushita et al., 2002). Additionally, two more Cre lines, *Tmem233^{Cre}* and *Tmem45b^{Cre}* were generated to investigate neuronal subsets flagged as important and in which Cre lines were, to that date, not commercially available.

Herein, I validated the Cre lines crossed to a tomato reporter line by performing RNA scope *in situ* hybridization to investigate if each Cre is expressed in a neuronal population in development, outside from the expected expression profile in adult mice (see Table 2). Their promoter-driven neuronal expression pattern was verified in the DRG with specific marker labelling. Overall, I observed a large overlap between tdTomato expression and the Cre promoter (target), indicating

that Cre activity was in general consistent with the expression of the endogenous mRNA marker gene (Figure 26) (Santana-Varela et al., 2021).

Subsequently, each target gene was assessed for colocalization with *Nfh* to help us categorise the cellular population profile by a classic cell diameter distribution. RNAscope data showed *Ntrk2* (TrkB) Cre expression in large neurons marked by NF200. This correlates with the transcriptomic data (Zeisel et al., 2018b), as well as published studies that identify TrkB DRG positive neurons as Aδ-LTMR proprioceptors and putative mechanoreceptors, that reported the same level of expression and distribution (7-10% of total DRG neurons) (Rutlin et al., 2014a) (Dhandapani et al., 2018).

Tmem233^{Cre} and *Tmem45b^{Cre}* have been predicted to have similar transcriptome signatures to *Scn10a,* with expression in PSNP2, PSNP3, PSNP4, PSNP5 and PSNP6. Unsurprisingly, I found positive Cre activity in small-diameter unmyelinated sensory afferents (or *Nfh*-negative neurons), analogously to published *Scn10a* data (Abrahamsen et al., 2008, Tadashi et al., 2021). Unlike *Tmem233^{Cre}*, *Tmem45b^{Cre}* expression is also present in C-LTMRs *Th*-rich neurons (PSNP1) which was verified via immunohistochemistry (Figure 19).

Likewise, RNAscope studies confirmed that Cre activity and population distribution was following the predicted single-cell RNAseq data for *NetrinG1 (Ntng1),* active in Nefh-positive neurons, and *CGRP^{CreER}* Cre lines in both Nefh-positive and -negative neurons.

Previous studies on the PSNP1 population have reported certain discrepancies between *Th* mRNA (~37%) and protein (~15%) detected in adult mouse lumbar DRG (Brumovsky, 2016), where *Th* transcripts might not be translated into protein. When I investigated the *Th^{CreERT2}* line by RNAscope, I found incomplete overlap between tdTomato expression and the target endogenous *Th* mRNA (Figure 23). Furthermore, I performed immunohistochemistry and confirmed that the tomato signal observed is indeed immunoreactive to the Th antibody (Figure 24). However, to confirm fully the findings, RNAscope quantification techniques would be necessary which would benefit also the characterisation of the other Cre lines listed above (see future directions in chapter 3.6).

Importantly, a recent RNAscope study on mouse and human DRG has revealed strong interspecies divergence when investigating expression patterns, cell body

diameter classification and functionality of different pain processing markers (Shiers et al., 2020). Their results on the classic large-diameter Aβ mechanoreceptor marker NF200 suggests that the labelling is not specific for this neuronal subpopulation in some mammals, and it is expressed in all sensory neurons in humans instead. Similarly, in the past few years, researchers have been reporting critical differences and similarities in molecular and cellular characteristics of DRG (Haberberger et al., 2019) with potential functional consequences. This highlights the importance of confirming mice-human homology when translating results to the clinic.

The second aim of this project was to identify the role of transcriptomically different subpopulations of DRG neurons in different types of pain perception. Using the chosen library of gene-specific promoter-driven Cre lines, I ablated specific subpopulations of neurons by crossing them with the *Advillin* Flox-tdTomato-Stop-DTA BAC strain. The characterisation of this newly generated reporter mouse is included in this thesis.

The construct of the ablative reporter line contains an *Advillin* promoter for spatial control. Mainly restricted to DRG (Emery and Ernfors, 2018, Lau et al., 2011), this promoter has been proven essential when targeting genes that lead to neonatal deaths when deleted globally, such as *Scn9a* (Nassar et al., 2004a). The loxP-flanked tomato-STOP cassette allows the transcription of the downstream red fluorescent protein variant (tdTomato) in all sensory neurons (Figure 14) while preventing the downstream diphtheria toxin A (DTA). Unfortunately, the tomato signal generated by these animals was too weak to be used for quantification and imaging distribution analysis (Figure 27), possibly due to a weak Kozak consensus sequence for translation initiation.

(sequence of 476 amino acids with 0.63 Kozak score:

MVSKGEEVIKEFMRFKVRMEGSMNGHEFEIEGEGEGRPYEGTQTAKLKVTKGGPLP
FAWDILSPQFMYGSKAYVKHPADIPDYKKLSFPEGFKWERVMNFEDGGLVTVTQDSS
LQDGTLIYKVKMRGTNFPPDGPVMQKKTMGWEASTERLYPRDGVLKGEIHQALKLKD
GGHYLVEFKTIYMAKKPVQLPGYYYVDTKLDITSHNEDYTIVEQYERSEGRHHLFLGH
GTGSTGSGSSGTASSEDNNMAVIKEFMRFKVRMEGSMNGHEFEIEGEGEGRPYEGT
QTAKLKVTKGGPLPFAWDILSPQFMYGSKAYVKHPADIPDYKKLSFPEGFKWERVMN
FEDGGLVTVTQDSSLQDGTLIYKVKMRGTNFPPDGPVMQKKTMGWEASTERLYPRD

GVLKGEIHQALKLKDGGHYLVEFKTIYMAKKPVQLPGYYYVDTKLDITSHNEDYTIVEQ
YERSEGRHHLFLYGMDELYK).

Recombination between LoxP sites is catalysed by Cre recombinase which allowed the expression of the toxin, leading to a controlled DRG neuron cell ablation in cells where the Cre was expressed. *Advillin* Flox-tdTomato-Stop-DTA BAC strain efficacy was validated after crossing it to a well characterised $Na_v1.8^{Cre}$ line (Abrahamsen et al., 2008). It resulted in a Cre expression pattern (

Figure 28) and deficits in noxious mechanosensation (Figure 29) common to known $Na_v1.8$ ablative studies using a different DTA knockin line (Abrahamsen et al., 2008). In conclusion, although the tomato expression in *Advillin* Flox-tdTomato-Stop-DTA was not strong enough to be used as a marker for post mortem immuno-studies, its ablation mechanism was effective and was used to examine the consequences of ablating subsets of DRG neurons.

Furthermore, *Scn10a* and *Tmem45b* mRNA gene expression levels in $Na_v1.8^{Cre}$ and Tmem45b^{Cre} lines crossed to *Advillin* Flox-tdTomato-Stop-DTA mice were found negligible when compared to their controls by RT-PCR quantification (Figure 30 and Figure 31), further confirming successful ablation. However, when analysing Tmem45b^{Cre+}/ *Advillin* Flox-tdTomato-Stop-DTA individual values within their control group, I unexpectedly observed a considerable level of segregation with some Cre negative mice having reduced Tmem45b expression (albeit still much higher than in Cre positive, AdvDTA positive mice). One possible explanation is that there is some leaky expression, with read-through of the transcriptional stop sequences in some control mice. A better design to prevent this would be to use a Cre dependent Flex-Knockin strategy instead with the DTA sequence inverted in the absence of Cre activity (see chapter 3.6. Future directions). Initially reported in 2003, this method has proven to improve functional redundancies and background unexpected gene expression or even lethality (Schnütgen et al., 2003).

Since our breeding strategy and initial behavioural characterisation was already ongoing when we came across this potential limitation, I continued the project and decided to pool all *Advillin* Flox-tdTomato-Stop-DTA control littermates from every Cre line crossing. This way I intended to dilute any potential effects of leaky

DTA expression within a bigger n number group while facilitating the comparison between the Cre lines.

Sensitivity to innocuous mechanical stimuli was found overall normal when ablating the chosen neuronal subpopulations with only one exception. Not without surprise (McCoy et al., 2012), the current data shows that the conditional deletion of *CGRP*-positive DRG neurons had an impaired effect in mechanical sensitivity in the von Frey test in a mixed-sex analysis (Figure 36). This hypersensitivity appeared to be stronger in male than female mice. However, and as mentioned in this thesis, sex-specific graphs were considered merely informative due to some groups' low n number. CGRP-expressing excitatory interneurons present in lamina III of the spinal cord dorsal horn and trigeminal nucleus caudalis have been reported producing mechanical hypersensitivity in response to von Frey stimulation after chemogenetic activation whilst normal in resting conditions (Löken et al., 2021). Since this subset is widely expressed in the nervous system it would be interesting to interrogate the hyperexcitability of neurons located in other areas (ie spinal cord) as a consequence of its ablation in the DRG. Similarly, when interrogating Ntrk2-positive DRG neuron implication on non-noxious mechanical pain processing, I found significant differences in the female group when compared to the littermate controls. Males, however, were found normo-reactive in the von Frey test, correlating to the already reported characterisation of TrkB positive neurons by the Heppenstall group (Dhandapani et al., 2018) performed in males. It would be necessary to increase n number of males and/or females in some of the groups to be able to be certain of any sex specific effects.

CGRP positive DRG neurons partially overlap with the *TRPV1* positive subpopulation and have been linked to itch, heat and cool temperature perception (McCoy et al., 2013, McCoy et al., 2012). Whilst *CGRP* neurons were unexpectedly found to be implicated in innocuous mechanosensation, I confirmed their expected role in noxious heat and cooling. *CGRP* [CreER]/*Advillin* Flox-tdTomato-Stop-DTA mice showed significant hyposensitivity to noxious heat both in the Hargreaves' (Figure 38), and 50°C heated plate tests (Figure 39), suggesting that this nocifensive impairment is linked to a mechanistic supraspinal response as well as a spinal reflex to heat (Minett et al., 2011, Chapman et al.,

1985). Although I could not recapitulate delayed withdrawal responses to dry ice stimuli in animals lacking CGRP positive neurons (Figure 40) as predicted, I performed a further noxious cooling assay and showed that their ablation does inhibit the development of acetone induced cold allodynia when compared to their control littermates (Figure 41). This confirms the implication of *CGRP* expressing primary afferents in noxious cold processing mechanisms already reported (McCoy et al., 2013).

When characterising *Tmem45b* expressing primary afferents I confirmed an analogous Cre expression pattern to $Na_v1.8$ (PSNP1 to 6). I found a sex independent deficit in noxious mechanosensation (Figure 37) with no effects in innocuous stimuli (Figure 36) and thermal responses, corroborating previous $Na_v1.8$ ablated findings when using other DTA carrier strategies (Abrahamsen et al., 2008). Also expressed in the PSNP subpopulation (except PSNP1), a new *Tmem233*[Cre] was also created. It would have been interesting to characterise it and compare phenotypes for a better understanding of non Peptidergic C nociceptors, but their breeding rate was abnormally inefficient, and they could not be included in the behavioural analyses.

In terms of basic exploratory behaviour (Figure 33) and responses to motor function (Figure 34), the ablation of each target neuronal subpopulation was without significant effect. However, I observed some motor coordination difficulties in animals lacking *Th* expressing neurons. The performance of these animals on a vertical and horizontal pole was investigated further and revealed significantly higher difficulties when performing the task when compared to their littermate controls (Figure 35). Per definition, proprioceptive neurons are essential for the proper execution of all our movements by providing muscle sensory feedback to the central motor network. In addition, Calcium-binding protein parvalbumin (PV) expression has been found co-localizing with Tyrosine receptor kinase C (Trk C) and Neurotrophin-3 proteins, which are linked to the development of proprioceptive receptors and their primary afferent neurons and muscle (Ernfors et al., 1994). Since PV is considered a reliable neurochemical marker for the proprioceptive subset of DRG fibres, our unexpected behavioural phenotype could be explained by a certain level of colocalization within the parvalbumin (PV) positive neurons observed by RNAscope *in situ* hybridization (

Figure 25). Whilst it does not correspond to the predictive transcriptomic data, it would require a substantial increase in the n number of the groups of the study in order to draw final conclusions.

To summarise, this thesis has contributed to the current repertoire of transgenic tool strains by characterising a novel *Advillin* Flox-tdTomato-Stop-DTA and proved it useful in ablative functional studies. I foresee this mouse to be a useful resource for the neuroscience community. I have tested acute pain thresholds in mice where subpopulations of DRG neurons have been killed through expression of DTA, identified the *Tmem45b* population of neurons important for detecting noxious mechanical pain and the *Cgrp* population of neurons important noxious thermal sensation. Due to low n numbers for some lines, sex-specific conclusions are difficult to draw. This is a limitation of the study and was caused by difficulties and unpredictable breeding of the BAC transgenic line. However, the data in this thesis is a strong foundation for further more in-depth studies on the functional importance of specific subpopulations of DRG neurons. Lastly, since the nervous system must be considered as a dynamic circuit with the ability to change and adapt to changes in the microenvironment (Leslie and Nedivi, 2011), any characterisation of primary afferents would be incomplete without including their implication in pain under pathological conditions. This is addressed in chapter four of this thesis.

3.5 Conclusions

-The characterisation of a novel *Advillin* Flox-tdTomato-Stop-DTA line shows this transgenic reporter as useful in ablative functional studies when combined with Cre recombinase lines.

-Expression pattern analyses and phenotyping carried out in this thesis provide information about diverse sets of peripheral sensory neurons and their role in pain under non-pathological conditions.

3.6 Future directions

RNAscope *in situ* hybridization allowed us to validate a wide array of Cre lines and in general there was a high correlation between Cre activity and expression of the endogenous mRNA marker gene. The RNAscope experiments could be further expanded by using more markers to fully characterise which neuronal subsets each Cre is active in.

Besides, although using mice as a preclinical model for translational studies has proven to be useful, recent discoveries have identified critical interspecies differences that highlight the importance of mice-human homology confirmation when designing experiments (Shiers et al., 2020). Furthermore, since historical and novel information about the size and location of human and mice DRG is continuously updating, future expression studies should be tuned to any potential refinements.

Advillin Flox-tdTomato-Stop-DTA limitations mentioned in this report include weak tomato signal and potential leakiness in DTA expression in some control mice. Whilst the weak tomato expression issue was not a major problem, the potential leaky expression of DTA could have led to inaccurate behavioural results. In the future, a new Cre dependent Flex(flip-excision)-Knock-in strategy could potentially reduce the chance of leaky expression of DTA.

Another limitation of the study that could benefit from an improved reporter mouse design is the low breeding rate of the strain. I faced great difficulties in obtaining enough n number of animals per group to perform the behavioural experiments, without compromising the age factor. I accept that mixed-sex results are not ideal

to delineate sex-specific differences and I have tried to account for gender diversity when examining the consequences of deleting individual genes. However, breeding inefficiency has led to an insufficient number of males and females in some of the groups and prevented us to draw reliable gender-specific conclusions. One of the possible reasons for this could be inherent to the reporter strain design. Libraries constructed in the bacterial chromosome (BAC) vectors have been widely used due to their large carrying capacity, cost efficiency and high clonal stability (Kelley et al., 1999). However, they can integrate randomly into the genome and, if inserted in germ cell-expressed genes, then this can affect breeding capacity.

Chapter 4 - Conditional ablation of subsets of neurons by advillin driven floxed-stop-diphtheria toxin in models of disease

4.1 Summary

This chapter focuses on the analysis of the roles of unique classes of sensory neurons in particular types of pain relevant to human conditions. Using transcriptomics and transgenic functional studies, I aim to associate precise subsets of neurons with particular pain syndromes including, inflammatory pain, cancer pain and neuropathic.

In chapter three, I characterised a comprehensive set of Cre recombinase lines driven by genes that are differentially expressed across the eighteen sensory neuron subtypes (Zeisel et al., 2018b). I included both currently available as well as novel Cre lines to investigate different promoter driven neuronal ablation in cells that are flagged as important in pain processing. The deletion of specific DRG neuronal subsets using our DTA tool mouse has been proven to be successful, and a useful resource for functional characterisation of somatosensory processing at an acute level; howbeit, the behavioural results shown represent the physiological and not the pathological states of DRG neurons. The literature is full of evidence about changes in gene expression patterns of DRG cell bodies under pathological conditions. Animal models of chronic pain induced by peripheral nerve injury, for example, have shown that the amount of Galanin-expressing DRG neurons is increased after surgery, whereas the expression of Tac1 (Tachykinin Precursor 1) is reduced (Schreiber et al., 1994). Taking this into consideration:

- The first aim of this chapter is to study the adaptability of the nervous system to an injured status and analyse changes in Galanin (Gal) expression profile after an inflammatory insult. By using the Cre recombinase system and tomato reporters, I generated a Gal ^{Cre}/*Rosa-CAG-flox-stop-tdTomato* line that was treated with complete Freund's adjuvant (CFA). The neuronal galanin expression pattern in DRG was observed against littermates injected with saline via RNAscope and by immunostaining.

- Secondly, I applied the same breeding strategy as in chapter three to investigate well-established pain models that are potentially useful in addressing the diversity

of pain mechanisms, and to study whether they involve a unique or several subpopulations of cells.

Offspring from the already verified Cre lines crossed with *Advillin* Flox-tdTomato-Stop-DTA BAC mouse were tested to assess the neuronal depletion effect in an inflammatory formalin test.

Lastly and in parallel to the model above, TrkB positive neurons were also further investigated in cancer induced bone pain and a neuropathic partial nerve ligation model to identify the role of this neuronal population in these specific mechanisms of pain processing within the DRG.

4.2 Introduction

The developmental complexity of sensory neuron specification has been extensively analysed but the link from transcriptome to function is still relatively unclear. Recent breakthrough technical advances in genetic techniques for the analysis and manipulation of sensory neurons, have allowed the Ernfors and Linnarsson groups to reveal eighteen major subtypes of mouse sensory neurons (Usoskin et al., 2015b, Zeisel et al., 2018b) that could potentially be linked to particular pain mechanisms. In parallel, the Zeilhofer and Ma labs have pioneered intersectional genetic approaches using multiple recombinases to address the function of genetically defined small subsets of neurons. They have also generated a range of rapid delivery viral vectors based on AAV that can infect DRG neurons and manipulate neuronal activity to analyse behavioural consequences (Foster et al., 2015). All these and other discoveries are currently providing a potential technical platform for addressing peripheral mechanisms in human pain.

In chapter three of this thesis, I interrogated if transcriptomic heterogeneity among DRG neuron types correlates with the somatosensory diversity. Combining mouse transcriptomics and functional studies in transgenic mice have allowed us to characterise the acute thresholds of selected subpopulations of neurons in the DRG under physiological conditions (Santana-Varela et al., 2021). Thus, our study provides new insights into the biological function of somatosensory neurons, particularly for the nociceptors, and suggests that neuron types are defined by their transcriptomic, morphological and functional characteristics. However, since the nervous system is dynamic and adaptable to for example epigenetic changes, this study would be incomplete without studying neuronal subsets in different pain states.

Analogously, previous studies of voltage-gated sodium channels in different pain syndromes have successfully uncovered a diversity of mechanisms in peripheral pain pathways and revealed pain-modality specific roles for genes such as $Na_v1.3$, 1.7, 1.8 & 1.9. Moreover, studies in $Na_v1.7$ have shown that the oxaliplatin neuropathic pain or cancer pain model, for example, has a distinct $Na_v1.7$-independent mechanism from surgical neuropathic models (Minett et al., 2014a). Likewise, other studies have reported enough evidence to be able to confirm that

those identical behavioural outcomes have distinct underlying mechanisms in different neuropathic and other pain models and does not necessarily involve a classical nociceptor activation. This mechanistic redundancy is a major problem for drug development and must be addressed by analysing neuronal types and their markers independently under pathological conditions to identify their potentially causative role while observing potential plasticity.

On this line, one classic example of neuronal plasticity is the study of Galanin. Galanin a neuropeptide involved in pain processing (Xu et al., 2010), linked to addiction and Alzheimer's disease (Counts et al., 2008), and more recently has been identified as a modulator in male and female parenting behaviour (Wu et al., 2014). It is expressed in several CNS regions, spinal cord and DRG where galanin expressing neurons belong to the small C fibre nociceptors (Skofitsch and Jacobowitz, 1985). Despite being present in only circa 5% of DRG neurons, the role of this biomarker is very complex and has been reported facilitatory and inhibitory on nociception when applied exogenously (Holmes et al., 2003a). Interestingly, transgenic studies on mice encoding this gene have shown significantly increased levels of endogenous galanin after different neuropathic models in DRG lumbar areas (Villar et al., 1989). This temporal change in peptide expression is a molecular adaptative response of the nervous system to injury in continuous investigation. Intrathecal administration of Galanin has been translated into reduced allodynia after nerve injury in animals (Liu and Hökfelt, 2000) suggesting this peptide and its receptor, as a good analgesic target.

4.2.1 Complete Freund's Adjuvant

Complete Freund's Adjuvant (CFA) is a suspension of mycobacterium tuberculosis emulsified in mineral oil and mannide monooleate widely used to induce inflammation, tissue necrosis, and ulceration in murine models. Individuals receive a single intraplantar injection of 20µl of 100% CFA (Sigma) which leads to lasting inflammatory hypersensitivity (Larson et al., 1986) after an onset period of 24h. It causes thermal and mechanical hyperalgesia believed to be linked to pro-inflammatory cytokine release in the periphery, as well as spinal changes such as increased density of postsynaptic NMDA receptors (Yang et al., 2009) (see chapter 1.2.2).

The adjuvant activity derived from the injection is able to produce an immunologic response which can be also used to induce arthritis in rodents. Adjuvant-induced arthritis (AIA) is a disease produced in rats by immunization with CFA, characterized by primary arthritic lesions appearing rapidly from day zero in the injected hind paw, followed by the development of secondary arthritic lesions in the contralateral paw at around day fifteen from the injection of CFA (Cui et al., 2019).

Both CFA-induced inflammatory and arthritis murine models (AIA) have been successfully used for studying anti-inflammatory pain drugs (Cui et al., 2019, Deval et al., 2008) however, the inflammatory or arthritogenic elements are still unclear. Assessing potential transcriptional changes in DRG could help to identify which primary afferents subsets are involved in CFA- induced pain (Bangash et al., 2018).

4.2.2 Formalin

One of the most predictive models of inflammatory pain is the Formalin test, used to assess intense, short-lasting persistent pain. This model of nociception has been widely used in rodents for drug screening and consists of injecting a noxious diluted formaldehyde solution into the hind paw of the animal (Murray et al., 1988). It produces a biphasic pain response, where spontaneous evoked behaviours are recorded on a freely unrestrained animal, when every licking, biting or tapping is timed. Its main advantage is that it contains inflammatory, neurogenic and central mechanisms of nociception. It starts with an early phase or phase I that corresponds to the first 10 minutes after injection, resulting from the direct activation of primary sensory neurons with no prostaglandin involvement. It is followed by a period of quiescence or sensitization, and a late second phase or phase II, lasting till 60 min. This last phase contains pain-like behaviours resulting from central sensitization (Le Bars et al., 2001).

Further research has investigated the involvement of inflammatory processes in the two phases by testing different drugs in both independently. It has been reported that, although paracetamol, opioids and other centrally acting analgesics were antinociceptive in both phases, local anaesthetics appeared to be

suppressing the first but not the second phase, whilst nonsteroidal anti-inflammatory drugs (NSAIDs), N-methyl-D-aspartate (NMDA) antagonists and gabapentin inhibit only phase II responses (Hunskaar and Hole, 1987, Jourdan et al., 1997). These findings suggest that both phases I and II are in fact mechanistically different, providing duality to the utility of the test and its analysis.

The application of this model in mouse transgenics has allowed us to identify the mammalian TRPA1 as being important in formalin-evoked mechanical hyperalgesia (Kerstein et al., 2009) as shown by the use of channel blockers. Another example is the calcium voltage channel Cav2.3, whose knockout mice show an attenuated response to the second phase of the formalin test (Saegusa et al., 2002). And more recently, $Na_v1.9$ voltage-gated sodium channel function has been linked to maintaining peripheral inflammatory pain using this specific test (Lolignier et al., 2011).

I assessed the role of transcriptomically distinct neuronal subpopulations (previously characterised in chapter three), by using the same promoter driven ablation strategy to identify their potential involvement in a classic inflammatory Formalin model.

4.2.3 Neuropathic pain models

Neuropathic pain is a relevant human condition characterised by acute mechanical allodynia or hypersensitivity to touch, where standard analgesia has almost no beneficial effect without affecting the quality of life. We know it can be either sympathetically maintained or sympathetically independent (Roberts, 1986) but the identity of the neurons responsible to transmit this condition is still unclear.

Chemotherapy-induced peripheral neuropathy is a common type of neuropathic pain that can be replicated by a series of oxaliplatin injections in mice. Similarly, models of diabetic neuropathy can be chemically induced too, by the administration of streptozotocin (STZ), a pancreatic selective Beta cell toxin that induces irreversible necrosis of insulin producing cells (Field et al., 1999).

Neuropathic pain can also be surgically provoked to recreate what occurs in the clinic after injury and has been widely applied in the identification of potential pain

genes. Such is the case of several voltage-gated sodium channels (VGSCs) like $Na_v1.3$ (Hains, 2004; Lindia et al., 2005), $Na_v1.7$ (Ghelardini et al., 2010), $Na_v1.8$ (Lai et al., 2002; Joshi et al., 2006; Dong et al., 2007) and $Na_v1.9$ (Leo et al., 2010). Different surgical interventions such as spared nerve transection SNT, partial nerve ligation (Malmberg and Basbaum, 1998) or chronic constriction injury CCI in mice lead to a neuropathic-derived allodynia phenotype, all of which have been reported as different mechanistically (Minett et al., 2014a).

Within the different neuronal subpopulations innervating the skin, I examined neuropathic pain behaviour in mice lacking *Ntrk2*-positive neurons in the DRG. *Ntrk2* encodes the surface receptor tyrosine kinase TrkB and is expressed in myelinated mechanoreceptors where it binds to BDNF. Loss of function studies using Cre recombinase ablation studies have identified TrkB expressing DRG neurons as necessary for producing pain from light touch after nerve injury in mice (Dhandapani et al., 2018). Analogously to these latest studies, I used a CreERT2 line (Rutlin et al., 2014b) and followed the Cre driven ablation strategy already explained in chapter three to interrogate the role of TrkB expressing DRG cell bodies in response to a partial sciatic nerve ligation injury, which to date has not been reported.

4.2.4 Cancer model

Metastases to the bone are considered to be the most common causes of pain in cancer patients and the skeleton seems to be the principal target of different primary tumours. Post-mortem examinations reveal bone metastasis incidence ranging from 14-45% in melanoma up to 70-95% in myeloma, followed by 65-75% in both breast and prostate cancer (Currie et al., 2013). Improvement in cancer patient survival is inevitably accompanied by longer suffering, where pain management of cancer-induced bone pain (CIBP) is to date, ineffective and insufficient in the latter stages of the disease. Due to this, a better understanding of the process that led to cancer-induced bone pain could provide crucial help in the development of a more specifically targeted treatment.

Although translational cancer research is still very limited, the use and development of mouse models in cancer are one of the most important

achievements in research both for the process of understanding and drug screening purposes. In particular, loss of function strategies represent an important tool in assessing the potential validity of targeted therapy thanks to spatial and temporal control strategies such as the one explained in this thesis.

The CIBP mouse model was initially described in 1999 (Schwei et al., 1999) and after continuous refinement has provided the perfect platform to study the main players and interactions. The model is based on the injection of cancer LLC cells into the intramedullary space of the femur, which is then sealed to confine the cancer progression to the bone. Animals develop severe pain 2-3 weeks after cell implantation as well as showing signs of osteolytic bone destruction.

The complex CIBP involves not only inflammation and neuropathic mechanisms, but also ischemia and nerve compression (Falk and Dickenson, 2014). Tumour growth derived pressure into the bone cavity sensitizes primary afferents, whilst inflammatory mediators released as a consequence to the tumour interaction with bone marrow has been reported to also play a crucial role in the pain mechanism (Basbaum et al., 2009a). Furthermore, the microenvironmental acidosis derived from osteoclast activity and immune cell proton release could also contribute to peripheral sensitization through the activation of the newly identified acid-sensing bone primary afferents (Yoneda et al., 2011). Two major receptors are known to respond to acidosis; transient receptor potential cation channel subfamily V member 1 (TRPV1) and acid sensing ion channels (ASICs). TRPV1 belongs to the channel trio mediating acute noxious thermal sensing (Vandewauw et al., 2018), and it is increased after CIBP in the DRG of mice (Niiyama et al., 2007). Similarly, proton-gated sodium channels ASICs also detect pH changes, some of which (ASIC1b and ASIC3) have been found also upregulated following bone cancer (Nagae et al., 2007).

In the same way that detailed mapping of genotype could be linked to a phenotype based on the transcriptome for different cell types, research has been trying to determine if a specific subpopulation of sensory neurons drives CIBP. A comparative study between single-cell RNA-seq gene expression datasets of sensory neurons (Usoskin et al., 2015b) to genes that were dysregulated in animals with bone cancer pain, found no clear trends (Bangash et al., 2018). In this analysis, microarray samples were collected at a clinically relevant middle

term time point (when limb score of 2 was reached, which ranged from day 8 to 16 post surgery), suggesting that at least that particular stage of bone cancer pain is not mediated by a particular subset of DRG neurons but not discarding an earlier effect. Furthermore, there could be a large degree of plasticity not restricted to sensory subpopulations which show gene expression changes.

Interestingly, the discovery of *NTRK1* (TrkA), *NTRK2* (TrkB) and *NTRK3* (TrkC) gene fusions and oncogenic alterations in several tumour types, has increased the interest in the study of the Trk family in human cancers (Joshi et al., 2019). In fact, Trk inhibitors such as Entrectinib (formerly RXDX-101) have provided promising results in clinical trials (Doebele et al., 2020), however, little is known about their implication in cancer derived pain. This question will be addressed herein.

4.3 Results

4.3.1 Galanin expression was up-regulated in DRG neurons after CFA injection with NF200 positive neurons co-expression.

Here I further investigated the nervous system plasticity and analysed the DRG *Galanin* profile expression after a CFA-induced inflammatory model. I used a *Galanin* Cre animal previously described (Gong et al., 2007) and crossed it with a tomato reporter line following the strategy explained in chapter three. Subsequently, I injected saline or Complete Freund's adjuvant (CFA) intraplantarly in a representative group of the newly generated *Galanin Cre + / Rosa-CAG-flox-stop-tdTomato* offspring, and extracted their lumbar DRGs.

Immunohistochemistry and Nissl staining results showed a stronger neuronal immunoreactivity in animals 5 days after CFA injection when compared to the saline group. A subsequent count on total cell bodies (stained by Nissl) and *Gal* expressing neurons (in red) showed a significant peptide upregulation in samples from CFA injured animals which were not observed in saline-injected littermates (Figure 42).
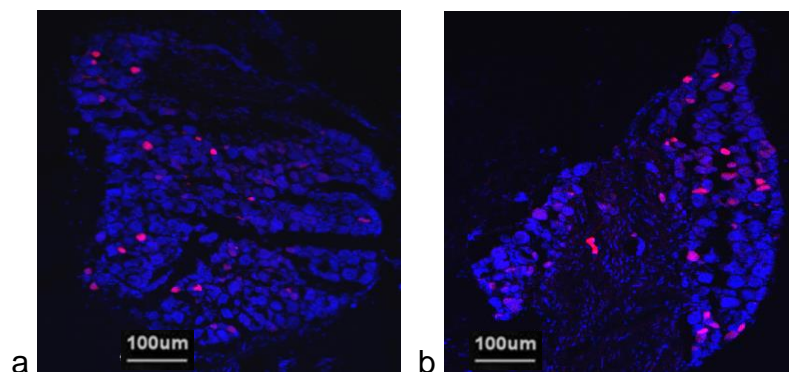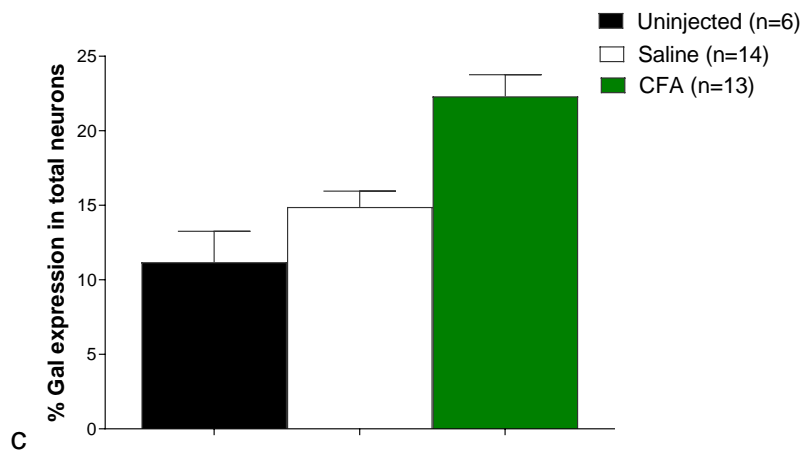
Figure 42. Representative Nissl staining image in lumbar DRG sections of *Galanin Cre+* / Rosa-CAG-flox-stop-tdTomato after CFA.

tdTomato (pink) expression is seen in lumbar DRG sensory neurons with Galanin promoter activity driving Cre expression in mice 5 days after being injected with saline (a) and CFA (b). (c) Staining quantification on mouse DRG sections showing upregulation of *Galanin* Cre activity after CFA injury. Data are shown as Mean±SEM mixed gender with t-test analysis (P ≤ 0.001).

I then co-stained with neurofilament (NF-200), a classic big and medium neuronal marker (in green), and confirmed *Galanin* Cre activity to be significantly increased in NF200 positive neurons in CFA treated samples (Figure 43), similar to what has been reported after peripheral nerve injury (Villar et al., 1989).

C
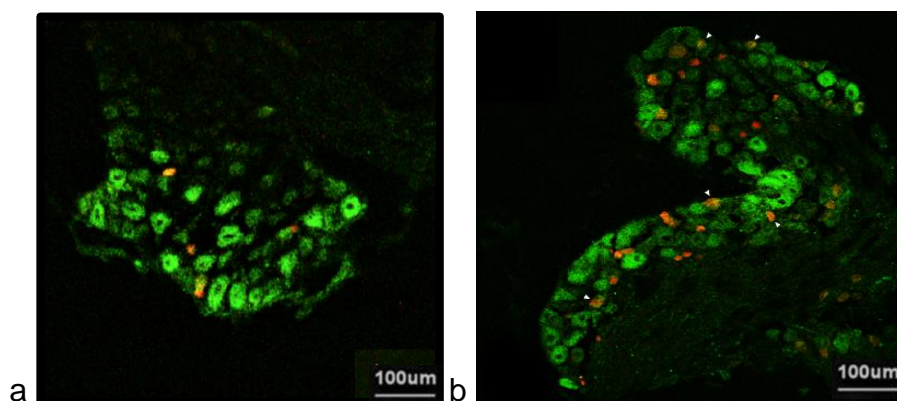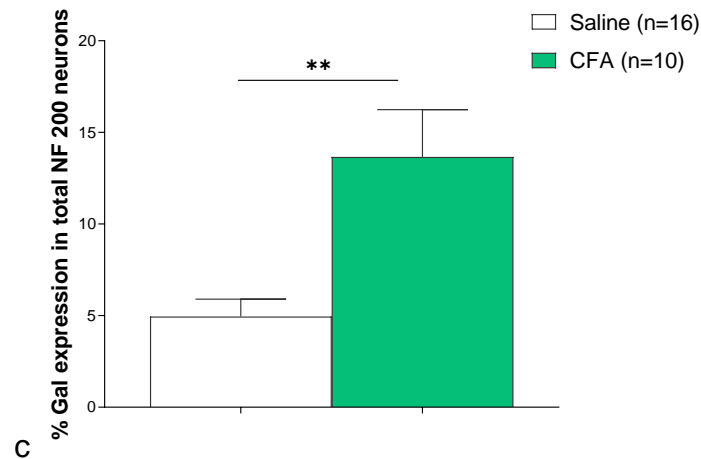
Figure 43. Representative immunofluorescence image of lumbar DRG sections of *Galanin Cre* +/ Rosa-CAG-flox-stop-tdTomato mice.

Galanin Cre expressing neurons (orange) colocalise (arrowheads) with NF200 positive neurons (green) in animals injected with CFA (b), unlike in the saline-injected group. (c) Staining quantification on mouse DRG sections showing a significantly increased expression of Galanin in NF200 positive neurons after CFA. Data are shown as Mean±SEM mixed gender with t-test analysis (P ≤ 0.01).

4.3.2 Galanin Cre + neurons correspond to small-diameter C fibres and have low expression in DRG

In situ hybridization on both groups of animals was analysed following the protocol already explained (see chapter 3). Samples from animals injected with saline (Figure 55) showed expression of *Galanin* mRNA in DRG neurons (in green) colocalised with tomato fluorescence (red), confirming the Cre activity of the promoter driven strain. I observed a low level of expression of gal positive neurons in DRG with almost none detected in big to medium neurons when using a *Nfh* probe (blue). This corroborates what has been already published and identify galanin positive neurons as small-diameter C fibres.
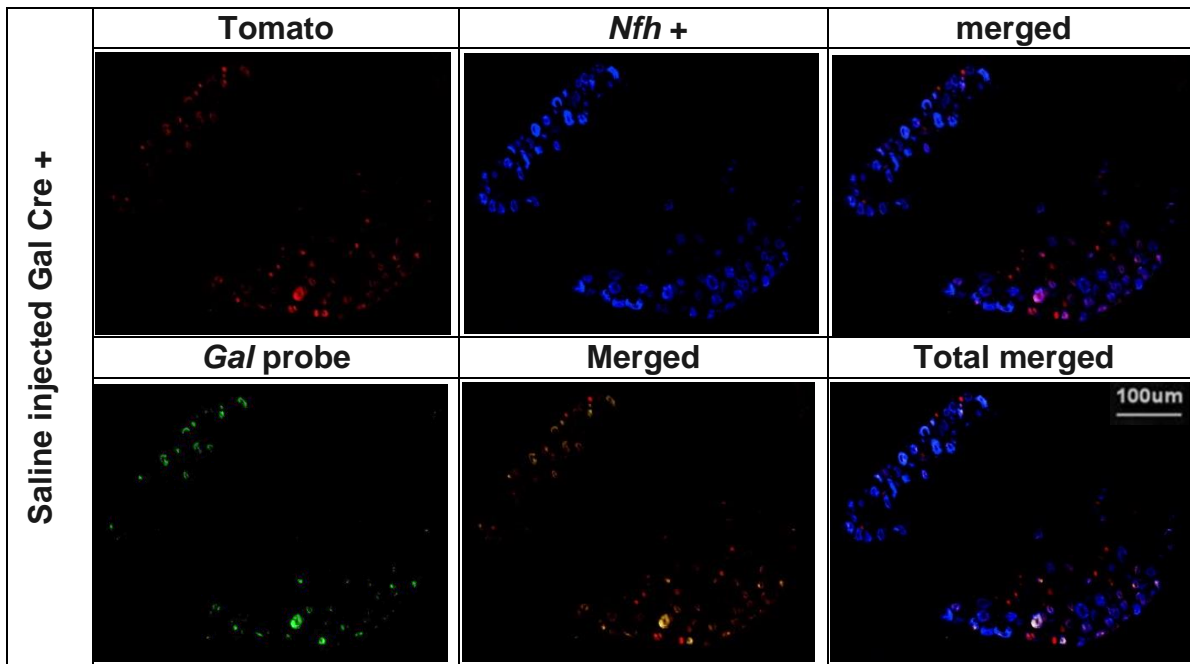
Figure 44. Representative images of *Gal* Cre +/ Rosa-CAG-flox-stop-tdTomato expression pattern in mouse DRG.

(1st row) large-diameter neurons *Nfh* positive in blue colocalised with *Gal* positive in red (merged). (2nd row) *Gal* mRNA expressing cells in green and their colocalization with Cre induced tomato red protein, confirming Cre activity.

RNAscope in the CFA injected animals (Figure 45) showed *Galanin* expression (red) and its messenger RNA (green) not only upregulated but colocalising in *Nfh* expressing neurons, confirming what has been seen at protein level.
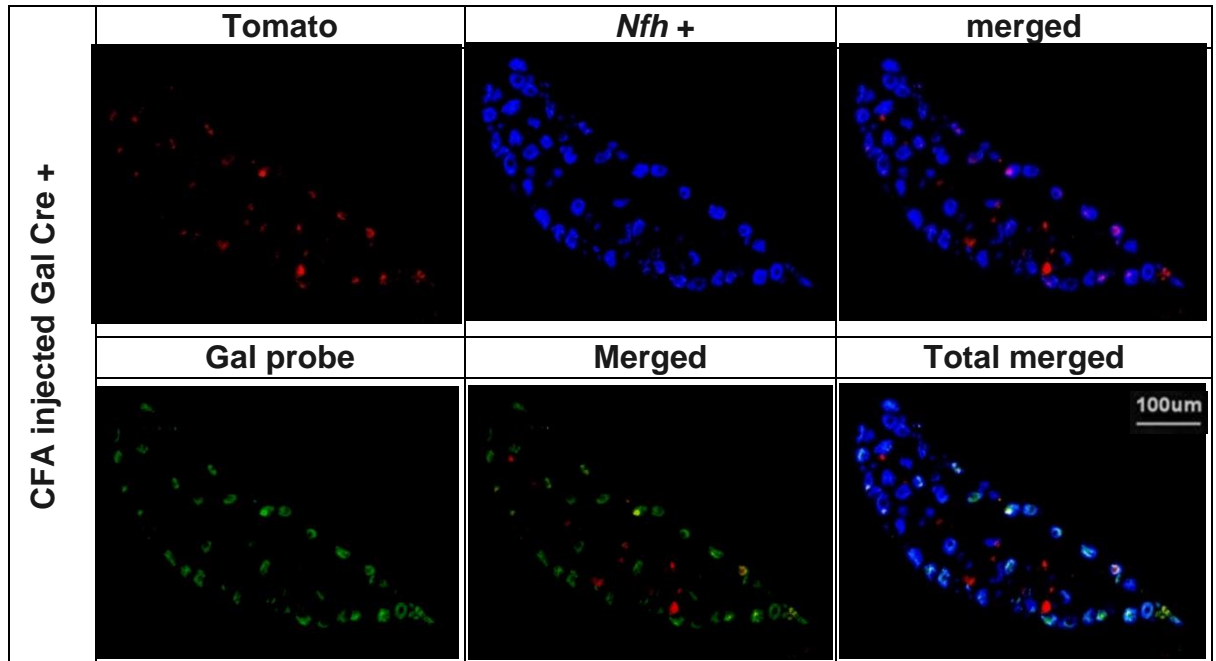
Figure 45. RNAscope representative images of *Gal* Cre +/ Rosa-CAG-flox-stop-tdTomato expression pattern in mouse DRG after CFA injection by situ hybridization. (1st row) large-diameter neurons *Nfh* positive in blue colocalised with *Gal* positive in red (merged). (2nd row) High levels of *Gal* mRNA in green and their colocalization with Cre induced tomato red protein, confirming Cre activity of the strain and *Gal* upregulation after injury.

4.3.3 Ablation of Cgrp DRG neurons is linked to altered responses in the inflammatory formalin test whilst the rest of the Cre lines analysed are normo-reactive.

I ablated different subpopulations of DRG neurons and analysed the possible deficits in sensory function during inflammatory pain in mice. Following the strategy already explained in the last chapter (see 3.3.2), I measured nocifensive responses of the different offspring following the intraplantar injection of 20 μl of 5% diluted formalin. This test comprises two phases, a short phase I or acute linked to direct nociceptor activation, and a subsequent phase II which involves inflammatory mediators (see chapter 4.2.2) (sampling recordings using a Python script obtained by Dr De Clausser).

Animals with different neuronal subpopulations ablated showed comparable pain behaviour to the common control without Cre, *Advillin* Flox-tdTomato-Stop-DTA (BAC) during the first 10 minutes corresponding to the first phase. However, the ablation of DRG CGRP positive neurons caused a significant behavioural deficit during the second phase, suggesting a role of CGRP expressing DRG fibres in inflammatory processing (Figure 46) whilst their associated paw oedema developed normally (data not shown). The number of males and females were not enough for statistical sex analysis in *Ntrk2* (TRKB), *Ntng1* and Th Cre/CreERT2 lines, so the graphs just show trends on males and or females when compared to the mixed sex analysis. Further experiments would be needed in order to conclude any sex dependent link to inflammatory responses.

a

b

c
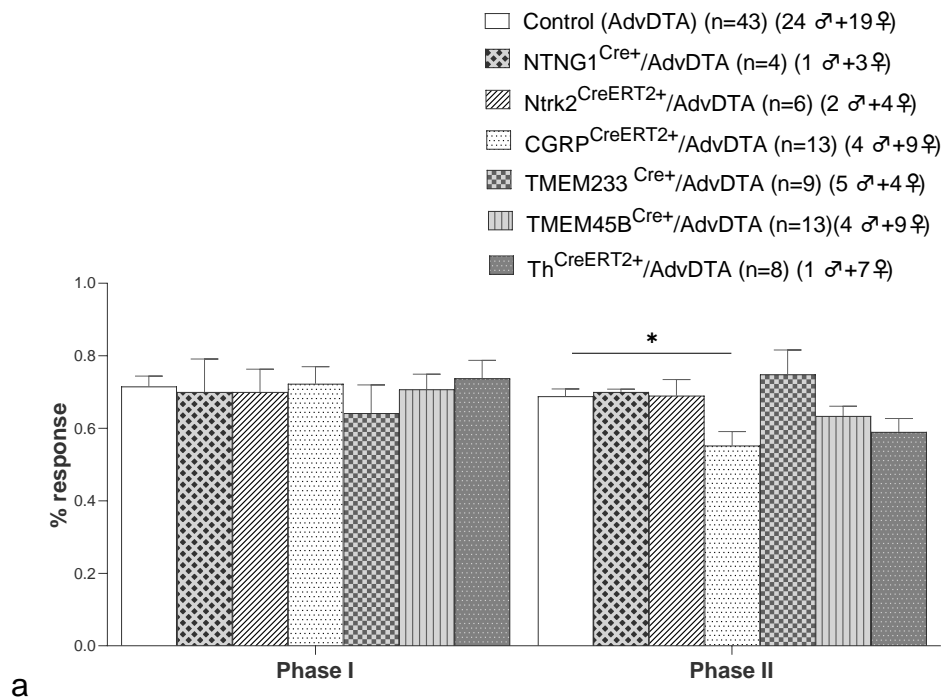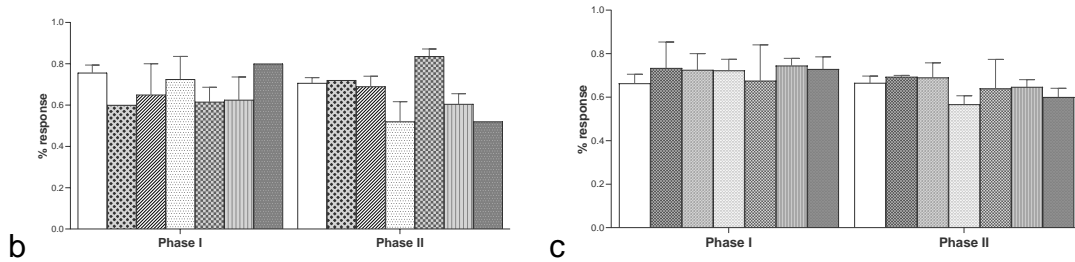
Figure 46. Behavioural responses of different neuronal ablated mice during the formalin inflammatory model.

(a)   Mixed gender analysis appears normal during phase I whilst animals lacking CGRP-positive DRG neurons show a decrease in response during phase II. (b) and (c) are representative graphs of males and females respectively. Data are shown as Mean±SEM with one-way ANOVA analysis ($P \leq 0.05$) on mixed gender graph.

4.3.4 Mice lacking TrkB positive DRG neurons have deficits in light touch sensitivity

In 2018, Heppenstall et al. identified peripheral sensory neurons expressing TrkB as light touch transmitters (Dhandapani et al., 2018) by using Cre targeted ablation and optogenetics. They generated a TrkB^{CreERT2} and crossed it with an Avil diphtheria toxin receptor line, allowing for the selective deletion of this subpopulation of neurons in male mice.

I used *Ntrk2*(TrkB)$^{creER+}$ mice already described (Rutlin et al., 2014b) and followed the conditional ablation strategy already explained in the last chapter three. Similarly to Heppenstall et al, I observed no differences in responses to various thermal and noxious mechanical tests (see 3.3.2) when compared with the controls. Furthermore, when I performed the cotton swab test, I again confirmed a significant reduction of responsiveness to the lightest mechanical stimuli in basal conditions when compared to animals where the diphtheria toxin is not present (Figure 47) analogously to the mentioned group findings.
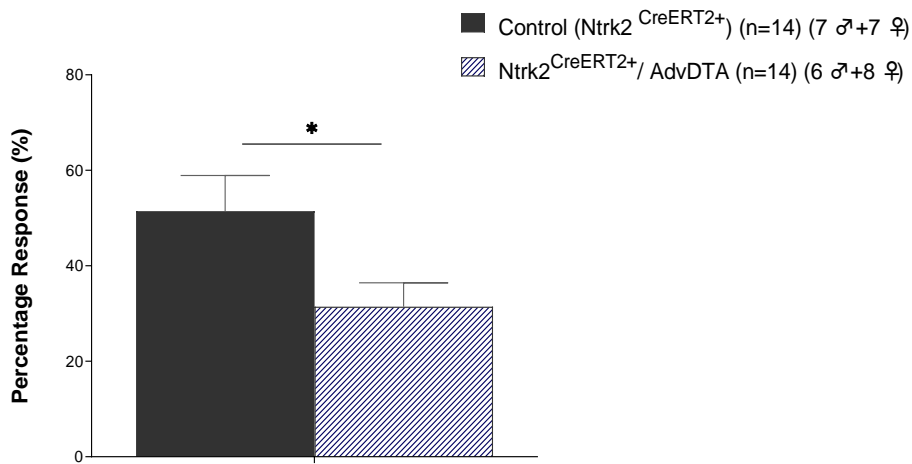
Figure 47. Light mechanical sensitivity is impaired in mice lacking Trkb (*Ntrk2*) positive DRG neurons

($P \leq 0.05$) when compared to controls (Ntrk2 CreERT2+ control). Data are shown as Mean±SEM mixed gender with t-test analysis.

4.3.5 TrkB positive DRG neurons are necessary for producing mechanical allodynia after a PSL neuropathic model

I performed a partial nerve ligation (PSL) neuropathic model in a group of male and female mice lacking TrkB positive DRG neurons (*Ntrk2* CreERT2+/ *Advillin* Flox-tdTomato-Stop-DTA) and compared them to their controls (*Ntrk2* Cre+). When assessing mechanical sensitivity to von Frey for 16 days, I found a reversed mechanical hyperalgesia associated with neuropathic models (Figure 48). This suggests a possible contribution to neuropathic pain of TrkB positive DRG neurons in this specific model, analogously to the effect after spared nerve injury (SNI) already reported (Dhandapani et al., 2018).
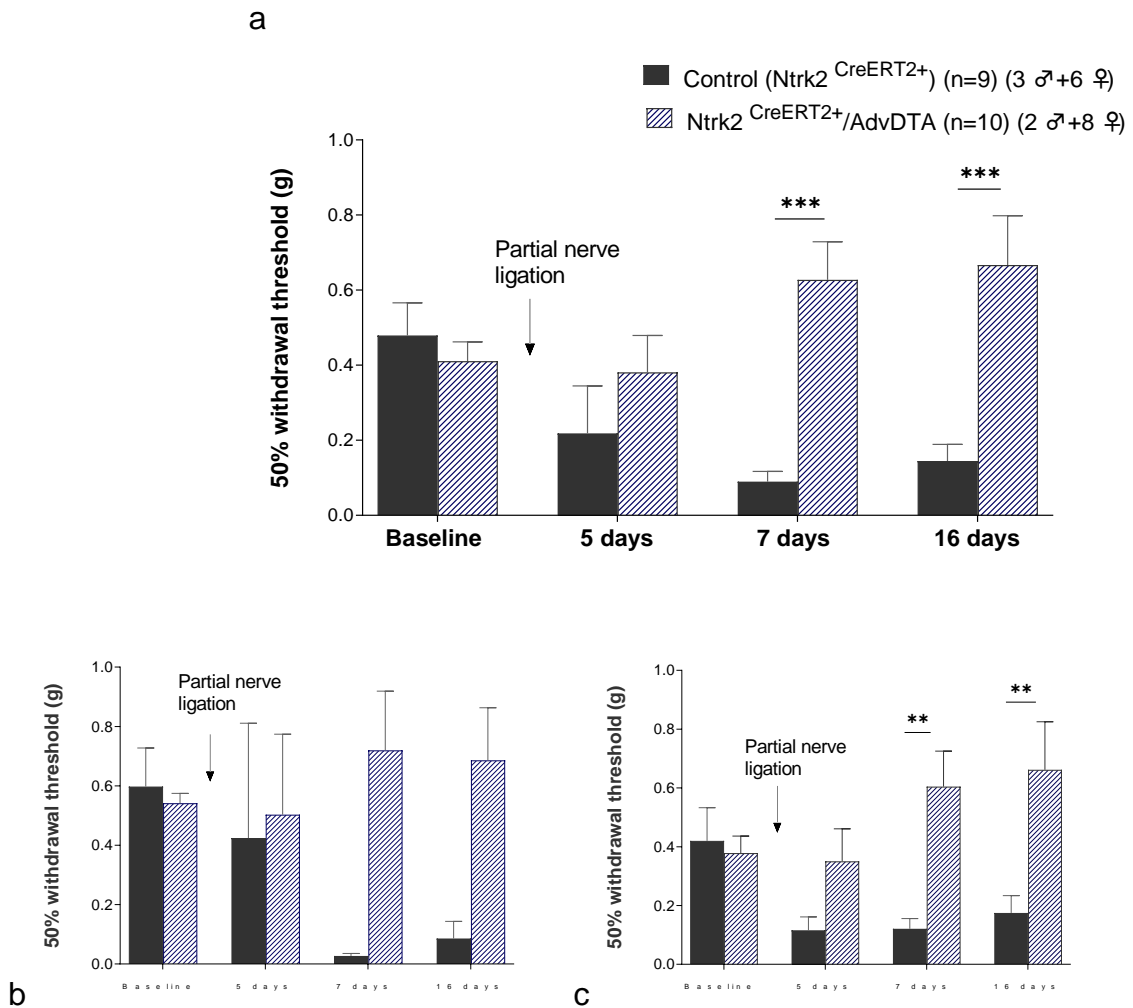
Figure 48. Mechanical behavioural responses of *Ntrk2*[Cre+] */Adv*DTA (blue stripes) and littermate Cre controls following PSL.

Response to Von Frey hairs show significantly attenuated mechanical sensitivity over 16 days (a) (P ≤ 0.001). (b) Males and (c) females (P ≤ 0.01) trend respectively. Data are shown as Mean±SEM with ANOVA analysis in mixed gender and female graphs.

We were unable to draw sex difference conclusions due to the lack of male individuals to perform statistical analysis, albeit still useful to observe trends.

4.3.6 Mice lacking TrkB positive DRG neurons develop bone cancer associated pain normally

To investigate the role of TrkB positive peripheral fibres in cancer pain, I implanted Lewis Lung carcinoma cells into the femur of adult mice lacking DRG TrkB positive neurons and their littermates. I analysed their behaviour over 20 days, and approximately 9 days after the cancer induction, I started to observe a reduction of limb use and weight bearing of the affected leg in all animal groups (Figure 49). A limb score of 0 (lack of use of the affected limb) was used as the endpoint. The severity of these deficits, as well as survival rate, did not significantly differ between $Ntrk2^{Cre+}$/AdvDTA animals and their controls, suggesting no implication of this subset of neurons in the development of CIBP.

a
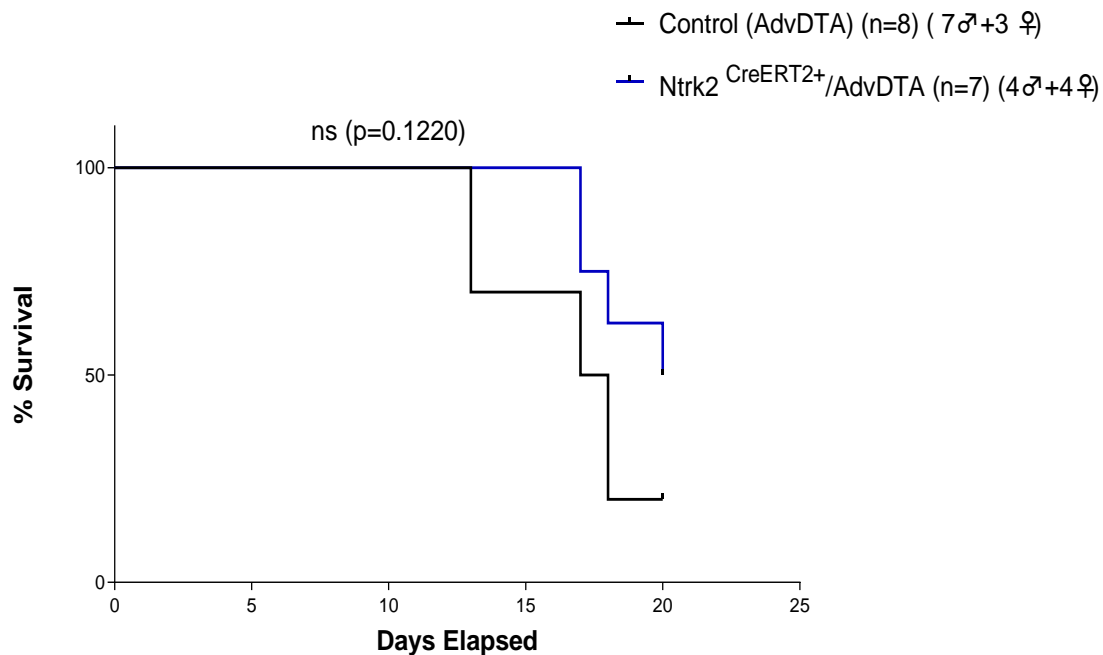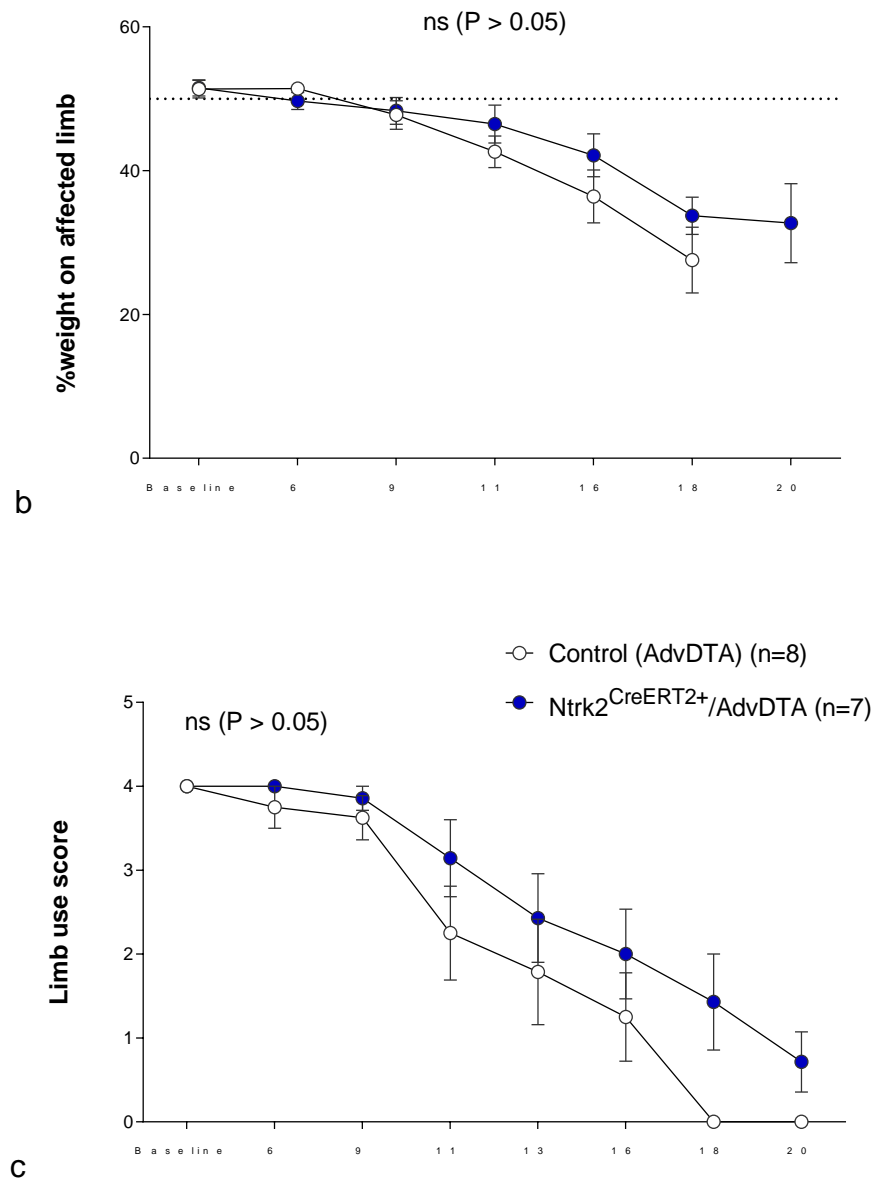
Figure 49. Bone cancer pain develops normally in *Ntrk2*CreERT2+ */Advillin* Flox-tdTomato-Stop-DTA mice.

(a). Survival curve for littermates *Ntrk2*Cre+ */Adv*DTA (black line) and *Adv*DTA (blue line) does not significantly differ. (b). Weight bearing on the affected limb decreases with the progression of CIBP in both groups. (c) Limb score reduction curve. Data are shown as Mean±SEM mixed gender with Log-rank (Mantel-Cox) test analysis in a and ANOVA analysis in b and c.

4.4   Discussion

The dorsal root ganglion (DRG) is composed of first-order neuron cell bodies and serves as a communication centre between the peripheral and central nervous systems. Initially it was considered a passive supporting structure, but recent findings reporting anatomic and physiologic changes as a result of the micro-environment, suggest that DRGs have a dynamic role in neuromodulation.

The gene expression patterns of DRG neurons are markedly changed in animal models of chronic pain, induced by peripheral nerve injury or inflammation. The reasoning behind this relies in the understanding of chronic pain not as a prolonged form of acute pain, but as the result of plastic modifications occurring at several levels of the pain circuitry beyond the healing process (Wood, 2020). The maladaptive transition from protective pain to persistent is initially triggered by tissue damage or inflammation. Immediately after the insult, both neuronal and immune cells infiltrate the injured tissue ultimately leading to the sensitisation of primary afferents driven by the inflammatory soup. The stimulus-driven pain relies not only on injured nerves but also upon intact, uninjured sensory neurons that transmit the signals to the central nervous system. Injured, uninjured or silent nociceptors suffer neurophysiological changes and become active participants in both initial sensitivity and transmission (Basbaum et al., 2009a, Torsney, 2019). Importantly, *in vivo* calcium imaging studies during cold and heat stimulation have shown that stimuli-specific nociceptors can become polymodal after a persistent and more intense input (Emery et al., 2016), and different mouse pain models have been reported with a unique set of altered transcripts and therefore underlying mechanisms (Bangash et al., 2018). Whilst the literature contains examples of genes found relevant in pain-modality specific disorders (Minett et al., 2014a, Habib et al., 2017), plasticity and redundancy in the pain circuitry reduce the chances of finding one single target in the race for an improved analgesia.

This chapter constitutes an extension of chapter three, where I explored if transcriptomic heterogeneity among DRG neuron types correlates with the functional diversity in somatosensory processing. The expression pattern analysis and phenotyping described in the last chapter provide valuable information to understanding the primary afferent molecular architecture and their

associated functions. However, they represent only the physiological, and not the pathological states of DRG neurons. Given the importance of plasticity and redundancy to address the diversity of pain mechanisms, it is important to tune any newly established census of DRG primary afferents (Zeisel et al., 2018b) in different disease-like scenarios.

Firstly, I studied the potential plastic adaptive expression changes of *Galanin* after an inflammatory injury. Following the strategy from chapter three (see chapter 3.2.2), I crossed *Galanin* promoter-driven Cre mice (Gong et al., 2007) with a reporter tomato mouse, and analysed the expression pattern changes after a CFA hind paw injection, by RNAscope and immunohistochemistry. Cre targeted gene expression in control animals injected with saline recapitulates the predicted endogenous *Galanin* distribution pattern in uninjured DRG neurons (Zeisel et al., 2018b). Following CFA induced injury, galanin expression significantly increased in the DRG Figure 42). I report the newly expressed *Galanin* to be within the NF200 positive neurons (Figure 43), confirming previous findings on gene expression changes after nerve injury (Villar et al., 1989). Phenotypically, functional studies have shown increased neuropathic pain-like responses in animals lacking the *Galanin* receptor (Blakeman et al., 2003) and reduced constriction injury derived allodynia after intrathecal administration of this peptide (Holmes et al., 2003b). Whether exogenous administration of Galanin and its antagonists in CFA injured animals leads to a comparable effect remains unknown and could be interrogated in follow up experiments (see future directions in chapter 4.6).

The newly developed experimental framework on hyperalgesic priming (see 1.5.2) has appointed neuronal plasticity as one of the key mechanisms for pain chronicity (Ferrari et al., 2015), and they have contributed to the identification of glial cells and their neuroimmune interaction as transition modulators from acute to chronic pain (Torsney, 2019). Considered the inherent immune cells of the nervous system, microglia have the ability to adopt a variety of morphological and functional phenotypes not only to adapt to motor skill learning (Xiao et al., 2016) but also as a consequence of injury and inflammation (Salter & Stevens, 2017). Among the studies on their main players, DTX-induced ablation of oligodendrocytes have shown pain hypersensitivity even before the initial

inflammatory response and loss of myelin (Gritsch et al., 2014). Whether or not the recently discovered heterogeneity in their transcriptomic profile leads to different functionality is still to be discovered (Zeisel et al., 2018b, Marques et al., 2016). In addition, astrocyte inhibitors have been reporting successful results in attenuating hyperalgesia induced by nerve injury and CFA injection in males (Sorge et al., 2011). Interestingly, female mice insensitivity to microglial inhibition was found to switch to a microglial dependent pathway in the absence of adaptive immune cells.

Plasticity and sex specificity have been reported across almost all forms of chronic pain with increasingly uncovered peripheral nociceptive mechanisms, spinal pain processing, and descending regulatory control (Wood, 2020). Although it is not limited to microglia, it highlights the importance of follow up experiments to determine not only male/female differences in chronic pain development but also to incorporate the increasing information about neuroglia and their connections with the nervous system.

Given the revolution in transcriptomic discoveries and data to hand, I exploited the battery of Cre lines available from the last chapter in order to identify any nociceptor subtype as key for inflammatory pain, by using the formalin test.

The injection of formalin into the hind paw induces a biphasic pain response by directly activating the transient receptor potential A1 (TRPA1), a cation channel that plays an important role in inflammatory pain. At behavioural level, pharmacologic blockade (by TRPA1-selective antagonist) or genetic ablation of TRPA1 produced marked attenuation of the nocifensive responses derived from the injection of formalin in phase I and II (McNamara et al., 2007). According to transcriptomic data, all lines studied herein with the exception *Ntng1* , present *TRPA1* expression of some degree (Zeisel et al., 2018a). Whilst we have not found significant differences during the first phase on none of them, nocifensive behaviour during the second phase was found to be significantly reduced in mice lacking *CGRP* positive afferent population (Figure 46) seemingly, in a sex independent fashion. The associated paw oedema developed normally suggesting that lacking this neuronal subpopulation does not inhibit the inflammatory processes but the nociceptors' activity. The behavioural deficit in phase II shown in this study correlates with phenotypic and electrophysiological

results on *CGRP*–null mutant mice that identify this cluster as an attenuating contributor to mechanisms of sensitization in animal models of inflammation and neuropathic pain (Salmon et al., 2001). The phenotype has been reported only on the phase II of the formalin test, proposed to reflect the combined effects of afferent input and central sensitization in the dorsal horn. This contributes to the increasingly strong evidence towards a pronociceptive sensitizing role of *CGRP* not only of primary afferents but also of second-order pain transmission neurons within the central nervous system. Recent studies using immunofluorescent histochemistry and anterograde axonal tracing techniques found that the large-diameter CGRP neurons most likely are high-threshold mechanosensitive Aβ and Aδ fibres that synapse with wide-dynamic-range (WDR) neurons of laminae IV and V, allowing this fibres to influence nociceptive inputs and central sensitization by the development and maintenance of a sensitized, hyperresponsive state (Kestell et al., 2015). This contribution to central sensitization has already been pragmatically translated into the development of CGRP blockers to treat migraine in the clinic (Benemei et al., 2009). Besides, CFA and carrageenan induced inflammatory models have also revealed that central sensitization associated with the enhanced abnormal pain responses in the inflammatory pain state is mediated in large part by elevated CGRP expression in DRG neurons (Benemei et al., 2009).

Along with *CGRP*, ablation studies on *Ginip (Phf24)* positive neurons whose expression signature falls within MRGPRD and C-LTMRs, have been found to significantly alter formalin-evoked pain responses (Urien et al., 2017). Since *MRGPRD* positive afferents have already been identified as dispensable for formalin-inflammatory hypersensitivity (Shields et al., 2010), the study goes into predicting C-LTMRs as essential in this type of pain. Whilst I cannot categorically void this prediction due to the low n numbers in some of the groups, I could not find any behavioural deficit in this test when the *Th* positive subpopulation was ablated (Figure 46). Further investigation would be required to confirm a possible combinatorial effect of both MRGPRD and C-LTMRs as responsible for *Ginip* behavioural deficits in the formalin test instead of additive phenotypes.

The identification and targeting of the specific components driving chronic pain could potentially improve currently inefficient pain management in the clinic. Evidence suggests the existence of different mechanisms and neuronal

subpopulations in different types of pain, which makes this task very complicated. For example, DTA mediated ablation of *Scn10a* DRG neurons have been reported essential after inflammatory insults while dispensable after nerve injury (Abrahamsen et al., 2008). In contrast, TrkB positive neurons have been found responsible for the reversal of mechanical allodynia on SNI neuropathic pain with no effect in a CFA model (Dhandapani et al., 2018).

Since even phenotypically identical neuropathic pain models have been suggested to have different underlying mechanisms in *Scn9a* studies (Minett et al., 2014a), I interrogated the implication of TrkB (*Ntrk2*) positive neurons in a partial nerve ligation neuropathic pain, to date not reported. Belonging to the large-diameter low-threshold mechanoreceptive (LTMRs) group of fibres, I used the Trkb^{CreERT2} already characterised in the last chapter and showed a reversed mechanical hyperalgesia after surgically induced nerve injury (Figure 48). This is analogous with previous work by Heppenstall et al. and suggests a possible common contribution of TrkB positive DRG neurons to different sub-modalities of neuropathic pain. Whether this mechanism is sexually dimorphic as suggested by transcriptomic studies after several peripheral nerve injury models (Ghazisaeidi et al., 2019) (Lopes et al., 2017) remains unknown and it would be necessary to increase n number in order to obtain sex specific conclusions. Besides, the TrkB receptor binds to BDNF which has been recently identified as the link through microglia to neurons during neuropathic pain (Coull et al., 2005). Further studies on BDNF expression changes in microglia in these animals would be interesting for a deeper mechanistic understanding.

Lastly, I interrogated the role of TrkB rich peripheral fibres in bone cancer pain. Since the discovery of the oncogenic properties of certain *Ntrk* gene family fusions (Joshi et al., 2019), several lines of investigation have been interrogating their role in cancer. Overexpression of TrkB in the tumour has been found to inhibit programmed cell death, resulting in an oncogenic effect (Geiger and Peeper, 2007). Even when these results contribute to the increasing cancer patient life expectancy, pain management is still underdeveloped. Wide range *NTRK* neurotrophin receptor inhibitors such as Entrectinib (Doebele et al., 2020) or ARRY-470 have been shown to attenuate evoked pain behaviours in models like the cancer-induced bone pain (CIBP) and suggests neurotrophins as involved in its mechanism (Ghilardi et al., 2010). Since that study does not

distinguish between the three *Ntrk* receptors, I interrogated the role of Trkb coded by *Ntrk2* on a CIBP model. I report that the deletion of Trkb expressing neurons in mice DRG does not have any effect on the pain development (Figure 49) when compared to their controls, suggesting other neurotrophin subclusters or the summative effect of all of them as responsible for the analgesic effect reported by Ghilardi.

Furthermore, tomography imaging and histology studies on metastatic prostate cancer tissues have found increased TrkB expression and are believed to drive metastatic bone formation (Faltermeier et al., 2016). Elevated osteoclast activity and associated resorption are one of the hallmarks of many metastatic cancers (Mundy, 2002). Bone targeting agents such as Denosumab have shown promising analgesic results in cancer patients however its mechanism of action is unknown. There is a complex interaction between cancer cells and bone-resident cells, where the tandem osteoclast/osteoblast differs depending on the type of cancer. Breast cancer has been reported to spread in the bone by osteolytic metastases, while prostate does it via osteoblastic (Maroni and Bendinelli, 2020). Whilst bone density quantification would benefit our study, we cannot ignore that the current results depend on variability in the osteoclastogenic potential of the cancer cells used, both in terms of cell passage as well as the type of cancer used as an initiator (Lewis Lung carcinoma in this study).

Lastly, a final consideration should be made to investigate changes in the bone microenvironment such as the sensitising acidosis derived from osteoclast activity or pro-inflammatory cytokine release potentially translated into pain behaviour in mice.

In summary, our results contribute to the key scientific findings suggesting the existence of different pathways involved in pain states, and the importance of both developmental plasticity and sex in determining the nociceptive function leading to the individual pain experience. In addition, our investigation continues last chapter's validation of the use of the novel *Advillin* Flox-tdTomato-Stop-DTA BAC strain as a useful resource for further functional characterization of somatosensory processing, neuro-immune interactions and chronic pain disorders.

4.5   Conclusions

-Peripheral neuron *Galanin* expression analysis is significantly upregulated after CFA induced inflammatory injury. These results are analogous to those reported after nerve injury and highlight a functional role for this peptide in nociception.

-Although I could not confirm or discard the previously suggested role of C-LTMRs as essential in formalin-induced pain, I report the ablation of CGRP positive neurons as an attenuating contributor to sensitisation mechanisms in this model.

-Behavioural analyses herein have identified *Ntrk2* rich DRG neurons as necessary for the mechanical pain hypersensitivity derived from a PSL neuropathic model, whilst dispensable for the development of cancer-induced bone pain.

4.6   Future directions

The work in this thesis used transgenic techniques to explore the mechanisms responsible for pain both in physiological (chapter three) and pathological conditions where plasticity has been identified as key in the transition from acute to chronic pain.

Our findings on *Galanin* as a modulator of CFA induced pain could benefit from further behavioural experiments to evaluate if its reported upregulation corresponds to increased pain like responses. Based on promising results on the exogenous administration of Galanin after nerve injury reported (Holmes et al., 2003b), it would be interesting to extend the study of this peptide as an analgesic target in a CFA inflammatory model.

Newly discovered evidence appoints glial cells and neuroimmune interactions as pain chronification modulators (Wood, 2020) which had not been addressed in this report. Extending the study of DRG neurons to their surrounding glia and reciprocal interactions between the immune and nervous systems would improve our understanding of the transition mechanisms from acute to chronic pain.

Since the present chapter is a continuation of chapter three, the limitations discussed there do apply also here. As such, and since sex specificity has been

reported across almost all forms of chronic pain, it would be necessary to increase the n number of animals in the groups for statistical male/female analyses. The discovery of male and female potentially different phenotypes would uncover if the herein identified role of Trkb rich neurons in neuropathic pain is sexually dimorphic.

On this line, including more animals in the formalin test investigation would also contribute to resolving the inconclusive results obtained in respect to the role of C-LTMRs previously suggested as essential for this model in the *GINIP* study (Urien et al., 2017).

The contribution of the *Ntrk2* neuronal subpopulation in cancer-induced bone pain is, albeit informative, incomplete on its own. Subsequent bone degradation quantification via micro-CT would be very important not only for further confirmation of the existence of cancer in the bone but also to link the observed behaviour with bone density changes. In addition, we could investigate the putative TrkB driven metastatic bone formation (Geiger and Peeper, 2007) and its subsequent effect on the surrounding microenvironment. Lastly, we could adjust the CIBP model by modulating the osteoclastogenic potential of the cancer cells to evaluate any neuronal depletion effect in a milder survival rate curve in males and females independently.

Chapter 5 - *Zfhx*2 gene targeted mouse models

5.1   Summary

Congenital analgesia is a human heritable disorder characterised by an absence of pain to normally noxious stimuli. Although rare, the study of affected families and the identification of the causative mutations can provide important insights into the pain system. For example, recessive loss of function mutations in the *SCN9A* gene cause a complete inability to perceive pain and for some years has been heavily studied as an analgesic drug target.

By exome sequencing an Italian family with pain insensitivity, a potential causative missense mutation was identified in *ZFHX*2. Whilst the normal function of this gene in mice is poorly understood, the high expression of this transcriptional regulator in the brain and DRG nociceptors suggests that it may play a role in pain pathways.

The aim of this chapter is, by using transgenic techniques, to explore the contribution of the *Zfhx2* gene in physiological and pathological pain conditions in rodents. By establishing a model for a better understanding of the Marsili family hypoalgesia syndrome I have provided a platform for possible future gene therapy analgesic treatments.

-Initially, I used an already reported *Zfhx2-/-* global functional knockout mouse model to investigate the role of *Zfhx2* as a gene in pain perception both in acute nociception and under normally painful conditions.

-Secondly, a new BAC transgenic mouse line overexpressing copies of the orthologous *Zfhx*2 mutation (R1907K) was analysed. I studied the pain phenotype in acute, inflammatory, and neuropathic pain models.

Pain behavioural analyses show that the *Zfhx2* gene affects pain thresholds with the BAC transgenic mouse displaying significantly longer withdrawal latencies to noxious thermal stimuli. Although the transgenic mouse model does not fully recapitulate the phenotype observed in the human family, the model has helped to validate the *ZFHX2* gene as a potential new analgesic drug target.

5.2   Introduction. Marsili family clinical background

The pain insensitive phenotype in the Italian Marsili family was first described in 2008. Six members of the same family were phenotypically characterized by hyposensitivity to noxious heat and painless bone fractures (Figure 50) (Spinsanti et al., 2008): The subjects were belonging to the same family (spread in three generations), including a 75-year-old woman, her two daughters (40-year- old and 34-year-old sisters) and two nephews (two brothers, 14 and 11 years old). Subsequently a female cousin of the two brothers was also identified as presenting with the disorder. All these individuals were apparently healthy, with normal mental ability and high performance in physical activities, with an apparently normal quality of life. The main clinical data refers to their absence of pain in response to usual painful stimuli (all subjects), low sensitivity to capsaicin (all subjects), history of clinical autonomic disability, plus several episodes of hyperthermia, increased warm and cold thresholds, recurrent infections (three subjects), absence of corneal reflex (all subjects) and rare episodes of orthostatic hypotension (three subjects).
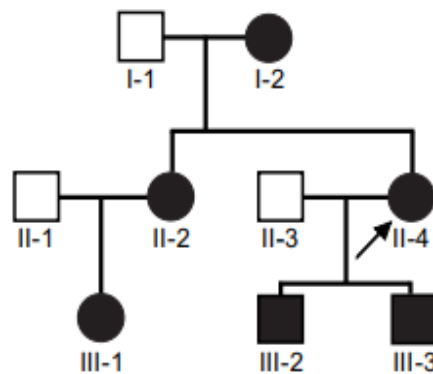
Figure 50. Autosomal dominant inheritance of the pain insensitivity Marsili syndrome. In black, individuals are affected by pain insensitivity. Individual II-4 (arrow) also reported a pleasurable sensation at high mechanical thresholds.

The inherited pain phenotype was evident in all six affected members. In contrast to *SCN9A*-CIP patients, the pain insensitivity was not global with, for example, some visceral pain being normally perceived by them. They reported significantly low sensitivity to capsaicin, however, it is worth mentioning that during the test an

immediate very intense pain following capsaicin injection was recorded that, very unusually, abruptly disappeared.

Analysis of a skin biopsy indicated a normal intraepidermal nerve fibre density for age and sex, after staining with anti Pgp9.5 (Data from Prof Bennett, University of Oxford) indicating that the phenotype was likely not related to a neuropathy (Figure 51). Consequently, genomic DNA was isolated from the blood of all affected members and analysed by exome sequencing to identify the pathogenic variant.
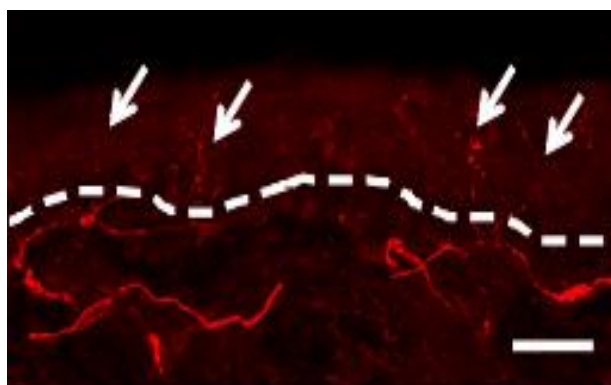
Figure 51. II-4 Individual's skin biopsy from the lower leg.
Dermal-epidermal intersection represented by a discontinued line and nerve fibres with arrows stained with anti-Pgp9.5 (red). Data from Prof Bennett, University of Oxford.

Sanger sequencing data were analysed by Habib et al. (2008) and a novel point mutation was identified in the Zinc finger homeobox (Hox) 2 gene (*ZFHX2*), which encodes a large transcription factor of 2572 amino acids. The point mutation (R1913K) maps to the second Hox domain in *ZFHX*2. A Hox domain is a structure with 60 amino acids folded in three helical regions folded again in a tight globular structure (Qian et al., 1989) that binds to DNA and regulates downstream gene expression and function. Mutations in Hox domains have been reported as pathogenic, causing several diseases and abnormalities of the brain due to a change in their rigid structure and binding specificity to DNA, leading to downstream transcriptional inactivity (D'Elia et al., 2001).

In order to assess the likely pathogenicity of the *ZFHX2* genetic variant, it was important to know how conserved the mutated Hox domain is across species.

Located at position 1913, the mutation changes a Guanine (G) to Adenine (A) which translates into an amino acid change from a highly evolutionarily Arginine (Arg-R) into a Lys(K) (Figure 52).

G→A mutation

AGGGCCCGGGAGANGAAAGGCCAGTTTCG
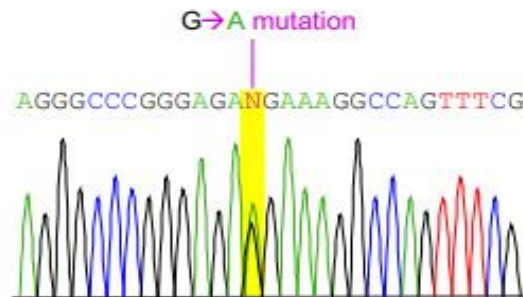
Figure 52. Sanger sequencing from Marsili samples.

It confirms the point mutation (G>A) in all affected individuals (as heterozygotes) and is absent in all controls. In yellow is the position of the mutation.

Interestingly, the *ZFHX2* point mutation resulting in that amino acid change has been found invariantly conserved across all known orthologous Tetrapoda (four-limbed animal superclass) (HomoloGene 52657) for that position (Figure 53), when comparing across species using data provided by the UCSC Genome Browser.

Mutation	QVWFQNTRARE**K**KGQFRSTP
Human	QVWFQNTRARE**R**KGQFRSTP
Chimp	QVWFQNTRARE**R**KGQFRSTP
Dog	QVWFQNTRARE**R**KGQFRSTP
Cow	QVWFQNTRARE**R**KGQFRSTP
Mouse	QVWFQNTRARE**R**KGQFRSTP
Rat	QVWFQNTRARE**R**KGQFRSTP
Frog	QVWFQNTRARE**R**KGQYRGAP

Figure 53. The protein sequence of *ZFHX*2 homolog across species.

Arg 1913 (humans R1913 aa /mouse R1907aa) is highly conserved at the residue.

In mice, the *Zfhx2* homolog is highly expressed in the thalamus, hypothalamus and midbrain (Komine et al., 2006) as well as in small-diameter DRG neurons (Usoskin et al., 2015b), both essential areas in pain perception and processing (Figure 54).
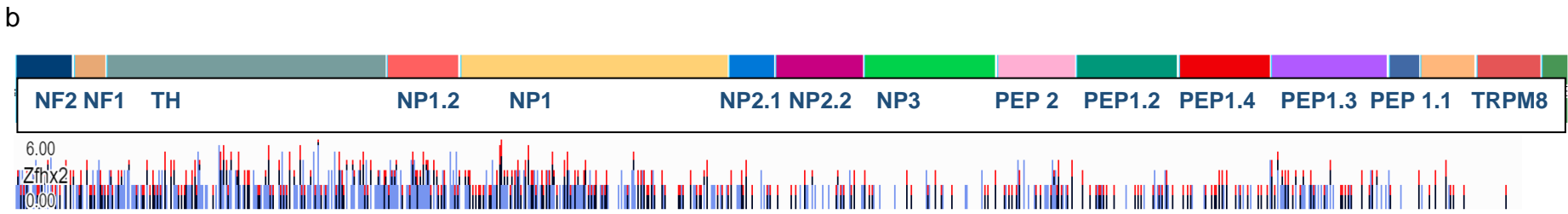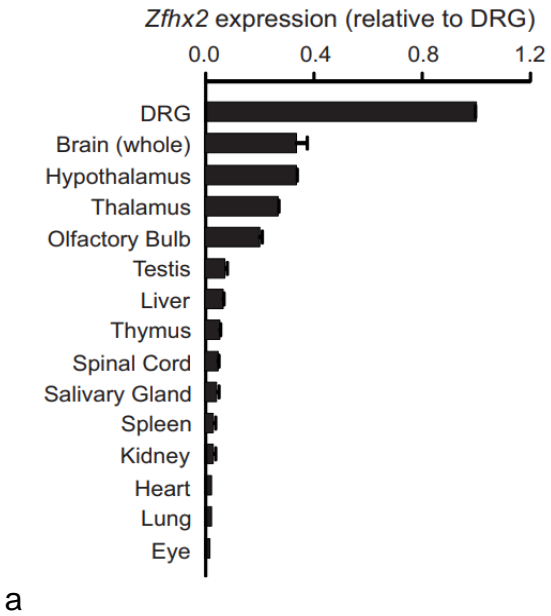
Figure 54. (a) *Zfhx2* expression relative to DRG in different mouse tissue. (b) Single-cell RNAseq data of *Zfhx2* expression in DRG relative to the major subtypes of mouse sensory neurons revealed by Ernfors group (Usoskin et al., 2015a) showing an enriched expression in nociceptors.

5.3   Results. *Zfhx2* gene targeted mouse models

Genetically engineered mouse models can mimic human phenotypes and help to evaluate underlying mechanisms and potential treatments once a "disease allele" is identified (see chapter 1.5). In this chapter, two different mouse models are characterized that can be used to better understand *Zfhx2* function in pain pathways.

5.3.1 *Zfhx2* global functional gene knockout

Mouse and human *Zfhx2*/*ZFHX2* genes (initially called *Zfh-5*) each consist of ten exons located on chromosomes 14C2 and 14q11 respectively with the genes cloned in 2006 (Komine et al., 2006). Isolated from the developing mouse brain, this novel transcription factor is expressed in most differentiating neurons of the CNS (central nervous system). Where it is not expressed, like in pyramidal and granule cells in the hippocampus, *Zfh-2* antisense RNA transcripts were reported.

Komine et al. created two gene-targeting mouse lines. One presented a 6kb deletion in the antisense control region (ASC). A second one was a knock-in *Zfh-2* mouse line with insertion of an EGFP-stop codon (polyA) cassette within the *Zfh-2* coding region open reading frame (ORF or translating frame), translating into a global functional *Zfhx2* targeted knockout mouse. When studying expression profiles by *in situ* and northern hybridization, the generated mutant mice with deleted *Zfh-2* antisense RNA appeared to have up-regulation of *Zfh-2* RNA, suggesting a *Zfh-2* antisense RNA negative regulatory role on *Zfh-2* expression.

5.3.1.1 Zfhx2-deficient mice (Zfhx-egfp). Breeding strategy

An initial behavioural characterisation of the *Zfhx2*-deficient mouse line was first published in 2013 (Komine et al., 2013), reporting hyperactivity, enhanced depression and altered anxiety. We initially received homozygous knockout (Zfhx2$^{-/-}$ KO) animals (from the National Institute for Basic Biology, Okazaki, Japan), which were crossed with C57BL/6J mice to generate heterozygous offspring. Several heterozygous breeding pairs were set up concurrently to gather

a battery of age (9-12 weeks old) and sex matched *Zfhx2-/-* KO mice and wild type (WT) littermate controls.

The genotype of every pup was confirmed using PCR of genomic DNA isolated from ear samples (2.2), identifying WT, Zfhx2+/- heterozygous or homo Zfhx2-/- KO mice for the gene.

5.3.1.2 Zfhx2 homozygous knockout mice have altered pain thresholds

After confirming normal motor-coordination by the Rotarod test (Jones and Roberts, 1968) (Figure 55), animals were tested for innocuous mechanosensation in the glabrous skin of the paw, where they showed no change in paw withdrawal threshold (PWT) during the von Frey test nor in response to stimulation with a cotton swab (light touch) (Figure 55). All data are shown as adults (9-12 weeks) mixed gender.
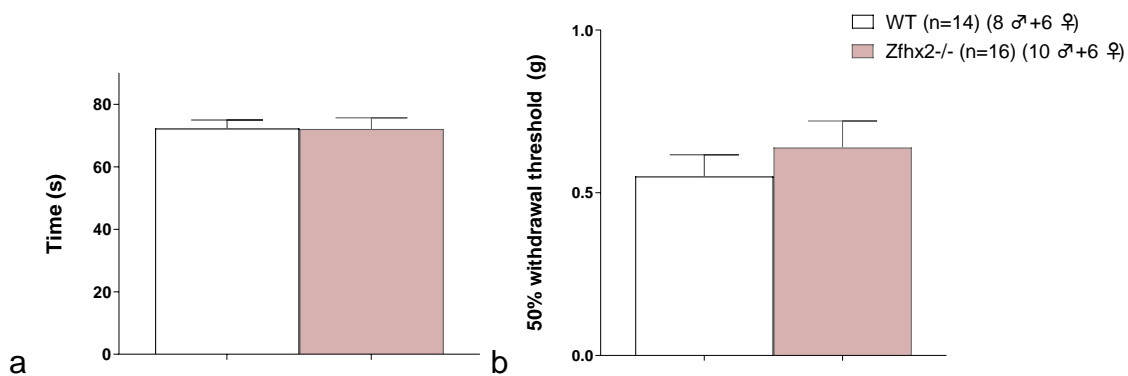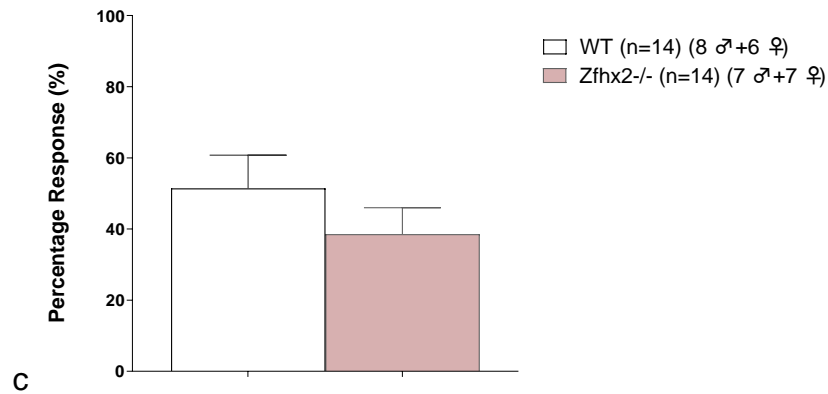
Figure 55. *Zfhx2*^{-/-} KO mice are normal in von Frey, rotarod and cotton swab tests. Unimpaired motor coordination compared to WT control littermates with comparable latency to fall from an accelerating rotarod (a) Unaltered paw withdrawal in response to von Frey hairs (b) or a cotton swab (c) on paw when compared to control littermates. Data are shown as mean ± S.E.M., mixed gender and analysed by t-test.

Data obtained from the Randall-Selitto test showed a significant difference in sensitivity to noxious mechanical stimuli when applied to the tail of the animals lacking functional Zfhx2 (Figure 56) compared to their littermate controls both in male and female cohorts. The force at which Zfhx2-/- KO animals responded to noxious mechanical stimulation on the tail was greater than in WT. This phenotype correlates with what has been reported in human Marsili patients.
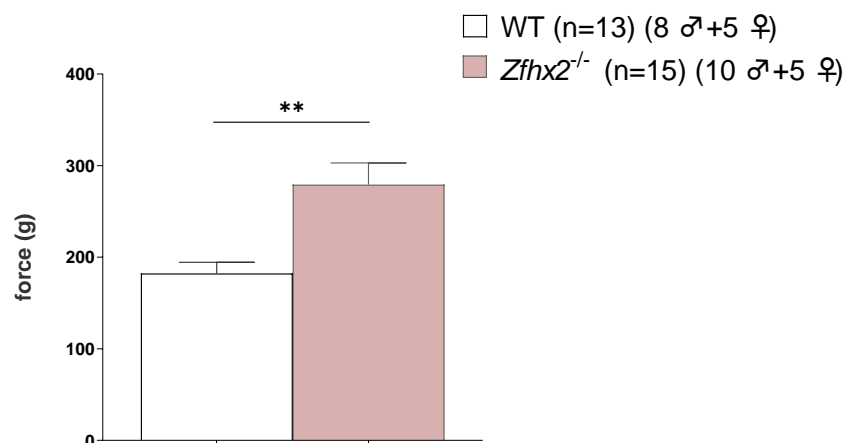
Figure 56. Noxious mechanosensation is impaired in *Zfhx2*^{-/-} KOs.
Hyposensitivity was observed when using the Randall-Selitto apparatus applied to the tail. Data are shown as mean ± S.E.M., mixed gender and analysed by t-test.

Responses to cold stimuli were tested using the acetone and thermal place preference tests. Both tests showed no differences in cold sensitivity between WT and *Zfhx2*-/- KOs (Figure 57).
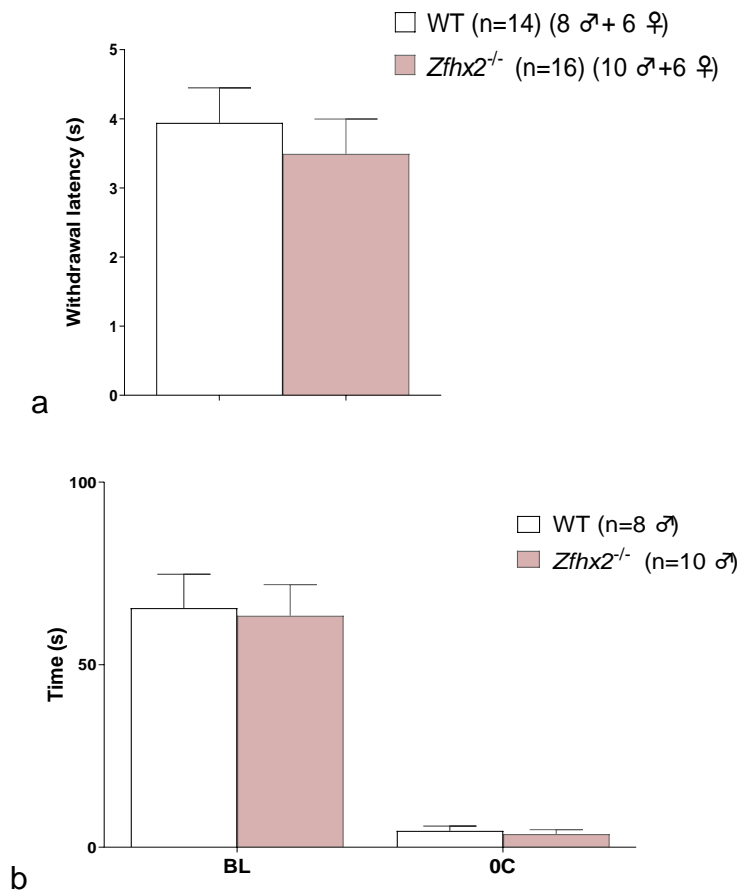
Figure 57. Unimpaired noxious cooling (a) and thermal place preference (b) in *Zfhx2*-/- KO

(TPP performed by Dr Minett). Data are shown as mean ± S.E.M., mixed gender and analysed by t-test

I observed hypersensitivity to noxious heat when the animals were placed on a 50°C and a 55°C heated plate (Figure 58). Interestingly, no differences in response to noxious heat were observed in the Hargreaves' test (Figure 59), suggesting that this nocifensive impairment is linked to a supraspinal response to heat (Minett et al., 2011, Chapman et al., 1985) and not a spinal reflex.
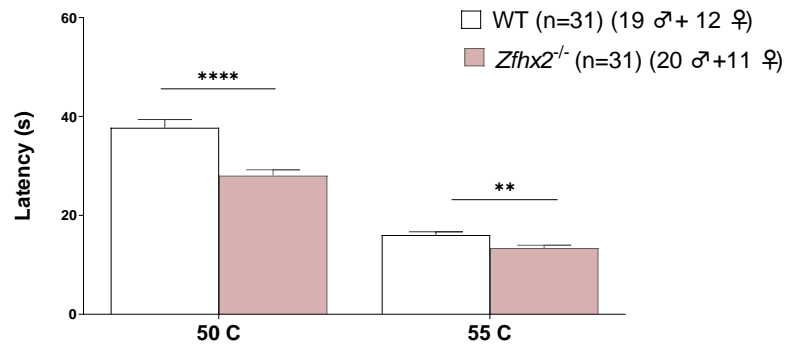
Figure 58. Thermosensation is impaired when animals are on a plate at 50 and 55 ˚C. Significant hypersensitivity is observed in *Zfhx2-/-* global KO mice compared to WT littermates. Data are shown as mean ± S.E.M., mixed gender and analysed by t-test.
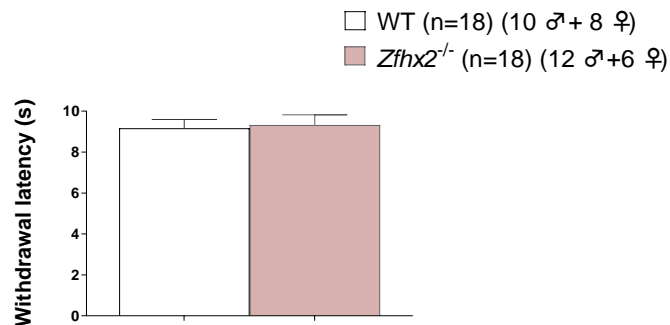
Figure 59. Thermosensation in the Hargreaves' test is unimpaired, shown by comparable responses to a radiant heat stimulus.

Data are shown as mean ± S.E.M., mixed gender and analysed by t-test.

5.3.1.3 *Zfhx2 altered pain thresholds observed in homozygous functional knockout mice whilst hetero animals appear normo-reactive*

After observing altered pain behaviour in the homozygous *Zfhx2-/-* KO animals, I then studied heterozygous animals to understand whether this was a recessive phenotype. This is of interest because the Marsili patients carry the point mutation in a heterozygous state.

Our results showed that *Zfhx2+/-* heterozygous mice show normo-sensitivity in the Hargreaves', hot plate and Randall Selitto tests (Figure 60) when compared with their littermate controls. All data are shown as female adults (8-9 weeks).
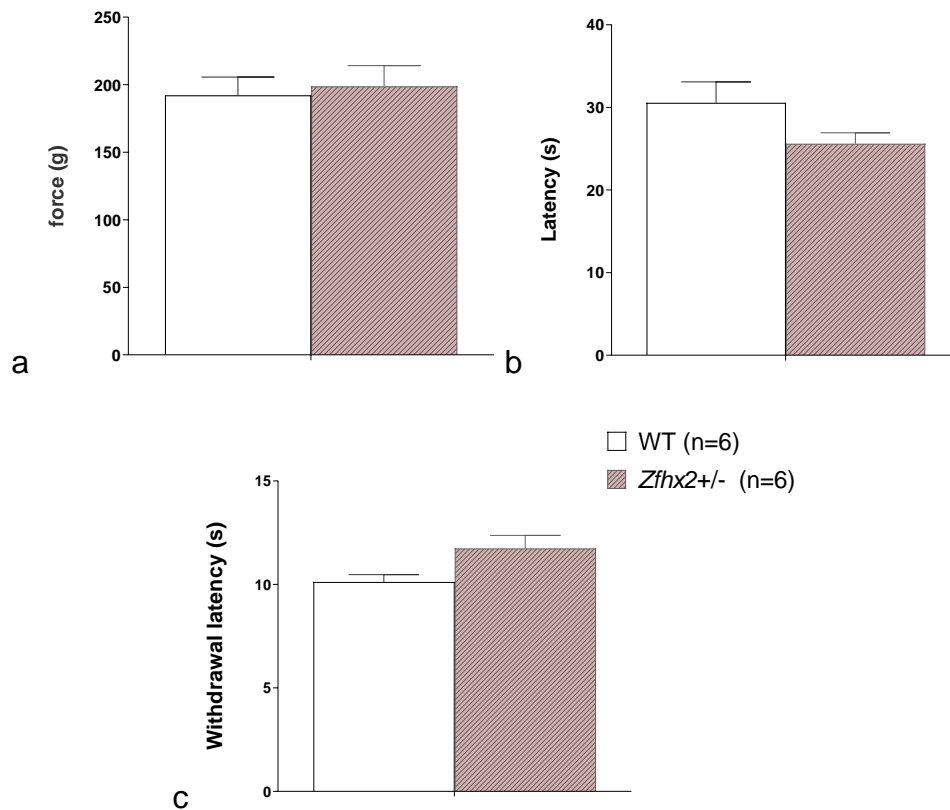
Figure 60. Normal acute nociceptive responses of heterozygous Zfhx2$^{+/-}$ mice and littermates (mixed gender).

(a) Mechanical pain: Randall-Selitto test (b) Supraspinal thermal: Hotplate test at 50°C (c) Thermal spinal reflex: Hargreaves' test. Data are shown as mean ± S.E.M., females and analysed by t-test.

5.3.1.4 Global deletion of Zfhx2 does not have an effect on inflammatory pain behaviour in the formalin test when compared to their littermates

A mixed sex group of KO adult animals and WT littermates received an intraplantar injection of formalin to study possible deficits in sensory neuron function by analysing their nocifensive responses over an hour. No significant difference was observed between the groups during the acute phase (Phase I, 0-10min), linked to direct nociception activation of fibres, nor during the second phase (Phase II, 10-60min), associated with a more complex spinal response and inflammatory messengers (Figure 61).
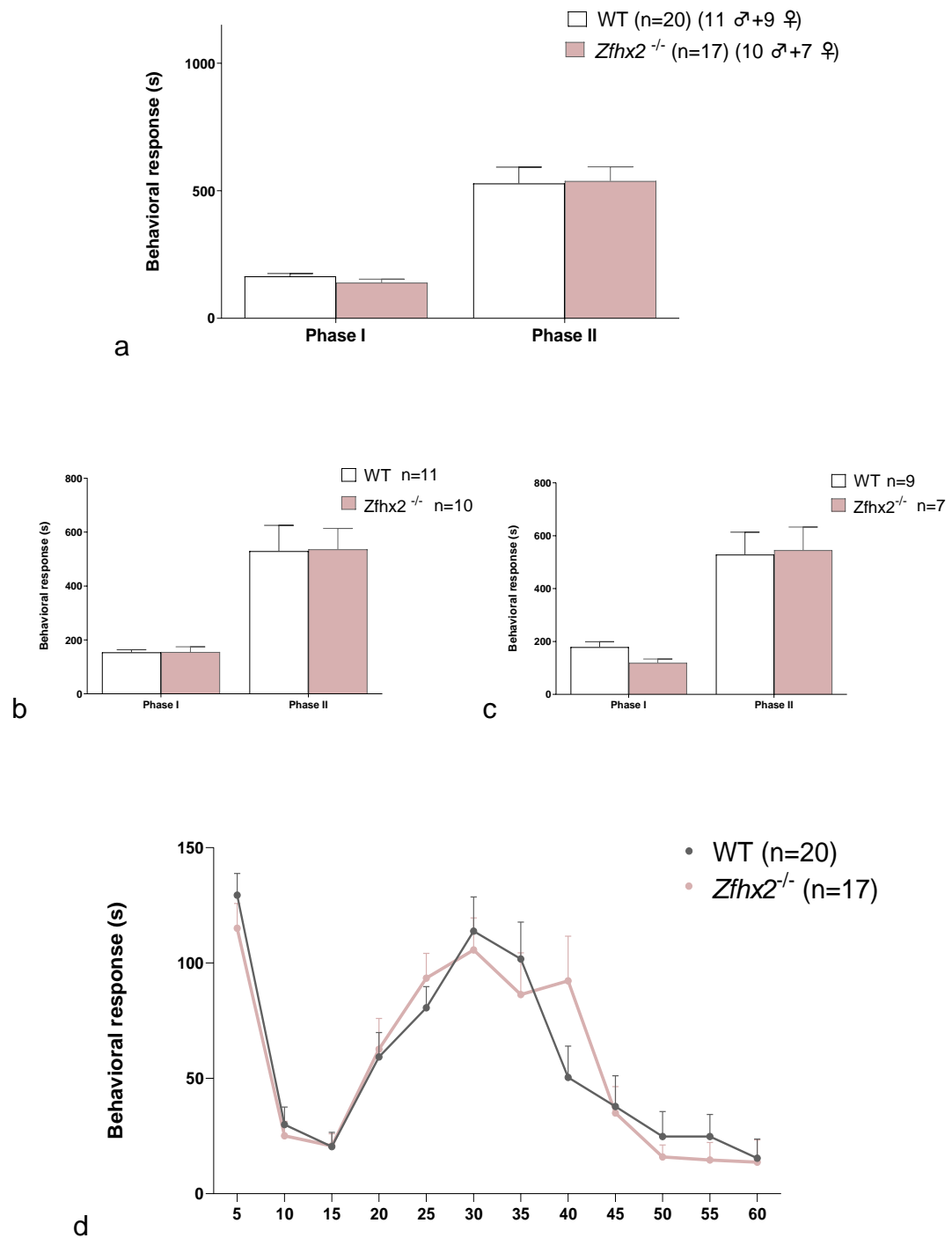
Figure 61. I and II phase behavioural responses after formalin injection in *Zfhx2⁻/⁻* KO mice compared to WT littermate controls.

Data are shown as mean ± S.E.M., mixed gender in a and d. Graphs b and c are male and female data respectively. All were analysed by two-way ANOVA (Bonferroni post hoc test).

5.3.1.5 Global deletion of Zfhx2 has no evident effect on pain sensitivity after CCI induced neuropathic pain

To study whether *Zfhx2* expression affects neuropathic pain, I performed a surgical chronic constriction injury in the sciatic nerve (see 2.4.3) on a cohort of mixed gender and age matched $Zfhx2^{-/-}$ KO and WT controls. As an internal negative control, half of the KO animals in each group were put through the procedure of exposing the nerve but with no ligation carried out (Sham group).

Although mild, mechanical allodynia was found in all groups as a consequence of the surgery when compared with the sham group.

Comparison of behavioural responses to von Frey paw withdrawal at 7 and 15 days after surgery suggests that deleting *Zfhx2* globally does not inhibit the development of the mild mechanical allodynia found 15 days after CCI. Thermal responses to radiant heat as measured by Hargreaves' also show no significant differences between genotypes 7 and 15 days after injury (Figure 62).

a

b
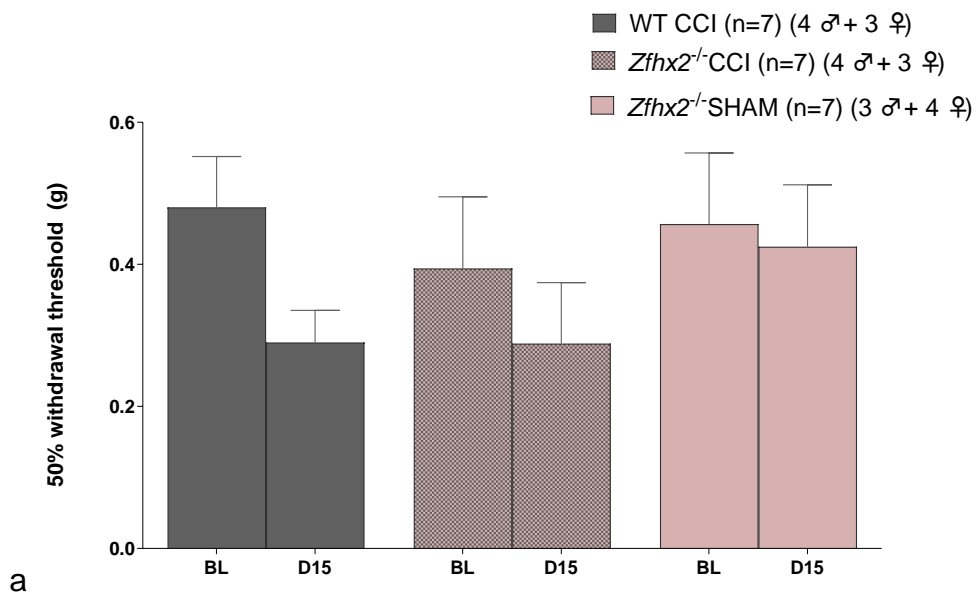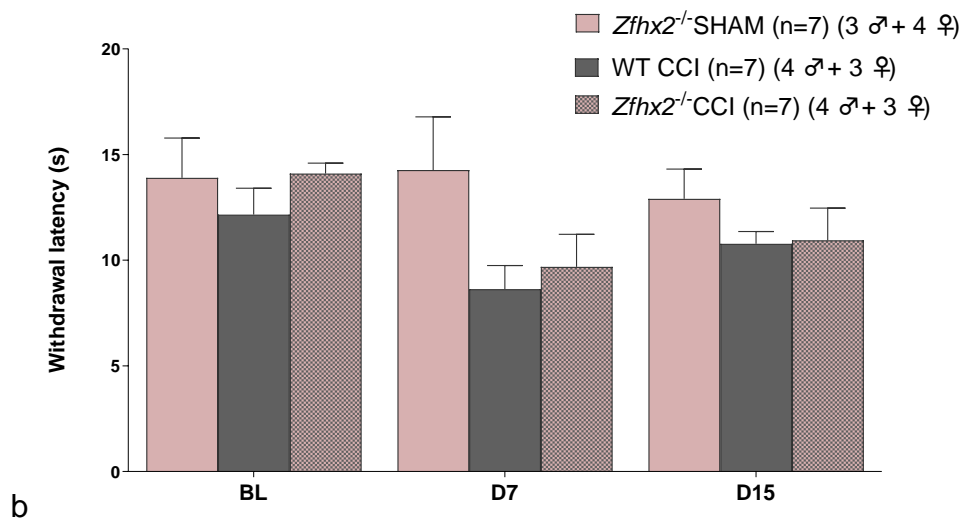
Figure 62. Behavioural responses of *Zfhx2*^{-/-} KO and littermate mice following CCI surgery

(a) von Frey data shows mild mechanical allodynia following CCI in *Zfhx2*^{-/-} KOs and WTs but not in sham. Data are shown as mean ± S.E.M., mixed gender and analysed by two-way ANOVA (Bonferroni post hoc test) comparing the baseline data to day 15 for each group (b) Hargreaves data shows no difference between genotypes in response to radiant heat after surgery. Data are shown as mean ± S.E.M., mixed gender and analysed by two-way ANOVA (Bonferroni post hoc test) comparing the each genotype group to WT sham in each time point (Baseline, day 7 and day 15).

5.3.1.6 Immuno-staining shows no neuronal loss when lacking the Zfhx2 gene

Although the skin punch biopsy of the distal leg performed in one of the Marsili affected individuals excluded the likelihood of a small fibre neuropathy (chapter 5.2-Figure 51), I did perform a further immunohistochemistry analysis to investigate whether loss of *Zfhx2* results in any sensory neuron loss in mouse DRG.

Cell counts were performed on lumbar (4th segment) fresh frozen DRG 11µm thick sections (see chapter 2.5) that were double stained with anti-neurofilament N200 (A-fibre marker) as well as anti-peripherin (nociceptive sensory neurons marker) to cover the entire spectrum of sensory neurons. N200-positive neurons

were labelled in green and peripherin-positive neurons were labelled in red with cell counts showing no significant differences between WT and *Zfhx2*^{-/-} KO DRGs (Figure 63), confirming our observations in humans.
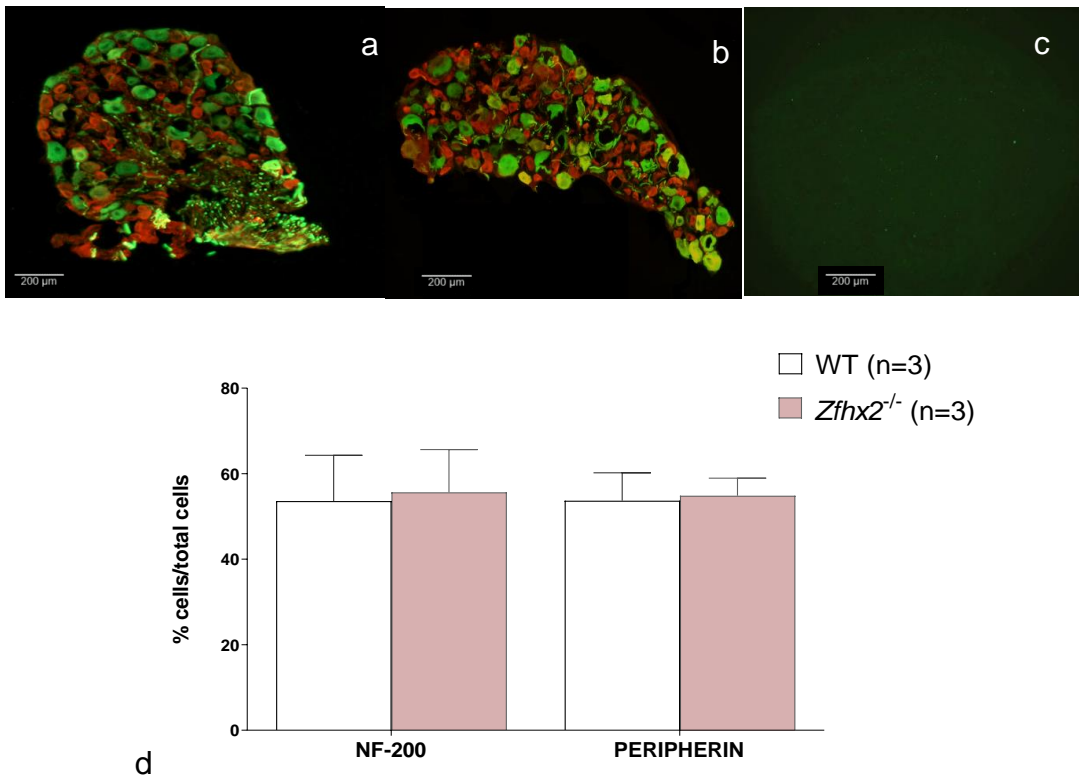
Figure 63: Representative images of FF *Zfhx2*^{-/-} global KO DRG immuno-stained Number of N200 (green) and peripherin positive (red) L4 DRG neurons in littermate control (a), homozygous *Zfhx2*^{-/-} KO animals (b) and Negative control (c). Unchanged percentage of N200 and peripherin positive neurons over the total of DRG neurons in both groups (n=3 each) (d). Data are shown as mean ± S.E.M., mixed gender and analysed by t-test.

5.3.2 *Zfhx2* BAC transgenic line

5.3.2.1 Zfhx2- BAC transgenic generation and breeding strategy

Pain behaviour analyses of the *Zfhx2* global KO mice showed hyposensitivity to noxious mechanical stimuli and hypersensitivity to noxious thermal stimuli in the hot plate test. These data indicate that disrupting the *Zfhx2* gene alters acute pain behaviour. However, we were keen to generate a mouse model that more accurately represented the missense mutation (R1913K) that was observed in the Marsili family. We, therefore, ordered a transgenic mouse line from Cyagen in which the orthologous murine *Zfhx2* amino acid (R1907K) was mutated in BAC RP23-248M20. We received from Cyagen three founders (denoted *Zfhx2**BAC A, B and C) in which copies of the mutated BAC were randomly inserted into the mouse genome.
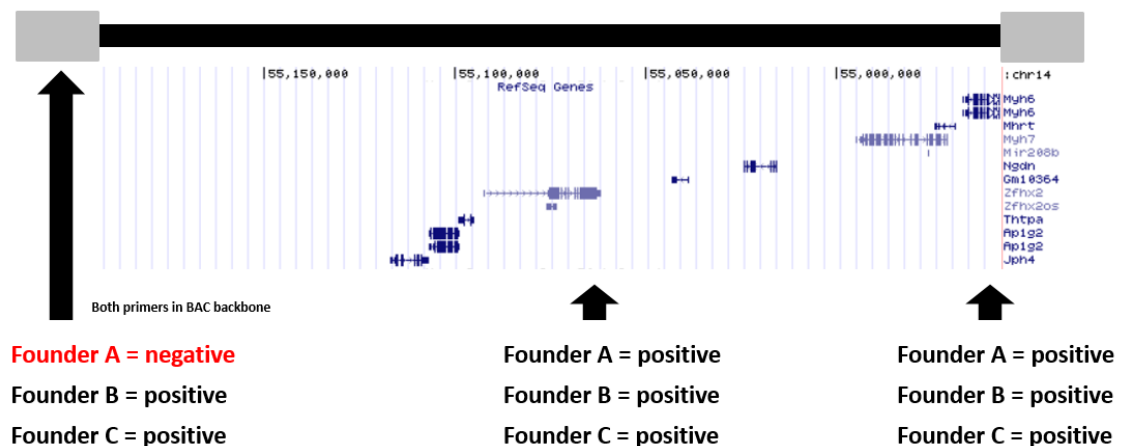
Figure 64. Diagram of the *Zfhx2**BAC RP23-24M20 where *Zfhx2* mutation is inserted (chr14: 54957179-55195089). A group of genes also included are listed on the right hand side (not obviously pain-related).

I treated each founder independently due to the potential variability in both insertion site locus and copy number. Each founder was initially crossed with C57BL/6J mice and then further bred to generate an initial small trial cohort of age (9-12 weeks old) and sex matched *Zfhx2**BAC mutant and WT littermate mice. Every animal used for the study was Sanger sequenced in order to confirm the presence/absence of the mutation with template DNA isolated from ear samples of each mouse.

5.3.2.2 Behavioural assays in Zfhx2 R1907K BAC transgenic mice: Initial trial shows hyperactivity and hyposensitivity to noxious thermal stimuli in the hot plate test for founder C mice

*Zfhx*2 R1907K (*Zfhx2**) BAC animals bred normally, and no motor coordination deficits were observed on the Rotarod apparatus (Figure 65). It is, therefore, reasonable to assume that responses to subsequent sensory tests are not altered as a result of motor impairment.
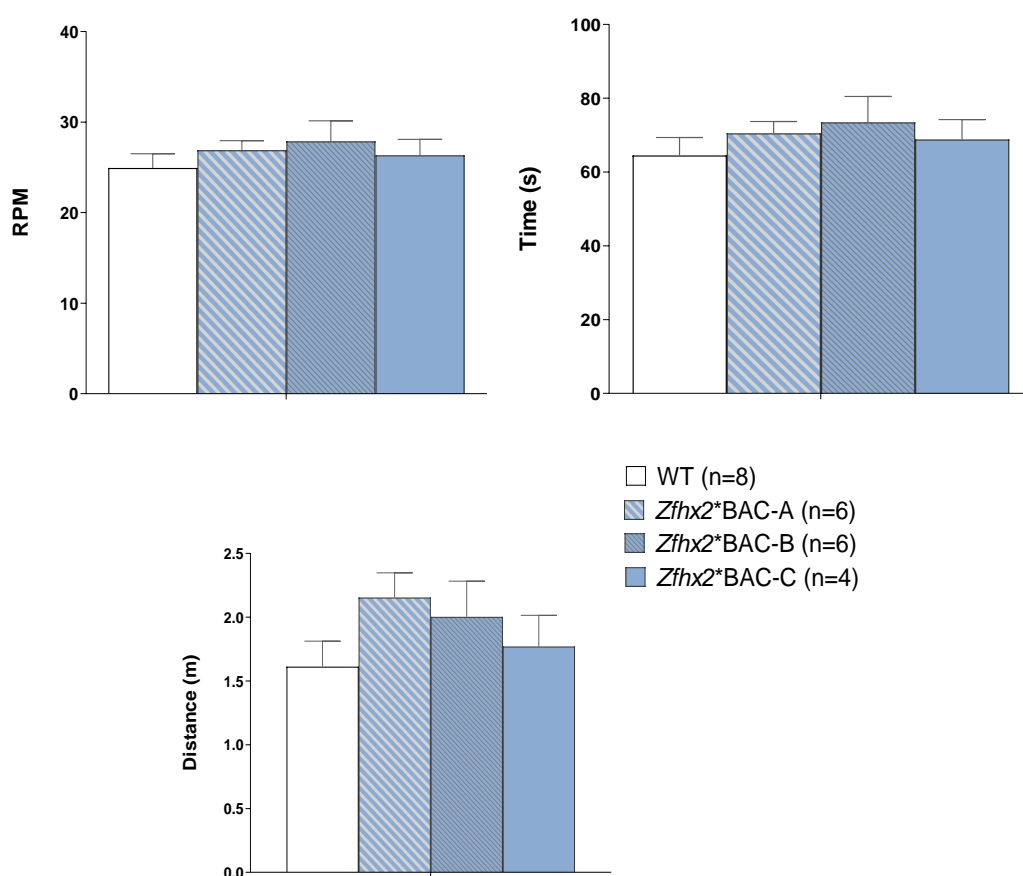
Figure 65. Behavioural responses of *Zfhx2**BAC transgenic mice in the rotarod test (derived from founders A, B and C) and littermate controls (RPM, time and distance). Data are shown as mean ± S.E.M., mixed gender and analysed by one ANOVA (Bonferroni correction).

No marked differences between founders A, B or C lines and littermates were observed for light touch (von Frey and cotton swab test), mechanical (Randall-Selitto test) or radiant thermal stimuli (Hargreaves' test). Founder C mice seemed to show a slightly lower reaction to noxious cooling by the acetone test, but this

was not significant when compared to their controls. No difference in the time spent at 0˚C in the place preference test corroborates this. All tests were performed in adults (8-9 weeks old) and mixed gender (Figure 66). Due to the nature of the comparative analysis, the low number in each founder group did not allow to split groups into males and females. However, expanded further studies with the selected founder C enabled a more comprehensive pain behavioural analysis.
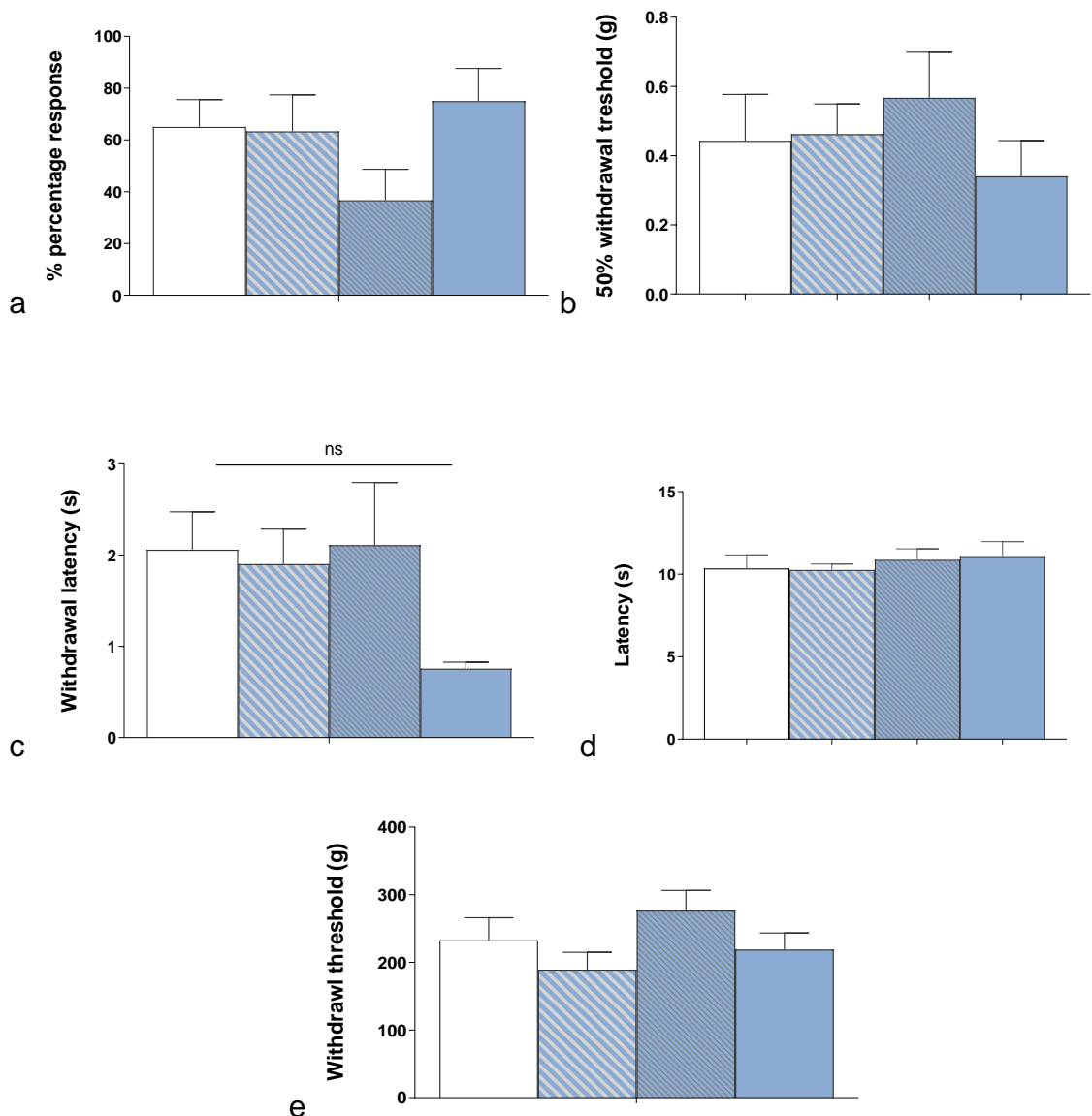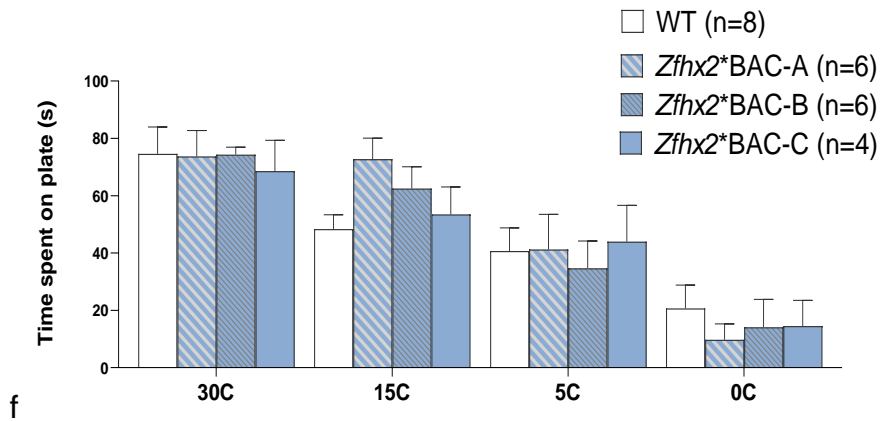
Figure 66. Acute normal behavioural responses of *Zfhx2**BAC transgenic mice (derived from founders A, B and C) bearing the orthologous mutation and littermate mice to (a) Cotton Swab, (b) von Frey, (c) Acetone, (d) Hargreaves', (e) Randall-Selitto, (f) Thermal Place Preference test. No significant differences were found. Data are shown as mean ± S.E.M., mixed gender and analysed by one ANOVA (Bonferroni correction).

In line with previous work for *Zfhx2*^{-/-} KO mice (Komine et al., 2013) I report significant hyperactivity in the open field test for all founders, and seemingly (n=4) greater for founder C animals (Figure 67). Interestingly for the hot plate test, the founder C mice showed significant hyposensitivity compared to their controls.
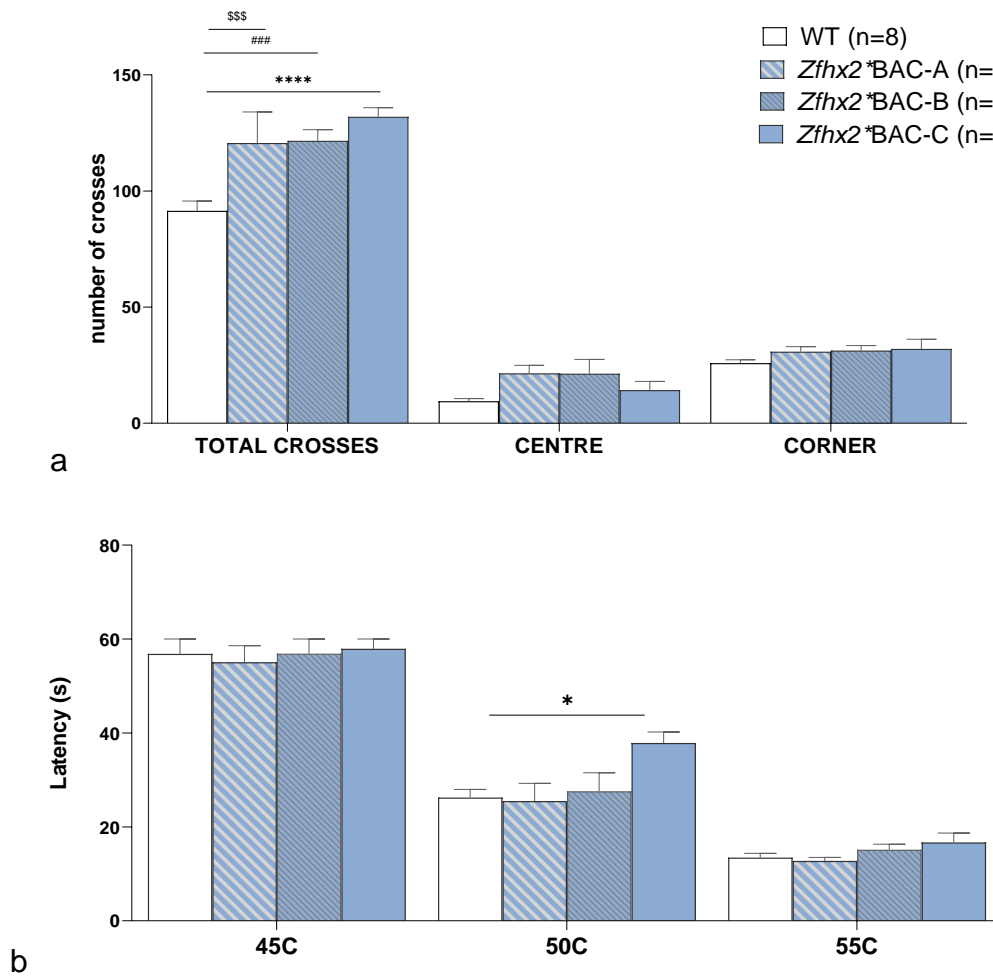
Figure 67. Behavioural responses of *Zfhx2**BAC transgenic mice to (a) Open field and (b) Hot plate

(derived from founders A, B and C) and controls,

They report signs of hyperactivity as well as hyposensitivity at 50°C hot plate in founder C. Data are shown as mean ± S.E.M., mixed gender and analysed by one ANOVA (Bonferroni correction).

This initial trial (with relatively low n numbers) suggested that there were thermal pain sensing deficits for animals in the founder C line, which I were keen to see if they could be replicated in a larger trial. Before commencing a larger trial, Dr Abdella Habib investigated whether there were any differences in the number of copies of the mutated BAC between the different founders. qRT-PCR results of mRNA levels of *Zfhx2* in DRG from mice derived from these founders showed that Founder A had four copies (although the 5' end of the BAC was absent); Founder B had one copy and Founder C had 5 copies. Data were calculated

using the comparative ΔΔCt (Ct) method (see 2.7.1) and normalised by a WT mouse.
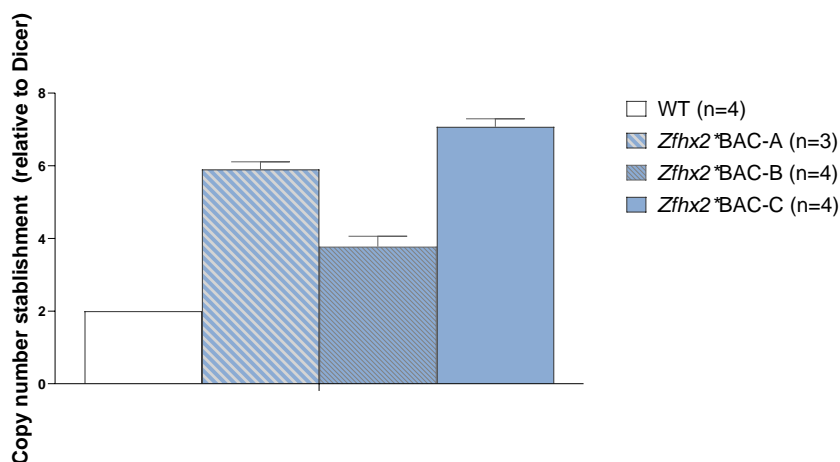
Figure 68. Real-time qRT-PCR analysis of *Zfhx2* mRNA expression in DRG relative to Dicer in WT and mice derived from BAC founder A, B and C for copy number establishment. Data from Dr Abdella Habib at WIBR, UCL. Data were calculated using the comparative ΔΔCt (Ct) method (see 2.7.1) and normalised by a WT mouse. Data are shown as mean ± S.E.M., mixed gender

5.3.2.3 *Zfhx2 R1907K BAC transgenic animals bred from founder C show hyperactivity and hyposensitivity to noxious heat, with the phenotype more severe in animals with a higher BAC copy number*

The initial small-scale pain behaviour trial indicated that mice derived from founder C have (a) the most copies of the mutant *Zfhx2* allele and (b) show hyposensitivity to noxious thermal stimuli on the hot plate test. We, therefore, decided to focus on founder C animals in order to obtain a full testing cohort.

Behaviour tests on the founder C-derived mice showed that motor co-ordination was normal (rotarod) and no differences were reported in mechanical sensitivity tests (von Frey, cotton swab, Randall Selitto), nor altered reactivity to cooling stimuli (dry ice) when compared to their littermate controls (Figure 69).
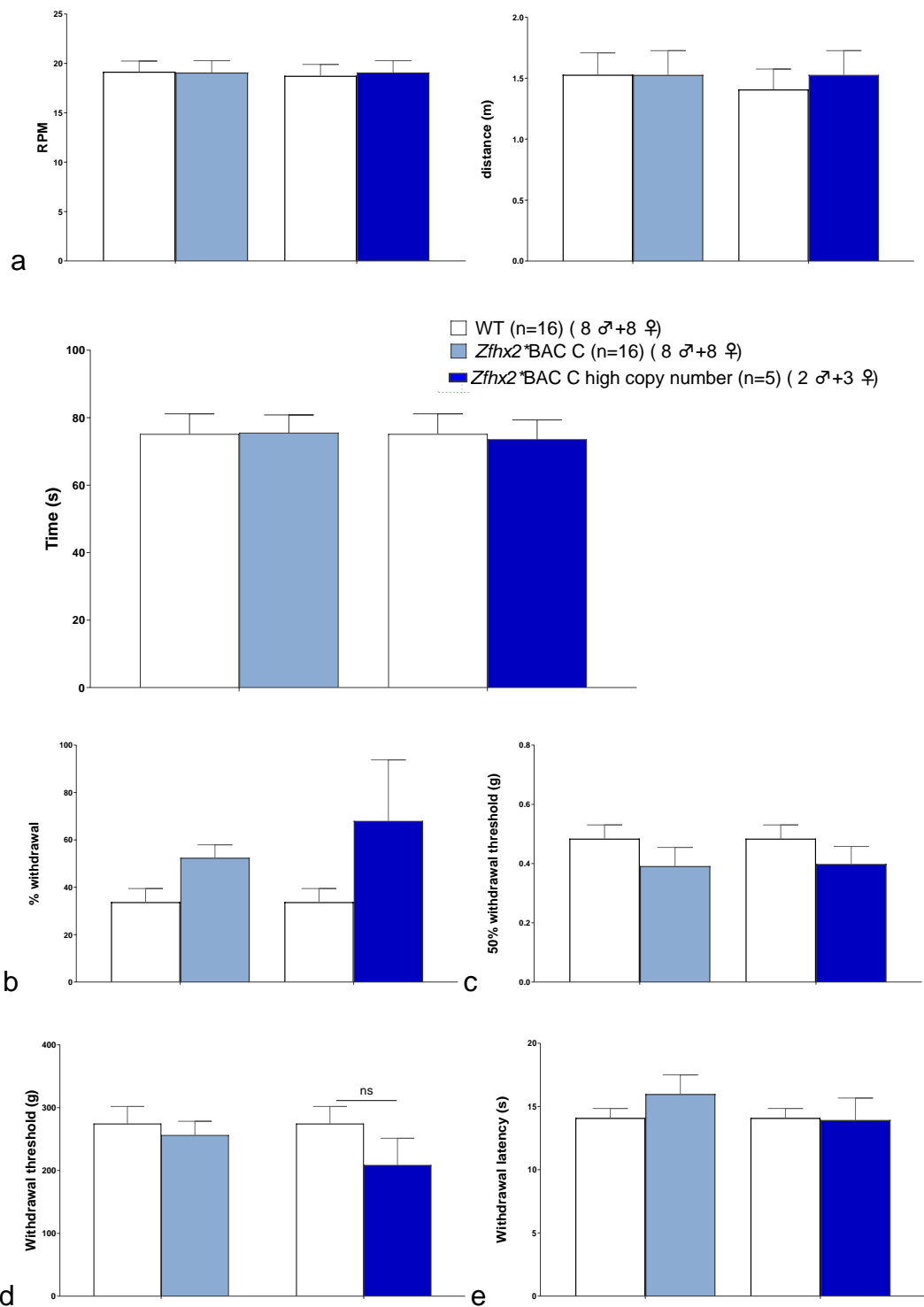
Figure 69. Acute behavioural responses of *Zfhx2**BAC transgenic C founder mice, bearing the R1907K *Zfhx2* mutation and littermates to (a) Rotarod (RPM, time and distance), (b) Cotton Swab, (c) von Frey, (d) Randall-Selitto, (e) Dry Ice. No significant differences were found in adults males or females. BAC C (copy number 1-5); high copy number (copy number 4-5). Data are shown as mean ± S.E.M., mixed gender and analysed by one ANOVA (Bonferroni correction).

Open field tests showed mice with a high copy number of the mutant BAC (4-5 copies) were hyperactive compared to their WT littermates (Figure 70). Importantly, *Zfhx2**BAC transgenic mutants showed reduced sensitivity to thermal stimuli both in the Hargreaves' and hot plate tests (Figure 70), with the difference more pronounced in animals with a higher copy number of the mutant *Zfhx2* gene.

C
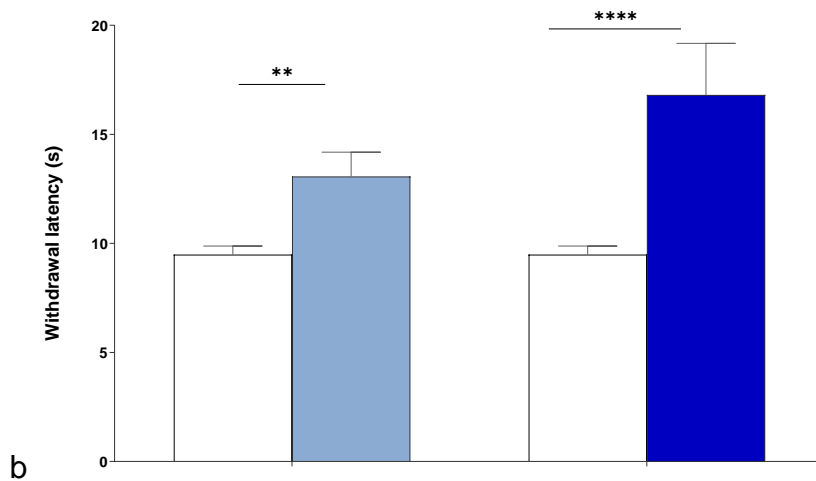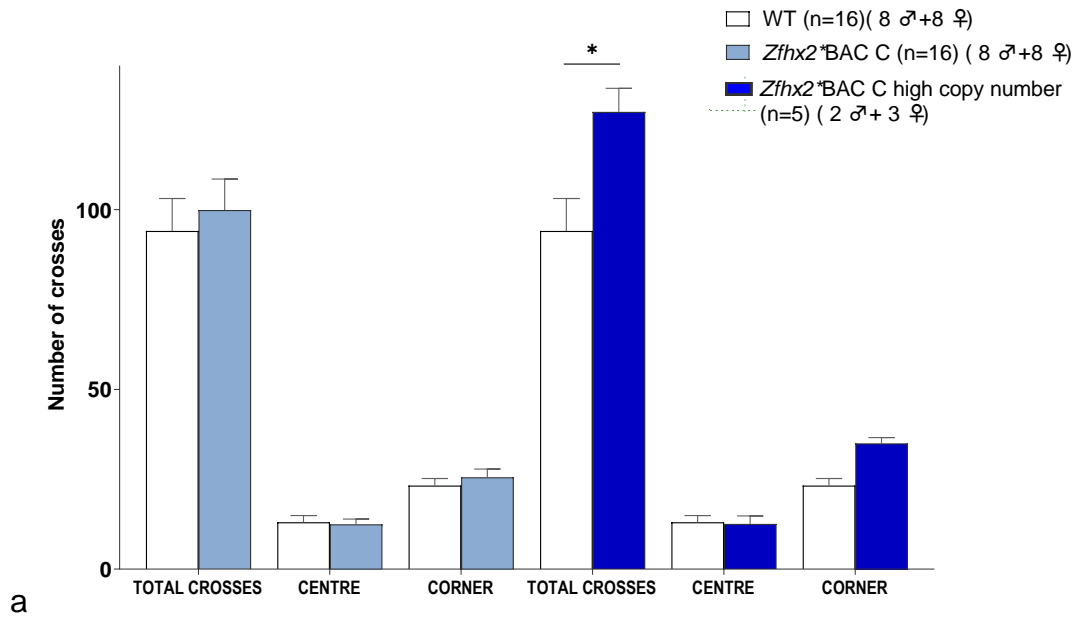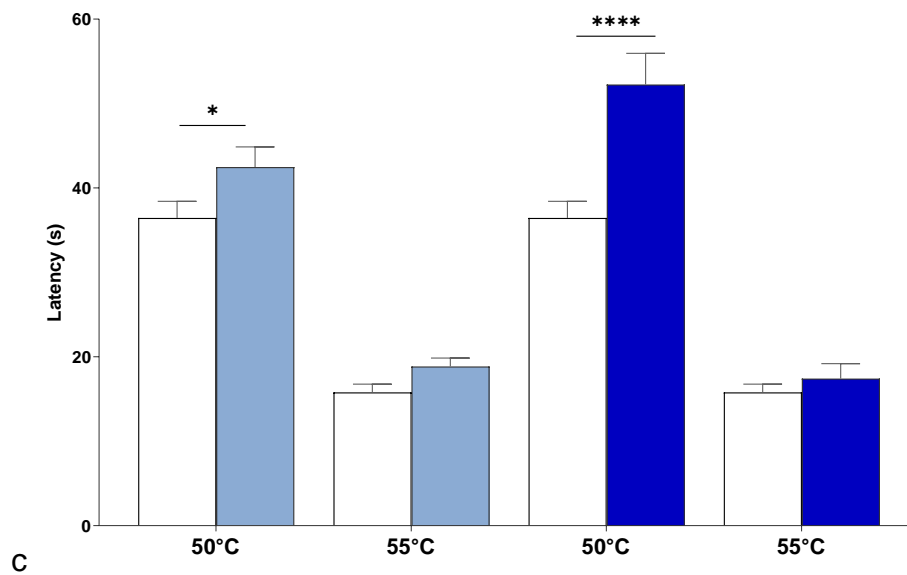
Figure 70. Impaired exploratory and thermal behavioural responses of mixed gender adult *Zfhx2***BAC transgenic mice derived from founder C,
and littermates to (a) Open field, (b) Hargreaves', (c) Hot plate. A significant increase in values was found for the 3 tests, being greater in animals with higher copy numbers (4-5 copies). Data are shown as mean ± S.E.M., mixed gender and analysed by one ANOVA (Bonferroni correction).

All tests were performed in age-matched adult mice and analysed separately per sex. Once confirmed that the results were gender independent, they were pooled into mixed gender for easier graph representation and understanding.

5.3.2.4 Mechanical and thermal hypersensitivity develops normally in Zfhx2 R1907K BAC transgenic mice following intraplantar injection of CFA

After the acute pain behaviour trials, we decided to move on to an inflammatory pain test where mechanical and thermal hypersensitivity was measured following intraplantar injection of CFA. Our findings showed that both thermal and mechanical inflammatory hyperalgesia develop independently of overexpression of the mutated *Zfhx2 (Zfhx2*)* with no changes in the associated paw oedema between WT and mutant mice (Figure 71).
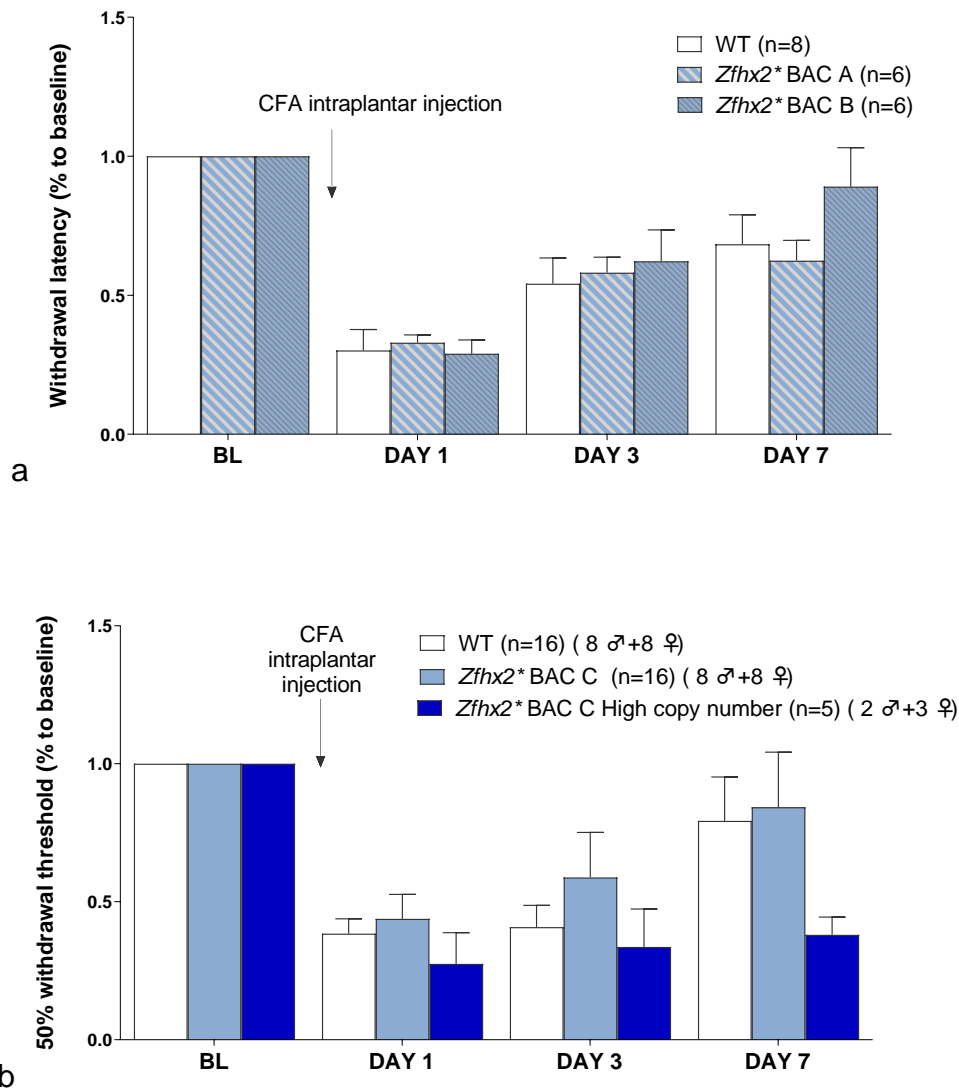
Figure 71. Behavioural responses following intraplantar CFA injection of littermate and *Zfhx2**BAC (*Zfhx2* R1907K mutant) transgenics derived from founders A, B and C. Mechanical hypersensitivity induced by CFA was present in *Zfhx2** BAC regardless of the founder (a) or copy number (b) at 1-, 3- and 7-days following injection. Data are shown as mean ± S.E.M. percentage to baseline mixed gender and analysed by two way ANOVA (Bonferroni correction) after normalisation.

On the other hand, under CFA induced painful conditions, sensitivity to radiant heat observed in animals bred from founder A, B or C is not different at day 1, 3 or 7 post injection when analysing normalised to baseline data (Figure 72).
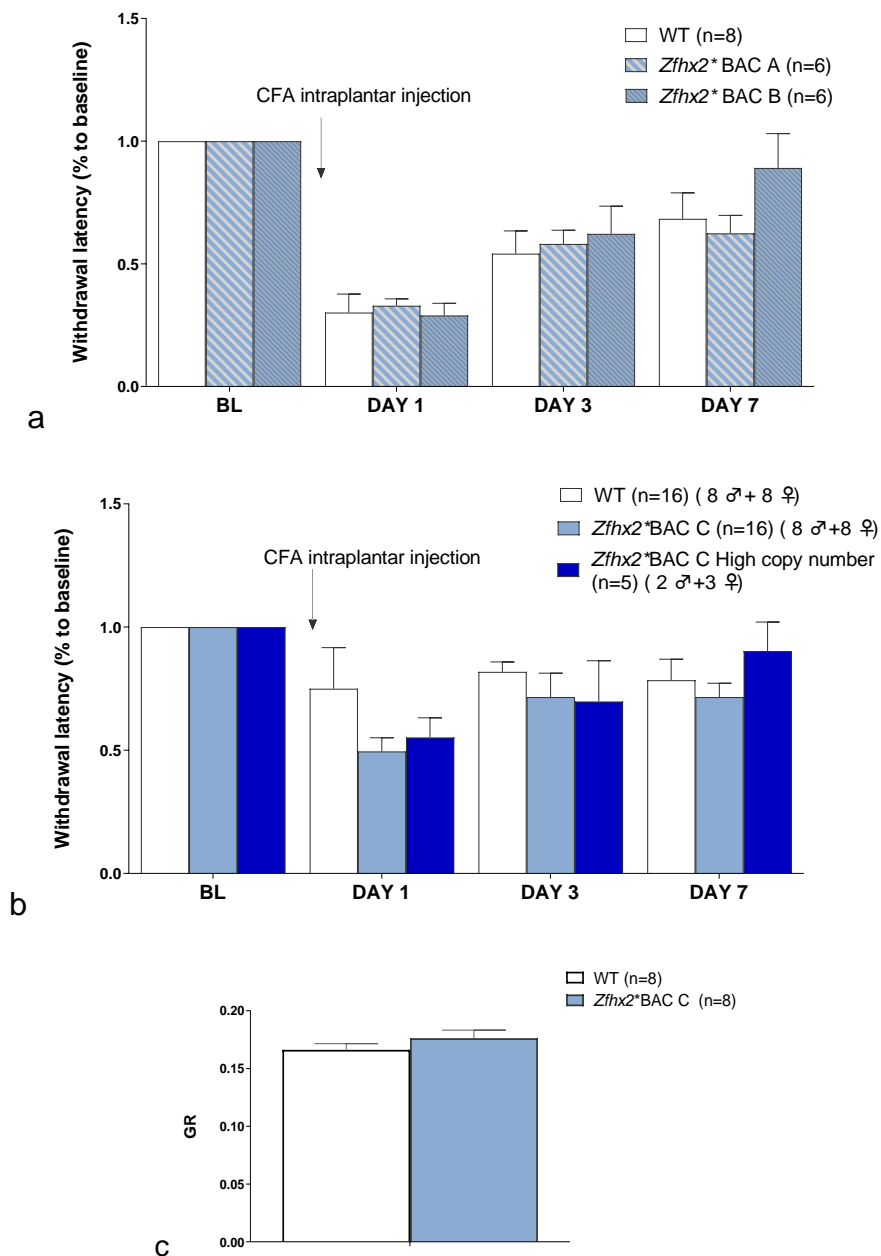
Figure 72. Behavioural responses following intraplantar CFA injection on littermate and *Zfhx2**BAC (*Zfhx2* R1907K mutant) transgenics derived from founders A, B and C. Thermal sensitivity to radiant heat observed in animals bred from founder A, B or C is not significantly different than controls during the CFA model (b). (c) Paw oedema in BAC *Zfhx2** and WT mice after intraplantar injection of CFA. Data are shown as mean±S.E.M. percentage to baseline, mixed gender and analysed by two way ANOVA (Bonferroni correction) after normalisation. (a,b) and t-test (c).

5.3.2.5 Immuno-staining shows no changes in the number of peripherin positive neurons in animals overexpressing Zfhx2 R1907K

Lumbar 11µm thick DRG sections were double stained (see chapter 2.5) with anti-NeuN anti-rabbit (SIGMA) protein (classic total neuronal marker) as well as anti-peripherin anti-mouse (SIGMA) (nociceptive sensory neurons marker). No significant differences were observed in the number of peripherin positive neurons in DRG derived from *Zfhx2*BAC (Zfhx2 R1907K mutant)* transgenic mice and littermate controls (Figure 73).
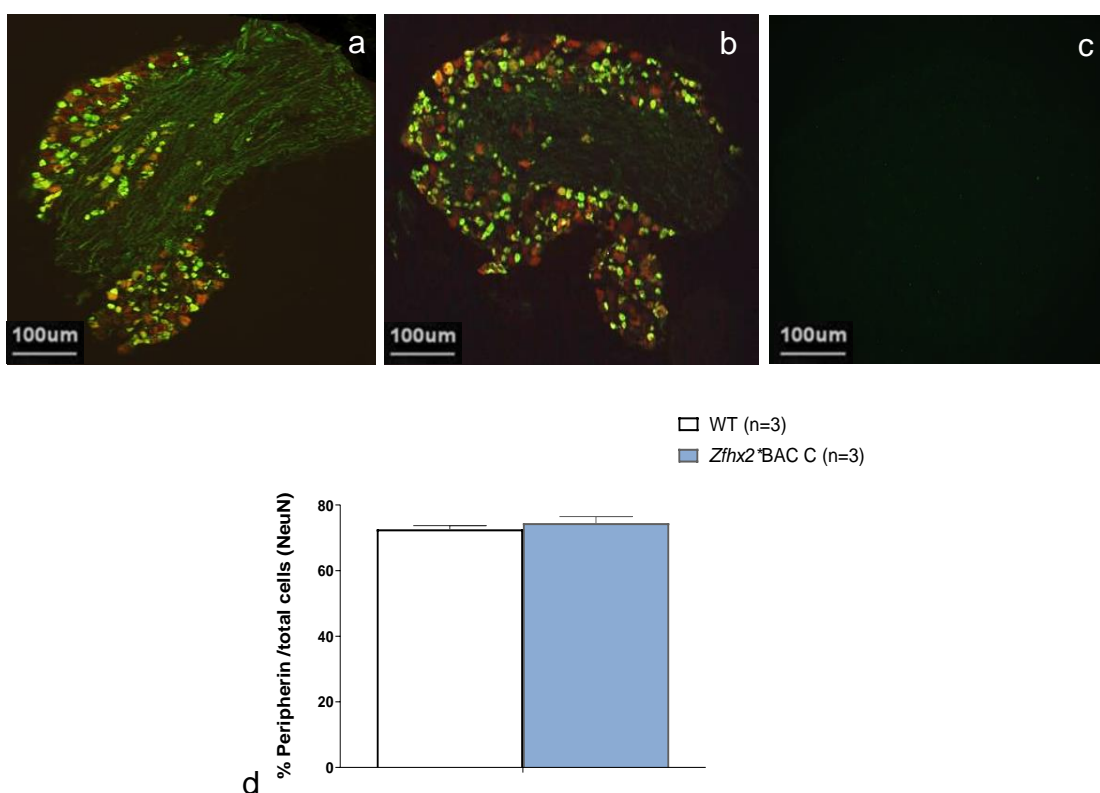
Figure 73. Representative images of FF *Zfhx2*BAC C* and littermate control DRGs (4th lumbar segment) sections.

Peripherin positive (green) in total NeuN (red) in littermate control (a), *Zfhx2*BAC C* mouse (b), negative control (no primary antibody treated sample) (c), Unchanged percentage of Peripherin positive neurons over the total of NeuN positive DRG neurons in both groups (d). Data are shown as mean ± S.E.M., mixed gender and analysed by t-test.

5.4   Discussion

The human genome project, development of molecular cloning and advances in gene manipulation technology have dramatically changed the future of science and medicine (Gurumurthy and Lloyd, 2019). For example, in-depth gene sequencing in patients with painless phenotypes have identified mutant genes which in turn can be new analgesic drug targets (see Table 4) In a time when animal models are widely used to mimic human diseases, here I use a transgenic model approach to explore the effects in mice of knocking out and also expressing the orthologous point mutation in *Zfhx2* that was identified in the heritable pain insensitive Marsili syndrome disorder.

Patients with heritable pain-free disorders can experience a lower life expectancy due to accumulated injuries and unnoticed illnesses that can become lethal due to their lack of self-protection strategies. Ironically however, whilst rare, the existence of these families is highly attractive for researchers as they have led us to identify and validate new genes as analgesic targets. Such is the case of the discovery of families with the recessive loss of function *SCN9A* mutations encoding the $Na_v1.7$ voltage-gated sodium channel (Cox et al., 2006), widely proven to be essential in pain perception. Or the more recently discovered pain insensitivity condition linked to co-inheritance of a deletion in a long non-coding RNA gene (*FAAH-OUT*) and a hypomorphic SNP in the fatty acid amide hydrolase (*FAAH*) gene. These mutations result in a loss of function of the enzyme which translates into raised endocannabinoid anandamide levels in the affected individual, consequently inducing an analgesic effect (Habib et al., 2019b).

Marsili syndrome is a disorder named after the family where it was first described, characterised by congenital insensitivity to pain whilst normal cognitive abilities were present (Spinsanti et al., 2008). As mentioned in chapter 5.2, they reported: a decreased corneal reflex, hypohidrosis, painless fractures and impaired thermal sensitivity. However, whilst evident, the inherited pain phenotype was not global (with visceral and birth pain present as well as headaches) but more complex. They were reporting in fact, an occasional perception of something abnormal (Shaer, 2019), or an initial "unpleasant sensation" that soon after dissipated following a fracture. Similarly, when subjects were injected with capsaicin into

their skin, they reported an immediate very intense pain, again unusually fading after around 15 s (Habib et al., 2018a). Intradermal injection of this compound obtained from chilli peppers normally causes an immediate burn like pain sensation and prolonged hyperalgesia to both heat and mechanical stimuli, due to its effect on C-fibre polymodal nociceptors (Baumann et al., 1991) (Simone et al., 1987). Importantly, a normal intraepidermal nerve fibre density was observed from a skin biopsy isolated from the proband suggesting that the abnormal capsaicin response may be related to dysfunction of the intact nociceptors.

Exome sequencing identified a heterozygous point mutation in Zfhx2 that was present in all affected individuals from the Marsili family. This mutation maps to a homeodomain and is predicted to change a conserved Arg (R) into a Lys (K) residue. Whilst we accept that both amino acids are very similar, and the change R to K does not seem to be a big change, R is very highly conserved and there is a hypothesis centred around the methylation of the arginine. In more detail, changing R1913 to K could mean that R1911 is predicted to no longer be methylated, which potentially affect DNA binding of the Hox domain (hypothesis and results serving Ayako's Matsusama's thesis).

ZFHX2 is highly expressed in important pain processing regions of the human CNS (Komine et al., 2013), as well as in mouse DRG nociceptors (Usoskin et al., 2015). To study the importance of *Zfhx2* for pain perception, I characterised the sensory function of two different mouse models: a *Zfhx2* global KO line and *Zfhx2**BAC transgenic mice bearing the orthologous mutation.

The current data shows that the global deletion of the mouse *Zfhx2* gene has a direct impact on pain perception. The sensitivity to noxious mechanosensation was impaired in homozygous *Zfhx2* deficient mice compared to WT controls, reporting significant hyposensitivity in the Randall Selitto test (Figure 56). These findings correlate with what has been reported in the Marsili affected individuals. Interestingly, I observed hypersensitivity to noxious heat when the animals were placed on a 50˚C and a 55˚C heated plate (Figure 58) but not in the Hargreaves' test (Figure 59), suggesting that this nocifensive impairment is linked to a mechanistic supraspinal response to heat (Minett et al., 2011, Chapman et al., 1985) and not a spinal reflex, not observed in the human carriers.

Having shown that knockout of *Zfhx2* alters pain thresholds, I then studied a potential gain of function transgenic model which overexpresses the *Zfhx2* gene

with the mutation R1907K (orthologous to the human R1913K). From three different founders obtained, initial acute characterisation seemed to be stronger in founder C, and comparative analysis of qRT-PCR results of mRNA levels of *Zfhx2* in mouse DRG (Figure 68) showed that *Zfhx2* mRNA expression relative to β-Actin was higher in founder C derived mice and was therefore chosen for further tests.

Pain behavioural phenotyping of transgenic mice expressing multiple copies of the mutant *Zfhx2* showed significantly delayed responses to noxious heat in both the Hargreaves' and hot plate tests (Figure 70), although unaltered mechanical thresholds when compared with their littermate controls. Interestingly, while evident, the thermal low sensitivity readings were quite variable within the mice mutant group. This inter-individual variability in response to heat is consistent with the reported one after quantitative sensory testing (QST) performed in the affected Marsili members (Habib et al., 2019b). Measuring changes in sensitivity to different types of noxious stimuli revealed different levels of pain impairment in response to heat across family members with one proband showing extreme deficits in response to noxious heat. I then explored the idiosyncrasy observed in mice by qPCR and copy number determination, uncovering that in fact, it was in animals with a higher number of copies of the inserted mutated *Zfhx2* allele where the phenotype was more pronounced. These findings suggest, not only that R1913K seems to be a causative point mutation leading to a pain insensitive phenotype in mice; but also the existence of a cause-effect relationship in direct proportion with the amount of the gene expressed in mice. This suggests that overexpression of mutant *Zfhx2* could be an attractive candidate for gene therapy but we cannot discard that the effect could be due to an increase number of copies of the gene and not necessarily its mutation. Similar strategies of overexpressing proteins such as the mu-opioid receptor (Xu et al., 2003) in rodent primary sensory neurons have proven successful.

Altogether, although acute pain deficits have been reported in both models, the *Zfhx2**BAC model seems to be closer to the Marsili phenotype. This should be somehow expected, since the first model is a global deletion of the whole gene, and the second is a gain of function of the gene bearing the missense mutation, where two unaltered copies of the *Zfhx2* allele are still present. A recently

developed model of bone fracture pain in rodents (Magnusdottir et al., 2021) or a capsaicin induced pain model (Sakurada et al., 2003) would be required to confirm a fully recapitulation of the phenotype described.

Another factor to consider when interpreting the data is that even when designing experiments accounting for sex and age as modulators of the pain experience in mice and humans, I would not be able to escape the inherent interspecies differences not only in pain processing mechanisms but also its quantification. Although mouse models have provided specific, sensitive and reproducible results (Minett et al., 2015), a direct "bench-to-bedside" relationship would be an oversimplification of the multidimensional pain experience (Mogil, 2009), and have led to numerous failures in the aim to recapitulate human conditions. A recent pain study has characterised a set of spinal cord neurons involved in a novel neural pain pathway responsible for "coping" with ongoing pain whilst exhibiting normal first evoked reflex behaviour (Huang et al., 2019a). This calls into question whether current reflex-based nociception tests are adequate while phenotyping a genetically manipulated animal, even more importantly when trying to mimic a human phenotype where "there is an initial pain which soon dissipates"(Shaer, 2019).

This new insight in the pain field, as well as the already mentioned human-mice translational discrepancies, could be partially resolved by the use of a more extensive array of behavioural tests and pain models when characterising our transgenic animal models. In fact, comparative characterisation of different $Na_v1.7$ transgenic mouse strains have revealed differences not only within the distinct neuronal subpopulations where they are expressed but also reporting different results depending on the neuropathic model performed (Minett et al., 2014b). A deeper understanding of neuronal plasticity along with detailed microarray analyses in DRG obtained in different chronic pain models, revealed transcriptomic changes in gene expression, sometimes specific to the model, implying distinct cellular responses to different painful stimuli (Bangash et al., 2018).

Although in the inflammatory formalin test (Figure 61) and CFA model (Figure 71 and Figure 72), as well as CCI derived allodynia (Figure 62) pain appeared to develop normally regardless of genetic manipulation in the *Zfhx2* gene; it would

be useful to expand the range of tests to more clinically relevant pain models for a better understanding on how good *Zfhx2* could be as a target for different chronic pain disorders.

Additionally, coincident with what has been already published with global *Zfhx2* KOs (Komine et al., 2012), mice with a high copy number of the mutant BAC (4-5 copies) were hyperactive compared to their WT littermates (Figure 70) in the open field maze. This test, initially designed to estimate emotionality in rodents, is now widely used to assess locomotor activity, spontaneous pain and willingness to explore as well as, not without controversy, anxiety levels (Walsh and Cummins, 1976). I could not find differences in the amount of time the animals spent in the corner versus central areas, but exploratory behaviour was overall significantly higher, with no associated motor coordination impairment (Figure 55, Figure 65). This altered cognitive function, essential for decision-making and survival is processed in the brain, where, interestingly, the *Zfhx2* mouse homolog seems to be highly expressed (Figure 54) (Komine et al., 2006). Although the expression pattern of *Zfhx2* in human and mouse nervous tissue may not be necessarily the same, it is safe to assume that there is a possible role of the *Zfhx2* gene in the CNS in both species. Nevertheless, further studies should be required to confirm its central implication in the pain insensitivity phenotype found. This could include more central processing behavioural tests (like an elevated plus maze, light dark box, or sociability chamber), as well as microarray or RNA sequencing in different areas of the brain to determine whether impairing the function of *Zfhx2* alters the expression of other genes in the brain with implication in pain perception, and whether they could represent viable gene therapy targets themselves.

In conclusion, the work in this study demonstrates that the *Zfhx2* gene plays a selective role in pain sensitivity, suggesting that targeting this transcription factor and mimicking the R1913K missense mutation may be used as a new analgesic therapy.

5.5   Conclusions

-Pain behavioural analyses show that the *Zfhx2* gene affects pain thresholds both when lacking expression and when overexpressed.

-Although it would be difficult to fully recapitulate the "almost no pain" phenotype observed in the human family on a mouse, the transgenic mouse model does recapitulate the thermal phenotype observed in the affected members and has helped to validate the *ZFHX2* gene as a potential new analgesic drug target

5.6   Future directions

As previously discussed, It would be interesting to expand the range of pain tests, including more clinically relevant nociception disease-like models for a better understanding of the gene under painful conditions and its use as a target for different humanized chronic pain disorders. When doing so, and albeit the Marsili syndrome seems to affect both males and females, it would be necessary to analyse any potential sex differences in both mouse models. When doing so, it would be interesting to expand the behaviour tests and to introduce more relevant ones to the reported human phenotype such as a bone fracture model (Magnusdottir, 2021 #84} or a capsaicin induced pain model (Sakurada et al., 2003).

Although a list of genes dysregulated in DRG in both *Zfhx2* KO and *Zfhx2**BAC mice has already been published, it is still to be clarified which ones are likely to be responsible for the pain insensitivity. Screening this cohort of genes and the use of antisense oligonucleotides delivered intrathecally to the DRG, will artificially isolate the individual effect of each of them, providing *Zfhx2* mechanistic clues as well as revealing them as potential gene therapy targets themselves. A similar approach could be performed by overexpressing the chosen candidate gene under tissue specific promoters in the DRG or even brain specific ones.

Lastly, developing a viral way of delivering mutant *Zfhx2* coding sequence to DRG by using tissue- specific promoters is also a consideration for future projects especially to confirm an effect due to the mutation and not overexpression of the

gene itself. However, the gene of interest is very large and AAV vectors only have ~4.7 kb packaging capacity. This could be addressed by potentially trialling the use of lentivirus to deliver mutant *Zfhx2* in cells or using a split-intein approach and 2 AAVs to deliver the gene in two halves (Truong et al., 2015). So, although manipulating the *ZFHX2* gene or downstream targets could provide useful pain relief, challenges remain in effectively targeting this gene therapeutically.

Chapter 6 - References

ABRAHAMSEN, B., ZHAO, J., ASANTE, C. O., CENDAN, C. M., MARSH, S., MARTINEZ-BARBERA, J. P., NASSAR, M. A., DICKENSON, A. H. & WOOD, J. N. 2008. The cell and molecular basis of mechanical, cold, and inflammatory pain. *Science,* 321**,** 702-5.

ABRAIRA, V. E., KUEHN, E. D., CHIRILA, A. M., SPRINGEL, M. W., TOLIVER, A. A., ZIMMERMAN, A. L., OREFICE, L. L., BOYLE, K. A., BAI, L., SONG, B. J., BASHISTA, K. A., O'NEILL, T. G., ZHUO, J., TSAN, C., HOYNOSKI, J., RUTLIN, M., KUS, L., NIEDERKOFLER, V., WATANABE, M., DYMECKI, S. M., NELSON, S. B., HEINTZ, N., HUGHES, D. I. & GINTY, D. D. 2017. The Cellular and Synaptic Architecture of the Mechanosensory Dorsal Horn. *Cell,* 168**,** 295-310.e19.

AXELROD, F. B. & GOLD-VON SIMSON, G. 2007. Hereditary sensory and autonomic neuropathies: types II, III, and IV. *Orphanet journal of rare diseases,* 2**,** 39-39.

BANGASH, M. A., ALLES, S. R. A., SANTANA-VARELA, S., MILLET, Q., SIKANDAR, S., DE CLAUSER, L., TER HEEGDE, F., HABIB, A. M., PEREIRA, V., SEXTON, J. E., EMERY, E. C., LI, S., LUIZ, A. P., ERDOS, J., GOSSAGE, S. J., ZHAO, J., COX, J. J. & WOOD, J. N. 2018. Distinct transcriptional responses of mouse sensory neurons in models of human chronic pain conditions. *Wellcome Open Res,* 3**,** 78.

BASBAUM, A. I., BAUTISTA, D. M., SCHERRER, G. & JULIUS, D. 2009a. Cellular and molecular mechanisms of pain. *Cell,* 139**,** 267-284.

BASBAUM, A. I., BAUTISTA, D. M., SCHERRER, G. & JULIUS, D. 2009b. Cellular and molecular mechanisms of pain. *Cell,* 139**,** 267-84.

BAUMANN, T. K., SIMONE, D. A., SHAIN, C. N. & LAMOTTE, R. H. 1991. Neurogenic hyperalgesia: the search for the primary cutaneous afferent fibers that contribute to capsaicin-induced pain and hyperalgesia. *J Neurophysiol,* 66**,** 212-27.

BAUTISTA, D. M., SIEMENS, J., GLAZER, J. M., TSURUDA, P. R., BASBAUM, A. I., STUCKY, C. L., JORDT, S.-E. & JULIUS, D. 2007. The menthol receptor TRPM8 is the principal detector of environmental cold. *Nature,* 448**,** 204-208.

BENEMEI, S., NICOLETTI, P., CAPONE, J. G. & GEPPETTI, P. 2009. CGRP receptors in the control of pain and inflammation. *Curr Opin Pharmacol,* 9**,** 9-14.

BERGE, O.-G. 2011. Predictive validity of behavioural animal models for chronic pain. *British journal of pharmacology,* 164**,** 1195-1206.

BLAKEMAN, K. H., HAO, J. X., XU, X. J., JACOBY, A. S., SHINE, J., CRAWLEY, J. N., IISMAA, T. & WIESENFELD-HALLIN, Z. 2003. Hyperalgesia and increased neuropathic pain-like response in mice lacking galanin receptor 1 receptors. *Neuroscience,* 117**,** 221-7.

BOLDING, K. A., NAGAPPAN, S., HAN, B.-X., WANG, F. & FRANKS, K. M. 2020. Recurrent circuitry is required to stabilize piriform cortex odor representations across brain states. *eLife,* 9**,** e53125.

BREIVIK, H., COLLETT, B., VENTAFRIDDA, V., COHEN, R. & GALLACHER, D. 2006. Survey of chronic pain in Europe: prevalence, impact on daily life, and treatment. *Eur J Pain,* 10**,** 287-333.

BRENNER, D. S., GOLDEN, J. P. & GEREAU, R. W. T. 2012. A novel behavioral assay for measuring cold sensation in mice. *PloS one,* 7**,** e39765-e39765.

BRUMOVSKY, P., STANIC, D., SHUSTER, S., HERZOG, H., VILLAR, M. & HÖKFELT, T. 2005. Neuropeptide Y2 receptor protein is present in peptidergic and nonpeptidergic primary sensory neurons of the mouse. *J Comp Neurol,* 489**,** 328-48.

BRUMOVSKY, P., VILLAR, M. J. & HÖKFELT, T. 2006. Tyrosine hydroxylase is expressed in a subpopulation of small dorsal root ganglion neurons in the adult mouse. *Exp Neurol,* 200**,** 153-65.

BRUMOVSKY, P. R. 2016. Dorsal root ganglion neurons and tyrosine hydroxylase--an intriguing association with implications for sensation and pain. *Pain,* 157**,** 314-320.

CHAPLAN, S. R., BACH, F. W., POGREL, J. W., CHUNG, J. M. & YAKSH, T. L. 1994. Quantitative assessment of tactile allodynia in the rat paw. *J Neurosci Methods,* 53**,** 55-63.

CHAPMAN, C. R., CASEY, K. L., DUBNER, R., FOLEY, K. M., GRACELY, R. H. & READING, A. E. 1985. Pain measurement: an overview. *Pain,* 22**,** 1-31.

CHOI, Y., YOON, Y. W., NA, H. S., KIM, S. H. & CHUNG, J. M. 1994. Behavioral signs of ongoing pain and cold allodynia in a rat model of neuropathic pain. *Pain,* 59**,** 369-76.

CIOFFI, C. L. 2018. Modulation of Glycine-Mediated Spinal Neurotransmission for the Treatment of Chronic Pain. *Journal of Medicinal Chemistry,* 61**,** 2652-2679.

COPELAND, N. G., JENKINS, N. A. & COURT, D. L. 2001. Recombineering: a powerful new tool for mouse functional genomics. *Nat Rev Genet,* 2**,** 769-79.

COSTE, B., MATHUR, J., SCHMIDT, M., EARLEY, T. J., RANADE, S., PETRUS, M. J., DUBIN, A. E. & PATAPOUTIAN, A. 2010. Piezo1 and Piezo2 are essential components of distinct mechanically activated cation channels. *Science,* 330**,** 55-60.

COULL, J. A. M., BEGGS, S., BOUDREAU, D., BOIVIN, D., TSUDA, M., INOUE, K., GRAVEL, C., SALTER, M. W. & DE KONINCK, Y. 2005. BDNF from microglia causes the shift in neuronal anion gradient underlying neuropathic pain. *Nature,* 438**,** 1017-1021.

COUNTS, S. E., PEREZ, S. E. & MUFSON, E. J. 2008. Galanin in Alzheimer's disease: neuroinhibitory or neuroprotective? *Cellular and molecular life sciences : CMLS,* 65**,** 1842-1853.

COX, J. J., REIMANN, F., NICHOLAS, A. K., THORNTON, G., ROBERTS, E., SPRINGELL, K., KARBANI, G., JAFRI, H., MANNAN, J., RAASHID, Y., AL-GAZALI, L., HAMAMY, H., VALENTE, E. M., GORMAN, S., WILLIAMS, R., MCHALE, D. P., WOOD, J. N., GRIBBLE, F. M. & WOODS, C. G. 2006. An SCN9A channelopathy causes congenital inability to experience pain. *Nature,* 444**,** 894-8.

COX, J. J., SHEYNIN, J., SHORER, Z., REIMANN, F., NICHOLAS, A. K., ZUBOVIC, L., BARALLE, M., WRAIGE, E., MANOR, E., LEVY, J., WOODS, C. G. & PARVARI, R. 2010. Congenital insensitivity to pain: novel SCN9A missense and in-frame deletion mutations. *Human mutation,* 31**,** E1670-E1686.

CUI, X., WANG, R., BIAN, P., WU, Q., SESHADRI, V. D. D. & LIU, L. 2019. Evaluation of antiarthritic activity of nimbolide against Freund's adjuvant induced arthritis in rats. *Artificial Cells, Nanomedicine, and Biotechnology,* 47**,** 3391-3398.

CURRIE, G. L., DELANEY, A., BENNETT, M. I., DICKENSON, A. H., EGAN, K. J., VESTERINEN, H. M., SENA, E. S., MACLEOD, M. R., COLVIN, L. A. & FALLON, M. T. 2013. Animal models of bone cancer pain: systematic review and meta-analyses. *Pain,* 154**,** 917-26.

D'ELIA, A. V., TELL, G., PARON, I., PELLIZZARI, L., LONIGRO, R. & DAMANTE, G. 2001. Missense mutations of human homeoboxes: A review. *Hum Mutat,* 18**,** 361-74.

DE CLAUSER, L., LUIZ, A. P., SANTANA-VARELA, S., WOOD, J. N. & SIKANDAR, S. 2020. Sensitization of Cutaneous Primary Afferents in Bone Cancer Revealed by In Vivo Calcium Imaging. *Cancers,* 12**,** 3491.

DE CLAUSER, L., SANTANA-VARELA, S., WOOD, J. N. & SIKANDAR, S. 2021. Physiologic osteoclasts are not sufficient to induce skeletal pain in mice. *European journal of pain (London, England),* 25**,** 199-212.

DEUIS, J. R., DVORAKOVA, L. S. & VETTER, I. 2017. Methods Used to Evaluate Pain Behaviors in Rodents. *Front Mol Neurosci,* 10**,** 284.

DEVAL, E., NOËL, J., LAY, N., ALLOUI, A., DIOCHOT, S., FRIEND, V., JODAR, M., LAZDUNSKI, M. & LINGUEGLIA, E. 2008. ASIC3, a sensor of acidic and primary inflammatory pain. *The EMBO journal,* 27**,** 3047-3055.

DHANDAPANI, R., AROKIARAJ, C. M., TABERNER, F. J., PACIFICO, P., RAJA, S., NOCCHI, L., PORTULANO, C., FRANCIOSA, F., MAFFEI, M., HUSSAIN, A. F., DE CASTRO REIS, F., REYMOND, L., PERLAS, E., GARCOVICH, S., BARTH, S., JOHNSSON, K., LECHNER, S. G. & HEPPENSTALL, P. A. 2018. Control of mechanical pain hypersensitivity in mice through ligand-targeted photoablation of TrkB-positive sensory neurons. *Nat Commun,* 9**,** 1640.

DOEBELE, R. C., DRILON, A., PAZ-ARES, L., SIENA, S., SHAW, A. T., FARAGO, A. F., BLAKELY, C. M., SETO, T., CHO, B. C., TOSI, D., BESSE, B., CHAWLA, S. P., BAZHENOVA, L., KRAUSS, J. C., CHAE, Y. K., BARVE, M., GARRIDO-LAGUNA, I., LIU, S. V., CONKLING, P., JOHN, T., FAKIH, M., SIGAL, D., LOONG, H. H., BUCHSCHACHER, G. L., JR., GARRIDO, P., NIEVA, J., STEUER,

C., OVERBECK, T. R., BOWLES, D. W., FOX, E., RIEHL, T., CHOW-MANEVAL, E., SIMMONS, B., CUI, N., JOHNSON, A., ENG, S., WILSON, T. R. & DEMETRI, G. D. 2020. Entrectinib in patients with advanced or metastatic NTRK fusion-positive solid tumours: integrated analysis of three phase 1-2 trials. *Lancet Oncol,* 21**,** 271-282.

DUBIN, A. E. & PATAPOUTIAN, A. 2010. Nociceptors: the sensors of the pain pathway. *The Journal of clinical investigation,* 120**,** 3760-3772.

EDDY, N. B. & LEIMBACH, D. 1953. Synthetic analgesics. II. Dithienylbutenyl- and dithienylbutylamines. *J Pharmacol Exp Ther,* 107**,** 385-93.

EMERY, E. C. & ERNFORS, P. 2018. Dorsal root ganglion neuron types and their functional specialization. *The oxford handbook of the neurobiology of pain***,** 1-30.

EMERY, E. C., LUIZ, A. P., SIKANDAR, S., MAGNÚSDÓTTIR, R., DONG, X. & WOOD, J. N. 2016. In vivo characterization of distinct modality-specific subsets of somatosensory neurons using GCaMP. *Sci Adv,* 2**,** e1600990.

ERNFORS, P., LEE, K. F., KUCERA, J. & JAENISCH, R. 1994. Lack of neurotrophin-3 leads to deficiencies in the peripheral nervous system and loss of limb proprioceptive afferents. *Cell,* 77**,** 503-12.

ESPEJO, E. F. & MIR, D. 1993. Structure of the rat's behaviour in the hot plate test. *Behav Brain Res,* 56**,** 171-6.

FALK, S. & DICKENSON, A. H. 2014. Pain and nociception: mechanisms of cancer-induced bone pain. *J Clin Oncol,* 32**,** 1647-54.

FALK, S., ULDALL, M., APPEL, C., DING, M. & HEEGAARD, A. M. 2013. Influence of sex differences on the progression of cancer-induced bone pain. *Anticancer Res,* 33**,** 1963-9.

FALTERMEIER, C. M., DRAKE, J. M., CLARK, P. M., SMITH, B. A., ZONG, Y., VOLPE, C., MATHIS, C., MORRISSEY, C., CASTOR, B., HUANG, J. & WITTE, O. N. 2016. Functional screen identifies kinases driving prostate cancer visceral and bone metastasis. *Proc Natl Acad Sci U S A,* 113**,** E172-81.

FARROW, L., GARDNER, W. T., TANG, C. C., LOW, R., FORGET, P. & ASHCROFT, G. P. 2021. Impact of COVID-19 on opioid use in those awaiting hip and knee arthroplasty: a retrospective cohort study. *BMJ Quality & Safety***,** bmjqs-2021-013450.

FERRARI, L. F., ARALDI, D. & LEVINE, J. D. 2015. Distinct terminal and cell body mechanisms in the nociceptor mediate hyperalgesic priming. *J Neurosci,* 35**,** 6107-16.

FIELD, M. J., MCCLEARY, S., HUGHES, J. & SINGH, L. 1999. Gabapentin and pregabalin, but not morphine and amitriptyline, block both static and dynamic components of mechanical allodynia induced by streptozocin in the rat. *Pain,* 80**,** 391-8.

FILLINGIM, R. B. 2017. Individual differences in pain: understanding the mosaic that makes pain personal. *Pain,* 158 Suppl 1**,** S11-S18.

FINNERUP, N. B., HAROUTOUNIAN, S., KAMERMAN, P., BARON, R., BENNETT, D. L. H., BOUHASSIRA, D., CRUCCU, G., FREEMAN, R., HANSSON, P., NURMIKKO, T., RAJA, S. N., RICE, A. S. C., SERRA, J., SMITH, B. H., TREEDE, R. D. & JENSEN, T. S. 2016. Neuropathic pain: an updated grading system for research and clinical practice. *Pain,* 157**,** 1599-1606.

FOSTER, E., WILDNER, H., TUDEAU, L., HAUETER, S., RALVENIUS, W. T., JEGEN, M., JOHANNSSEN, H., HÖSLI, L., HAENRAETS, K., GHANEM, A., CONZELMANN, K.-K., BÖSL, M. & ZEILHOFER, H. U. 2015. Targeted ablation, silencing, and activation establish glycinergic dorsal horn neurons as key components of a spinal gate for pain and itch. *Neuron,* 85**,** 1289-1304.

GARRISON, S. R., DIETRICH, A. & STUCKY, C. L. 2012. TRPC1 contributes to light-touch sensation and mechanical responses in low-threshold cutaneous sensory neurons. *J Neurophysiol,* 107**,** 913-22.

GEIGER, T. R. & PEEPER, D. S. 2007. Critical role for TrkB kinase function in anoikis suppression, tumorigenesis, and metastasis. *Cancer Res,* 67**,** 6221-9.

GHAZISAEIDI, S., RAMANI, A., SHOOSHTARI, P., TU, A., HALIEVSKI, K., FINN, D., ASSI, S., MULEY, M., WANG, V., SENGAR, A., WEKSBERG, R., BRUDNO, M. & SALTER, M. 2019. Characterization of Key Sexually Dimorphic Regulators in Pain Processing. *Canadian Journal of Pain*.

GHILARDI, J. R., FREEMAN, K. T., JIMENEZ-ANDRADE, J. M., MANTYH, W. G., BLOOM, A. P., KUSKOWSKI, M. A. & MANTYH, P. W. 2010. Administration of a tropomyosin receptor kinase inhibitor attenuates sarcoma-induced nerve sprouting, neuroma formation and bone cancer pain. *Mol Pain,* 6**,** 87.

GONG, S., DOUGHTY, M., HARBAUGH, C. R., CUMMINS, A., HATTEN, M. E., HEINTZ, N. & GERFEN, C. R. 2007. Targeting Cre Recombinase to Specific Neuron Populations with Bacterial Artificial Chromosome Constructs. *The Journal of Neuroscience,* 27**,** 9817-9823.

GONG, S., ZHENG, C., DOUGHTY, M. L., LOSOS, K., DIDKOVSKY, N., SCHAMBRA, U. B., NOWAK, N. J., JOYNER, A., LEBLANC, G., HATTEN, M. E. & HEINTZ, N. 2003. A gene expression atlas of the central nervous system based on bacterial artificial chromosomes. *Nature,* 425**,** 917-25.

GREGORY, N. S., HARRIS, A. L., ROBINSON, C. R., DOUGHERTY, P. M., FUCHS, P. N. & SLUKA, K. A. 2013. An overview of animal models of pain: disease models and outcome measures. *J Pain,* 14**,** 1255-69.

GRITSCH, S., LU, J., THILEMANN, S., WÖRTGE, S., MÖBIUS, W., BRUTTGER, J., KARRAM, K., RUHWEDEL, T., BLANFELD, M., VARDEH, D., WAISMAN, A., NAVE, K.-A. & KUNER, R. 2014. Oligodendrocyte ablation triggers central pain independently of innate or adaptive immune responses in mice. *Nature Communications,* 5**,** 5472.

GUIGO, R. & DE HOON, M. 2018. Recent advances in functional genome analysis. *F1000Res,* 7.

GURUMURTHY, C. B. & LLOYD, K. C. K. 2019. Generating mouse models for biomedical research: technological advances. *Disease models & mechanisms,* 12**,** dmm029462.

HABERBERGER, R. V., BARRY, C., DOMINGUEZ, N. & MATUSICA, D. 2019. Human Dorsal Root Ganglia. *Frontiers in Cellular Neuroscience,* 13.

HABIB, A. M., MATSUYAMA, A., OKOROKOV, A. L., SANTANA-VARELA, S., BRAS, J. T., ALOISI, A. M., EMERY, E. C., BOGDANOV, Y. D., FOLLENFANT, M., GOSSAGE, S. J., GRAS, M., HUMPHREY, J., KOLESNIKOV, A., LE CANN, K., LI, S., MINETT, M. S., PEREIRA, V., PONSOLLES, C., SIKANDAR, S., TORRES, J. M., YAMAOKA, K., ZHAO, J., KOMINE, Y., YAMAMORI, T., MANIATIS, N., PANOV, K. I., HOULDEN, H., RAMIREZ, J. D., BENNETT, D. L. H., MARSILI, L., BACHIOCCO, V., WOOD, J. N. & COX, J. J. 2017. A novel human pain insensitivity disorder caused by a point mutation in ZFHX2. *Brain,* 141**,** 365-376.

HABIB, A. M., MATSUYAMA, A., OKOROKOV, A. L., SANTANA-VARELA, S., BRAS, J. T., ALOISI, A. M., EMERY, E. C., BOGDANOV, Y. D., FOLLENFANT, M., GOSSAGE, S. J., GRAS, M., HUMPHREY, J., KOLESNIKOV, A., LE CANN, K., LI, S., MINETT, M. S., PEREIRA, V., PONSOLLES, C., SIKANDAR, S., TORRES, J. M., YAMAOKA, K., ZHAO, J., KOMINE, Y., YAMAMORI, T., MANIATIS, N., PANOV, K. I., HOULDEN, H., RAMIREZ, J. D., BENNETT, D. L. H., MARSILI, L., BACHIOCCO, V., WOOD, J. N. & COX, J. J. 2018a. A novel human pain insensitivity disorder caused by a point mutation in ZFHX2. *Brain,* 141**,** 365-376.

HABIB, A. M., MATSUYAMA, A., OKOROKOV, A. L., SANTANA-VARELA, S., BRAS, J. T., ALOISI, A. M., EMERY, E. C., BOGDANOV, Y. D., FOLLENFANT, M., GOSSAGE, S. J., GRAS, M., HUMPHREY, J., KOLESNIKOV, A., LE CANN, K., LI, S., MINETT, M. S., PEREIRA, V., PONSOLLES, C., SIKANDAR, S., TORRES, J. M., YAMAOKA, K., ZHAO, J., KOMINE, Y., YAMAMORI, T., MANIATIS, N., PANOV, K. I., HOULDEN, H., RAMIREZ, J. D., BENNETT, D. L. H., MARSILI, L., BACHIOCCO, V., WOOD, J. N. & COX, J. J. 2018b. A novel human pain insensitivity disorder caused by a point mutation in ZFHX2. *Brain : a journal of neurology,* 141**,** 365-376.

HABIB, A. M., OKOROKOV, A. L., HILL, M. N., BRAS, J. T., LEE, M.-C., LI, S., GOSSAGE, S. J., VAN DRIMMELEN, M., MORENA, M., HOULDEN, H., RAMIREZ, J. D., BENNETT, D. L. H., SRIVASTAVA, D. & COX, J. J. 2019a. Microdeletion in a FAAH pseudogene identified in a patient with high anandamide concentrations and pain insensitivity. *British journal of anaesthesia,* 123**,** e249-e253.

HABIB, A. M., OKOROKOV, A. L., HILL, M. N., BRAS, J. T., LEE, M. C., LI, S., GOSSAGE, S. J., VAN DRIMMELEN, M., MORENA, M., HOULDEN, H., RAMIREZ, J. D., BENNETT, D. L. H.,

SRIVASTAVA, D. & COX, J. J. 2019b. Microdeletion in a FAAH pseudogene identified in a patient with high anandamide concentrations and pain insensitivity. *Br J Anaesth*.

HAN, L., MA, C., LIU, Q., WENG, H.-J., CUI, Y., TANG, Z., KIM, Y., NIE, H., QU, L., PATEL, K. N., LI, Z., MCNEIL, B., HE, S., GUAN, Y., XIAO, B., LAMOTTE, R. H. & DONG, X. 2012. A subpopulation of nociceptors specifically linked to itch. *Nature Neuroscience,* 16**,** 174.

HAN, L., MA, C., LIU, Q., WENG, H.-J., CUI, Y., TANG, Z., KIM, Y., NIE, H., QU, L., PATEL, K. N., LI, Z., MCNEIL, B., HE, S., GUAN, Y., XIAO, B., LAMOTTE, R. H. & DONG, X. 2013a. A subpopulation of nociceptors specifically linked to itch. *Nature Neuroscience,* 16**,** 174-182.

HAN, L., MA, C., LIU, Q., WENG, H. J., CUI, Y., TANG, Z., KIM, Y., NIE, H., QU, L., PATEL, K. N., LI, Z., MCNEIL, B., HE, S., GUAN, Y., XIAO, B., LAMOTTE, R. H. & DONG, X. 2013b. A subpopulation of nociceptors specifically linked to itch. *Nat Neurosci,* 16**,** 174-82.

HANESCH, U., PFROMMER, U., GRUBB, B. D. & SCHAIBLE, H. G. 1993. Acute and chronic phases of unilateral inflammation in rat's ankle are associated with an increase in the proportion of calcitonin gene-related peptide-immunoreactive dorsal root ganglion cells. *Eur J Neurosci,* 5**,** 154-61.

HARGREAVES, K., DUBNER, R., BROWN, F., FLORES, C. & JORIS, J. 1988. A new and sensitive method for measuring thermal nociception in cutaneous hyperalgesia. *Pain,* 32**,** 77-88.

HASSELMANN, J., COBURN, M. A., ENGLAND, W., FIGUEROA VELEZ, D. X., KIANI SHABESTARI, S., TU, C. H., MCQUADE, A., KOLAHDOUZAN, M., ECHEVERRIA, K., CLAES, C., NAKAYAMA, T., AZEVEDO, R., COUFAL, N. G., HAN, C. Z., CUMMINGS, B. J., DAVTYAN, H., GLASS, C. K., HEALY, L. M., GANDHI, S. P., SPITALE, R. C. & BLURTON-JONES, M. 2019. Development of a Chimeric Model to Study and Manipulate Human Microglia In Vivo. *Neuron,* 103**,** 1016-1033.e10.

HILL, R. 2000. NK1 (substance P) receptor antagonists - Why are they not analgesic in humans? *Trends in pharmacological sciences,* 21**,** 244-6.

HJERLING-LEFFLER, J., ALQATARI, M., ERNFORS, P. & KOLTZENBURG, M. 2007. Emergence of functional sensory subtypes as defined by transient receptor potential channel expression. *J Neurosci,* 27**,** 2435-43.

HOLMES, F. E., BACON, A., POPE, R. J., VANDERPLANK, P. A., KERR, N. C., SUKUMARAN, M., PACHNIS, V. & WYNICK, D. 2003a. Transgenic overexpression of galanin in the dorsal root ganglia modulates pain-related behavior. *Proc Natl Acad Sci U S A,* 100**,** 6180-5.

HOLMES, F. E., BACON, A., POPE, R. J. P., VANDERPLANK, P. A., KERR, N. C. H., SUKUMARAN, M., PACHNIS, V. & WYNICK, D. 2003b. Transgenic overexpression of galanin in the dorsal root ganglia modulates pain-related behavior. *Proceedings of the National Academy of Sciences,* 100**,** 6180-6185.

HUANG, T., LIN, S.-H., MALEWICZ, N. M., ZHANG, Y., ZHANG, Y., GOULDING, M., LAMOTTE, R. H. & MA, Q. 2019a. Identifying the pathways required for coping behaviours associated with sustained pain. *Nature,* 565**,** 86-90.

HUANG, T., LIN, S. H., MALEWICZ, N. M., ZHANG, Y., ZHANG, Y., GOULDING, M., LAMOTTE, R. H. & MA, Q. 2019b. Identifying the pathways required for coping behaviours associated with sustained pain. *Nature,* 565**,** 86-90.

HUNSKAAR, S. & HOLE, K. 1987. The formalin test in mice: dissociation between inflammatory and non-inflammatory pain. *Pain,* 30**,** 103-114.

HWANG, B., LEE, J. H. & BANG, D. 2018. Single-cell RNA sequencing technologies and bioinformatics pipelines. *Experimental & molecular medicine,* 50**,** 96-96.

JI, R. R. & STRICHARTZ, G. 2004. Cell signaling and the genesis of neuropathic pain. *Sci STKE,* 2004**,** reE14.

JONES, B. J. & ROBERTS, D. J. 1968. The quantiative measurement of motor inco-ordination in naive mice using an acelerating rotarod. *J Pharm Pharmacol,* 20**,** 302-4.

JOSHI, S. K., DAVARE, M. A., DRUKER, B. J. & TOGNON, C. E. 2019. Revisiting NTRKs as an emerging oncogene in hematological malignancies. *Leukemia,* 33**,** 2563-2574.

JOURDAN, D., ARDID, D., BARDIN, L., BARDIN, M., NEUZERET, D., LANPHOUTHACOUL, L. & ESCHALIER, A. 1997. A new automated method of pain scoring in the formalin test in rats. *Pain,* 71**,** 265-70.

JUSTICE, M. J. & DHILLON, P. 2016. Using the mouse to model human disease: increasing validity and reproducibility. *Disease models & mechanisms,* 9**,** 101-103.

KANDEL, E. R. S. J. H. J. T. M. 1991. Principles of neural science.

KARPOVA, N. N., SALES, A. J. & JOCA, S. R. 2017. Epigenetic Basis of Neuronal and Synaptic Plasticity. *Curr Top Med Chem,* 17**,** 771-793.

KELLEY, J. M., FIELD, C. E., CRAVEN, M. B., BOCSKAI, D., KIM, U. J., ROUNSLEY, S. D. & ADAMS, M. D. 1999. High throughput direct end sequencing of BAC clones. *Nucleic Acids Res,* 27**,** 1539-46.

KERSTEIN, P. C., DEL CAMINO, D., MORAN, M. M. & STUCKY, C. L. 2009. Pharmacological blockade of TRPA1 inhibits mechanical firing in nociceptors. *Molecular pain,* 5**,** 19-19.

KESTELL, G. R., ANDERSON, R. L., CLARKE, J. N., HABERBERGER, R. V. & GIBBINS, I. L. 2015. Primary afferent neurons containing calcitonin gene-related peptide but not substance P in forepaw skin, dorsal root ganglia, and spinal cord of mice. *J Comp Neurol,* 523**,** 2555-69.

KNOWLTON, W. M., PALKAR, R., LIPPOLDT, E. K., MCCOY, D. D., BALUCH, F., CHEN, J. & MCKEMY, D. D. 2013. A sensory-labeled line for cold: TRPM8-expressing sensory neurons define the cellular basis for cold, cold pain, and cooling-mediated analgesia. *The Journal of neuroscience : the official journal of the Society for Neuroscience,* 33**,** 2837-2848.

KOMINE, Y., NAKAMURA, K., KATSUKI, M. & YAMAMORI, T. 2006. Novel transcription factor zfh-5 is negatively regulated by its own antisense RNA in mouse brain. *Mol Cell Neurosci,* 31**,** 273-83.

KOMINE, Y., TAKAO, K., MIYAKAWA, T. & YAMAMORI, T. 2013. Behavioral Abnormalities Observed in Zfhx2-Deficient Mice. *PLOS ONE,* 7**,** e53114.

KUPARI, J., USOSKIN, D., PARISIEN, M., LOU, D., HU, Y., FATT, M., LÖNNERBERG, P., SPÅNGBERG, M., ERIKSSON, B., BARKAS, N., KHARCHENKO, P. V., LORÉ, K., KHOURY, S., DIATCHENKO, L. & ERNFORS, P. 2021. Single cell transcriptomics of primate sensory neurons identifies cell types associated with chronic pain. *Nature Communications,* 12**,** 1510.

LALLEMEND, F. & ERNFORS, P. 2012. Molecular interactions underlying the specification of sensory neurons. *Trends Neurosci,* 35**,** 373-81.

LANGE, A. M. & LO, H. W. 2018. Inhibiting TRK Proteins in Clinical Cancer Therapy. *Cancers (Basel),* 10.

LARSON, A. A., BROWN, D. R., EL-ATRASH, S. & WALSER, M. M. 1986. Pain threshold changes in adjuvant-induced inflammation: a possible model of chronic pain in the mouse. *Pharmacol Biochem Behav,* 24**,** 49-53.

LAU, J., MINETT, M. S., ZHAO, J., DENNEHY, U., WANG, F., WOOD, J. N. & BOGDANOV, Y. D. 2011. Temporal control of gene deletion in sensory ganglia using a tamoxifen-inducible Advillin-Cre-ERT2 recombinase mouse. *Mol Pain,* 7**,** 100.

LE BARS, D., GOZARIU, M. & CADDEN, S. W. 2001. Animal models of nociception. *Pharmacol Rev,* 53**,** 597-652.

LEE, C. S., BISHOP, E. S., ZHANG, R., YU, X., FARINA, E. M., YAN, S., ZHAO, C., ZHENG, Z., SHU, Y., WU, X., LEI, J., LI, Y., ZHANG, W., YANG, C., WU, K., WU, Y., HO, S., ATHIVIRAHAM, A., LEE, M. J., WOLF, J. M., REID, R. R. & HE, T.-C. 2017. Adenovirus-Mediated Gene Delivery: Potential Applications for Gene and Cell-Based Therapies in the New Era of Personalized Medicine. *Genes & diseases,* 4**,** 43-63.

LESLIE, J. & NEDIVI, E. 2011. Activity-Regulated Genes as Mediators of Neural Circuit Plasticity. *Progress in neurobiology,* 94**,** 223-37.

LEWIS, V. A. & GEBHART, G. F. 1977. Evaluation of the periaqueductal central gray (PAG) as a morphine-specific locus of action and examination of morphine-induced and stimulation-produced analgesia at coincident PAG loci. *Brain Res,* 124**,** 283-303.

LI, C.-L., LI, K.-C., WU, D., CHEN, Y., LUO, H., ZHAO, J.-R., WANG, S.-S., SUN, M.-M., LU, Y.-J., ZHONG, Y.-Q., HU, X.-Y., HOU, R., ZHOU, B.-B., BAO, L., XIAO, H.-S. & ZHANG, X. 2016. Somatosensory neuron types identified by high-coverage single-cell RNA-sequencing and functional heterogeneity. *Cell Research,* 26**,** 83-102.

LIPTON, A. & BALAKUMARAN, A. 2012. Denosumab for the treatment of cancer therapy-induced bone loss and prevention of skeletal-related events in patients with solid tumors. *Expert Rev Clin Pharmacol,* 5**,** 359-71.

LIU, H. & HÖKFELT, T. 2000. Effect of intrathecal galanin and its putative antagonist M35 on pain behavior in a neuropathic pain model. *Brain Res,* 886**,** 67-72.

LIU, Q. & DONG, X. 2015. The role of the Mrgpr receptor family in itch. *Handb Exp Pharmacol,* 226**,** 71-88.

LÖKEN, L. S., BRAZ, J. M., ETLIN, A., SADEGHI, M., BERNSTEIN, M., JEWELL, M., STEYERT, M., KUHN, J., HAMEL, K., LLEWELLYN-SMITH, I. J. & BASBAUM, A. 2021. Contribution of dorsal horn CGRP-expressing interneurons to mechanical sensitivity. *Elife,* 10.

LOLIGNIER, S., AMSALEM, M., MAINGRET, F., PADILLA, F., GABRIAC, M., CHAPUY, E., ESCHALIER, A., DELMAS, P. & BUSSEROLLES, J. 2011. Nav1.9 channel contributes to mechanical and heat pain hypersensitivity induced by subacute and chronic inflammation. *PLoS One,* 6**,** e23083.

LOLIGNIER, S., GKIKA, D., ANDERSSON, D., LEIPOLD, E., VETTER, I., VIANA, F., NOËL, J. & BUSSEROLLES, J. 2016. New Insight in Cold Pain: Role of Ion Channels, Modulation, and Clinical Perspectives. *J Neurosci,* 36**,** 11435-11439.

LOPES, D. M., MALEK, N., EDYE, M., JAGER, S. B., MCMURRAY, S., MCMAHON, S. B. & DENK, F. 2017. Sex differences in peripheral not central immune responses to pain-inducing injury. *Scientific Reports,* 7**,** 16460.

LUIZ, A. P., MACDONALD, D. I., SANTANA-VARELA, S., MILLET, Q., SIKANDAR, S., WOOD, J. N. & EMERY, E. C. 2019. Cold sensing by NaV1.8-positive and NaV1.8-negative sensory neurons. *Proc Natl Acad Sci U S A,* 116**,** 3811-3816.

LUONG, T. N., CARLISLE, H. J., SOUTHWELL, A. & PATTERSON, P. H. 2011. Assessment of motor balance and coordination in mice using the balance beam. *J Vis Exp*.

MACDONALD, D. I., SIKANDAR, S., WEISS, J., PYRSKI, M., LUIZ, A. P., MILLET, Q., EMERY, E. C., MANCINI, F., IANNETTI, G. D., ALLES, S. R. A., ARCANGELETTI, M., ZHAO, J., COX, J. J., BROWNSTONE, R. M., ZUFALL, F. & WOOD, J. N. 2021. A central mechanism of analgesia in mice and humans lacking the sodium channel Na(V)1.7. *Neuron,* 109**,** 1497-1512.e6.

MADISEN, L., ZWINGMAN, T. A., SUNKIN, S. M., OH, S. W., ZARIWALA, H. A., GU, H., NG, L. L., PALMITER, R. D., HAWRYLYCZ, M. J., JONES, A. R., LEIN, E. S. & ZENG, H. 2010. A robust and high-throughput Cre reporting and characterization system for the whole mouse brain. *Nat Neurosci,* 13**,** 133-40.

MAGNUSDOTTIR, R., GOHIN, S., TER HEEGDE, F., HOPKINSON, M., MCNALLY, I. F., FISHER, A., UPTON, N., BILLINTON, A. & CHENU, C. 2021. Fracture-induced pain-like behaviours in a femoral fracture mouse model. *Osteoporos Int,* 32**,** 2347-2359.

MALMBERG, A. B. & BASBAUM, A. I. 1998. Partial sciatic nerve injury in the mouse as a model of neuropathic pain: behavioral and neuroanatomical correlates. *Pain,* 76**,** 215-22.

MARONI, P. & BENDINELLI, P. 2020. Bone, a Secondary Growth Site of Breast and Prostate Carcinomas: Role of Osteocytes. *Cancers,* 12**,** 1812.

MARQUES, S., ZEISEL, A., CODELUPPI, S., VAN BRUGGEN, D., MENDANHA FALCÃO, A., XIAO, L., LI, H., HÄRING, M., HOCHGERNER, H., ROMANOV, R. A., GYLLBORG, D., MUÑOZ MANCHADO, A., LA MANNO, G., LÖNNERBERG, P., FLORIDDIA, E. M., REZAYEE, F., ERNFORS, P., ARENAS, E., HJERLING-LEFFLER, J., HARKANY, T., RICHARDSON, W. D., LINNARSSON, S. & CASTELO-BRANCO, G. 2016. Oligodendrocyte heterogeneity in the mouse juvenile and adult central nervous system. *Science,* 352**,** 1326-1329.

MASON, P. 2007. Placing pain on the sensory map: classic papers by Ed Perl and colleagues. *J Neurophysiol,* 97**,** 1871-3.

MATSUSHITA, N., OKADA, H., YASOSHIMA, Y., TAKAHASHI, K., KIUCHI, K. & KOBAYASHI, K. 2002. Dynamics of tyrosine hydroxylase promoter activity during midbrain dopaminergic neuron development. *J Neurochem,* 82**,** 295-304.

MATSUURA, K., KABUTO, H., MAKINO, H. & OGAWA, N. 1997. Pole test is a useful method for evaluating the mouse movement disorder caused by striatal dopamine depletion. *J Neurosci Methods,* 73**,** 45-8.

MAY, E. S., TIEMANN, L., SCHMIDT, P., NICKEL, M. M., WIEDEMANN, N., DRESEL, C., SORG, C. & PLONER, M. 2017. Behavioral responses to noxious stimuli shape the perception of pain. *Sci Rep,* 7**,** 44083.

MCCARTHY, P. W. & LAWSON, S. N. 1990. Cell type and conduction velocity of rat primary sensory neurons with calcitonin gene-related peptide-like immunoreactivity. *Neuroscience,* 34**,** 623-632.

MCCOY, E. S., TAYLOR-BLAKE, B., STREET, S. E., PRIBISKO, A. L., ZHENG, J. & ZYLKA, M. J. 2013. Peptidergic CGRPα primary sensory neurons encode heat and itch and tonically suppress sensitivity to cold. *Neuron,* 78**,** 138-51.

MCCOY, E. S., TAYLOR-BLAKE, B. & ZYLKA, M. J. 2012. CGRPα-Expressing Sensory Neurons Respond to Stimuli that Evoke Sensations of Pain and Itch. *PLOS ONE,* 7**,** e36355.

MCNAMARA, C. R., MANDEL-BREHM, J., BAUTISTA, D. M., SIEMENS, J., DERANIAN, K. L., ZHAO, M., HAYWARD, N. J., CHONG, J. A., JULIUS, D., MORAN, M. M. & FANGER, C. M. 2007. TRPA1 mediates formalin-induced pain. *Proc Natl Acad Sci U S A,* 104**,** 13525-30.

MELZACK, R. & WALL, P. D. 1965. Pain Mechanisms: A New Theory. *Science,* 150**,** 971-979.

MERCADANTE, S., VILLARI, P., FERRERA, P. & CASUCCIO, A. 2004. Optimization of opioid therapy for preventing incident pain associated with bone metastases. *J Pain Symptom Manage,* 28**,** 505-10.

METZGER, D. & CHAMBON, P. 2001. Site- and time-specific gene targeting in the mouse. *Methods,* 24**,** 71-80.

MINETT, M. S., FALK, S., SANTANA-VARELA, S., BOGDANOV, Y. D., NASSAR, M. A., HEEGAARD, A.-M. & WOOD, J. N. 2014a. Pain without nociceptors? Nav1.7-independent pain mechanisms. *Cell reports,* 6**,** 301-312.

MINETT, M. S., FALK, S., SANTANA-VARELA, S., BOGDANOV, Y. D., NASSAR, M. A., HEEGAARD, A. M. & WOOD, J. N. 2014b. Pain without nociceptors? Nav1.7-independent pain mechanisms. *Cell Rep,* 6**,** 301-12.

MINETT, M. S., NASSAR, M. A., CLARK, A. K., PASSMORE, G., DICKENSON, A. H., WANG, F., MALCANGIO, M. & WOOD, J. N. 2012a. Distinct Nav1.7-dependent pain sensations require different sets of sensory and sympathetic neurons. *Nature communications,* 3**,** 791-791.

MINETT, M. S., NASSAR, M. A., CLARK, A. K., PASSMORE, G., DICKENSON, A. H., WANG, F., MALCANGIO, M. & WOOD, J. N. 2012b. Distinct Nav1.7-dependent pain sensations require different sets of sensory and sympathetic neurons. *Nat Commun,* 3**,** 791.

MINETT, M. S., PEREIRA, V., SIKANDAR, S., MATSUYAMA, A., LOLIGNIER, S., KANELLOPOULOS, A. H., MANCINI, F., IANNETTI, G. D., BOGDANOV, Y. D., SANTANA-VARELA, S., MILLET, Q., BASKOZOS, G., MACALLISTER, R., COX, J. J., ZHAO, J. & WOOD, J. N. 2015. Endogenous opioids contribute to insensitivity to pain in humans and mice lacking sodium channel Nav1.7. *Nature communications,* 6**,** 8967-8967.

MINETT, M. S., QUICK, K. & WOOD, J. N. 2011. Behavioral Measures of Pain Thresholds. *Curr Protoc Mouse Biol,* 1**,** 383-412.

MIZUMURA, K. 1997. Peripheral mechanism of hyperalgesia--sensitization of nociceptors. *Nagoya J Med Sci,* 60**,** 69-87.

MOGIL, J. S. 2009. Animal models of pain: progress and challenges. *Nat Rev Neurosci,* 10**,** 283-94.

MOGIL, J. S. & CHANDA, M. L. 2005. The case for the inclusion of female subjects in basic science studies of pain. *Pain,* 117**,** 1-5.

MURRAY, C. W., PORRECA, F. & COWAN, A. 1988. Methodological refinements to the mouse paw formalin test. An animal model of tonic pain. *J Pharmacol Methods,* 20**,** 175-86.

NAGAE, M., HIRAGA, T. & YONEDA, T. 2007. Acidic microenvironment created by osteoclasts causes bone pain associated with tumor colonization. *Journal of Bone and Mineral Metabolism,* 25**,** 99-104.

NAGATSU, T., LEVITT, M. & UDENFRIEND, S. 1964. TYROSINE HYDROXYLASE. THE INITIAL STEP IN NOREPINEPHRINE BIOSYNTHESIS. *J Biol Chem,* 239**,** 2910-7.

NASSAR, M. A., STIRLING, L. C., FORLANI, G., BAKER, M. D., MATTHEWS, E. A., DICKENSON, A. H. & WOOD, J. N. 2004a. Nociceptor-specific gene deletion reveals a major role for Nav1.7 (PN1) in acute and inflammatory pain. *Proc Natl Acad Sci U S A,* 101**,** 12706-11.

NASSAR, M. A., STIRLING, L. C., FORLANI, G., BAKER, M. D., MATTHEWS, E. A., DICKENSON, A. H. & WOOD, J. N. 2004b. Nociceptor-specific gene deletion reveals a major role for Nav1.7 (PN1) in acute and inflammatory pain. *Proceedings of the National Academy of Sciences of the United States of America,* 101**,** 12706-12711.

NIIYAMA, Y., KAWAMATA, T., YAMAMOTO, J., OMOTE, K. & NAMIKI, A. 2007. Bone cancer increases transient receptor potential vanilloid subfamily 1 expression within distinct subpopulations of dorsal root ganglion neurons. *Neuroscience,* 148**,** 560-72.

PERINI, I., OLAUSSON, H. & MORRISON, I. 2015. Seeking pleasant touch: neural correlates of behavioral preferences for skin stroking. *Front Behav Neurosci,* 9**,** 8.

PERL, E. R. 2011. Pain mechanisms: a commentary on concepts and issues. *Prog Neurobiol,* 94**,** 20-38.

QIAN, Y. Q., BILLETER, M., OTTING, G., MÜLLER, M., GEHRING, W. J. & WÜTHRICH, K. 1989. The structure of the Antennapedia homeodomain determined by NMR spectroscopy in solution: comparison with prokaryotic repressors. *Cell,* 59**,** 573-80.

QUADROS, A. U., PINTO, L. G., FONSECA, M. M., KUSUDA, R., CUNHA, F. Q. & CUNHA, T. M. 2015. Dynamic weight bearing is an efficient and predictable method for evaluation of arthritic nociception and its pathophysiological mechanisms in mice. *Sci Rep,* 5**,** 14648.

RADHAKRISHNAN, R., MOORE, S. A. & SLUKA, K. A. 2003. Unilateral carrageenan injection into muscle or joint induces chronic bilateral hyperalgesia in rats. *Pain,* 104**,** 567-577.

RAJA, S. N., CARR, D. B., COHEN, M., FINNERUP, N. B., FLOR, H., GIBSON, S., KEEFE, F. J., MOGIL, J. S., RINGKAMP, M., SLUKA, K. A., SONG, X. J., STEVENS, B., SULLIVAN, M. D., TUTELMAN, P. R., USHIDA, T. & VADER, K. 2020. The revised International Association for the Study of Pain definition of pain: concepts, challenges, and compromises. *Pain,* 161**,** 1976-1982.

RAMACHANDRAN, V. S. & ROGERS-RAMACHANDRAN, D. 2000. Phantom limbs and neural plasticity. *Arch Neurol,* 57**,** 317-20.

RAMÓN Y CAJAL, S. 1909. *Histologie du système nerveux de l'homme & des vertébrés,* Paris :, Maloine.

RANDALL, L. O. & SELITTO, J. J. 1957. A method for measurement of analgesic activity on inflamed tissue. *Arch Int Pharmacodyn Ther,* 111**,** 409-19.

RAOUF, R., QUICK, K. & WOOD, J. N. 2010. Pain as a channelopathy. *J Clin Invest,* 120**,** 3745-52.

REICHLING, D. B. & LEVINE, J. D. 2009. Critical role of nociceptor plasticity in chronic pain. *Trends in neurosciences,* 32**,** 611-618.

REIMANN, F., COX, J. J., BELFER, I., DIATCHENKO, L., ZAYKIN, D. V., MCHALE, D. P., DRENTH, J. P., DAI, F., WHEELER, J., SANDERS, F., WOOD, L., WU, T. X., KARPPINEN, J., NIKOLAJSEN, L., MÄNNIKKÖ, M., MAX, M. B., KISELYCZNYK, C., PODDAR, M., TE MORSCHE, R. H., SMITH, S., GIBSON, D., KELEMPISIOTI, A., MAIXNER, W., GRIBBLE, F. M. & WOODS, C. G. 2010. Pain perception is altered by a nucleotide polymorphism in SCN9A. *Proc Natl Acad Sci U S A,* 107**,** 5148-53.

RHODES, D. 2018. NHS accused of fuelling rise in opioid addiction. *BBC News*, 15 March 2018.

RUTLIN, M., HO, C. Y., ABRAIRA, V. E., CASSIDY, C., BAI, L., WOODBURY, C. J. & GINTY, D. D. 2014a. The cellular and molecular basis of direction selectivity of Adelta-LTMRs. *Cell,* 159**,** 1640-51.

RUTLIN, M., HO, C. Y., ABRAIRA, V. E., CASSIDY, C., BAI, L., WOODBURY, C. J. & GINTY, D. D. 2014b. The cellular and molecular basis of direction selectivity of Aδ-LTMRs. *Cell,* 159**,** 1640-51.

SAEGUSA, H., MATSUDA, Y. & TANABE, T. 2002. Effects of ablation of N- and R-type Ca(2+) channels on pain transmission. *Neurosci Res,* 43**,** 1-7.

SAKURADA, T., MATSUMURA, T., MORIYAMA, T., SAKURADA, C., UENO, S. & SAKURADA, S. 2003. Differential effects of intraplantar capsazepine and ruthenium red on capsaicin-induced desensitization in mice. *Pharmacol Biochem Behav,* 75**,** 115-21.

SALMON, A.-M., DAMAJ, M. I., MARUBIO, L. M., EPPING-JORDAN, M. P., MERLO-PICH, E. & CHANGEUX, J.-P. 2001. Altered neuroadaptation in opiate dependence and neurogenic inflammatory nociception in αCGRP-deficient mice. *Nature Neuroscience,* 4**,** 357-358.

SANGER, F., NICKLEN, S. & COULSON, A. R. 1977. DNA sequencing with chain-terminating inhibitors. *Proc Natl Acad Sci U S A,* 74**,** 5463-7.

SANTANA-VARELA, S., BOGDANOV, Y., GOSSAGE, S., OKOROKOV, A., LI, S., DE CLAUSER, L., ALVES-SIMOES, M., SEXTON, J., ISEPPON, F., LUIZ, A., ZHAO, J., WOOD, J. & COX, J. 2021. Tools for analysis and conditional deletion of subsets of sensory neurons [version 1; peer review: 1 approved]. *Wellcome Open Research,* 6.

SCHMIDT, R., SCHMELZ, M., FORSTER, C., RINGKAMP, M., TOREBJÖRK, E. & HANDWERKER, H. 1995. Novel classes of responsive and unresponsive C nociceptors in human skin. *J Neurosci,* 15**,** 333-41.

SCHNÜTGEN, F., DOERFLINGER, N., CALLÉJA, C., WENDLING, O., CHAMBON, P. & GHYSELINCK, N. B. 2003. A directional strategy for monitoring Cre-mediated recombination at the cellular level in the mouse. *Nature Biotechnology,* 21**,** 562-565.

SCHOLZ, J., FINNERUP, N. B., ATTAL, N., AZIZ, Q., BARON, R., BENNETT, M. I., BENOLIEL, R., COHEN, M., CRUCCU, G., DAVIS, K. D., EVERS, S., FIRST, M., GIAMBERARDINO, M. A., HANSSON, P., KAASA, S., KORWISI, B., KOSEK, E., LAVAND'HOMME, P., NICHOLAS, M., NURMIKKO, T., PERROT, S., RAJA, S. N., RICE, A. S. C., ROWBOTHAM, M. C., SCHUG, S., SIMPSON, D. M., SMITH, B. H., SVENSSON, P., VLAEYEN, J. W. S., WANG, S.-J., BARKE, A., RIEF, W., TREEDE, R.-D. & CLASSIFICATION COMMITTEE OF THE NEUROPATHIC PAIN SPECIAL INTEREST, G. 2019. The IASP classification of chronic pain for ICD-11: chronic neuropathic pain. *Pain,* 160**,** 53-59.

SCHOUENBORG, J. & SJÖLUND, B. H. 1983. Activity evoked by A- and C-afferent fibers in rat dorsal horn neurons and its relation to a flexion reflex. *J Neurophysiol,* 50**,** 1108-21.

SCHREIBER, R. C., HYATT-SACHS, H., BENNETT, T. A. & ZIGMOND, R. E. 1994. Galanin expression increases in adult rat sympathetic neurons after axotomy. *Neuroscience,* 60**,** 17-27.

SCHWEDT, T. J. 2013. Multisensory integration in migraine. *Curr Opin Neurol,* 26**,** 248-53.

SCHWEI, M. J., HONORE, P., ROGERS, S. D., SALAK-JOHNSON, J. L., FINKE, M. P., RAMNARAINE, M. L., CLOHISY, D. R. & MANTYH, P. W. 1999. Neurochemical and cellular reorganization of the spinal cord in a murine model of bone cancer pain. *J Neurosci,* 19**,** 10886-97.

SHAER, M. 2019. THE FAMILY THAT FEELS ALMOST NO PAIN. *Smithsonian magazine.*

SHIELDS, S. D., CAVANAUGH, D. J., LEE, H., ANDERSON, D. J. & BASBAUM, A. I. 2010. Pain behavior in the formalin test persists after ablation of the great majority of C-fiber nociceptors. *PAIN®,* 151**,** 422-429.

SHIERS, S., KLEIN, R. M. & PRICE, T. J. 2020. Quantitative differences in neuronal subpopulations between mouse and human dorsal root ganglia demonstrated with RNAscope in situ hybridization. *Pain,* 161**,** 2410-2424.

SIKANDAR, S., MINETT, M. S., MILLET, Q., SANTANA-VARELA, S., LAU, J., WOOD, J. N. & ZHAO, J. 2018. Brain-derived neurotrophic factor derived from sensory neurons plays a critical role in chronic pain. *Brain : a journal of neurology,* 141**,** 1028-1039.

SIMONE, D. A. & KAJANDER, K. C. 1997. Responses of cutaneous A-fiber nociceptors to noxious cold. *J Neurophysiol,* 77**,** 2049-60.

SIMONE, D. A., NGEOW, J. Y., PUTTERMAN, G. J. & LAMOTTE, R. H. 1987. Hyperalgesia to heat after intradermal injection of capsaicin. *Brain Res,* 418**,** 201-3.

SKOFITSCH, G. & JACOBOWITZ, D. M. 1985. Immunohistochemical mapping of galanin-like neurons in the rat central nervous system. *Peptides,* 6**,** 509-46.

SNIDER, W. D. & MCMAHON, S. B. 1998. Tackling pain at the source: new ideas about nociceptors. *Neuron,* 20**,** 629-32.

SONG, H., YAO, E., LIN, C., GACAYAN, R., CHEN, M. H. & CHUANG, P. T. 2012. Functional characterization of pulmonary neuroendocrine cells in lung development, injury, and tumorigenesis. *Proc Natl Acad Sci U S A,* 109**,** 17531-6.

SORGE, R. E., LACROIX-FRALISH, M. L., TUTTLE, A. H., SOTOCINAL, S. G., AUSTIN, J. S., RITCHIE, J., CHANDA, M. L., GRAHAM, A. C., TOPHAM, L., BEGGS, S., SALTER, M. W. & MOGIL, J. S. 2011. Spinal cord Toll-like receptor 4 mediates inflammatory and neuropathic hypersensitivity in male but not female mice. *J Neurosci,* 31**,** 15450-4.

SPINSANTI, G., ZANNOLLI, R., PANTI, C., CECCARELLI, I., MARSILI, L., BACHIOCCO, V., FRATI, F. & ALOISI, A. M. 2008. Quantitative Real-Time PCR detection of TRPV1-4 gene expression in human leukocytes from healthy and hyposensitive subjects. *Mol Pain,* 4**,** 51.

TADASHI, T., MASAYOSHI, N., YASUYUKI, T., KOHTAROU, K., MASAHIKO, W., HIROAKI, H., YURI, O., TSUNEYASU, K. & TOMOYUKI, K. 2021. *Nature Portfolio*.

TAN, C. H. & MCNAUGHTON, P. A. 2016. The TRPM2 ion channel is required for sensitivity to warmth. *Nature,* 536**,** 460-3.

TER HEEGDE, F., LUIZ, A. P., SANTANA-VARELA, S., CHESSELL, I. P., WELSH, F., WOOD, J. N. & CHENU, C. 2019. Noninvasive Mechanical Joint Loading as an Alternative Model for Osteoarthritic Pain. *Arthritis Rheumatol,* 71**,** 1078-1088.

TODD, A. J. 2010. Neuronal circuitry for pain processing in the dorsal horn. *Nature reviews. Neuroscience,* 11**,** 823-836.

TORSNEY, C. 2019. Inflammatory pain neural plasticity. *Current Opinion in Physiology,* 11**,** 51-57.

TRUONG, D. J., KÜHNER, K., KÜHN, R., WERFEL, S., ENGELHARDT, S., WURST, W. & ORTIZ, O. 2015. Development of an intein-mediated split-Cas9 system for gene therapy. *Nucleic Acids Res,* 43**,** 6450-8.

URIEN, L., GAILLARD, S., LO RE, L., MALAPERT, P., BOHIC, M., REYNDERS, A. & MOQRICH, A. 2017. Genetic ablation of GINIP-expressing primary sensory neurons strongly impairs Formalin-evoked pain. *Scientific Reports,* 7**,** 43493.

USOSKIN, D., FURLAN, A., ISLAM, S., ABDO, H., LONNERBERG, P., LOU, D., HJERLING-LEFFLER, J., HAEGGSTROM, J., KHARCHENKO, O., KHARCHENKO, P. V., LINNARSSON, S. & ERNFORS, P. 2015a. Unbiased classification of sensory neuron types by large-scale single-cell RNA sequencing. *Nat Neurosci,* 18**,** 145-53.

USOSKIN, D., FURLAN, A., ISLAM, S., ABDO, H., LÖNNERBERG, P., LOU, D., HJERLING-LEFFLER, J., HAEGGSTRÖM, J., KHARCHENKO, O., KHARCHENKO, P. V., LINNARSSON, S. & ERNFORS, P. 2015b. Unbiased classification of sensory neuron types by large-scale single-cell RNA sequencing. *Nat Neurosci,* 18**,** 145-53.

VAISHNAVI, A., LE, A. T. & DOEBELE, R. C. 2015. TRKing down an old oncogene in a new era of targeted therapy. *Cancer Discov,* 5**,** 25-34.

VANDEWAUW, I., DE CLERCQ, K., MULIER, M., HELD, K., PINTO, S., VAN RANST, N., SEGAL, A., VOET, T., VENNEKENS, R., ZIMMERMANN, K., VRIENS, J. & VOETS, T. 2018. A TRP channel trio mediates acute noxious heat sensing. *Nature,* 555**,** 662-666.

VARDEH, D., MANNION, R. J. & WOOLF, C. J. 2016. Toward a Mechanism-Based Approach to Pain Diagnosis. *The journal of pain,* 17**,** T50-T69.

VILLAR, M. J., CORTÉS, R., THEODORSSON, E., WIESENFELD-HALLIN, Z., SCHALLING, M., FAHRENKRUG, J., EMSON, P. C. & HÖKFELT, T. 1989. Neuropeptide expression in rat dorsal root ganglion cells and spinal cord after peripheral nerve injury with special reference to galanin. *Neuroscience,* 33**,** 587-604.

VOLINIA, S., CALIN, G. A., LIU, C. G., AMBS, S., CIMMINO, A., PETROCCA, F., VISONE, R., IORIO, M., ROLDO, C., FERRACIN, M., PRUEITT, R. L., YANAIHARA, N., LANZA, G., SCARPA, A., VECCHIONE, A., NEGRINI, M., HARRIS, C. C. & CROCE, C. M. 2006. A microRNA expression

signature of human solid tumors defines cancer gene targets. *Proc Natl Acad Sci U S A,* 103**,** 2257-61.

VRIENS, J. & VOETS, T. 2019. Heat sensing involves a TRiPlet of ion channels. *Br J Pharmacol,* 176**,** 3893-3898.

WALSH, R. N. & CUMMINS, R. A. 1976. The Open-Field Test: a critical review. *Psychol Bull,* 83**,** 482-504.

WANG, S., KIM, M., ALI, Z., ONG, K., PAE, E.-K. & CHUNG, M.-K. 2019. TRPV1 and TRPV1-Expressing Nociceptors Mediate Orofacial Pain Behaviors in a Mouse Model of Orthodontic Tooth Movement. *Frontiers in physiology,* 10**,** 1207-1207.

WEISS, J., PYRSKI, M., JACOBI, E., BUFE, B., WILLNECKER, V., SCHICK, B., ZIZZARI, P., GOSSAGE, S. J., GREER, C. A., LEINDERS-ZUFALL, T., WOODS, C. G., WOOD, J. N. & ZUFALL, F. 2011. Loss-of-function mutations in sodium channel Nav1.7 cause anosmia. *Nature,* 472**,** 186-90.

WERCBERGER, R. & BASBAUM, A. I. 2019. Spinal cord projection neurons: a superficial, and also deep, analysis. *Curr Opin Physiol,* 11**,** 109-115.

WISE, B. L., SEIDEL, M. F. & LANE, N. E. 2021. The evolution of nerve growth factor inhibition in clinical medicine. *Nature Reviews Rheumatology,* 17**,** 34-46.

WOLFF, M., VOGEL, W. & SAFRONOV, B. V. 1998. Uneven distribution of K+ channels in soma, axon and dendrites of rat spinal neurones: functional role of the soma in generation of action potentials. *The Journal of physiology,* 509 (Pt 3)**,** 767-776.

WOOD, J. N. 2020. *The Oxford Handbook of the Neurobiology of Pain*, Oxford University Press, Incorporated.

WOOD, J. N. & EIJKELKAMP, N. 2012. Noxious mechanosensation – molecules and circuits. *Current Opinion in Pharmacology,* 12**,** 4-8.

WU, Z., AUTRY, A. E., BERGAN, J. F., WATABE-UCHIDA, M. & DULAC, C. G. 2014. Galanin neurons in the medial preoptic area govern parental behaviour. *Nature,* 509**,** 325-330.

XIAO, L., OHAYON, D., MCKENZIE, I. A., SINCLAIR-WILSON, A., WRIGHT, J. L., FUDGE, A. D., EMERY, B., LI, H. & RICHARDSON, W. D. 2016. Rapid production of new oligodendrocytes is required in the earliest stages of motor-skill learning. *Nature Neuroscience,* 19**,** 1210-1217.

XU, X. J., HÖKFELT, T. & WIESENFELD-HALLIN, Z. 2010. Galanin and spinal pain mechanisms: past, present, and future. *Exp Suppl,* 102**,** 39-50.

XU, Y., GU, Y., XU, G. Y., WU, P., LI, G. W. & HUANG, L. Y. M. 2003. Adeno-associated viral transfer of opioid receptor gene to primary sensory neurons: a strategy to increase opioid antinociception. *Proceedings of the National Academy of Sciences of the United States of America,* 100**,** 6204-6209.

YANG, X., YANG, H. B., XIE, Q. J., LIU, X. H. & HU, X. D. 2009. Peripheral inflammation increased the synaptic expression of NMDA receptors in spinal dorsal horn. *Pain,* 144**,** 162-9.

YAO, L.-C., RIESS, J., CHENG, M., WANG, M., BANCHEREAU, J., SHULTZ, L., PALUCKA, K. & KECK, J. G. 2016. Patient-derived tumor xenografts in humanized NSG-SGM3 mice: A new immuno-oncology platform. *Journal of Clinical Oncology,* 34**,** 3074-3074.

YONEDA, T., HATA, K., NAKANISHI, M., NAGAE, M., NAGAYAMA, T., WAKABAYASHI, H., NISHISHO, T., SAKURAI, T. & HIRAGA, T. 2011. Involvement of acidic microenvironment in the pathophysiology of cancer-associated bone pain. *Bone,* 48**,** 100-5.

ZEISEL, A., HOCHGERNER, H., LONNERBERG, P., JOHNSSON, A., MEMIC, F., VAN DER ZWAN, J., HARING, M., BRAUN, E., BORM, L. E., LA MANNO, G., CODELUPPI, S., FURLAN, A., LEE, K., SKENE, N., HARRIS, K. D., HJERLING-LEFFLER, J., ARENAS, E., ERNFORS, P., MARKLUND, U. & LINNARSSON, S. 2018a. Molecular Architecture of the Mouse Nervous System. *Cell,* 174**,** 999-1014.e22.

ZEISEL, A., HOCHGERNER, H., LÖNNERBERG, P., JOHNSSON, A., MEMIC, F., VAN DER ZWAN, J., HÄRING, M., BRAUN, E., BORM, L. E., LA MANNO, G., CODELUPPI, S., FURLAN, A., LEE, K., SKENE, N., HARRIS, K. D., HJERLING-LEFFLER, J., ARENAS, E., ERNFORS, P.,

MARKLUND, U. & LINNARSSON, S. 2018b. Molecular Architecture of the Mouse Nervous System. *Cell,* 174**,** 999-1014.e22.

ZHANG, J., CAVANAUGH, D. J., NEMENOV, M. I. & BASBAUM, A. I. 2013. The modality-specific contribution of peptidergic and non-peptidergic nociceptors is manifest at the level of dorsal horn nociresponsive neurons. *J Physiol,* 591**,** 1097-110.

ZHANG, Q., SANO, C., MASUDA, A., ANDO, R., TANAKA, M. & ITOHARA, S. 2016. Netrin-G1 regulates fear-like and anxiety-like behaviors in dissociable neural circuits. *Scientific Reports,* 6**,** 28750.

ZHU, F., NAIR, R. R., FISHER, E. M. C. & CUNNINGHAM, T. J. 2019. Humanising the mouse genome piece by piece. *Nature Communications,* 10**,** 1845.

ZIMMERMANN, K., LEFFLER, A., BABES, A., CENDAN, C. M., CARR, R. W., KOBAYASHI, J., NAU, C., WOOD, J. N. & REEH, P. W. 2007. Sensory neuron sodium channel Nav1.8 is essential for pain at low temperatures. *Nature,* 447**,** 855-8.

Chapter 7 - Appendix Publications

Appendix A
Tools for analysis and conditional deletion of subsets of sensory neurons

RESEARCH ARTICLE

Tools for analysis and conditional deletion of subsets of sensory neurons

Sonia Santana-Varela[1], Yury D. Bogdanov[1,2], Samuel J. Gossage[1], Andrei L. Okorokov[1], Shengnan Li[1], Larissa de Clauser[1,3], Marta Alves-Simoes[1], Jane E. Sexton[1], Federico Iseppon[1], Ana P. Luiz[1], Jing Zhao [1], John N. Wood [1], James J. Cox [1]

[1]Molecular Nociception Group, University College London, London, WC1E 6BT, UK
[2]Cancer Sciences, Faculty of Medicine, University of Southampton, Southampton, SO166YD, UK
[3]Institute for Biomedicine, Affiliated Institute of the University of Lubeck, Bolzano, Italy

Open Peer Review

Reviewer Status *AWAITING PEER REVIEW*

Any reports and responses or comments on the article can be found at the end of the article.

Abstract

Background: Somatosensation depends on primary sensory neurons of the trigeminal and dorsal root ganglia (DRG). Transcriptional profiling of mouse DRG sensory neurons has defined at least 18 distinct neuronal cell types. Using an advillin promoter, we have generated a transgenic mouse line that only expresses diphtheria toxin A (DTA) in sensory neurons in the presence of Cre recombinase. This has allowed us to ablate specific neuronal subsets within the DRG using a range of established and novel Cre lines that encompass all sets of sensory neurons.

Methods: A floxed-tdTomato-stop-DTA bacterial artificial chromosome (BAC) transgenic reporter line (AdvDTA) under the control of the mouse advillin DRG promoter was generated. The line was first validated using a Nav1.8[Cre] and then crossed to CGRP[CreER] (Calca), Th[CreERT2], Tmem45b[Cre], Tmem233[Cre], Ntng1[Cre] and TrkB[CreER] (Ntrk2) lines. Pain behavioural assays included Hargreaves', hot plate, Randall-Selitto, cold plantar, partial sciatic nerve ligation and formalin tests.

Results: Motor activity, as assessed by the rotarod test, was normal for all lines tested. Noxious mechanosensation was significantly reduced when either Nav1.8 positive neurons or Tmem45b positive neurons were ablated whilst acute heat pain was unaffected. In contrast, noxious mechanosensation was normal following ablation of CGRP-positive neurons but acute heat pain thresholds were significantly elevated and a reduction in nocifensive responses was observed in the second phase of the formalin test. Ablation of TrkB-positive neurons led to significant deficits in mechanical hypersensitivity in the partial sciatic nerve ligation neuropathic pain model.

Conclusions: Ablation of specific DRG neuronal subsets using the AdvDTA line will be a useful resource for further functional

characterization of somatosensory processing, neuro-immune
interactions and chronic pain disorders.

Corresponding authors: Jing Zhao (jing02.zhao@ucl.ac.uk), John N. Wood (j.wood@ucl.ac.uk), James J. Cox (j.j.cox@ucl.ac.uk)

Author roles: Santana-Varela S: Conceptualization, Data Curation, Formal Analysis, Investigation, Methodology, Project Administration, Supervision, Validation, Visualization, Writing – Original Draft Preparation, Writing – Review & Editing; **Bogdanov YD**: Conceptualization, Investigation, Methodology, Visualization, Writing – Original Draft Preparation, Writing – Review & Editing; **Gossage SJ**: Conceptualization, Investigation, Methodology, Validation, Writing – Review & Editing; **Okorokov AL**: Conceptualization, Data Curation, Investigation, Methodology, Visualization, Writing – Original Draft Preparation, Writing – Review & Editing; **Li S**: Investigation, Methodology, Writing – Review & Editing; **de Clauser L**: Formal Analysis, Investigation, Methodology, Writing – Review & Editing; **Alves-Simoes M**: Investigation, Writing – Review & Editing; **Sexton JE**: Investigation, Visualization, Writing – Review & Editing; **Iseppon F**: Investigation, Writing – Review & Editing; **Luiz AP**: Investigation, Writing – Review & Editing; **Zhao J**: Conceptualization, Formal Analysis, Funding Acquisition, Investigation, Methodology, Project Administration, Supervision, Writing – Review & Editing; **Wood JN**: Conceptualization, Funding Acquisition, Methodology, Project Administration, Resources, Supervision, Writing – Original Draft Preparation, Writing – Review & Editing; **Cox JJ**: Conceptualization, Funding Acquisition, Investigation, Methodology, Project Administration, Supervision, Writing – Original Draft Preparation, Writing – Review & Editing

Introduction

Somatosensory neurons have been classified into distinct sets first on the basis of action potential velocity, later with histochemical markers, and more recently by single cell transcriptional profiling[1–4]. Gasser's original observations of three sets of sensory neurons (A fibres, A delta fibres and C fibres) all of which could contribute nociceptive input, demonstrated the complexity of damage-sensing in the periphery. It was only in the 1960s that Perl demonstrated the existence of functionally specialised nociceptors[5]. The debate about polymodality as opposed to modality-specific sensory neurons has been lively. It is clear that the *in vivo* properties of sensory neurons are altered when they are cultured, so that polymodality is often encountered in the dish and may be artefactual[6]. The plasticity of sensory neurons caused by inflammatory mediators is also a complication.

The existence of defined transcripts that distinguish particular sets of sensory neurons provides an opportunity to analyse their function through genetic ablation studies. Recent studies suggest that the subdivisions of sensory neuron subsets identified in mice are in the main evolutionarily conserved in primates, which is of great significance for human studies[3,4,7]. Thus analysis of rodent sensory neuron function is a useful tool for a better understanding of human somatosensation. Here we have used established and new Cre recombinase lines to ablate subsets of sensory neurons and carried out a preliminary analysis of the consequences for acute pain behaviour. It was important to rule out effects on other tissues, and so we developed a floxed stop diphtheria toxin mouse driven by a sensory neuron specific promoter, advillin. Advillin is selectively expressed in all sensory neurons and Merkel cells[8]. This allowed us to ablate only sensory neurons with no effect on other tissue that may express the same transcripts as sensory neurons but in which advillin and hence diphtheria toxin is not expressed.

Methods

Ethical considerations

All experiments were performed in accordance with the UK Animals (Scientific Procedures) Act 1986 with prior approval under a Home Office project licence (PPL 70/7382). This study is reported in line with the ARRIVE guidelines[9].

Mouse husbandry

The study took place at University College London in 2018–2021. Mice were kept on a 12-hr light/dark cycle with cage enrichment (e.g. disposable igloos) and provided with food and water *ad libitum*. Surgical procedures were performed by trained researchers and under aseptic conditions. For genotyping, genomic DNA was isolated from ear tissue for polymerase chain reaction (PCR) using GoTaq DNA Polymerase (Promega) (see *Extended data*, Supplementary Methods for primer sequences and cycling conditions[9]). Cre[ER/ERT2] mouse lines received 200 µl doses i.p. of a 1% tamoxifen solution on five consecutive days (once per day) between 8–10 weeks of age. Tamoxifen was prepared in 15% ethanol/85% sunflower oil.

Mouse lines

Advillin Flox-tdTomato-Stop-DTA BAC transgenic (AdvDTA).
We generated a floxed-tdTomato-stop-DTA bacterial artificial

chromosome (BAC) transgenic reporter line under the control of the mouse *Advillin* (*Avil*) promoter. The construct was generated using a recombineering protocol described in detail by Copeland *et al.*[10] (*Extended data*, Supplementary Figure 1[9]). BAC clone RPCI23-424F19 containing part of the *Advillin* gene was used as a template to prepare a targeting construct. To construct the shuttle vector for recombineering the 5'-homology arm (432 bp) and the 3'-homology arm (274 bp) flanking exon 2 of the *Advillin* gene were cloned into a vector containing a floxTomatoDTA cassette and a Kanamycin cassette, the latter being flanked by flippase recognition target (FRT) sites. The floxTomatoDTA cassette consists of the sequence encoding tdTomato protein followed by three SV40 polyadenylation signals and flanked by the loxP sites. This sequence was fused with the sequence encoding DTA protein followed by bGH and SV40 polyA signals. The start codon in the exon 2 of the *Advillin* gene corresponds to the start codon of tdTomato. The completed shuttle construct was sequenced and the targeting cassette was isolated from the plasmid by AscI/PacI digest.

EL250 E. coli cells transformed with the BAC clone were co-transformed with the shuttle targeting construct and recombination was induced by heat-shock according to the recombineering protocol. The induced bacterial clones were isolated by growing on Kanamycin-containing plates. The Kanamycin resistance cassette was removed by inducing Flp-recombinase expression by arabinose. The final construct was verified by PCR and analytical restriction digests. The resulting BAC containing the targeting cassette was sent to Cyagen for pronucleus injection. The founder line was bred with wild-type C57BL6/J mice to obtain germline transmission.

Cre and floxed stop tdTomato reporter lines

The following lines were provided as generous gifts: CGRP[CreER][11], TrkB[CreER][12] (Jackson Lab stock number 027214), Th[CreERT2][13] (Jackson Lab stock number 025614), Ntng1[Cre][14] and Rosa-CAG-flox-stop-tdTomato[15] (Jackson Lab stock number 007905). The Nav1.8[Cre] line was in house and previously described[16].

Tmem45b[Cre] and Tmem233[Cre] lines were generated by Cyagen on a C57BL/6 background. The Tmem45b[Cre] line is a BAC transgenic in which a fragment containing the Cre-SV40 pA together with Frt-Kanamycin cassette-Frt was introduced in exon 2 of the murine *Tmem45b* gene within BAC clone RP24-249I6. The Kanamycin cassette was removed from the recombinant BAC by Flp-mediated recombination. The recombinant clone was verified by PCR and end-sequencing and then injected into fertilized eggs for transgenic mouse production. Pups were genotyped by PCR using GoTaq DNA Polymerase (Promega) (see *Extended data*, Supplementary Methods for primer sequences and cycling conditions[9]). Founder 'R' was used for further breeding and characterization.

The Tmem233[Cre] line is a constitutive knockin line in which the Kozak-Cre-pA cassette replaced the ATG start codon of the murine *Tmem233* gene. The Cre is under the control of *Tmem233* regulatory elements with homozygotes being knockouts of the *Tmem233* gene. The homology arms of the targeting vector were generated by PCR using BAC clones RP23-182O14 and

RP23-375I17. In the targeting vector the Neo cassette was flanked by Rox sites and DTA was used for negative selection. The final constitutive KI allele was obtained after Dre-mediated recombination with C57BL/6 ES cells used for gene targeting. Pups were genotyped by PCR using GoTaq DNA Polymerase (Promega) (see *Extended data*, Supplementary Methods for primer sequences and cycling conditions[9]).

Behavioural tests

For all behavioural assays, the animals in the test groups carried both the Cre gene and the AdvDTA BAC. Animals in the control groups were negative either for the Cre gene or the AdvDTA BAC (see each figure legend for specific details). Sample sizes (1 unit=1 animal) were calculated based on our previous experience for each assay[17] and animals were excluded from the study if they became unwell. All data points were included in the statistical analyses. Animals were acclimatized to the behavioural equipment for at least 2 days prior to testing; control and test groups were assayed on the same day. Observers who performed behavioural experiments were blind to the genotype of the animals. Animals were selected and placed into the apparatus randomly by an independent experimenter. The unblinding of each group followed input of the raw behavioural data into the analysis software. Experiments were conducted using both male and female adult transgenic mice and wild-type littermates (all >7 weeks in age).

Mechanical nociceptive thresholds were measured using a modified version of the Randall Selitto test for mice (Ugo Basile) that applies pressure to the tail with a 500g cut-off[17,18]. Punctate mechanical sensitivity was measured using the up-down method for obtaining the 50% threshold using von Frey hairs (Ugo Basile stand; Aesthesio hairs), as previously described[17,19]. Thermal nociceptive thresholds were determined by measuring paw-withdrawal latency using the Hargreaves' apparatus (IITC Life Science)[17,20] with a ramp of 1.5°C/s and a 30-s cut-off and also by use of the 50°C hot-plate test (Ugo Basile)[21]. The response to noxious cold was measured using the cold plantar assay (Ugo Basile)[22]. The rotarod test (IITC Life Science) was performed as described in 23. The formalin model was performed by intraplantar injection (subcutaneously) of 20 µl of a 5% formalin solution into the left hindpaw after a 15 min acclimatization to individual observation cages. Time spent engaged in nociceptive behaviour (biting or licking the affected region) was recorded over 1 hr immediately after injection. The video recordings were sampled for 10 sec at 1 min intervals using a Python script and scored for the presence or absence of nocifensive behaviours toward the injected hind paw (licking, biting, flinching). Data is expressed as a percentage of nocifensive responses out of all responses. The early acute phase (Phase 1, 0-10 min) and the latter inflammatory phase (Phase 2, 10–60 min) were separately analysed.

Partial sciatic nerve ligation model

Surgical procedures were performed under isoflurane anaesthesia (inhalation) (2–3%). A partial nerve injury in adult mice was induced by tying a tight ligature with 6-0 silk suture around approximately 1/3 to 1/2 the diameter of the sciatic nerve, similar to the approach described in rats[24].

In situ hybridization (ISH) sample preparation and RNAscope

Animals were deeply anesthetized with pentobarbital (i.p.) and transcardially perfused with heparinized saline (0.9%NaCl) followed by 25 ml of cold 4% paraformaldehyde in phosphate-buffered saline (pH 7.4). Dorsal root ganglia were extracted from the lumbar area and post-fixed with the same fixative solution for 2 hours at 4°C before being embedded in cryopreservative solution (30% sucrose) overnight at 4°C. Tissue samples were then placed in optimal cutting temperature (OCT) compound blocks for posterior sectioning by cryostat. 11 µm thick sections were mounted onto Superfrost Plus (Fisher Scientific) slides, allowed to freeze-dry overnight at -80 °C, for an immediate use, or were stored at −80 °C for no longer than a month for subsequent experiments.

In situ hybridization was performed using the RNAscope system (Advanced Cell Diagnostics) following a two-day protocol for fresh-frozen samples with 1hr post-fixing with 4% paraformaldehyde (PFA) in phosphate buffered saline (PBS) at 4°C and stepwise dehydration with 50%, 70% and 100% ethanol. Tissue pre-treatment consisted of hydrogen peroxide and protease IV (10 and 20 min, respectively) at room temperature (RT). Following pre-treatment, probe hybridization and detection with the Multiplex Fluorescence Kit v2 were performed according to the manufacturer's protocol.

Probes included Tmem233 (#519851), Tmem45b (#420461-c3), NEFH (#443671 or #443671-c4), Th (#317621-c4), CGRP (Calca #417961-c3), Ntng1 (#488871-C2), Ntrk2 (#423611-c3) and tdTomato (#317041-c4). Ribonucleic acid (RNA) localisation was detected with Alexa Fluor™ 488 Tyramide (Cat# B40953, green, for all target gene RNA products) and Opal 570 (Cat# FP1488001KT, red, when a probe against tdTomato was used) fluorochrome dyes (Perkin Elmer) compared to DAPI staining (nuclei) or TS-coumarin (TS405, blue, Cat# NEL703001KT, Perkin Elmer) used for neurofilament heavy chain (NEFH). *In situ* hybridisation slides were mounted using Prolong Gold (ThermoFisher Scientific #P36930).

Fluorescence was detected using Zeiss LSM 880 Airyscan microscope. Images were taken at 10x or 20x magnification with 4x averaging, airyscan processed, stitched whenever required and exported as 16-bit uncompressed tiff files for further basic editing in Adobe Lightroom v6 (Adobe) on colour calibrated iMac retina monitor. Final images were exported as jpeg files with 7,200 pix on longest side at 300 ppi.

RNA extraction and real-time qPCR

RNA was extracted from dorsal root ganglia tissue using TRIzol Reagent (Life Technologies) and Purelink RNA micro kit (Thermo Fisher) and then reverse transcribed according to standard protocols. Real-time RT-PCR using technical triplicates was performed with the BioRad CXF Connect™. PCR was carried out using the Universal SYBR Green Supermix protocol (Bio-Rad) and primers to *Scn10a* and *Gapdh* (see *Extended data*, Supplementary Methods for primer sequences and cycling conditions[9]). *Scn10a* expression was compared with that of

Gapdh measured on the same sample in parallel on the same plate, giving a CT difference (ΔCT) for *Gapdh* minus *Scn10a*. Mean and standard error were performed on the ΔCT data and converted to relative expression levels (2^ΔCT).

Statistics
Data was analysed using GraphPad Prism 9 (GraphPad Software, Inc), and results presented as mean ± SEM with n referring to the number of samples tested per group, as indicated in figure legends. SOFA Statistics is an alternative open access package that can be used.

Results
Single cell RNA sequencing of mouse dorsal root ganglia neurons has provided an unbiased classification of neuronal subpopulations based on their genetic profiles[3,4]. Using these data, we selected marker genes that could be used to drive expression of Cre recombinase in restricted DRG neuron populations to enable further functional analyses of neuronal subsets (Table 1). We recruited existing lines and generated new lines for further analyses (see Materials and Methods): Cgrp[CreER] (Calca), Th[CreERT2], Scn10a[Cre] (Na$_v$1.8), Tmem45b[Cre], Tmem233[Cre], Ntng1[Cre], and TrkB[CreER] (Ntrk2). Lines were crossed to a Rosa-CAG-flox-stop-tdTomato line and following tamoxifen administration for the CreER/CreERT2 lines, lumbar DRGs were isolated from adult mice for RNAscope testing. Figure 1 shows representative images of tdTomato expression (i.e. following Cre activity) and expression of the 'target gene' (i.e. an *in situ* probe against each marker gene mRNA)[9]. For each line tested, there was a large overlap between tdTomato expression and the target, indicating that Cre activity was in general consistent with expression of the endogenous marker gene. Figure 1 also shows expression of neurofilament (*Nefh*) mRNA, which is expressed in NF1, NF2, NF3, NF4, PEP1.2 and PEP2 neurons, according to single cell RNAseq data[3,4,25]. Comparison of Cre activity (tdTomato expression) and *Nefh* expression was as predicted from single cell RNAseq data (Table 1 and Figure 1). For example, Tmem45b Cre activity was present in Nefh-negative neurons; Ntng1 Cre was active in Nefh-positive neurons; and Calca Cre activity was in both Nefh-positive and -negative neurons.

Advillin Flox-tdTomato-Stop-DTA BAC transgenic
The library of validated Cre lines enables specific DRG neuronal populations to be ablated via Cre-dependent expression of Diphtheria toxin A (DTA). However, as many of the Cre lines drive expression in tissues outside of the DRG, we generated a floxed-tdTomato-stop-DTA BAC transgenic reporter line under the control of DRG-enriched mouse *Advillin* (*Avil*) promoter to enable restricted ablation[25] (*Extended data,* Supplementary Figure 1[9]). The targeting construct used to generate the line consists of a tdTomato fluorescent reporter gene and transcriptional stop sequences that are flanked by loxP sites with a DTA sequence downstream. Advillin is expressed in all sensory neurons and has minimal expression elsewhere in the nervous system[27]. In Cre negative animals, the tdTomato gene is expressed with transcription of the DTA prevented by the upstream transcriptional stop sequences. In Cre positive animals, the tdTomato

and transcriptional stop sequences are excised and the DTA is transcribed leading to toxin production and cell ablation.

To validate this new reporter we crossed it with the Na$_v$1.8[Cre] line and were able to recapitulate the behavioural phenotype observed in our earlier work in which the Na$_v$1.8[Cre] was bred to a Rosa floxed stop DTA knockin line[28]. We used the Hargreaves' test to apply a latent heat stimulus to the hind paw and recorded the latency to a nocifensive response. We also used the Randall-Selitto test to apply steadily increasing mechanical pressure to the tail until a withdrawal response was observed. We showed that mice lacking the Na$_v$1.8 positive population of sensory neurons have unimpaired responses to noxious heat (Figure 2A), but responses to noxious mechanical stimuli are substantially impaired (Figure 2B) suggesting that we successfully ablated Na$_v$1.8 containing neurons in the BAC transgenic line. Real-time qPCR in DRG isolated from the Cre+/AdvDTA+ mice confirmed the ablation with a 97.5% decrease in Nav1.8 mRNA levels compared to WT DRGs (Figure 2C).

Pain behaviour tests following restricted ablation of subpopulations of DRG neurons
Following validation of the AdvDTA reporter we crossed this BAC transgenic line to five additional Cre-expressing lines with distinct expression profiles across DRG neuronal subsets (Table 1). As expected, motor co-ordination as assessed by the rotarod test, was normal for all lines compared to Cre-negative/ AdvDTA+ littermates (single cell RNAseq data indicates that all five Cre lines are expressed outside of the parvalbumin-positive PSNF3 proprioceptive DRG neurons) (Figure 3A). The Randall-Selitto assay on the tail showed that noxious mechanosensation was significantly reduced in the Tmem45b Cre+/ AdvDTA mice (Figure 3B). Tmem45b is expressed in a subset of Nav1.8 positive neurons, specifically the six non-peptidergic neuronal subsets (PSNP1-6) (Table 1). Punctate mechanical sensitivity, as assessed using von Frey filaments, was not different to controls for the Tmem45b, Th, Ntrk2 and Ntng1 Cre+/AdvDTA mice although surprisingly, increased sensitivity was observed in the CGRP Cre+/AdvDTA mice (Figure 3C). Noxious thermal pain thresholds were assessed by the Hargreaves' and hot plate tests and for both assays, CGRP Cre+/AdvDTA mice showed significant hyposensitivity to noxious heat (Figures 3D and 3E). However, CGRP Cre+/AdvDTA mice did not show significant higher cold pain thresholds in the cold plantar assay, although a trend was observed (Figure 3F). The AdvDTA reporter line was also tested in inflammatory and neuropathic pain assays. In the formalin test, no significant differences were observed for all AdvDTA+/Cre+ lines in the first phase (Figure 4A). However, in the second phase, the AdvDTA+/CGRP Cre+ mice displayed significantly reduced nocifensive responses (Figure 4A).

Next, we tested the AdvDTA+/Ntrk2Cre+ mice in the partial sciatic nerve ligation model to investigate the contribution of the PSNF1 and PSNF2 neuronal populations in the development of mechanical allodynia under neuropathic pain conditions. As expected mechanical hypersensitivity developed in the control littermates at 7 days and 16 days post-surgery (Figure 4B). However, the AdvDTA+/Ntrk2Cre+ mice did not develop

Table 1. Expression profile of selected marker genes within mouse dorsal root ganglia (DRG) neurons.

	PSPEP6 TrpM8.1	PSPEP7 TrpM8.2	PSPEP8 TRPM8.3	PSPEP5 PEP1.1	PSPEP2 PEP1.2	PSPEP4 PEP1.3	PSPEP3 PEP1.4	PSPEP1 PEP2	PSNF1 NF1	PSNF2 NF2	PSNF2 NF3	PSNF3 NF4	PSNP1 TH	PSNP3 NP1.1	PSNP2 NP1.2	PSNP4 NP2.1	PSNP5 NP2.2	PSNP6 NP3
Calca	■			■	■	■	■	■						■	■			
Th													■			■	■	
Pvalb												■						
Scn10a				■	■		■	■					■	■	■	■	■	■
Tmem45b													■	■	■	■	■	■
Tmem233							■	■						■	■	■	■	■
Ntng1									■	■	■							
Ntrk2				■					■	■								
Avil	■	■	■	■	■	■	■	■	■	■	■	■	■	■	■	■	■	■

The PSPEP, PSNF and PSNP nomenclature of neuron types on top refers to the classification presented in Zeisel *et al.,* 2018 (available at mousebrain.org)[4]. The TrpM8, PEP, NF, TH and NP nomenclature represents the relationship of these neuron types to the classification presented in Usoskin *et al.,* 2015[3]. PEP (peptidergic); NF (neurofilament); NP (non-peptidergic); TH (tyrosine hydroxylase). Marker genes listed in far center column. Table adapted from 24.
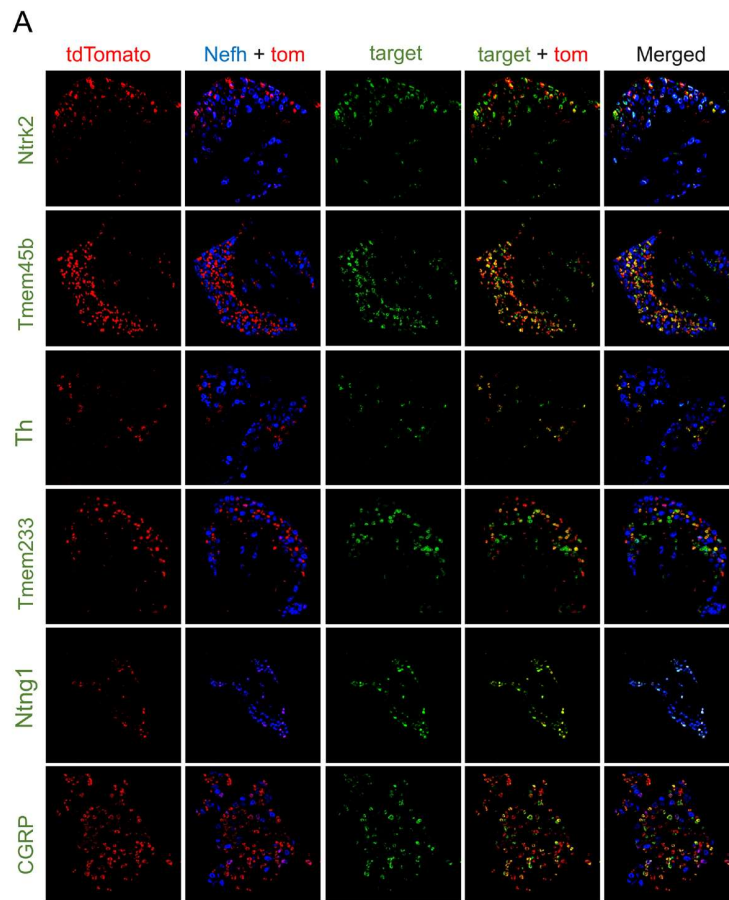
Figure 1. RNAscope analysis of Cre activity in dorsal root ganglia (DRG) neurons. Expression of tdTomato (red), Nefh RNA (detected with TS405, blue) and target marker gene RNA (detected with AF488, green). Cre lines indicated on the left: TrkB[CreER] (Ntrk2), Tmem45b[Cre], Th[CreERT2], Tmem233[Cre], Ntng1[Cre], CGRP[CreER] (Calca). These lines were crossed to a Rosa-CAG-flox-stop-tdTomato line and lumbar DRGs isolated from adult mice for RNAscope analyses.
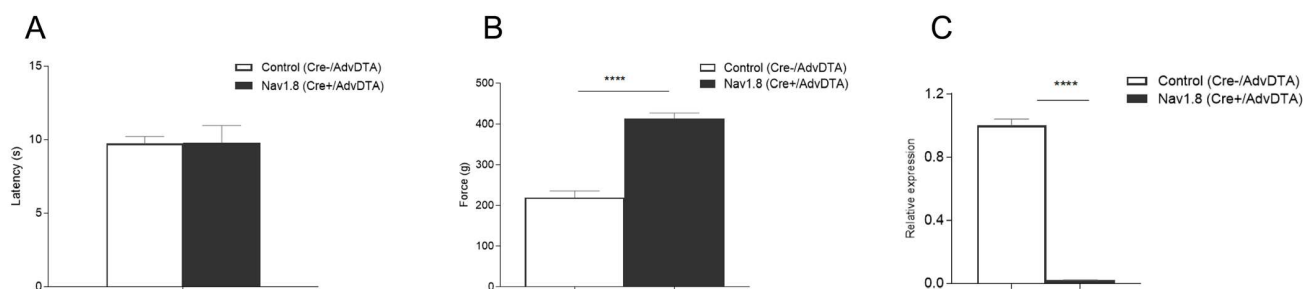
Figure 2. Validation of the *Advillin* Flox-tdTomato-Stop-DTA (AdvDTA) BAC transgenic. (**A**) Nav1.8 Cre+/AdvDTA mice show normal responses to noxious thermal stimuli in the Hargreaves' test (t-test: p>0.05 (ns)); Nav1.8 Cre-/AdvDTA n=6, Nav1.8 Cre+/AdvDTA n=5;. (**B**) Nav1.8 Cre+/AdvDTA mice show significantly impaired noxious mechanosensation in the Randall-Selitto test (t test: p<0.0001); Nav1.8 Cre-/AdvDTA n=6, Nav1.8 Cre+/AdvDTA n=5. (**C**) qPCR data shows a 97.5% decrease in levels of Nav1.8 mRNA following ablation of the Nav1.8-positive subset of sensory neurons in Nav1.8 Cre+/AdvDTA mice (t test: p<0.0001). Nav1.8 Cre-/AdvDTA n=3, Nav1.8 Cre+/AdvDTA n=3.
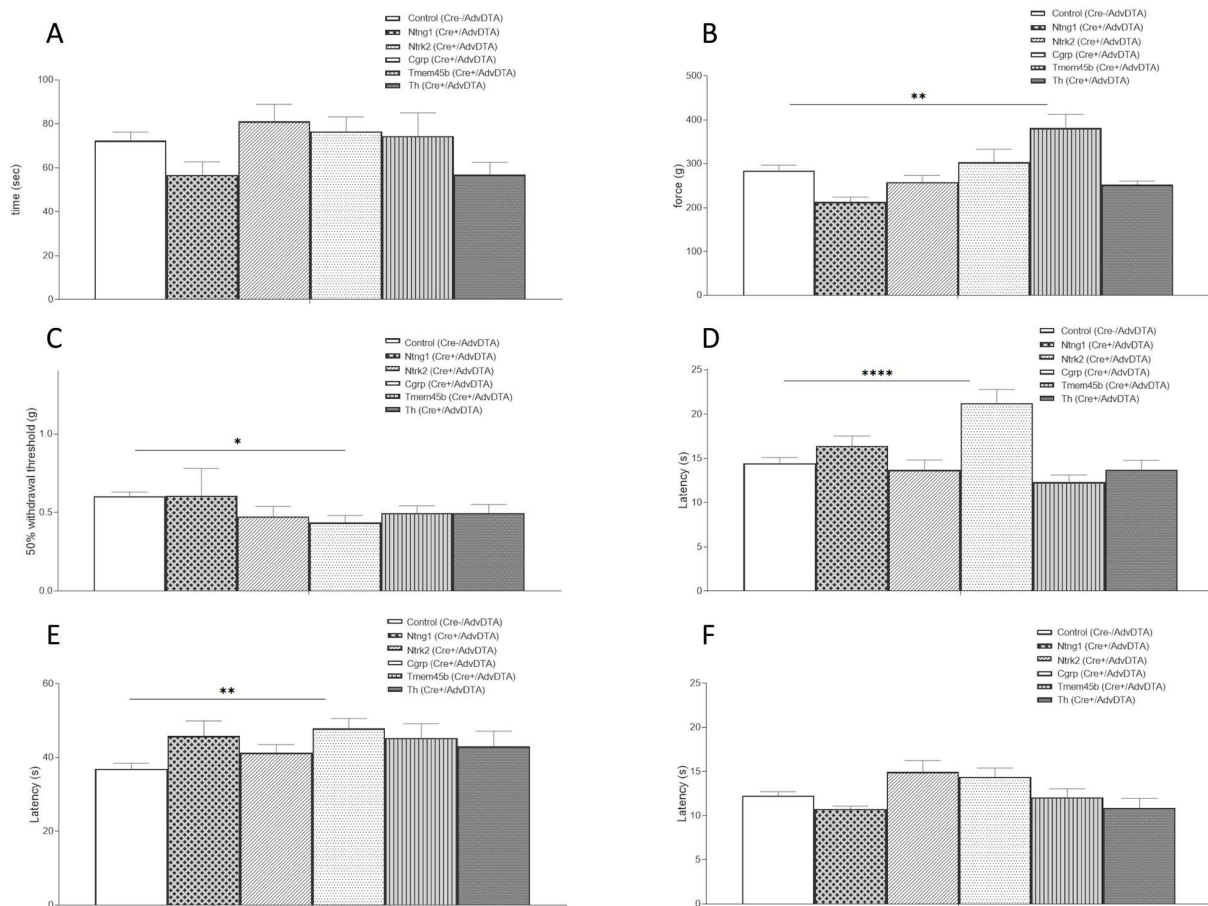
Figure 3. Behavioural analyses following ablation of subpopulations of dorsal root ganglia neurons. (**A**) All AdvDTA+/Cre+ mouse lines tested show normal motor co-ordination as assessed by the rotarod test (ANOVA, p>0.05 (ns)); (**B**) AdvDTA+/Tmem45b Cre+ mice show significantly impaired noxious mechanosensation in the Randall-Selitto test (ANOVA, p<0.005); (**C**) Increased sensitivity to punctate mechanical sensitivity was observed in the AdvDTA+/CGRP Cre+ line (ANOVA, p<0.05); (**D**) AdvDTA+/CGRP+ mice were hyposensitive to noxious heat in the Hargreaves's test (ANOVA, p<0.0001) and the (**E**) hot plate test (ANOVA, p<0.005); (**F**) All AdvDTA+/Cre+ mouse lines tested show normal responses in the cold plantar assay (ANOVA, p>0.05 (ns)). AdvDTA+/Cre- (n=52-54), AdvDTA+/Ntng1 Cre+ (n=5), AdvDTA+/Ntrk2 Cre+ (n=14), AdvDTA+/CGRP Cre+ (n=15-16), AdvDTA+/Tmem45b Cre+ (n=14) and AdvDTA+/Th Cre+ (n=7-8).
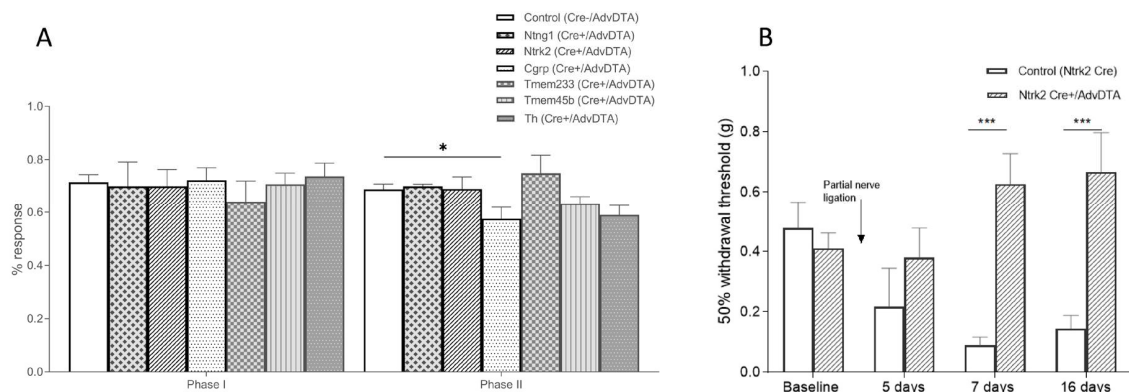
Figure 4. Inflammatory and neuropathic pain behaviour following ablation of subpopulations of DRG neurons. (**A**) Formalin test in all AdvDTA+/Cre+ mouse lines tested show normal phase 1 nocifensive responses to intraplantar injection of formalin. Ablation of CGRP+ neurons results in reduced responses in the second phase of the formalin test (ANOVA, p<0.05). AdvDTA+/Cre- (n=43), AdvDTA+/Ntng1 Cre+ (n=4), AdvDTA+/Ntrk2 Cre+ (n=6), AdvDTA+/CGRP Cre+ (n=13), AdvDTA+/Tmem233 Cre+ (n=9), AdvDTA+/Tmem45b Cre+ (n=13) and AdvDTA+/Th Cre+ (n=8). (**B**) Mechanical sensitivity following the partial sciatic nerve ligation model in Ntrk2 Cre (n=9) and AdvDTA+/Ntrk2 Cre+ (n=10) mice (ANOVA, p<0.0005).

mechanical hypersensitivity, highlighting the importance of the PSNF1 and PSNF2 neuronal subsets to mechanical allodynia in the partial sciatic nerve ligation (PSL) neuropathic pain model.

Discussion

Genetic tools have made a dramatic contribution to a better understanding of the nervous system. Thus human genetic studies have identified causative mutations for a variety of disorders[29], whilst gene and cell silencing[30] and in particular activity-based reporter systems such as CANE have proved extraordinarily informative[31].

The complexity of sensory neurons that play a key role in pain pathways has been highlighted by single cell transcriptional analysis[3]. This suggests that there are at least 18 subsets for sensory neurons in mice. Importantly very similar subsets of sensory neurons are present in primates[7], reinforcing the view that mouse genetic studies are likely to be relevant and useful for understanding human peripheral pain pathways[32].

Early experiments using a Nav1.8 Cre-recombinase to release diphtheria toxin and delete many peripherin-positive sensory neurons produced significant modality specific loss of function[28]. Recent GCaMP studies are also consistent with the presence of a high proportion of modality-specific sensory neurons although there remains considerable debate on this topic[6].

Linking transcriptional changes in pain states to particular sets of sensory neurons has proved problematic[33]. There is clearly extensive redundancy in pain mechanisms for example in temperature sensing[34] and cold sensation[35], whilst inflammation or damage changes the expression patterns of many transcripts including those encoding neuropeptides that are known to have a role in pain pathways. In addition, cells of the skin play a role as primary sensors for many painful stimuli indirectly signalling tissue damage to sensory neurons[36]. Neuro-immune interactions also play a major role in changing the gain of the pain system, and regulating nociceptive activity[37].

Despite these complexities, sets of sensory neurons with particular sensory modalities clearly exist, and we have assembled tools to address their specialised functional role. A major strength of this study is that we have exploited known and novel Cre lines that encompass all sensory neuron subsets, and generated an advillin floxed stop diphtheria toxin mouse that will release the toxin only in sets of sensory neurons in the presence of Cre recombinase. A limitation of the study is that there is random integration of the BAC into the genome of the reporter mice with the potential for leaky expression. An improvement would be to generate a knockin mouse line under the advillin promoter with expression of diphtheria toxin under the control of a Cre-dependent FLEx switch.

Expression patterns were analysed with tomato reporter mice and preliminary phenotyping has been carried out analysing acute pain in mice in which sets of sensory neurons have been deleted. This background information should prove useful as a platform for more complete analyses of pathways involved in pain states that are clearly mechanistically different, for example cold allodynia and chronic inflammatory pain[38]. The role of neurons normally associated with proprioception and innocuous sensation can also be addressed. Recent studies have demonstrated a significant efferent role for sensory neurons in immune responses, and conditions such as psoriasis[39]. Dissecting out the new roles of sets of peripheral sensory neurons in regulating immune responses can thus also be addressed with the assembled mouse lines.

Data availability

Underlying data
Open Science Framework: Tools for analysis and conditional deletion of subsets of sensory neurons. https://doi.org/10.17605/OSF.IO/KTHDU[9].

This project contains the following underlying data:

- Raw values for behavioural experiments (including gender-specific values) underlying Figure 2–Figure 4, in open access CSV format

- Raw unedited microscopy images for Figure 1

- Supplementary Methods.pdf (contains raw pictures of gels from PCR testing)

- Figure 2C – qPCR CT values.csv (raw Ct values for all samples and replicates from RT-PCR)

Extended data
Open Science Framework: Tools for analysis and conditional deletion of subsets of sensory neurons. https://doi.org/10.17605/OSF.IO/KTHDU[9].

This project contains the following extended data:

- Supplementary Figure 1.pdf

- Supplementary Figure 2 (from v6).pdf

- Supplementary Figure Legends.pdf

- Supplementary methods.pdf

Reporting guidelines
Open Science Framework: *ARRIVE checklist for 'Tools for analysis and conditional deletion of subsets of sensory neurons'.* https://doi.org/10.17605/OSF.IO/KTHDU[9].

Data are available under the terms of the Creative Commons Zero "No rights reserved" data waiver (CC0 1.0 Public domain dedication).

References

1. Gasser H: **The classification of nerve fibers.** *The Ohio Journal of Science.* 1941; **41**(3): 145–159.
    Reference Source

2. wson SN, Perry MJ, Prabhakar E, *et al.*: **Primary sensory neurones: neurofilament, neuropeptides, and conduction velocity.** *Brain Res Bull.* 1993; **30**(3–4): 239–43.
    PubMed Abstract | **Publisher Full Text**

3. Usoskin D, Furlan A, Islam S, *et al.*: **Unbiased classification of sensory neuron types by large-scale single-cell RNA sequencing.** *Nat Neurosci.* 2015; **18**(1): 145–53.
    PubMed Abstract | **Publisher Full Text**

4. eisel A, Hochgerner H, Lönnerberg P, *et al.*: **Molecular Architecture of the Mouse Nervous System.** *Cell.* 2018; **174**(4): 999–1014 e22.
    PubMed Abstract | **Publisher Full Text** | **Free Full Text**

5. Burgess PR, Perl ER: **Myelinated afferent fibres responding specifically to noxious stimulation of the skin.** *J Physiol.* 1967; **190**(3): 541–62.
    PubMed Abstract | **Publisher Full Text** | **Free Full Text**

6. Emery EC, Luiz AP, Sikandar S, *et al.*: ***In vivo* characterization of distinct modality-specific subsets of somatosensory neurons using GCaMP.** *Sci Adv.* 2016; **2**(11): e1600990.
    PubMed Abstract | **Publisher Full Text** | **Free Full Text**

7. Kupari J, Usoskin D, Parisien M, *et al.*: **Single cell transcriptomics of primate sensory neurons identifies cell types associated with chronic pain.** *Nat Commun.* 2021; **12**(1): 1510.
    PubMed Abstract | **Publisher Full Text** | **Free Full Text**

8. Lau J, Minett MS, Zhao J, *et al.*: **Temporal control of gene deletion in sensory ganglia using a tamoxifen-inducible *Advillin-Cre-ERT2* recombinase mouse.** *Mol Pain.* 2011; **7**: 100.
    PubMed Abstract | **Publisher Full Text** | **Free Full Text**

9. Cox J: **Tools for analysis and conditional deletion of subsets of sensory neurons**. 2021.
    http://www.doi.org/10.17605/OSF.IO/KTHDU

10. Copeland NG, Jenkins NA, Court DL: **Recombineering: a powerful new tool for mouse functional genomics.** *Nat Rev Genet.* 2001; **2**(10): 769–79.
    PubMed Abstract | **Publisher Full Text**

11. Song H, Yao E, Lin C, *et al.*: **Functional characterization of pulmonary neuroendocrine cells in lung development, injury, and tumorigenesis.** *Proc Natl Acad Sci U S A.* 2012; **109**(43): 17531–6.
    PubMed Abstract | **Publisher Full Text** | **Free Full Text**

12. Rutlin M, Ho CY, Abraira VE, *et al.*: **The cellular and molecular basis of direction selectivity of Aδ-LTMRs.** *Cell.* 2014; **159**(7): 1640–51.
    PubMed Abstract | **Publisher Full Text** | **Free Full Text**

13. Abraira VE, Kuehn ED, Chirila AM, *et al.*: **The Cellular and Synaptic Architecture of the Mechanosensory Dorsal Horn.** *Cell.* 2017; **168**(1–2): 295–310.e19.
    PubMed Abstract | **Publisher Full Text** | **Free Full Text**

14. Bolding KA, Nagappan S, Han BX, *et al.*: **Recurrent circuitry is required to stabilize piriform cortex odor representations across brain states.** *eLife.* 2020; **9**: e53125.
    PubMed Abstract | **Publisher Full Text** | **Free Full Text**

15. Madisen L, Zwingman TA, Sunkin SM, *et al.*: **A robust and high-throughput Cre reporting and characterization system for the whole mouse brain.** *Nat Neurosci.* 2010; **13**(1): 133–40.
    PubMed Abstract | **Publisher Full Text** | **Free Full Text**

16. Nassar MA, Stirling LC, Forlani G, *et al.*: **Nociceptor-specific gene deletion reveals a major role for Na$_v$1.7 (PN1) in acute and inflammatory pain.** *Proc Natl Acad Sci U S A.* 2004; **101**(34): 12706–11.
    PubMed Abstract | **Publisher Full Text** | **Free Full Text**

17. Minett MS, Quick K, Wood JN: **Behavioral Measures of Pain Thresholds.** *Curr Protoc Mouse Biol.* 2011; **1**(3): 383–412.
    PubMed Abstract | **Publisher Full Text**

18. Randall LO, Selitto JJ: **A method for measurement of analgesic activity on inflamed tissue.** *Arch Int Pharmacodyn Ther.* 1957; **111**(4): 409–19.
    PubMed Abstract

19. Chaplan SR, Bach FW, Pogrel JW, *et al.*: **Quantitative assessment of tactile allodynia in the rat paw.** *J Neurosci Methods.* 1994; **53**(1): 55–63.
    PubMed Abstract | **Publisher Full Text**

20. Hargreaves K, Dubner R, Brown F, *et al.*: **A new and sensitive method for measuring thermal nociception in cutaneous hyperalgesia.** *Pain.* 1988; **32**(1): 77–88.
    PubMed Abstract | **Publisher Full Text**

21. Eddy NB, Leimbach D: **Synthetic analgesics. II. Dithienylbutenyl- and dithienylbutylamines.** *J Pharmacol Exp Ther.* 1953; **107**(3): 385–93.
    PubMed Abstract

22. Brenner DS, Golden JP, Gereau RW 4th: **A novel behavioral assay for measuring cold sensation in mice.** *PLoS One.* 2012; **7**(6): e39765.
    PubMed Abstract | **Publisher Full Text** | **Free Full Text**

23. Stirling LC, Forlani Greta, Baker Mark D, *et al.*: **Nociceptor-specific gene deletion using heterozygous NaV1.8-Cre recombinase mice.** *Pain.* 2005; **113**(1–2): 27–36.
    PubMed Abstract | **Publisher Full Text**

24. Seltzer Z, Dubner R, Shir Y: **A novel behavioral model of neuropathic pain disorders produced in rats by partial sciatic nerve injury.** *Pain.* 1990; **43**(2): 205–18.
    PubMed Abstract | **Publisher Full Text**

25. Emery EC, Ernfors P: **Dorsal Root Ganglion Neuron Types and Their Functional Specialization.** *The Oxford Handbook of the Neurobiology of Pain*. (ed. Wood, J.N.) 2020.
    Publisher Full Text

26. Ravenall SJ, Gavazzi I, Wood JN, *et al.*: **A peripheral nervous system actin-binding protein regulates neurite outgrowth.** *Eur J Neurosci.* 2002; **15**(2): 281–90.
    PubMed Abstract | **Publisher Full Text**

27. Hasegawa H, Abbott S, Han BX, *et al.*: **Analyzing somatosensory axon projections with the sensory neuron-specific *Advillin* gene.** *J Neurosci.* 2007; **27**(52): 14404–14.
    PubMed Abstract | **Publisher Full Text** | **Free Full Text**

28. Abrahamsen B, Zhao J, Asante CO, *et al.*: **The cell and molecular basis of mechanical, cold, and inflammatory pain.** *Science.* 2008; **321**(5889): 702–5.
    PubMed Abstract | **Publisher Full Text**

29. Cox JJ, Reimann F, Nicholas AK, *et al.*: **An *SCN9A* channelopathy causes congenital inability to experience pain.** *Nature.* 2006; **444**(7121): 894–8.
    PubMed Abstract | **Publisher Full Text** | **Free Full Text**

30. Magnus CJ, Lee PH, Bonaventura J, *et al.*: **Ultrapotent chemogenetics for research and potential clinical applications.** *Science.* 2019; **364**(6436): eaav5282.
    PubMed Abstract | **Free Full Text**

31. Sakurai K, Zhao S, Takatoh J, *et al.*: **Capturing and Manipulating Activated Neuronal Ensembles with CANE Delineates a Hypothalamic Social-Fear Circuit.** *Neuron.* 2016; **92**(4): 739–753.
    PubMed Abstract | **Publisher Full Text** | **Free Full Text**

32. MacDonald DI, Sikandar S, Weiss J, *et al.*: **A central mechanism of analgesia in mice and humans lacking the sodium channel Na V 1.7.** *Neuron.* 2021; **109**(9): 1497–1512.e6.
    PubMed Abstract | **Publisher Full Text** | **Free Full Text**

33. Bangash MA, Alles SRA, Santana-Varela S, *et al.*: **Distinct transcriptional responses of mouse sensory neurons in models of human chronic pain conditions [version 1; peer review: 2 approved].** *Wellcome Open Res.* 2018; **3**: 78.
    PubMed Abstract | **Publisher Full Text** | **Free Full Text**

34. Vandewauw I, De Clercq K, Mulier M, *et al.*: **A TRP channel trio mediates acute noxious heat sensing.** *Nature.* 2018; **555**(7698): 662–666.
    PubMed Abstract | **Publisher Full Text**

35. MacDonald DI, Wood JN, Emery EC: **Molecular mechanisms of cold pain.** *Neurobiol Pain.* 2020; **7**: 100044.
    PubMed Abstract | **Publisher Full Text** | **Free Full Text**

36. Sadler KE, Moehring F, Stucky CL: **Keratinocytes contribute to normal cold and heat sensation.** *Elife.* 2020; **9**: e58625.
    PubMed Abstract | **Publisher Full Text** | **Free Full Text**

37. Sorge RE, Mapplebeck JCS, Rosen S, *et al.*: **Different immune cells mediate mechanical pain hypersensitivity in male and female mice.** *Nat Neurosci.* 2015; **18**(8): 1081–3.
    PubMed Abstract | **Publisher Full Text** | **Free Full Text**

38. MacDonald DI, Luiz AP, Iseppon F, *et al.*: **Silent cold-sensing neurons contribute to cold allodynia in neuropathic pain.** *Brain.* 2021; **144**(6): 1711–1726.
    PubMed Abstract | **Publisher Full Text** | **Free Full Text**

39. Riol-Blanco L, Ordovas-Montanes J, Perro M, *et al.*: **Nociceptive sensory neurons drive interleukin-23-mediated psoriasiform skin inflammation.** *Nature.* 2014; **510**(7503): 157–61.
    PubMed Abstract | **Publisher Full Text** | **Free Full Text**

Appendix B
Distinct transcriptional responses of mouse sensory neurons in models of human chronic pain conditions

RESEARCH ARTICLE

Distinct transcriptional responses of mouse sensory neurons in models of human chronic pain conditions [version 1; peer review: 2 approved]

M.A. Bangash [ID][1]*, Sascha R.A. Alles [ID][1]*, Sonia Santana-Varela[1]*,
Queensta Millet[1]*, Shafaq Sikandar[1]*, Larissa de Clauser[1]*, Freija ter Heegde[1,2]*,
Abdella M. Habib[1,3]*, Vanessa Pereira [ID][1]*, Jane E. Sexton[1], Edward C. Emery [ID][1],
Shengnan Li[1], Ana P. Luiz[1], Janka Erdos[1], Samuel J. Gossage[1], Jing Zhao [ID][1],
James J. Cox [ID][1], John N. Wood [ID][1]

[1]Molecular Nociception Group, Wolfson Institute for Biomedical Research, University College London, London, WC1E 6BT, UK
[2]Comparative Biomedical Science, Skeletal Biology Group, Royal Veterinary College, London, NW1 0TU, UK
[3]College of Medicine, Member of Qatar Health Cluster, Qatar University, Doha, Qatar

* Equal contributors

Abstract

Background: Sensory neurons play an essential role in almost all pain conditions, and have recently been classified into distinct subsets on the basis of their transcriptomes. Here we have analysed alterations in dorsal root ganglia (DRG) gene expression using microarrays in mouse models related to human chronic pain.
Methods: Six different pain models were studied in male C57BL/6J mice: (1) bone cancer pain using cancer cell injection in the intramedullary space of the femur; (2) neuropathic pain using partial sciatic nerve ligation; (3) osteoarthritis pain using mechanical joint loading; (4) chemotherapy-induced pain with oxaliplatin; (5) chronic muscle pain using hyperalgesic priming; and (6) inflammatory pain using intraplantar complete Freund's adjuvant. Microarray analyses were performed using RNA isolated from dorsal root ganglia and compared to sham/vehicle treated controls.
Results: Differentially expressed genes (DEGs) were identified. Known and previously unreported genes were found to be dysregulated in each pain model. The transcriptomic profiles for each model were compared and expression profiles of DEGs within subsets of DRG neuronal populations were analysed to determine whether specific neuronal subsets could be linked to each of the pain models.
Conclusions: Each pain model exhibits a unique set of altered transcripts implying distinct cellular responses to different painful

Open Peer Review

Reviewer Status ✔✔

	Invited Reviewers	
	1	**2**
version 1 25 Jun 2018	✔ report	✔ report

1. **David Wynick**, University of Bristol, Bristol, UK

2. **Mark D. Baker**, Queen Mary University of London, Whitechapel, UK

Any reports and responses or comments on the article can be found at the end of the article.

stimuli. No simple direct link between genetically distinct sets of neurons and particular pain models could be discerned.

Keywords
Chronic pain, mouse models, dorsal root ganglia, sensory neurons, microarrays, gene expression

Corresponding authors: Jing Zhao (jing02.zhao@ucl.ac.uk), James J. Cox (j.j.cox@ucl.ac.uk), John N. Wood (j.wood@ucl.ac.uk)

Author roles: Bangash MA: Conceptualization, Formal Analysis, Investigation, Methodology, Visualization, Writing – Original Draft Preparation, Writing – Review & Editing; **Alles SRA**: Conceptualization, Formal Analysis, Investigation, Methodology, Visualization, Writing – Original Draft Preparation, Writing – Review & Editing; **Santana-Varela S**: Conceptualization, Formal Analysis, Investigation, Methodology, Visualization, Writing – Review & Editing; **Millet Q**: Conceptualization, Formal Analysis, Investigation, Methodology, Visualization, Writing – Review & Editing; **Sikandar S**: Conceptualization, Formal Analysis, Investigation, Methodology, Visualization, Writing – Review & Editing; **de Clauser L**: Conceptualization, Formal Analysis, Investigation, Methodology, Visualization, Writing – Review & Editing; **ter Heegde F**: Conceptualization, Investigation, Methodology, Visualization, Writing – Review & Editing; **Habib AM**: Conceptualization, Formal Analysis, Investigation, Methodology, Visualization, Writing – Review & Editing; **Pereira V**: Conceptualization, Formal Analysis, Investigation, Methodology, Writing – Review & Editing; **Sexton JE**: Investigation; **Emery EC**: Methodology, Software; **Li S**: Investigation, Writing – Review & Editing; **Luiz AP**: Investigation, Methodology, Writing – Review & Editing; **Erdos J**: Formal Analysis; **Gossage SJ**: Investigation; **Zhao J**: Conceptualization, Formal Analysis, Funding Acquisition, Methodology, Project Administration, Supervision, Visualization, Writing – Original Draft Preparation, Writing – Review & Editing; **Cox JJ**: Conceptualization, Formal Analysis, Funding Acquisition, Methodology, Project Administration, Supervision, Visualization, Writing – Original Draft Preparation, Writing – Review & Editing; **Wood JN**: Conceptualization, Formal Analysis, Funding Acquisition, Methodology, Project Administration, Supervision, Visualization, Writing – Original Draft Preparation, Writing – Review & Editing

Introduction

Chronic pain is a major clinical problem affecting roughly 20% of the population with more than 6% suffering debilitating levels of pain[1,2]. Despite the huge clinical burden, little progress has been made in developing more effective analgesic agents. Dorsal root ganglion (DRG) sensory neurons are particularly exciting targets for drug development because of their essential role in driving pain sensations in the central nervous system. With the wider availability of high-throughput RNA-seq, there has been a major effort to define DRG transcriptomes, both at the level of whole ganglia[3] and single neurons[4,5]. This has allowed a new classification of sets of sensory neurons based on genetic identity, rather than on the rate of action potential propagation (A fibres and C fibres). As well as neurons, non-neuronal cells such as glia[6] and immune system cells are found within sensory ganglia, with leukocytes alone making up 5–10% of cells in DRG[7,8].

We wondered if the newly defined sensory neuron subsets were differentially activated in different pain models. We therefore performed microarray analyses of RNAs isolated from the DRG of male mice subjected to six different interventions that mimic common chronic pain in human patients. DRG were dissected after the development of peak pain behaviours in each case. The six different chronic pain models were: cancer cell injection in the intramedullary space of the femur as a model for bone cancer pain; partial sciatic nerve ligation (PSL) for neuropathic pain; mechanical joint loading for osteoarthritis pain; oxaliplatin-induced painful neuropathy for chemotherapy-induced pain; hyperalgesic priming model for chronic muscle pain and intraplantar complete Freund's adjuvant (CFA) for inflammatory pain. The rodent models for PSL[9], CFA[10], chemotherapy induced pain with oxaliplatin[11], bone cancer pain[12] and hyperalgesic priming[13–15] are well characterized. The mechanical joint loading model robustly recapitulates behavioural signs and symptoms of osteoarthritis[16].

By comparing altered levels of gene expression in six distinct chronic pain models we hoped to gain insights into the neuronal subsets that are particularly important in different pain conditions. We also could determine genes and related pathways that are common or unique to each condition. Here we show that there is no simple relationship between transcriptional changes in the newly defined subsets of sensory neurons and particular painful insults. However, we have identified several known and previously unreported genes altered in expression in each pain condition. Relevant pathways and upstream regulators were also analysed using Ingenuity Pathway Analysis including cytokines, transcription factors (TFs), G-protein coupled receptors (GCPRs) and ion channels. The results from these experiments highlight the complexity of sensory neuron cell types involved in nociceptive responses. Although altered DRG gene expression may not necessarily play a causal role in pain, some dysregulated genes are potential analgesic drug targets.

Methods

All experiments were performed in accordance with the UK Animals (Scientific Procedures) Act 1986 with prior approval under a Home Office project licence (PPL 70/7382). Mice were kept on a 12-h light/dark cycle and provided with food and water *ad libitum*. All animals were acclimatized for 1 week to the facility before the start of the experiment. Mice were housed in individually ventilated cages (Techniplast GM500 Mouse IVC Green line) containing Lignocel bedding with a maximum of 5 adult mice per cage. All tests and surgeries were conducted using adult male C57BL/6J mice supplied by Charles River and Envigo (specific numbers detailed in the figure legends and ages detailed below for each model). Sample size for each behavioural model was calculated using G*Power (Ver. 3.1.9.2) for a power of 0.8[17]. Surgical procedures were performed by trained researchers and under aseptic conditions. All efforts were made to ameliorate any suffering of the animals with surgery performed under anaesthesia. Mice were euthanized by CO_2 asphyxiation followed by cervical dislocation.

Cancer-induced bone pain

LL/2 Lewis Lung carcinoma cells (ATCC) were cultured in DMEM supplemented with 10% FBS and 100 units/ml Penicillin/Streptomycin for at least 2 weeks prior to surgery (cell culture reagents supplied by Thermo Fisher). Cells were split at 70–80% confluence four days prior to surgery. On the day of surgery, cells were harvested with 0.05% Trypsin-EDTA solution and resuspended in 1X DMEM at a final concentration of 2×10^7 cells/ml and kept on ice till used. Viability of Lewis lung carcinoma cells was confirmed at the end of surgery, showing 26% dead cells compared to 11% before surgery. The cancer cells were introduced to 12 week old mice, as previously described[18,19]. Sham-operated control mice underwent the same surgery, but were inoculated with DMEM medium alone. Ipsilateral L2-L4 DRGs from test and paired sham animals were collected when a limb score of 2 was measured in the test animals (see section *Behavioural tests*).

microCT (uCT) for bone cancer

Femurs were post-fixed in 4% PFA (Sigma-Aldrich) for 24h and kept in 70% ethanol (VWR) till scanning with microCT. Images were acquired with Skyscan software at 6.41um/pixel with 0.6 degrees rotation steps and 2 frame averaging. Image data was reconstructed with NRecon software. A CT-analyzer was used to select a 1mm volume of interest (VOI) region, starting at 0.6mm from the growth plate. Bone mineral density was determined by plotting attenuation coefficients against a standard curve determined with two phantoms with known density. Representative images were binarized with ImageJ (1.52c) and 3D Viewer extension (Java 3D 1.6 with 3D Viewer plugin 4.0.2) used for 3D reconstructions of femur scans.

Partial sciatic nerve ligation (PSL) model

Surgical procedures were performed under isoflurane anaesthesia (2–3%). A partial nerve injury in 14 week old mice was induced by tying a tight ligature with 6-0 silk suture around approximately 1/3 to 1/2 the diameter of the sciatic nerve, similar to the approach described in rats[9]. Ipsilateral and contralateral L3-L5 DRGs were dissected prior to RNA isolation on post-surgery day 16.

Mechanical joint loading (MJL) model

In vivo loading: Osteoarthritis was induced by subjecting 12 week old mice to a two week loading regimen using an electronic materials testing machine (Bose 3100). Throughout the loading episodes, mice were anaesthetised with isoflurane 3.5% (±0.5%) with the right tibia positioned vertically between two custom-made cups which fixate the knee and ankle joint in deep flexion[20]. The loading regimen was the same as previously described[16]. Loading was repeated three times per week for two consecutive weeks. The non-loaded control group consisted of age- and cage-matched mice that were not subjected to a loading regimen but received isoflurane anaesthesia for the same duration as loaded mice. Ipsilateral L3–L5 DRGs were dissected from loaded and non-loaded mice after three weeks.

Oxaliplatin pain model

Seven week old mice were injected with either oxaliplatin (6mg/kg/i.p., Sigma-Aldrich) or vehicle solution (5% glucose, Sigma-Aldrich) as a control twice weekly for four weeks[11,21]. Ipsilateral L3–L5 DRGs were dissected prior to RNA isolation from oxaliplatin and vehicle treated mice on day 28.

Chronic muscle pain model

Eight week old mice were injected twice, four days apart, with 30ul of 3% carrageenan (Sigma-Aldrich) (primed group; n=4) or saline (VWR) (control group; n=4) into the ipsilateral right gastrocnemius muscle[13]. Ipsilateral L3–L5 DRGs were dissected prior to RNA isolation on day 29.

Complete Freund's adjuvant (CFA) pain model

Eleven week old mice received intraplantar injection of 20 ul of Complete Freund's adjuvant (CFA, Sigma-Aldrich) or 0.9% sodium chloride solution (VWR) into the left hind paw[22,23]. Ipsilateral L3-L5 DRGs were then dissected prior to RNA isolation from CFA and saline treated mice 2 days after treatment.

Behavioural tests

For behavioural experiments, animals were acclimatized to the equipment for at least 2 days prior to testing. Observers who performed behavioural experiments were blind to the test/sham groups. The cancer induced bone pain model used a limb score assessment, as previously described[19]. A limb score of 2 (i.e. significant limping) was used as the checkpoint for ending the experiment with DRGs and ipsilateral femurs collected.

Mechanical sensitivity was measured using the up-down method[24] and static weight bearing[18] assays. Thermal nociceptive thresholds were determined by measuring paw withdrawal latency using the Hargreaves' apparatus[25]. The response to noxious cold was measured using the cold plantar assay[26].

RNA extraction and microarrays

RNA was extracted using TRIzol Reagent (Life Technologies) and Purelink RNA micro kit (Thermo Fisher) according to the manufacturer's instructions. RNA samples from four animals displaying the most marked pain behaviours for each model were sent for microarray analyses together with four controls (Eurofins AROS) using the Affymetrix GeneChip Mouse Transcriptome Array 1.0 and WT pico kit. Four replicates give a statistical power of >0.8 to detect a 2 fold change[27,28]. Microarray data has been deposited at Gene Expression Omnibus Array Express for public use with reference number E-MTAB-6864.

Differential gene expression (DGE) and splice variant analysis

Differential gene expression (DGE) and splice variant analysis of transcriptome array data was performed using Transcriptome Analysis Console (TAC Ver 4.0, Thermo Fisher). Normalization was carried out according to the manufacturer's default protocol converting probe cell intensity (CEL files) into signal data (CHP files). An ANOVA (eBayes) cut-off p-value of <0.05 was used to identify DEGs, with the fold change filter then used to sort genes. Genes without a curated gene symbol associated with the Affymetrix probe set were excluded from downstream DGE analyses. Differentially expressed genes (DEGs) were correlated with known expression in DRG neuronal subtypes[4]. Splice variant analysis was performed using the Gene + Exon function in TAC which uses a gene normalized intensity value (ratio of probe set intensity to gene expression level). The cut off was set at Splicing Index of 2, splicing ANOVA with p<0.05, gene expressed in both conditions, probe selection region (PSR)/ junction expressed in at least one condition and gene containing at least one PSR. Non-coding genes were excluded from the splicing analyses. An exon event score indicated consensus alternative splicing event score where a score of 1 represents a high likelihood of splicing event. Heatmaps, volcano plots and statistical analyses were generated using GraphPad Prism 7.

Ingenuity Pathway Analysis (IPA)

Ingenuity Pathway Analysis (IPA, Qiagen) for upstream regulators was performed according to the manufacturer's instructions. IPA primarily utilizes published results of knockdown or knockout studies of genes characterized as growth factor, kinase/phosphatase, transcription/translation regulator, cytokine, transmembrane receptor, enzyme, ion channel, transporter, G-protein coupled receptor, peptidase, and microRNA. This analysis examines target genes from the array dataset, compares their direction of change to what is expected from the literature to predict likely upstream regulators using overlap p-value (Fishers Exact Test, p<0.01) and an activation z-score corrected for bias. The top upstream regulators with an activation z-score were examined for each pain pathway. The activation z-score was used to make a prediction regarding activation or inhibition of the upstream regulator.

Results

We modelled six different chronic pain conditions in mice and used behavioural assays to confirm the development of mechanical or thermal hypersensitivity, followed by transcriptomic analyses of whole dorsal root ganglia tissue. Significant DGE between naïve and injured conditions and alternative splicing was assessed for each model. DGE values for every gene on the mouse transcriptome array and alternative splicing changes are available in Supplementary Table 1.

Cancer-induced bone pain

Carcinoma cells were introduced into the mouse femur and pain behaviour measured daily to determine the limb use score (4: normal use of limb, 3: slight limping, 2: clear limping; see *Methods*). Mice were culled when a limb score of 2 was reached, which ranged from Day 8–16 post surgery (Figure 1A). Weight bearing tests confirmed a significant reduction in use of the affected limb (Figure 1B). Bone mineral density (BMD) was evaluated as an additional indicator of the cancer phenotype and was shown to be significantly decreased in cancer mice compared to sham controls (Figure 1C, D). This is also shown in Figure 1E using a micro-CT reconstruction.

Dorsal root ganglia (ipsilateral L2–L4) were isolated from test mice and paired sham controls and RNA expression levels analysed using microarrays. The volcano plot (Figure 1F) shows that all significantly dysregulated genes (p<0.05) were differentially expressed between ±10-fold with only 1 non-coding gene (*Gm25931*) falling outside of this range (fold change of -10.75). Interestingly, very few of the differentially expressed DRG genes in the cancer induced bone pain model were shared with other models (Figure 1G). A heat map was generated for genes that were significantly up or down regulated by 2 fold or more (Figure 1H). Forty-five genes were found to be upregulated >2 fold and 15 genes downregulated. Dysregulated genes were coding and non-coding, with many genes annotated as 'predicted' (Supplementary Table 1). Excluding these 'predicted' genes, the top 5 most upregulated genes were *Nts*, *miR6898*, *Snord49b*, *Sprr1a* and *Gal* (Figure 1H). The cancer induced bone pain model induced significant changes in 23 microRNAs in the >1.5 fold range, indicating the potential role of miRNAs in cancer pain modulation (Supplementary Figure 2A).

Partial sciatic nerve ligation (PSL) model

In the PSL neuropathic pain model mice developed mechanical allodynia from Day 7 post surgery, as characterized by a significant reduction in the 50% paw withdrawal threshold (PWT) in the injured (ipsilateral) compared to the non-injured (contralateral) paw (Figure 2A). Pain persisted for 15 days post-surgery, with ipsilateral and contralateral L3-L5 DRGs isolated on day 16 and RNA analysed by microarrays.

The volcano plot (Figure 2B) shows that all significantly dysregulated genes (p<0.05) were differentially expressed between ±10-fold with the exception of *Nts*, *Gpr151* and *Npy* (respective fold changes of 13.21, 13.88 and 66.18). Similar to the cancer model, very few PSL stimulated genes were shared with other pain models (Figure 2C). The PSL model stimulated changes in the largest cohort of DRG genes in the 2 fold change range (97 genes) compared to the other 5 models (Figure 2D). The top 5 most upregulated genes, *Npy*, *Gpr151*, *Nts*, *Gal* and *Atf3*, have all been previously reported as being upregulated in neuropathic pain[29–32]. Eighty-six genes were identified as being upregulated more than 2 fold with several of these being non-coding RNAs (Supplementary Table 1). Fourteen microRNAs were upregulated >1.5-fold and 5 were downregulated <-1.5- fold (p<0.05, ANOVA) (Supplementary Figure 2B).

Mechanical joint loading (MJL) model

Osteoarthritis was induced through a two-week mechanical joint loading protocol after which animals developed significant mechanical hypersensitivity and altered weight bearing (Figure 3A). Ipsilateral L3–L5 DRGs from loaded and non-loaded mice were extracted 3 weeks after the loading regimen, RNA extracted and analysed for DEGs. The volcano plot (Figure 3B) shows that all significantly dysregulated genes (p<0.05) were differentially expressed between ±7-fold. Only fourteen genes were dysregulated >2 fold (Figure 3D) with only 1–2 of these genes also differentially expressed in the other pain models (Figure 3C). The top three upregulated genes (*Ppbp*, *DLEU2_5* and *Scarna9*) have no previous association with osteoarthritic pain.

Oxaliplatin-induced painful neuropathy

Oxaliplatin is a chemotherapeutic drug known to induce mechanical and cold allodynia[33]. Mice exposed to oxaliplatin were found to have a reduced cold pain threshold in the cold plantar test (Figure 4A). Twenty-eight days following the first oxaliplatin treatment, ipsilateral L3–L5 DRGs were extracted from test and vehicle treated mice and analysed for differential gene expression. The volcano plot (Figure 4B) shows that all significantly dysregulated genes (p<0.05) were differentially expressed between ±10-fold. Oxaliplatin treatment resulted in 58 dysregulated genes in the >2 fold range, which in contrast to other models, the majority (36 genes) being down- rather than up-regulated (Figure 4D). Out of the 58 DEGs, 7 were shared with the CFA model, 3 with the PSL model and 2 with the mechanical joint loading model (Figure 4C).

Chronic muscle pain (CMP)

A hyperalgesic priming model was used to study chronic muscle pain, whereby the gastrocnemius muscle was injected twice, four days apart, with 3% carrageenan. Prolonged mechanical hypersensitivity resulted from the hyperalgesic priming (Figure 5A). On Day 29, ipsilateral L3-L5 DRGs were extracted from test and vehicle treated mice and analysed for DGE. The volcano plot (Figure 5B) shows that all significantly dysregulated genes (p<0.05) were differentially expressed between ±5-fold. Interestingly, only ten genes were dysregulated >2 fold (Figure 5D) with *Snord49b* shared with the cancer-induced bone pain model and *Gm19860* shared with the mechanical joint loading model (Figure 5C).

CFA inflammatory pain model

Intraplantar injection of CFA was used to induce a robust inflammatory pain phenotype, with significant thermal hypersensitivity observed thirty-six hours post CFA injection (Figure 6A). Ipsilateral L3–L5 DRGs were extracted 2 days post CFA and RNA analysed for differential gene expression. The volcano plot (Figure 6B) shows that all significantly dysregulated genes (p<0.05) were differentially expressed between ±9-fold. Seventy genes were differentially expressed >2 fold with the majority of genes (52) being upregulated (Figure 6D). Once again, very few dysregulated genes were shared between CFA and the other models (Figure 6C).
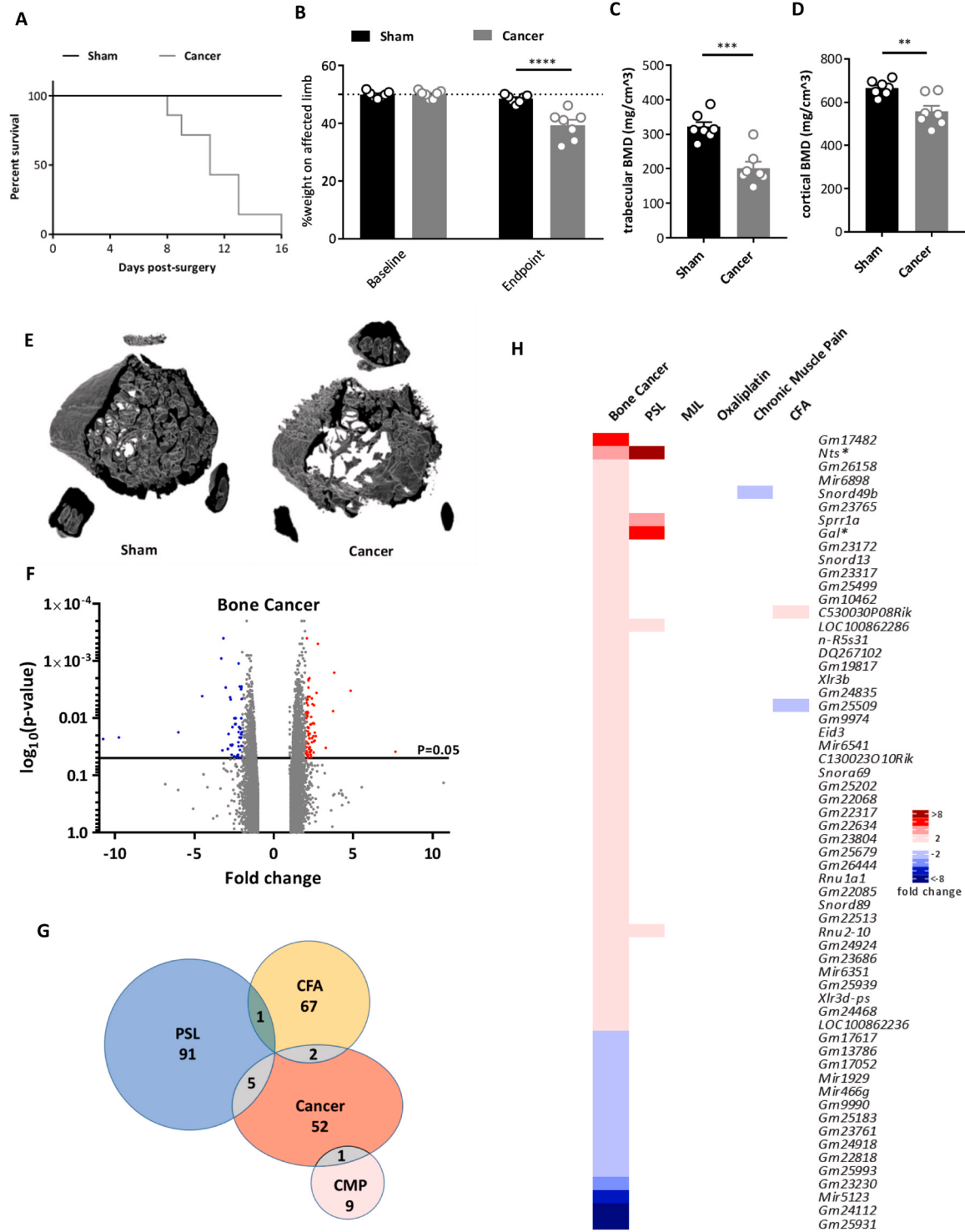
Figure 1. Differential gene expression in the cancer induced bone pain model. (**A**) Survival curve after surgery for sham (black line, n=7) and cancer (grey line, n=7) animals with endpoint defined as clear limping on the affected limb (limb score=2). Log-rank test: p=0.0056. (**B**) Percentage weight bearing on the affected limb is significantly reduced at the endpoint (limb score=2) for cancer compared to sham animals (2-way ANOVA with posthoc Bonferonni test: p<0.0001.) (**C**) Trabecular bone mineral density (unpaired t-test: p=0.0003) and (**D**) cortical bone mineral density (unpaired t-test: p=0.0033) in cancer vs. sham animals. (**E**) Representative 3D reconstructions of a 1mm VOI at 0.6mm from growth plate from uCT data (7 replicates per group). (**F**) Volcano plot for all genes identified in the bone cancer pain array. Each dot represents a single gene (red=upregulated; blue=downregulated). (**G**) Venn diagram showing the number of differentially expressed DRG genes (fold change >2, <-2, p<0.05) shared with other pain models. (**H**) Heat map of upregulated (red) and downregulated (blue) DRG genes (fold change >2, <-2, p<0.05) and a comparison of shared genes across models. Genes with an asterisk are present within the *Pain Genes Database* of pain-related transgenic knockout studies[34].

Figure 2. Differential gene expression in the partial sciatic nerve ligation (PSL) neuropathic pain model. (**A**) Mechanical sensitivity using von Frey filaments on ipsilateral and contralateral paws following PSL surgery (n=4, **indicates p<0.01, ****indicates p<0.0001, 2-way ANOVA with posthoc Bonferonni test). PWT = paw withdrawal threshold. (**B**) Volcano plot for all genes identified in the PSL pain model array. Each dot represents a single gene (red=upregulated; blue=downregulated). (**C**) Venn diagram showing the number of differentially expressed DRG genes (fold change >2, <-2, p<0.05) shared with other pain models. (**D**) Heat map of upregulated (red) and downregulated (blue) DRG genes (fold change >2, <-2, p<0.05) and a comparison of shared genes across models. Genes with an asterisk are present within the *Pain Genes Database* of pain-related transgenic knockout studies[34].

Figure 3. Differential gene expression in the mechanical joint loading (MJL) model. (**A**) Development of mechanical hypersensitivity and altered weight bearing after osteoarthritis (OA) induction by mechanical joint loading. Mice were loaded three times per week for two weeks at 9N (grey line, error bars given as SEM, n=6) in order to induce OA. Behavioural measurements were taken before OA induction and each week for three weeks post loading. These values were compared to a non-loaded isoflurane control (black hashed line, error bars given as SEM, n=6). Significant changes between non-loaded animals and loaded animals are indicated with a # (p<0.05, 2-way ANOVA with posthoc Dunnett or Sidak tests) whilst significant changes within experimental groups over time (compared to baseline value) are indicated with a * (p<0.05, 2-way ANOVA with posthoc Dunnett or Sidak tests). (**B**) Volcano plot for all genes identified in the MJL array. Each dot represents a single gene (red=upregulated; blue=downregulated). (**C**) Venn diagram showing the number of differentially expressed DRG genes (fold change >2, <-2, p<0.05) shared with other pain models. (**D**) Heat map of upregulated (red) and downregulated (blue) DRG genes (fold change >2, <-2, p<0.05) and a comparison of shared genes across models.
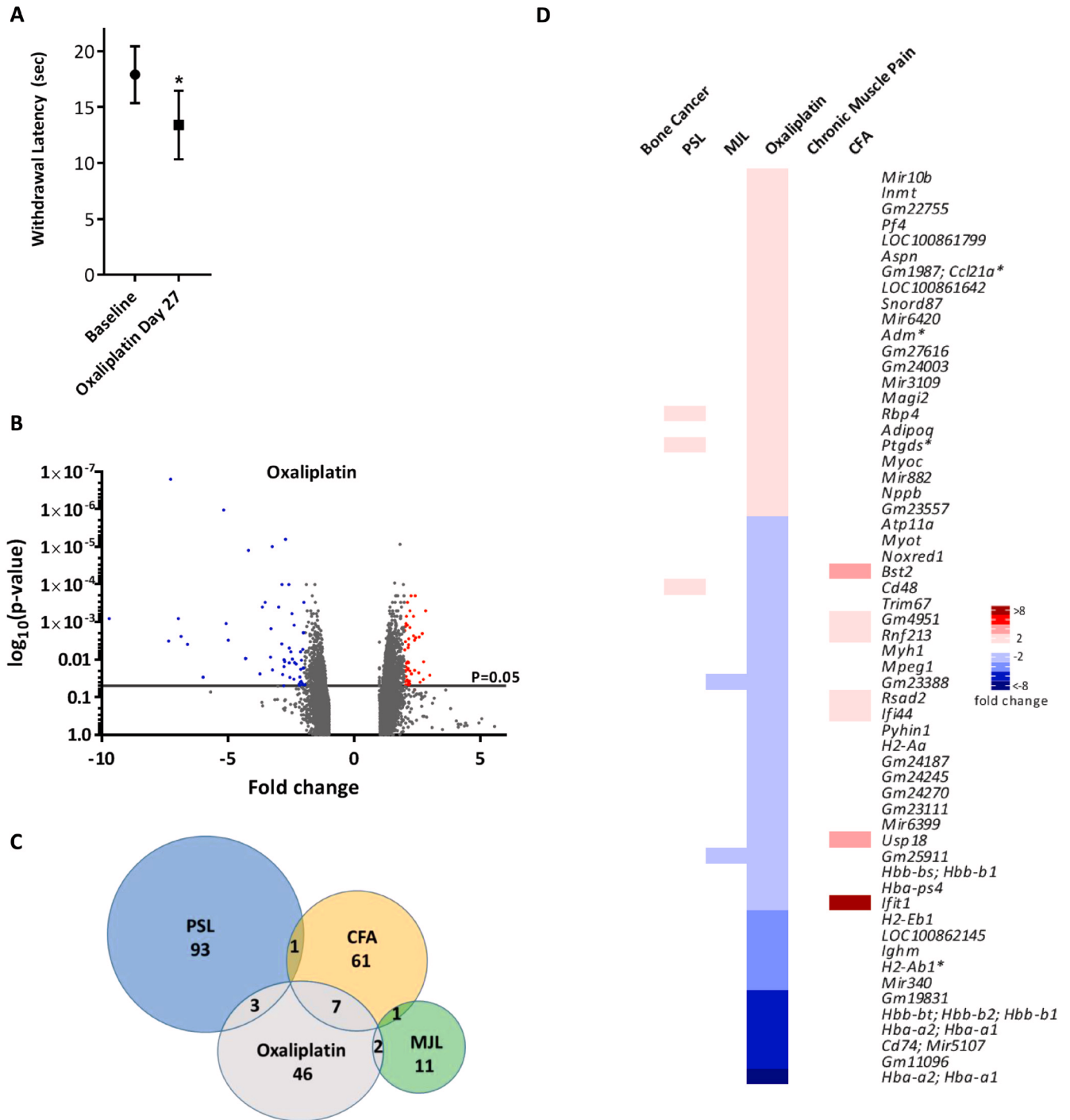
Figure 4. Differential gene expression in the oxaliplatin pain model. (**A**) Cold hypersensitivity induced by oxaliplatin (6 mg/kg, i.p.) at Day 27 (5% glucose solution was used as control). Significant changes are indicated with * (n=6 per group, *p<0.05, paired t-test). (**B**) Volcano plot for all genes identified in the oxaliplatin model array. Each dot represents a single gene (red=upregulated; blue=downregulated). (**C**) Venn diagram showing the number of differentially expressed DRG genes (fold change >2, <-2, p<0.05) shared with other pain models. (**D**) Heat map of upregulated (red) and downregulated (blue) DRG genes (fold change >2, <-2, p<0.05) and a comparison of shared genes across models. Genes with an asterisk are present within the *Pain Genes Database* of pain-related transgenic knockout studies[34].
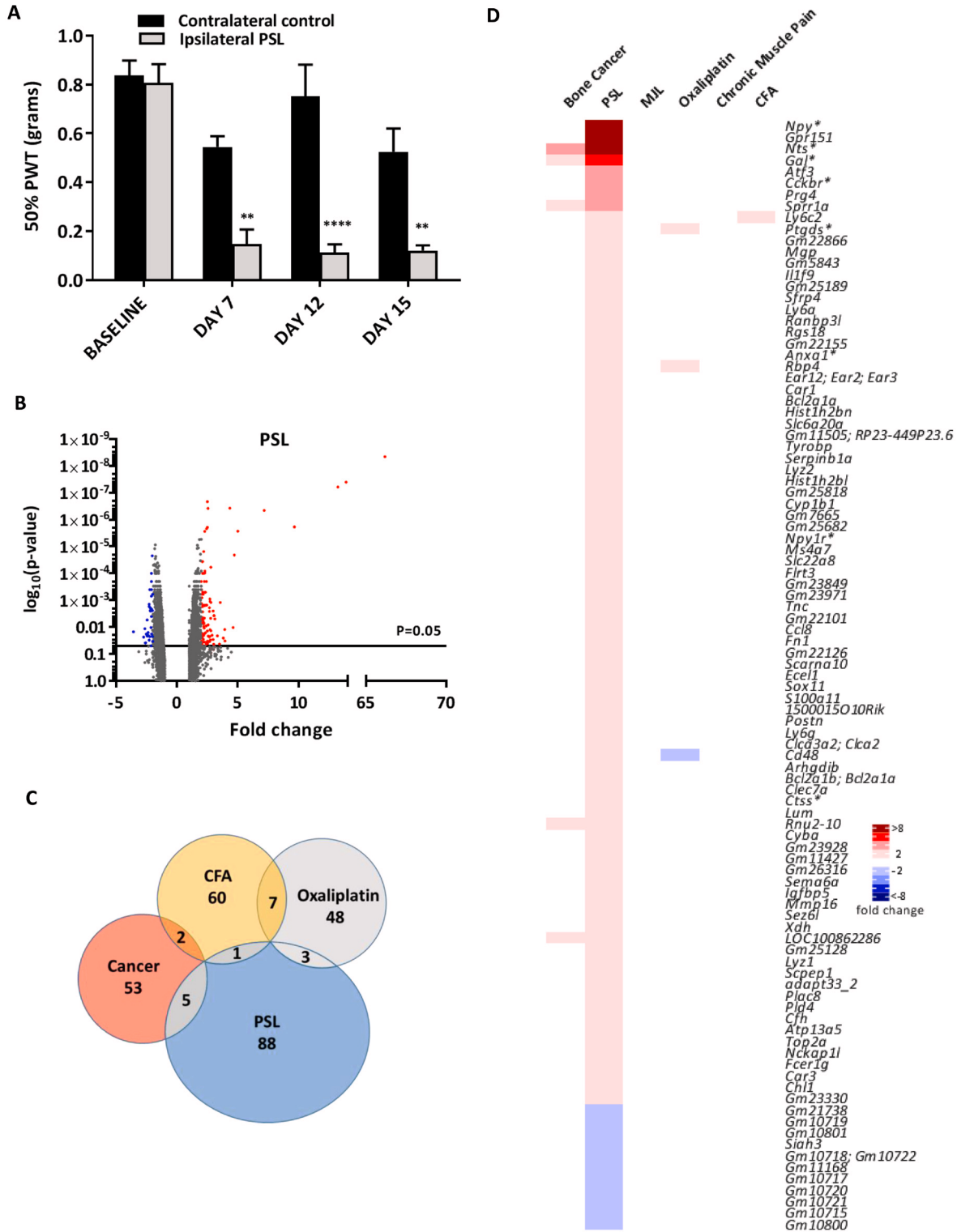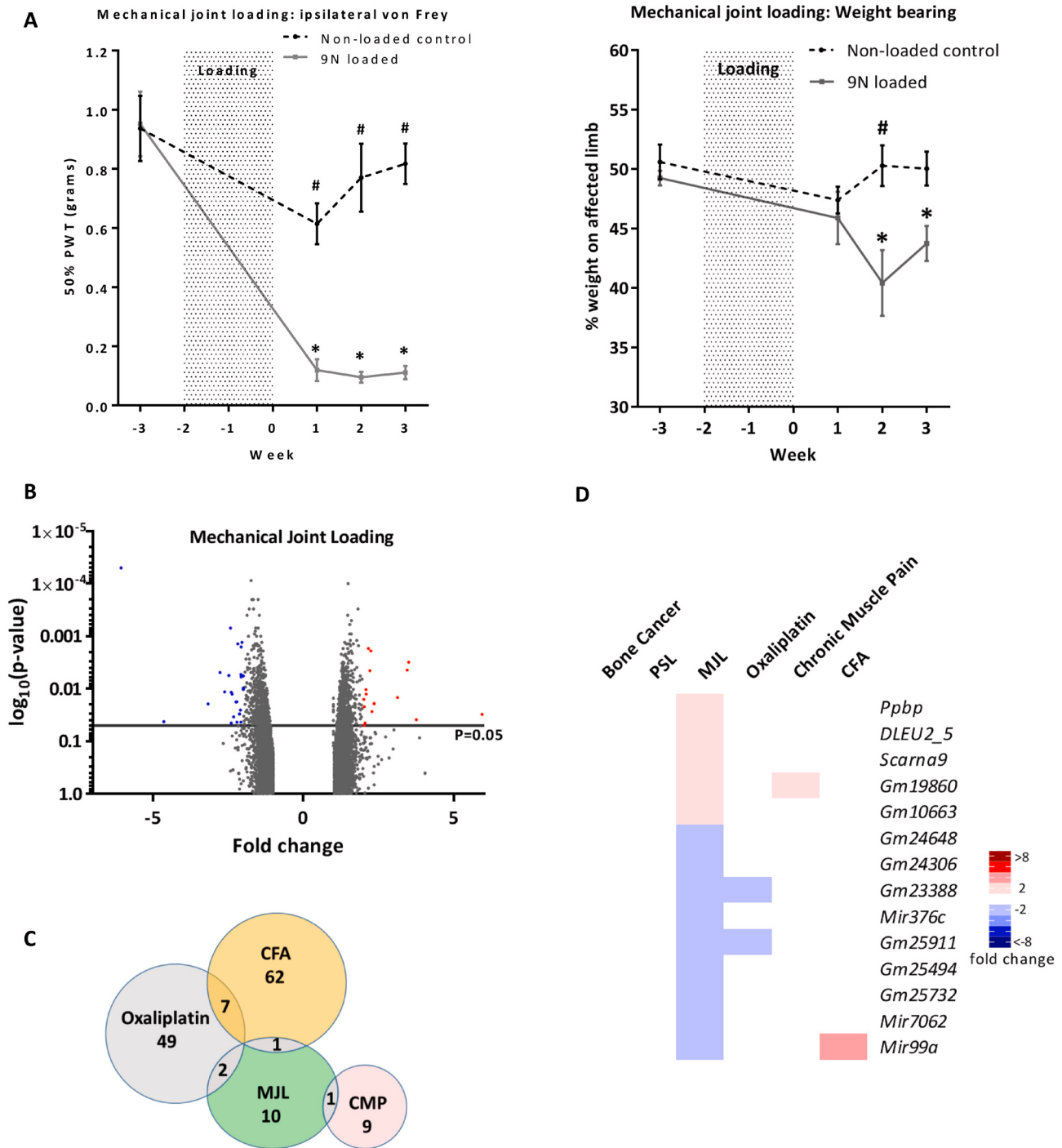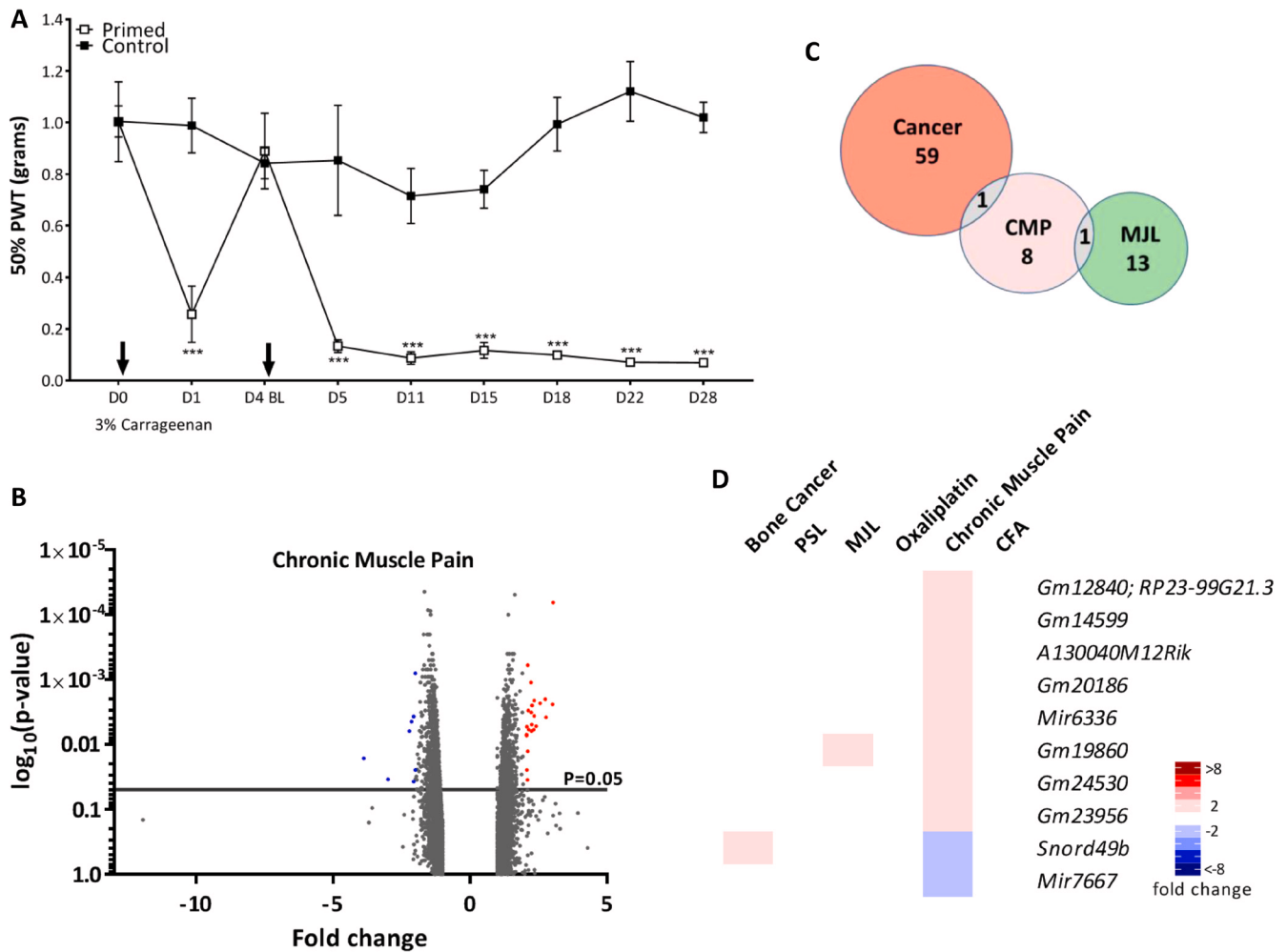
Figure 5. Differential gene expression in the chronic muscle pain model. (**A**) Widespread mechanical hypersensitivity in a mouse model of the transition from acute to chronic musculoskeletal pain. Mice were injected twice with 3% carrageenan i.m. (primed group) or saline (control group) into the gastrocnemius muscle (n=4 per group). Injections are indicated by arrows and mechanical withdrawal thresholds were assessed in the glabrous skin of the ipsilateral hind paw. Significant changes denoted by *** (***p<0.001 Primed vs Control, 2-way ANOVA with repeated measures and Bonferroni post hoc tests). (**B**) Volcano plot for all genes identified in the chronic muscle pain model array. Each dot represents a single gene (red=upregulated; blue=downregulated). (**C**) Venn diagram showing the number of differentially expressed DRG genes (fold change >2, <-2, p<0.05) shared with other pain models. (**D**) Heat map of upregulated (red) and downregulated (blue) DRG genes (fold change >2, <-2, p<0.05) and a comparison of shared genes across models.

Expression of pain-related DEGs in DRG neuronal subsets

Single cell RNA sequencing of mouse DRG neurons has identified 11 distinct subsets of neurons[4]. To determine whether particular DRG neuronal populations are enriched with DEGs, we created heat maps for each model that show expression of every neuronal DEG (fold change >±1.5 fold; p<0.05) and compared this with the basal expression of each gene in the Usoskin *et al.* dataset[4] (Figure 7A–F, Supplementary Figure 1A–F). Next, the percentage of DEGs was correlated with each subpopulation of DRG neurons (Figure 7G). This indicated that there were no clear trends for the expression pattern of the DEGs for each model, with the exception of oxaliplatin where DEGs clustered in the NF1-5 and PEP2 subgroups (myelinated neurofilament-heavy (*Nefh*) positive neurons).

Analysis of upstream regulators of neuronal DEGs in chronic pain models

Next, we analysed pathways and upstream regulators implicated in the four pain conditions with the highest number of DEGs using the Ingenuity Pathway Analysis program. The top upstream regulators in the bone cancer pain model are shown in Figure 8A (p-value of overlap <0.05, ANOVA) and includes cytokine IFNG (activation z-score 1.9); growth factor LEP (activation z-score 0.4); and transcription regulator NFE2L2 (activation z-score 1.9). The analysis was unable to determine whether these regulators were activated or inhibited. The top upstream regulators in the PSL model are depicted in Figure 8B (p-value of overlap<0.05, ANOVA), and includes growth factors TGFB1 (activation z-score 2.2, predicted to be activated) and
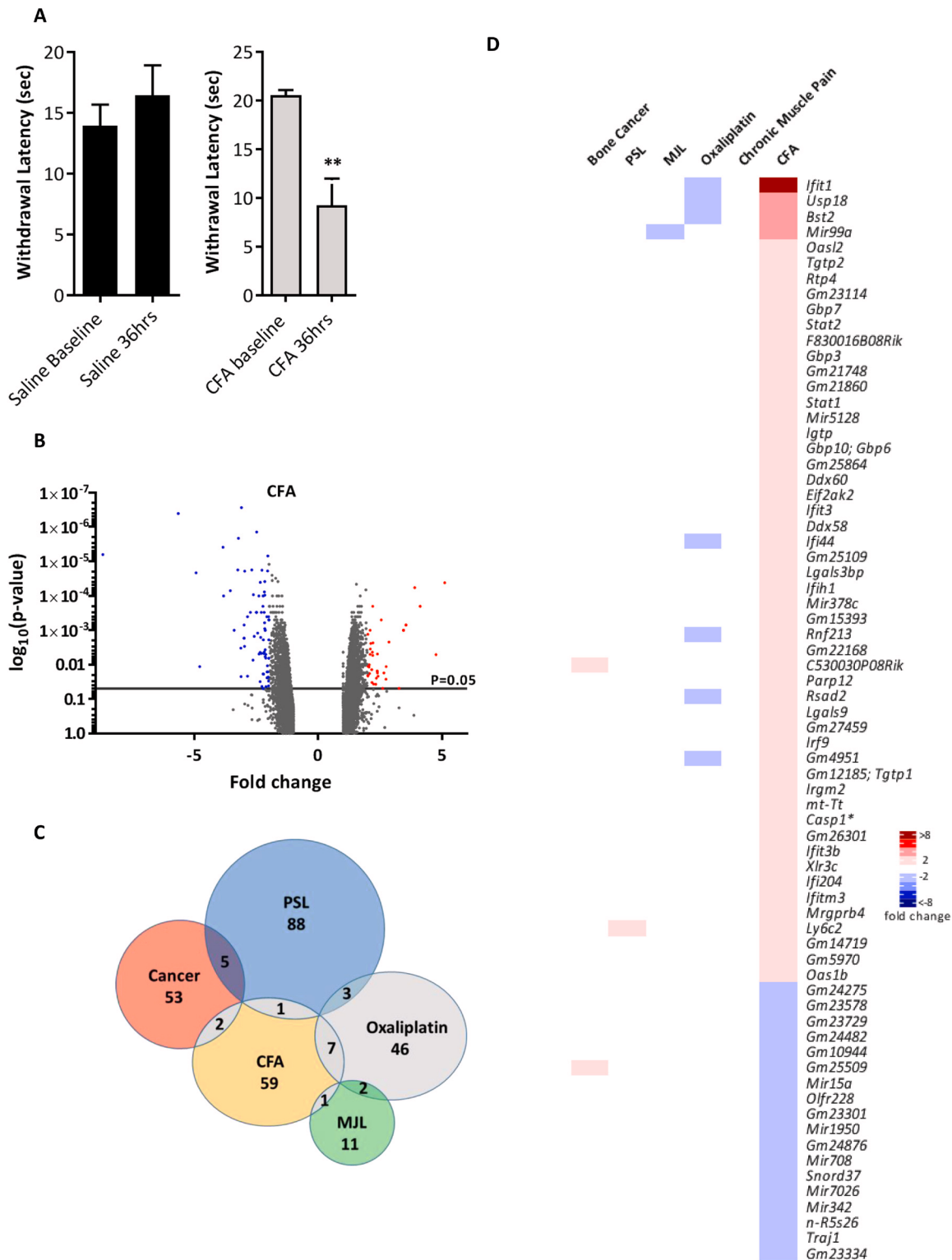
Figure 6. Differential gene expression in the complete Freund's adjuvant (CFA) inflammatory pain model. (**A**) Heat hypersensitivity post CFA intraplantar injection (20 microliters) in mice. Significant changes are indicated with ** (n=6 per group, ** p<0.01, 2-way ANOVA). (**B**) Volcano plot for all genes identified in the CFA pain model array. Each dot represents a single gene (red=upregulated; blue=downregulated). (**C**) Venn diagram showing the number of differentially expressed DRG genes (fold change >2, <-2, p<0.05) shared with other pain models. (**D**) Heat map of upregulated (red) and downregulated (blue) DRG genes (fold change >2, <-2, p<0.05) and a comparison of shared genes across models. Genes with an asterisk are present within the *Pain Genes Database* of pain-related transgenic knockout studies[34].
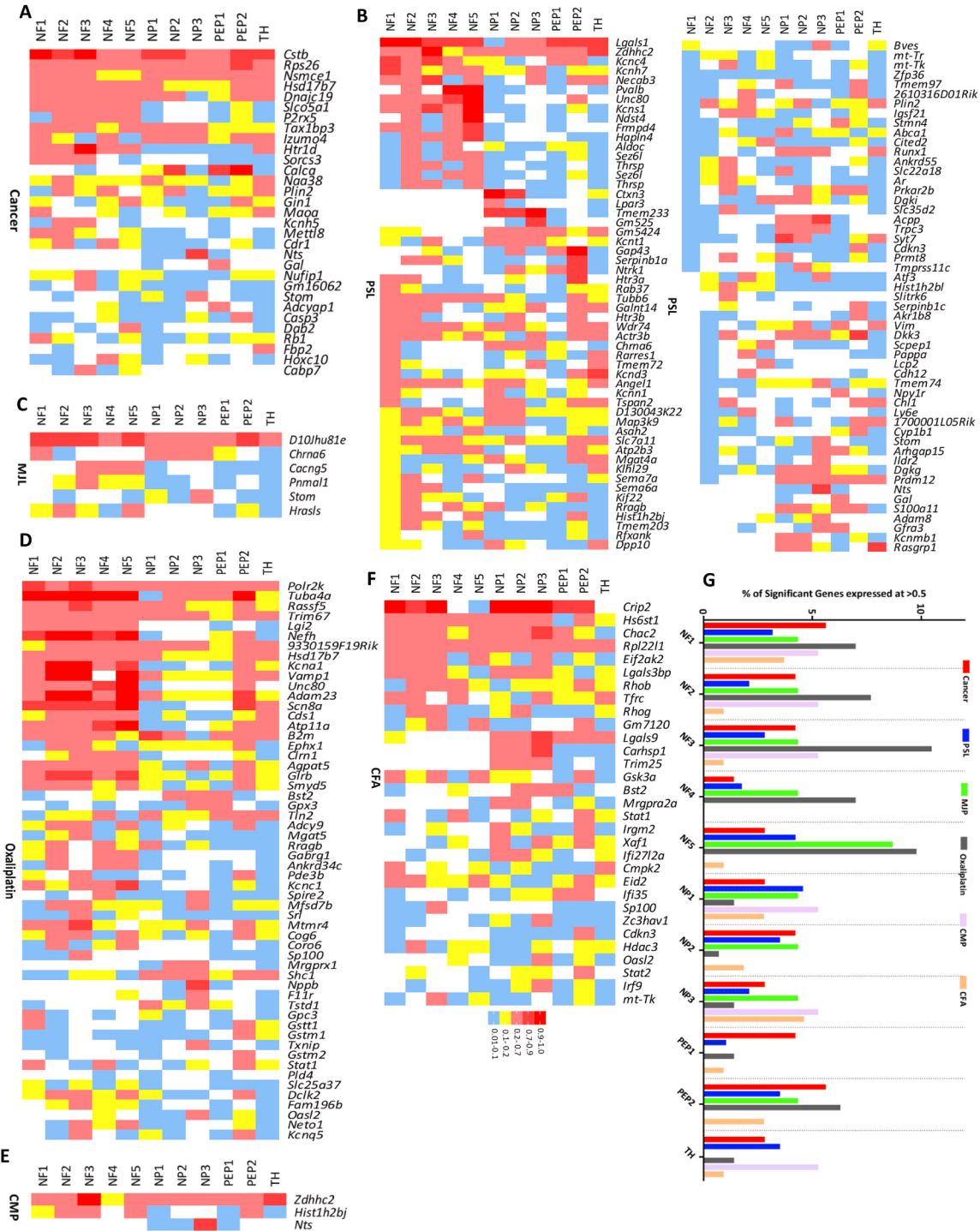
Figure 7. Pattern of dorsal root ganglion (DRG) neuron expression of differentially expressed genes (DEGs) identified in the six pain models. Expression pattern in (**A**) Bone cancer, (**B**) partial sciatic nerve ligation (PSL), (**C**) mechanical joint loading (MJL), (**D**) Oxaliplatin, (**E**) chronic muscle pain (CMP) and (**F**) complete Freund's adjuvant (CFA) models of the DEGs and their basal expression pattern in the 11 different subtypes of DRG neurons (NF1-5, NP1-3, PEP1-2, TH) based on the classification described by Usoskin *et al.*[4]. NF1, NF2 and NF3 correspond to low-threshold mechanoreceptors (LTMRs); NF4 and NF5 correspond to proprioceptors; NP1, NP2 and NP3 are unmyelinated, nonpeptidergic neurons; PEP1 are unmyelinated, peptidergic neurons; PEP2 are myelinated, peptidergic neurons; and TH neurons are type C low-threshold mechanoreceptors (C-LTMRs) that are unmyelinated. Analysis has been restricted to DEGs with a fold-change greater than 1.5 or less than -1.5 (p<0.05) with at least 20% expression in 1 or more of the neuronal subgroups in the Usoskin *et al.* dataset[4]. (**G**) Transcriptional preference for distinct DRG neuronal subpopulations (described previously) in each pain model. This graphical estimation is based on a particular gene being expressed in 50% or more of a particular neuronal subpopulation and presented as a percentage of the total DEGs shared with the Usoskin *et al.* dataset[4] at >1.5 or <-1.5 fold (p<0.05).

A

Cancer

Upstream Regulator	Gene Type	Activation z-score	p-value of overlap	Target genes in Cancer Pain Array
IFNG	cytokine	1.937	0.053	CABP7,CASP3,DUSP1,RB1,SPRR1A
NFE2L2	transcription regulator	1.925	0.0158	ADCYAP1,GSTM4,PLIN2,Xlr3c (includes others)
Cg	complex	0.763	0.00229	ADCYAP1,DUSP1,GAL,HSD17B7,SPRR1A
LEP	growth factor	0.447	0.00133	CASP3,FBP2,GAL,NTS,PLIN2
MGEA5	enzyme	-1.342	0.00442	ADAMTS5,DAB2,PLIN2,RB1,TGFBI

B

PSL

Upstream Regulator	Gene Type	Predicted Activation State	Activation z-score (bias corrected)	p-value of overlap	Target genes in PSL Pain Array
IL6	cytokine	Activated	2.17	7.32E-06	ABCA1,ANXA1,BMP6,CCL3L3,CRH,FN1,FOS,GAP43,HLA-DQA1,IGFBP5,LBP,LYZ,MYB,TF,THBS1
TNF	cytokine	Activated	3.143	1.14E-08	ABCA1,ADAM8,AEBP1,ARHGDIB,ATF3,BCL2A1,CCL3L3,CITED2,CSF1,CTSS,CYBA,CYP1B1,FN1,FOS,FST,GADD45A,IFI16,IGFBP6,IL1B,LBP,LYVE1,MGP,PTPRC,RBP1,RGS16,RRM2,SERPINB1,STEAP4,TF,THBS2,TNC,VIM
IL2	cytokine	Activated	2.419	0.000112	ABCA1,ADAM8,ANXA1,CCL3L3,CSF1,FOS,IL1B,LCP2,Ly6a (includes others),MYB,PLAC8,PTPRC,STK17B,VIM
IL1B	cytokine	Activated	2.355	1.71E-06	ACPP,ADAM8,ATF3,BCL2A1,CRH,CSF1,CTSS,FOS,FST,IGFBP5,IL1B,ITGB8,LBP,PTGDS,RGS16,SLC7A11,VIM,ZFP36
MTOR	kinase	Activated	2.306	0.0149	AR,FST,GAP43,IL1B,SERPINB1,SNAI2,UBE2C
TGFB1	growth factor	Activated	2.278	1.79E-09	BGN,CALB2,CASP8,CCL3L3,CDKN3,CITED2,COL12A1,FN1,FOS,GJB2,HLA-DQA1,IGFBP5,IGFBP7,IL1B,INPP5D,ITGBL1,LTBP1,Ly6a (includes others),POSTN,PRC1,S100A4,SEMA7A,SNAI2,THBS1,TNC,TOP2A,VIM,ZFP36
IFNG	cytokine	Activated	2.227	2.22E-09	ABCA1,ATF3,BCL2A1,BMP6,BTG1,C1QB,CALB2,CASP8,CCL3L3,CLEC7A,CLIC4,CSF1,CTSH,CTSS,DDR2,FCER1G,FCGR2A,FN1,GJB2,HLA-DQA1,IFI16,IL1B,Ly6a (includes others),LY6E,RARRES1,SEMA7A,SLC7A11,SPRR1A,SYT7,THBS1,TYROBP
CD44	other	Activated	2.191	3.03E-07	ADAM8,BGN,CLEC7A,CRABP2,FN1,IL1B,ITGBL1,LGALS1,LTBP1,Ly6a (includes others),THBS1,THBS2,VIM
Alpha catenin	group	Inhibited	-1.945	1.78E-08	ADAM8,BGN,GAP43,IGFBP6,IGFBP7,IL1B,LUM,LYZ,STEAP4,THBS2,TNC,VIM
BMP7	growth factor	Inhibited	-1.951	0.00318	FN1,IGFBP5,IGFBP6,IL1B
GATA4	transcription regulator	Inhibited	-2.084	0.0719	CRABP2,ECM2,S100A4,SPRR1A

C

Oxaliplatin

Upstream Regulator	Gene Type	Predicted Activation State	Activation z-score (bias corrected)	p-value of overlap	Target genes in Oxaliplatin Pain Array
TRIM24	transcription regulator	Activated	3.265	9.94E-13	Bst2,CALHM6,DDX60,HERC6,IFI44,IFIH1,IFIT1B,ISG15,ITIH2,SAMD9L,STAT1,USP18
SIRT1	transcription regulator	Activated	3.207	4.07E-09	ADIPOQ,DDX60,HLA-DQA1,HLA-DQB1,HLA-DRB5,IFI44,IFIT1B,MMP2,Oasl2,PCK1,RSAD2,STAT1,Trim30a/Trim30d,USP18
ACKR2	g-protein coupled receptor	Activated	3	1.1E-12	DDX60,IFI16,IFI44,IFIT1B,ISG15,Oasl2,RSAD2,STAT1,USP18
STAT3	transcription regulator	Activated	2.925	3.25E-10	ADIPOQ,ADM,ALAS2,CALHM6,HERC6,HLA-DQA1,HLA-DRB5,IFI16,IFIT1B,IL13RA2,ISG15,LBP,MMP2,PCK1,RSAD2,STAT1,USP18
IL10RA	transmembrane receptor	Activated	2.887	3.65E-07	ASPN,CALHM6,CLEC9A,CTSE,CYR61,GSTM1,GSTM5,IFI16,PCK1,PF4,RSAD2,STAT1
IL1RN	cytokine	Activated	2.646	1.95E-06	CTSS,HERC6,HLA-DQB1,IFI44,IFIH1,RSAD2,USP18
IFNG	cytokine	Inhibited	-2.802	4.06E-11	ADIPOQ,ADM,B2M,CALHM6,CCR2,CLEC7A,CTSS,GBP7,HERC6,HLA-DQA1,HLA-DQB1,HLA-DRB5,IFI16,IFI44,IFIH1,IFIT1B,ISG15,MMP2,PCK1,RSAD2,STAT1,THBS1,TXNIP,USP18
IFNL1	cytokine	Inhibited	-2.828	3.42E-09	DDX60,HERC6,IFI44,IFIH1,ISG15,RSAD2,STAT1,USP18
PRL	cytokine	Inhibited	-2.828	0.000044	CTSS,HERC6,IFI44,IFIH1,ISG15,RSAD2,SAMD9L,USP18
STAT1	transcription regulator	Inhibited	-3.044	8.76E-09	ALAS2,CALHM6,CTSS,DDX60,HERC6,HLA-DQA1,IFI16,IFIH1,IFIT1B,ISG15,RSAD2,SAMD9L,STAT1
Ifnar	group	Inhibited	-3.098	1.58E-10	B2M,Bst2,IFI16,IFIH1,IFIT1B,ISG15,RSAD2,Sp100,STAT1,USP18
IRF3	transcription regulator	Inhibited	-3.487	1.7E-12	Bst2,CALHM6,DDX60,IFI16,IFIH1,IFIT1B,ISG15,Oasl2,RSAD2,SAMD9L,STAT1,Trim30a/Trim30d,USP18

D

CFA

Upstream Regulator	Gene Type	Predicted Activation State	Activation z-score (bias corrected)	p-value of overlap	Target genes in CFA Pain Array
IFNG	cytokine	Activated	2.302	0.0147	CCR5,CD68,CXCL10,EIF2AK2,GBP6,IRF7,ISG15,MAP2K1,Ms4a4b (includes others),NLRC5,SP110,USP18
STAT1	transcription regulator	Activated	1.849	0.00418	CXCL10,EIF2AK2,GBP6,IRF7,ISG15,NLRC5,SP110
IFNB1	cytokine	Activated	1.763	0.00273	CXCL10,EIF2AK2,GBP6,IRF7,ISG15,USP18
IL1B	cytokine	Activated	1.746	0.2	CXCL10,EHF,GBP6,ISG15,PLA2G4A
HSPA5	enzyme	Activated	1.719	0.000167	ACADM,CD47,CXCL10,ISG15
PRL	cytokine	Activated	1.716	0.00541	CXCL10,EIF2AK2,IRF7,ISG15,SP110,USP18
TRIM24	transcription regulator	Inhibited	-1.478	0.000114	CXCL10,IRF7,ISG15,Ms4a4b (includes others),UBA7,USP18
PTGER4	g-protein coupled receptor	Inhibited	-1.774	0.0251	CXCL10,GBP6,IRF7,USP18
STAT3	transcription regulator	Inhibited	-2.036	0.0111	CD46,CXCL10,EIF2AK2,GBP6,IRF7,ISG15,SP110,USP18

Figure 8. Top upstream regulators of differentially expressed genes identified in bone cancer, partial sciatic nerve ligation (PSL), oxaliplatin, and complete Freund's adjuvant (CFA) models. Upstream regulators were identified for (**A**) Bone cancer, (**B**) PSL, (**C**) Oxaliplatin and (**D**) CFA. Bias corrected activation z-score predicts likelihood of activation (+ive score) or inhibition (-ive score) of the molecular pathway.

BMP7 (activation z-score -1.9); cytokines TNF, IL-6, IL-1-beta (activation z-scores > 2, all predicted to be activated in PSL); kinase MTOR (activation z-score 2.3, predicted to be activated); and the transcription regulator GATA4 (activation z-score -2.8). In the oxaliplatin model (Figure 8C) the top upstream regulators (p<0.05, ANOVA) involved included cytokines IFNG, IFNL1, PRL (activation z scores< -2, all predicted to be inhibited) and IL1RN (activation z score >2, predicted to be activated); G-protein coupled receptor ACKR2 (activation z score 3, predicted to be activated); and transcription regulators TRIM24, SIRT1, STAT3 (activation z scores > 2, all predicted to be activated) and STAT1 (activation z score <-3, predicted to be inhibited). Finally, for CFA the top upstream regulators (p<0.05, ANOVA) included cytokines IFNG, IL-1B and IFN-B1 (activation z scores>1.7, all predicted to be activated); transcription regulator STAT1 (activation z score 1.8, predicted to be activated) and TRIM24 (activation z score -1.47, predicted to be inhibited) (Figure 8D). We observed interesting patterns of activation compared to inhibition of upstream regulators between pain models. For example, STAT1 is activated in oxaliplatin, but inhibited in the CFA model; IFNG is activated in CFA and PSL, but inhibited in the oxaliplatin model.

Discussion

DRG sensory neurons are a heterogeneous population that have recently been classified according to their gene expression profiles[4]. By modelling six chronic pain conditions in mice we aimed to (1) identify dysregulated DRG genes in each model; (2) map dysregulated genes to one or more of the 11 neuronal subsets; and (3) determine whether different pain models shared similar dysregulated genes and/or neuronal subsets. Overall our analysis highlighted how dissimilar the different models were in respect to their transcriptomic profiles with the majority of dysregulated genes not shared between models (see Venn diagrams in Figure 1–Figure 6). This implies that chronic pain can arise from a diverse set of mechanisms involving different genes and pathways. Although transcriptional changes may not be causative in the pain induction, the present study suggests distinct cell and molecular mechanisms are involved with associated transcriptional correlates in the pain models studied. Although some key genes were shared between models, such as Neurotensin and Galanin being upregulated in cancer induced bone pain and PSL neuropathic pain models, the majority of dysregulated genes were exclusive to each pain model.

We also largely failed to link narrow subsets of DRG neurons to particular chronic pain models using microarray analyses (see Figure 7). Our aim was to identify dysregulated genes from the microarrays and map these genes to the neuronal populations previously outlined using single cell RNAseq data[4]. However, this approach was limited by the fact that the published RNAseq data is derived from naïve mice (i.e. not in pain) and potentially the gene expression patterns across the neuronal subsets may dynamically change in the pain models. This is certainly true for genes such as Galanin which is markedly upregulated and expressed in ~40–50% of DRG neurons following axotomy[32] and BDNF, which is upregulated in

medium and large diameter DRG neurons in neuropathic pain[35]. Furthermore, genes that have no DRG expression in the Usoskin *et al.* dataset (i.e. zero sequencing reads) were not included in our transcriptomic analyses, but could be expressed following injury. For example, Neuropeptide Y is dramatically upregulated in DRG neurons following peripheral nerve injury, but is not expressed in basal conditions[29]. Thirdly, many genes are broadly expressed in several DRG populations, meaning that restricted critical subsets are difficult to highlight.

Recent advances in deep sequencing have dramatically increased the number of known transcribed genes[36]. The Mouse Transcriptome Array that we used gives a comprehensive coverage of the mouse transcriptome, with >214,000 transcripts represented. Genes that are represented include both coding and non-coding genes (such an lncRNAs, small RNAs and expressed pseudogenes). Although such genes are now known to be expressed, gene annotation and understanding of gene function is lagging behind. This is highlighted in our transcriptomic analyses where a high number of predicted genes (typically with the 'Gm' prefix) showed differential expression. A major challenge is to determine the function of these types of genes and to ascertain the contribution, if any, to the pain phenotypes observed. Similarly, although the dense probe coverage on the array gives the opportunity to assess differential splicing patterns (Supplementary Figure 3), experimental verification is needed to prove that the changes in splicing patterns are relevant.

Given the unique sets of underlying genes, we attempted to identify potential common upstream regulators using IPA analyses. We identified several common cytokines as upstream regulators of DEGs in our pain models consistent with the role of cytokines in generation and maintenance of pain[37,38], pointing to the interaction of DRG neurons and immune cells as a key point of focus. T cells are known to infiltrate DRGs in models of neuropathic pain[39–41], however whether the cytokine related downstream DEGs identified in our pain models are being induced by immune cells remains to be investigated.

In summary, we present a systematic study of the transcriptomic changes in six different chronic mouse pain models as a resource for the pain community. Although gene expression changes may not be causally linked to the pain phenotypes observed, the transcriptomic profiles reported here highlight the diversity of cell and molecular mechanisms apparent in different pain conditions. Potential therapeutic gene targets for the distinct chronic pain conditions studied may also be identified after further mechanistic studies.

Data availability

Microarray data has been deposited at Gene Expression Omnibus Array Express for public use with reference number E-MTAB-6864.

DGE data (Supplementary Table 1), replicates for Figure 1E (3D reconstruction images) and raw values in a GraphPad Prism file for Figure 1A-D, Figure 2A, Figure 3A, Figure 4A, Figure 5A

and Figure 6A for all replicates are deposited in OSF: https://doi.org/10.17605/OSF.IO/DG7Z3[42]

Data are available under the terms of the Creative Commons Zero "No rights reserved" data waiver (CC0 1.0 Public domain dedication).

Competing interests
No competing interests were disclosed.

Supplementary material
Supplementary Table 1: Differential gene expression values for all genes on the mouse transcriptome array and alternative splicing changes. Differential gene expression and splice variant analysis of transcriptome array data was performed using Transcriptome Analysis Console (TAC Ver 4.0, Thermo Fisher). Normalization was carried out according to the manufacturer's default protocol converting probe cell intensity (CEL files) into signal data (CHP files).

Splice variant analysis was performed using the Gene + Exon function in TAC which uses a gene normalized intensity value (ratio of probe set intensity to gene expression level).
Click here to access the data.

Supplementary File 1: Supplementary figures.
Click here to access the data.

Supplementary Figure 1: Differentially expressed DRG neuron genes. Differentially expressed genes in (**A**) Bone cancer, (**B**) PSL, (**C**) MJL, (**D**) Oxaliplatin, (**E**) CMP and (**F**) CFA with known basal DRG neuron expression in the Usoskin *et al.* dataset[4]. Genes listed here correlate with those shown in Figure 7. Analysis has been restricted to DEGs with a fold-change greater than 1.5 or less than -1.5 (p<0.05) with at least 20% expression in 1 or more of the neuronal subgroups in the Usoskin *et al.* dataset[4]. Genes with an asterisk are present within the *Pain Genes Database* of pain-related transgenic knockout studies[34].

Supplementary Figure 2: Differentially expressed microRNA genes. Differentially expressed microRNA DRG genes in (**A**) Bone cancer, (**B**) PSL, (**C**) MJL, (**D**) Oxaliplatin, (**E**) CMP and (**F**) CFA pain models (fold change >1.5, <-1.5).

Supplementary Figure 3: Differential splicing analyses. Top 10 splice variants for (**A**) Bone Cancer, (**B**) PSL, (**C**) MJL, (**D**) Oxaliplatin, (**E**) Chronic Muscle Pain and (**F**) CFA. Attached heat map for each model shows the splicing index (SI) of the spliced genes (exon SI >2 or <-2, Exon p-val <0.05). Exon event score calculated by TAC software (see methods) where 1 represents a high likelihood for the spliced event. Exon events were defined in TAC as: Intron retention- when a sequence is spliced out as an intron or remains in the mature mRNA transcript; Cassette Exon (skipped exon) – when one exon is spliced out of the primary transcript together with its flanking introns; Alternative 3`acceptor site when two or more splice sites are recognized at the 5` end of an exon, an alternative 3` splice junction is used changing the 5` boundary of the downstream exon; Alternative 5` donor site when two or more splice sites are recognized at the 3` end of an exon, an alternative 5` splice junction is used changing the 3` boundary of the upstream exon.

References

1. Breivik H, Collett B, Ventafridda V, *et al.*: **Survey of chronic pain in Europe: prevalence, impact on daily life, and treatment.** *Eur J Pain.* 2006; **10**(4): 287–333.
   PubMed Abstract | **Publisher Full Text**

2. Nahin RL: **Estimates of pain prevalence and severity in adults: United States, 2012.** *J Pain.* 2015; **16**(8): 769–80.
   PubMed Abstract | **Publisher Full Text** | **Free Full Text**

3. LaCroix-Fralish ML, Austin JS, Zheng FY, *et al.*: **Patterns of pain: meta-analysis of microarray studies of pain.** *Pain.* 2011; **152**(8): 1888–98.
   PubMed Abstract | **Publisher Full Text**

4. Usoskin D, Furlan A, Islam S, *et al.*: **Unbiased classification of sensory neuron types by large-scale single-cell RNA sequencing.** *Nat Neurosci.* 2015; **18**(1): 145–53.
   PubMed Abstract | **Publisher Full Text**

5. Li CL, Li KC, Wu D, *et al.*: **Somatosensory neuron types identified by high-coverage single-cell RNA-sequencing and functional heterogeneity.** *Cell Res.* 2016; **26**(8): 967.
    PubMed Abstract | **Publisher Full Text** | **Free Full Text**

6. Huang LY, Gu Y, Chen Y: **Communication between neuronal somata and satellite glial cells in sensory ganglia.** *Glia.* 2013; **61**(10): 1571–81.
    PubMed Abstract | **Publisher Full Text** | **Free Full Text**

7. Iijima N, Iwasaki A: **Access of protective antiviral antibody to neuronal tissues requires CD4 T-cell help.** *Nature.* 2016; **533**(7604): 552–6.
    PubMed Abstract | **Publisher Full Text** | **Free Full Text**

8. Hidmark AS, Nawroth PP, Fleming T: **Analysis of Immune Cells in Single Sciatic Nerves and Dorsal Root Ganglion from a Single Mouse Using Flow Cytometry.** *J Vis Exp.* 2017; (130): e56538.
    PubMed Abstract | **Publisher Full Text**

9. Seltzer Z, Dubner R, Shir Y: **A novel behavioral model of neuropathic pain disorders produced in rats by partial sciatic nerve injury.** *Pain.* 1990; **43**(2): 205–18.
    PubMed Abstract | **Publisher Full Text**

10. Fraser GL, Gaudreau GA, Clarke PB, *et al.*: **Antihyperalgesic effects of delta opioid agonists in a rat model of chronic inflammation.** *Br J Pharmacol.* 2000; **129**(8): 1668–72.
    PubMed Abstract | **Publisher Full Text** | **Free Full Text**

11. Ling B, Authier N, Balayssac D, *et al.*: **Behavioral and pharmacological description of oxaliplatin-induced painful neuropathy in rat.** *Pain.* 2007; **128**(3): 225–34.
    PubMed Abstract | **Publisher Full Text**

12. Luger NM, Mach DB, Sevcik MA, *et al.*: **Bone cancer pain: from model to mechanism to therapy.** *J Pain Symptom Manage.* 2005; **29**(5 Suppl): S32–46.
    PubMed Abstract | **Publisher Full Text**

13. Aley KO, Messing RO, Mochly-Rosen D, *et al.*: **Chronic hypersensitivity for inflammatory nociceptor sensitization mediated by the epsilon isozyme of protein kinase C.** *J Neurosci.* 2000; **20**(12): 4680–5.
    PubMed Abstract | **Publisher Full Text**

14. Sluka KA, Kalra A, Moore SA: **Unilateral intramuscular injections of acidic saline produce a bilateral, long-lasting hyperalgesia.** *Muscle Nerve.* 2001; **24**(1): 37–46.
    PubMed Abstract | **Publisher Full Text**

15. Vadakkan KI, Wang H, Ko SW, *et al.*: **Genetic reduction of chronic muscle pain in mice lacking calcium/calmodulin-stimulated adenylyl cyclases.** *Mol Pain.* 2006; **2**: 7.
    PubMed Abstract | **Publisher Full Text** | **Free Full Text**

16. Poulet B, Hamilton RW, Shefelbine S, *et al.*: **Characterizing a novel and adjustable noninvasive murine joint loading model.** *Arthritis Rheum.* 2011; **63**(1): 137–47.
    PubMed Abstract | **Publisher Full Text**

17. Faul F, Erdfelder E, Lang AG, *et al.*: **G*Power 3: a flexible statistical power analysis program for the social, behavioral, and biomedical sciences.** *Behav Res Methods.* 2007; **39**(2): 175–91.
    PubMed Abstract | **Publisher Full Text**

18. Minett MS, Falk S, Santana-Varela S, *et al.*: **Pain without nociceptors? Nav1.7-independent pain mechanisms.** *Cell Rep.* 2014; **6**(2): 301–12.
    PubMed Abstract | **Publisher Full Text** | **Free Full Text**

19. Falk S, Uldall M, Appel C, *et al.*: **Influence of sex differences on the progression of cancer-induced bone pain.** *Anticancer Res.* 2013; **33**(5): 1963–9.
    PubMed Abstract

20. De Souza RL, Matsuura M, Eckstein F, *et al.*: **Non-invasive axial loading of mouse tibiae increases cortical bone formation and modifies trabecular organization: a new model to study cortical and cancellous compartments in a single loaded element.** *Bone.* 2005; **37**(6): 810–8.
    PubMed Abstract | **Publisher Full Text**

21. Pereira V, Busserolles J, Christin M, *et al.*: **Role of the TREK2 potassium channel in cold and warm thermosensation and in pain perception.** *Pain.* 2014; **155**(12): 2534–44.
    PubMed Abstract | **Publisher Full Text**

22. Cao YQ, Mantyh PW, Carlson EJ, *et al.*: **Primary afferent tachykinins are required to experience moderate to intense pain.** *Nature.* 1998; **392**(6674): 390–4.
    PubMed Abstract | **Publisher Full Text**

23. Ferreira J, Campos MM, Pesquero JB, *et al.*: **Evidence for the participation of kinins in Freund's adjuvant-induced inflammatory and nociceptive responses in kinin B_1 and B_2 receptor knockout mice.** *Neuropharmacology.* 2001; **41**(8): 1006–12.
    PubMed Abstract | **Publisher Full Text**

24. Chaplan SR, Bach FW, Pogrel JW, *et al.*: **Quantitative assessment of tactile allodynia in the rat paw.** *J Neurosci Methods.* 1994; **53**(1): 55–63.
    PubMed Abstract | **Publisher Full Text**

25. Hargreaves K, Dubner R, Brown F, *et al.*: **A new and sensitive method for measuring thermal nociception in cutaneous hyperalgesia.** *Pain.* 1988; **32**(1): 77–88.
    PubMed Abstract | **Publisher Full Text**

26. Brenner DS, Golden JP, Gereau RW: **A novel behavioral assay for measuring cold sensation in mice.** *PLoS One.* 2012; **7**(6): e39765.
    PubMed Abstract | **Publisher Full Text** | **Free Full Text**

27. Busby MA, Stewart C, Miller CA, *et al.*: **Scotty: a web tool for designing RNA-Seq experiments to measure differential gene expression.** *Bioinformatics.* 2013; **29**(5): 656–7.
    PubMed Abstract | **Publisher Full Text** | **Free Full Text**

28. Conesa A, Madrigal P, Tarazona S, *et al.*: **A survey of best practices for RNA-seq data analysis.** *Genome Biol.* 2016; **17**: 13.
    PubMed Abstract | **Publisher Full Text** | **Free Full Text**

29. Magnussen C, Hung SP, Ribeiro-da-Silva A: **Novel expression pattern of neuropeptide Y immunoreactivity in the peripheral nervous system in a rat model of neuropathic pain.** *Mol Pain.* 2015; **11**: 31.
    PubMed Abstract | **Publisher Full Text** | **Free Full Text**

30. Holmes FE, Kerr N, Chen YJ, *et al.*: **Targeted disruption of the orphan receptor Gpr151 does not alter pain-related behaviour despite a strong induction in dorsal root ganglion expression in a model of neuropathic pain.** *Mol Cell Neurosci.* 2017; **78**: 35–40.
    PubMed Abstract | **Publisher Full Text** | **Free Full Text**

31. Reinhold AK, Batti L, Bilbao D, *et al.*: **Differential transcriptional profiling of damaged and intact adjacent dorsal root ganglia neurons in neuropathic pain.** *PLoS One.* 2015; **10**(4): e0123342.
    PubMed Abstract | **Publisher Full Text** | **Free Full Text**

32. Hökfelt T, Wiesenfeld-Hallin Z, Villar M, *et al.*: **Increase of galanin-like immunoreactivity in rat dorsal root ganglion cells after peripheral axotomy.** *Neurosci Lett.* 1987; **83**(3): 217–20.
    PubMed Abstract | **Publisher Full Text**

33. Renn CL, Carozzi VA, Rhee P, *et al.*: **Multimodal assessment of painful peripheral neuropathy induced by chronic oxaliplatin-based chemotherapy in mice.** *Mol Pain.* 2011; **7**: 29.
    PubMed Abstract | **Publisher Full Text** | **Free Full Text**

34. Lacroix-Fralish ML, Ledoux JB, Mogil JS: **The *Pain Genes Database*: An interactive web browser of pain-related transgenic knockout studies.** *Pain.* 2007; **131**(1–2): 3 e1–4.
    PubMed Abstract | **Publisher Full Text**

35. Obata K, Yamanaka H, Kobayashi K, *et al.*: **The effect of site and type of nerve injury on the expression of brain-derived neurotrophic factor in the dorsal root ganglion and on neuropathic pain behavior.** *Neuroscience.* 2006; **137**(3): 961–70.
    PubMed Abstract | **Publisher Full Text**

36. ENCODE Project Consortium: **An integrated encyclopedia of DNA elements in the human genome.** *Nature.* 2012; **489**(7414): 57–74.
    PubMed Abstract | **Publisher Full Text** | **Free Full Text**

37. Schaible HG, von Banchet GS, Boettger MK, *et al.*: **The role of proinflammatory cytokines in the generation and maintenance of joint pain.** *Ann N Y Acad Sci.* 2010; **1193**(1): 60–9.
    PubMed Abstract | **Publisher Full Text**

38. Totsch SK, Sorge RE: **Immune System Involvement in Specific Pain Conditions.** *Mol Pain.* 2017; **13**: 1744806917724559.
    PubMed Abstract | **Publisher Full Text** | **Free Full Text**

39. Kobayashi Y, Kiguchi N, Fukazawa Y: **Macrophage-T cell interactions mediate neuropathic pain through the glucocorticoid-induced tumor necrosis factor ligand system.** *J Biol Chem.* 2015; **290**(20): 12603–13.
    PubMed Abstract | **Publisher Full Text** | **Free Full Text**

40. Draleau K, Maddula S, Slaiby A, *et al.*: **Phenotypic Identification of Spinal Cord-Infiltrating CD4+ T Lymphocytes in a Murine Model of Neuropathic Pain.** *J Pain Relief.* 2014; **Suppl 3**: 003.
    PubMed Abstract | **Publisher Full Text** | **Free Full Text**

41. Vicuña L, Strochlic DE, Latremoliere A, *et al.*: **The serine protease inhibitor SerpinA3N attenuates neuropathic pain by inhibiting T cell-derived leukocyte elastase.** *Nat Med.* 2015; **21**(5): 518–23.
    PubMed Abstract | **Publisher Full Text** | **Free Full Text**

42. James C: **Distinct Transcriptional Responses of Mouse Sensory Neurons in Models of Human Chronic Pain Conditions.** *Open Science Framework.* 2018.
    Data Source

Open Peer Review

Current Peer Review Status: ✓ ✓

Version 1

Reviewer Report 18 July 2018

https://doi.org/10.21956/wellcomeopenres.15942.r33489

✓ **Mark D. Baker**

Blizard Institute, Queen Mary University of London, Whitechapel, UK

The paper discovers differentially expressed genes in mouse primary sensory neurons (DRG) in a variety of pain models that are believed to be models of human pain states. Looking in the primary neurons the authors find that, although pain levels appear similar and significant in all the models studied, the changes in gene expression for each of the pain states is different. The paper is of great interest, and I have enjoyed trying to grapple with its contents. This is a way of saying that I like it, but I wanted to clarify a couple of things, that have raised a flag.

The discussion is written as though no gene expression data have ever been obtained before in pain models, and I agree with David Wynick that a more helpful approach would require that some context is offered in the discussion, particularly as this group of authors are generating a benchmark. For example, with reference to the findings on local inflammation, in Figure 2D I do not see a single sodium channel gene affected, and yet Na+ channel genes are reported by others to be dysregulated, for example NaV1.3 expression is reported to double in DRG in inflammatory circumstances[1]. Do the authors think this is surprising and what is the reader to make of this? In fact, is Na+ channel gene expression in DRG neurons affected at all by any of the induced pain states? What has happened to other potentially important pain related ion channels such as KCNQ and HCN channels?

Is one correct deduction then that while there may indeed be stereotyped gene expression changes taking place (given that somehow the maladaptive changes in the nervous system exist for all these pain scenarios) they must be in second and higher order neurons, involving glutamate gated ion channel subunits and so on?

Secondly, as it seems inescapable to conclude that the membrane behaviour of primary sensory neurons must be somehow 'abnormal' in pain states driven from the periphery, is the correct conclusion that this is precipitated without any necessity of modification of ion channel expression, completely by a combination of already latent functionality and post-translational modification.

I would like a little more clarification on Figure 7. I think the authors are looking a for a pattern of gene dysregulation that might conspicuously 'fit' the already discovered baseline gene expression profiles of sub-populations of neurons. I think I understand that fitting the profiles against each subtype (previously described) reveals nothing useful, but I would be happy with a bit more explanation for this (bottom page 10 and Figure 7), as I want to rid myself of (I think !) the erroneous impression that single cell analysis is going on.

References
1. Black JA, Liu S, Tanaka M, Cummins TR, et al.: Changes in the expression of tetrodotoxin-sensitive sodium channels within dorsal root ganglia neurons in inflammatory pain.*Pain*. 2004; **108** (3): 237-47 PubMed Abstract | Publisher Full Text

Is the work clearly and accurately presented and does it cite the current literature?
Yes

Is the study design appropriate and is the work technically sound?
Yes

Are sufficient details of methods and analysis provided to allow replication by others?
Partly

If applicable, is the statistical analysis and its interpretation appropriate?
Yes

Are all the source data underlying the results available to ensure full reproducibility?
Yes

Are the conclusions drawn adequately supported by the results?
Yes

Competing Interests: No competing interests were disclosed.

Reviewer Expertise: axons and ion channels

I confirm that I have read this submission and believe that I have an appropriate level of expertise to confirm that it is of an acceptable scientific standard.

Reviewer Report 13 July 2018

https://doi.org/10.21956/wellcomeopenres.15942.r33470

✔   **David Wynick**

Department of Translational Health Sciences, Bristol Medical School, University of Bristol, Bristol, UK

This is a well written paper that is clearly and accurately presented. The study design is appropriate and the work is technically sound. The data substantially expands the current evidence-base in this field.

The authors have used transcriptional profiling to identify differentially expressed genes in the mouse DRG following six different chronic pain models. Most interestingly and unexpectedly, they found almost no similarity between the transcriptional changes in expression with very little overlap in the genetic signatures between the models.

Points that could be further expanded upon in the discussion:
- Place the current dataset in the context of the previous published studies that have used transcriptional profiling on the DRG after different pain models (and in some cases comparing two different models), and whether the previous findings and genes identified are consistent with the current data.
- Identifying genes in the DRG on the basis of their fold-change after a pain model does not mean that those genes are necessarily involved in mediating pain. Indeed, many of the targets of the current analgesics used in clinical practice do not show >two-fold change in expression in mouse models. It is quite possible that many of the genes that do show large changes in each model play roles that relate to apoptosis, survival and/or regeneration, rather than pain transmission and nociception.
- The main finding of this paper provides further evidence that it may not be possible to identify targets in the final common nociceptive pathway that will target all causes of pain and would be amendable to drug discovery. A more targeted and mechanistic approach is likely to be necessary to focus more on specific pathways that are activated and thus on the individual diseases that cause the pain.

Is the work clearly and accurately presented and does it cite the current literature?
Yes

Is the study design appropriate and is the work technically sound?
Yes

Are sufficient details of methods and analysis provided to allow replication by others?
Yes

If applicable, is the statistical analysis and its interpretation appropriate?
Yes

Are all the source data underlying the results available to ensure full reproducibility?
Yes

Are the conclusions drawn adequately supported by the results?
Yes

Competing Interests: No competing interests were disclosed.

I confirm that I have read this submission and believe that I have an appropriate level of expertise to confirm that it is of an acceptable scientific standard.

Appendix C
A novel human pain insensitivity disorder caused by a point mutation in ZFHX2

BRAIN
A JOURNAL OF NEUROLOGY

A novel human pain insensitivity disorder caused by a point mutation in *ZFHX2*

Abdella M. Habib,[1,2,*] Ayako Matsuyama,[1,*] Andrei L. Okorokov,[1,*] Sonia Santana-Varela,[1,*] Jose T. Bras,[3,*] Anna Maria Aloisi,[4,*] Edward C. Emery,[1,*] Yury D. Bogdanov,[1] Maryne Follenfant,[1] Sam J. Gossage,[1] Mathilde Gras,[1] Jack Humphrey,[1] Anna Kolesnikov,[1] Kim Le Cann,[1] Shengnan Li,[1] Michael S. Minett,[1] Vanessa Pereira,[1] Clara Ponsolles,[1] Shafaq Sikandar,[1] Jesus M. Torres,[1,5] Kenji Yamaoka,[1] Jing Zhao,[1] Yuriko Komine,[6] Tetsuo Yamamori,[6] Nikolas Maniatis,[7] Konstantin I. Panov,[8] Henry Houlden,[3] Juan D. Ramirez,[9] David L. H. Bennett,[9] Letizia Marsili,[10] Valeria Bachiocco,[4] John N. Wood[1] and James J. Cox[1]

*These authors contributed equally to this work.

Chronic pain is a major global public health issue causing a severe impact on both the quality of life for sufferers and the wider economy. Despite the significant clinical burden, little progress has been made in terms of therapeutic development. A unique approach to identifying new human-validated analgesic drug targets is to study rare families with inherited pain insensitivity. Here we have analysed an otherwise normal family where six affected individuals display a pain insensitive phenotype that is characterized by hyposensitivity to noxious heat and painless bone fractures. This autosomal dominant disorder is found in three generations and is not associated with a peripheral neuropathy. A novel point mutation in *ZFHX2*, encoding a putative transcription factor expressed in small diameter sensory neurons, was identified by whole exome sequencing that segregates with the pain insensitivity. The mutation is predicted to change an evolutionarily highly conserved arginine residue 1913 to a lysine within a homeodomain. Bacterial artificial chromosome (BAC) transgenic mice bearing the orthologous murine p.R1907K mutation, as well as *Zfhx2* null mutant mice, have significant deficits in pain sensitivity. Gene expression analyses in dorsal root ganglia from mutant and wild-type mice show altered expression of genes implicated in peripheral pain mechanisms. The ZFHX2 variant and downstream regulated genes associated with a human pain-insensitive phenotype are therefore potential novel targets for the development of new analgesic drugs.

1 Molecular Nociception Group, Wolfson Institute for Biomedical Research, University College London, London, WC1E 6BT, UK
2 College of Medicine, Member of Qatar Health Cluster, Qatar University, PO Box 2713, Doha, Qatar
3 Department of Molecular Neuroscience, Institute of Neurology, University College London, London, WC1N 3BG, UK
4 Department of Medicine, Surgery and Neuroscience, University of Siena, via Aldo Moro, 2, 53100 Siena, Italy
5 Department of Biochemistry, Molecular Biology and Immunology, Faculty of Medicine, University of Granada, Granada 18012, Spain
6 National Institute for Basic Biology, Okazaki, 444-8585, Japan
7 Department of Genetics, Evolution and Environment, University College London, London, WC1E 6BT, UK
8 Medical Biology Centre, School of Biological Sciences, Queen's University Belfast, Belfast, BT9 7BL, UK
9 Nuffield Department of Clinical Neurosciences, University of Oxford, Oxford, OX3 9DU, UK
10 Department of Physical Sciences, Earth and Environment, University of Siena, 53100 Siena, Italy

Correspondence to: Dr James J Cox,
Lab 3.1, Molecular Nociception Group, Wolfson Institute for Biomedical Research
Cruciform Building, UCL, Gower Street, London, UK, WC1E 6BT
E-mail: j.j.cox@ucl.ac.uk

Introduction

Congenital hypoalgesia, in which patients are born with a reduced capacity to detect tissue-damage causing stimuli, is a rare inherited phenotype. In the most extreme forms, patients can suffer from a complete inability to perceive noxious stimuli which leads to dangerous, but painless, injuries such as biting off of fingertips, lips and the tongue, and frequent bone fractures (Nahorski *et al.*, 2015). Recessive loss of function mutations in the voltage-gated sodium channel gene *SCN9A*, which encodes Na$_v$1.7, are a major cause of this form of pain insensitivity (OMIM 243000) (Cox *et al.*, 2006; Habib *et al.*, 2015). A second, less frequent cause, are dominant gain of function mutations in the Na$_v$1.9 channel, which to date have been reported in only four families worldwide (OMIM 615548) (Leipold *et al.*, 2013; Woods *et al.*, 2015; Phatarakijnirund *et al.*, 2016). In both of these channelopathy disorders there is an absence of an associated peripheral neuropathy with the phenotype related to dysfunction of voltage-gated sodium channels within the intact sensory neurons. In the case of Na$_v$1.7, this dysfunction has been shown to result in an upregulation of endogenous opioids, with the painlessness capable of being partially reversed in both humans and mice through a systemic infusion of naloxone, an opioid receptor antagonist (Minett *et al.*, 2015).

Inherited pain insensitivity can also arise through congenital absence or a progressive degeneration of sensory and autonomic neurons, the so-called hereditary sensory and autonomic neuropathies (HSANs) (Rotthier *et al.*, 2012). This heterogeneous group of disorders differ in their age of onset (juvenile or adult) and degree of motor, sensory and autonomic disturbances, which correlates largely with the subtypes of neurons that are affected. In the case of HSAN IV (OMIM 256800) and HSAN V (OMIM 608654), in which there are recessive loss of function mutations in the genes encoding the nerve growth factor (NGF) receptor (TRK-A) and NGF, respectively, there is a congenital absence of damage- and temperature sensing neurons and a deficient innervation of sweat glands that can lead to anhidrosis (Indo *et al.*, 1996; Einarsdottir *et al.*, 2004; Carvalho *et al.*, 2011). The functions of HSAN genes are diverse, ranging from neurotrophic functions (*NTRK1*/TRK-A and *NGF*), sphingolipid metabolism (*SPTLC1* and *SPTLC2*), structural integrity of the endoplasmic reticulum (*ATL1*) and Golgi apparatus (*RETREG1*/FAM134B) and vesicular trafficking (*RAB7A* and *KIF1A*) (Rotthier *et al.*, 2012). Recently, several HSAN mutations were also reported in *PRDM12*, an epigenetic regulator that is expressed in nociceptors and their progenitors (OMIM 616488). Loss of function of PRDM12 leads to a severe congenital peripheral neuropathy, with a lack of nerve fibres crossing the dermal-epidermal border as assessed by staining of a skin biopsy, and a consequent pain-insensitive phenotype (Chen *et al.*, 2015).

Here, we have studied a family where congenital hypoalgesia is present in six affected individuals across three generations. Through a combination of whole exome sequencing and mouse model analyses we have shown that the genetic defect resides in *ZFHX2* (Zinc finger homeobox 2), a nociceptor-expressed transcriptional regulator. Gene expression analyses show that the missense mutation in *ZFHX2* causes significant gene deregulation within dorsal root ganglia (DRG), helping to explain the observed pain insensitive phenotype.

Materials and methods

Study subjects

The family was identified in Italy and was previously reported (Spinsanti *et al.*, 2008), although the full extent of the phenotype was only elucidated following publication. The family consists of a mother (aged 78), her two daughters (aged 52 and 50) and their children (two boys and one girl, aged 24, 21 and 16, respectively). In different severity and forms, these subjects presented a low ability to sense pain, to experience temperature and to sweat. Indeed, the members suffered unnoticed bone fractures in, for example, the arms and legs (Supplementary Table 1) and cutaneous injuries, but occasionally suffered from headaches and visceral pains. In addition, members manifested a low sensitivity to capsaicin (chilli pepper) and a normal or high sensitivity to odours. Sometimes the intense sensations were accompanied by autonomic reactions such as vomiting and fainting. Episodes of unexplained hyperthermia occasionally occurred. Cognitive ability and motor performances were normal or high. Written informed consent was obtained from all participants and the study was approved by the ethics committee at University College London, UK, with sensory phenotype assessments at the University of Siena, Italy.

Sensory phenotype assessment methods

Tender points

The number of positive tender points was assessed with a pressure algometer (footplate surface, 1 cm^2; scale range,

0–10 kg); the point was considered positive if the subject reported pain with a pressure lower than 4 kg. The pressure was applied once to 18 tender points (9 + 9) and 10 control points (5 + 5) (Wolfe *et al.*, 1990). The pressure gauge was advanced at a rate of ~1 kg/s and stopped when the subject declared that the pressure pain level had been reached.

Thermal detection pain threshold

Superficial cold and heat pain thresholds were determined with a thermal stimulator (Medical Instruments Facilities). Four cold and four heat stimuli were delivered on the thenar eminence of the dominant hand at 1.5°C/s starting from 32°C and passing to −10°C or 50°C, respectively, and the thresholds were expressed as the mean values of the four responses. The subject was asked to press a button to interrupt the stimulus when the thermal sensation became a nociceptive sensation.

Cold pressor test

Tonic cold pain was elicited by the cold pressor test (Wolf and Hardy, 1941) and pain onset and pain tolerance latencies (in seconds) were determined. Subjects kept their non-dominant hand fully immersed in a plastic box containing water at 37°C for 1 min, then immersed the same hand in another box containing cold water (0–1°C) and ice grains, and kept it there as long as possible (pain tolerance latency). During hand immersion, the subjects reported when the sensation became painful (pain threshold latency).

Mechanical threshold detection

A standard set of von Frey filaments, round tip ~0.5 mm (evaluator size 1.65–6.65; target force 0.008–300 g, Touch Test Sensory Evaluators), were administered in ascending and descending order five times (randomly) on the volar surface of the non-dominant forearm in an area along the midline, approximately midway from the wrist crease to elbow crease. The subject was asked to communicate when a touch sensation was perceived.

Mechanical pain threshold detection

A series of modified von Frey filaments with a sharp tip (0.25 mm, target force 4.56–6.45 i.e. 4–180 g) able to activate the cutaneous nociceptors (Rolke *et al.*, 2006), were applied till bending, in ascending and descending order five times (randomly) on the volar part of the arm with a contact of 1 s. The subject was asked to quantify the intensity of the painful/pleasurable sensation (VAS 0-100).

Capsaicin test

The volar surface of the non-dominant forearm in an area along the midline, approximately midway from the wrist to the elbow crease, an area of ~4 cm², was chosen for testing. From the centre of this area, radial spokes were traced out towards the periphery for ~6 cm. The proband was invited to fix her eyes on a precise point of the wall during each test when requested.

Basal responsiveness in the area was measured first. For touch evoked sensation, cotton wool was gently swept at a rate of 1 cm/s along each radial spoke starting at the point nearest to the elbow and moving to the centre point. The proband was asked to report if the stimulus was nothing, tactile, unpleasant, painful or other. For mechanical pain

detection, the von Frey filament (6.45) was applied along each radial spoke 1 cm apart (5 min after the cotton wool test).

Ten minutes later, a solution of capsaicin (0.250 µg capsaicin in 250 µl saline) was injected intradermally (25 µl) into the centre point of the map using a 0.5 ml insulin syringe using a 28-gauge needle.

The subject was asked to report the onset of whichever sensation and if painful to rate its intensity (VAS 0-100) and its unpleasantness (VAS 0-100) and all changes across time in order to build up the temporal profile. Cotton wool and von Frey filaments were used as described above following capsaicin injection.

Skin biopsy

A punch skin biopsy was taken from 10 cm above the lateral malleolus of the leg of the proband and fixed overnight with 2% periodate-lysine-paraformaldehyde and preserved in sucrose before blocked and processed into 50 µM sections. Nerve fibres were stained using rabbit anti-PGP (protein gene product) 9.5 antibody (1:2000; Ultraclone Ltd) and Cy3 anti-rabbit (1:500; Jackson Immunoresearch). By means of a Zeiss LSM 710 confocal microscope, z-stacks (2-µm intervals), maximum intensity projections were generated with a Plan-Apochromat objective at ×20 magnification (Carl Zeiss MicroImaging GmbH). Analysis was performed as per published guidelines (Lauria *et al.*, 2010). PGP9.5-positive nerve fibres crossing the dermal-epidermal junction were counted and intraepidermal nerve fibre density counts are given in number of fibres per millimetre of skin.

Whole exome sequencing

For enrichment of exons and flanking intronic sequences we used the Illumina TruSeq DNA Sample Prep Kit and Exome Enrichment Kit (Individuals III-1 and III-2) and the Agilent Human SureSelect V4 kit (Individuals I-2, II-2, II-4 and III-3). We performed 100 bp paired-end runs on a Genome Analyzer HiSeq 2000 system (Illumina) generating sequences of 2 (Individual III-1), 2.3 (Individual III-2), 6.0 (Individual I-2), 7.4 (Individual II-2), 6.9 (Individual II-4) and 7.0 (Individual III-3) Gb. This amount of data resulted in the following percentages of targets being covered at ⩾10×: 83.3 (Individual III-1), 83.1 (Individual III-2), 93.4 (Individual I-2), 98.3 (Individual II-2), 98.1 (Individual II-4) and 98.5 (Individual III-3). Sequence alignment and variant calling was performed against the reference human genome assembly (hg19) by using the Burrows-Wheeler Aligner (Li and Durbin, 2009) and the Genome Analysis Toolkit (McKenna *et al.*, 2010; DePristo *et al.*, 2011). Format conversion and indexing were performed with the Picard software. Single nucleotide variants and small insertions and deletions were checked against established databases (1000 Genomes Project and dbSNP v.142). Variants were further checked using the ExAC browser, dbSNP v.147 and in our in-house database of sequencing data for other diseases ($n > 2000$). The protein coding effects of variants was predicted using SIFT, PolyPhen-2 and M-CAP. Splicing changes were analysed using the NNSPLICE Splice Site Predictor. Novel variants were verified by Sanger sequencing and checked to see if they segregated in all six affected individuals (primers available on request).

Animal behaviour tests

All experiments were performed in accordance with the UK Animals (Scientific Procedures) Act 1986 with prior approval under a Home Office project licence (PPL 70/7382). Mice were kept on a 12-h light/dark cycle and provided with food and water *ad libitum*. Global *Zfhx2* knockout mice were previously generated (Komine *et al.*, 2012) and imported to the UK from the RIKEN Bio Resource Center (BRC No. 02262: B6.129S-Zfhx2<tm3Ymri>). Zfhx2 p.R1907K BAC (bacterial artificial chromosome) transgenic mice were generated by Cyagen Biosciences Inc (further details in the Supplementary material). Experiments were conducted using both male and female wild-type littermate and knockout/transgenic mice, all of which were at least 7 weeks old when tested. Observers who performed behavioural experiments were blind to the genotype of the animals. Mechanical nociceptive thresholds were measured using a modified version of the Randall Selitto test that applies pressure to the tail via a $3\,mm^2$ blunt conical probe with a 500-g cut-off (Randall and Selitto, 1957; Minett *et al.*, 2011). Touch perception was measured using the up-down method for obtaining the 50% threshold using von Frey hairs, as previously described (Chaplan *et al.*, 1994; Minett *et al.*, 2011). Thermal nociceptive thresholds were determined by measuring paw-withdrawal latency using the Hargreaves' apparatus (Hargreaves *et al.*, 1988; Minett *et al.*, 2011) with a ramp of $1.5°C/s$ and a 30-s cut-off and also by use of the $50°C$ hot-plate test (Eddy and Leimbach, 1953). The response to mild cooling was measured using the acetone evaporation test (Minett *et al.*, 2011) and the response to noxious cold measured using the cold plantar assay (Brenner *et al.*, 2012). The rotarod test was performed as described in Stirling *et al.* (2005).

In vivo electrophysiology

Electrophysiological recordings were performed by an experimenter blind to genotype. Mice were anaesthetized with isoflurane (4%; 66% N_2O and 33% O_2) and secured in a stereotaxic frame. Anaesthesia was reduced and maintained at 1.5% isoflurane for the remaining duration of the experiment. A laminectomy was performed to expose L3–L5 segments of the spinal cord and extracellular recordings were made from wide dynamic range (WDR) neurons in the deep dorsal horn (lamina III–V, 200–600 mm) using parylene-coated tungsten electrodes (A-M Systems) in *Zfhx2* knockout mice and littermate controls. Mechanical stimuli were applied to the peripheral receptive field of spinal neurons on the hindpaw glabrous skin and the evoked activity of neurons was visualized on an oscilloscope and discriminated on a spike amplitude and waveform basis using a CED 1401 interface coupled to Spike 2 software (Cambridge Electronic Design, UK). Mechanical stimuli (innocuous brush stroke and noxious prods, $100\,g/cm^2$ and $150\,g/cm^2$) were applied in ascending order of intensity to receptive fields for 10 s and the total number of evoked spikes recorded.

Microarrays

Following euthanization by inhalation of CO_2 and cervical dislocation, lumbar DRGs (L1–L6) were isolated from five mice bearing four genomic copies of the mutant *Zfhx2* gene and from seven wild-type controls. Total RNA was isolated using the PureLink™ RNA Micro Kit (Invitrogen) and run on the GeneChip Mouse Transcriptome Array 1.0 (Affymetrix). Expression data were analysed using the Expression and Transcriptome Analysis Consoles (Affymetrix). Microarray data have been deposited at Gene Expression Omnibus Array Express for public use with reference number E-MTAB-5650.

Calcium imaging

Mouse DRG neurons were extracted and dissociated as previously described (Emery *et al.*, 2016), and plated on poly-L-lysine and laminin coated glass coverslips (13 mm; size 0) and cultured in standard cell medium (Dulbecco's modified Eagle medium + GlutaMAX™, Life Technologies) supplemented with 10% foetal bovine serum and nerve growth factor (50 ng/ml). For calcium imaging experiments, neurons were preincubated with 5 µM fluo-4 AM (Life Technologies) in standard extracellular solution (in mM: 124 NaCl, 4 KCl, 10 HEPES, 1 $MgCl_2$, 2 $CaCl_2$, 5 glucose) for 30 min at 37°C. After the preincubation, neurons were washed in warmed standard extracellular solution and placed into a laminar flow imaging chamber (Warner Instruments). A gravity-fed perfusion system was used to continuously perfuse the neurons throughout the experiment. Image acquisition was performed using a confocal microscope (Leica SP8). For fluo-4 AM excitation, a laser wavelength of 488 nm was used, and the images were acquired at a bidirectional scan speed of 800 Hz. Image analysis was performed using LAS-X software (Leica).

Results

Clinical description

We studied a previously described family with a hypoalgesic phenotype in which six affected individuals have a history of painless injuries from childhood (Fig. 1A) (Spinsanti *et al.*, 2008). Bone fractures of the arms and legs are associated with an absence of pain, or pain present only for a few seconds and sometimes accompanied by fainting (Supplementary Table 1). Notably, broken limbs can be used without any painful sensations. The subjects did not record the occurrence of these events immediately and for this reason it is not clear if the time of healing was altered. Burning stimuli are also frequently reported to be not painful, with consequent lesions noticed only by sight. All individuals have severe corneal hyporeflexia but without corneal scarring and with normal tear production. Sweating is scarce or absent in all affected individuals and sensation of warm and cool temperatures is also reported to be altered in five of six subjects, with occasional episodes of hyperthermia (Spinsanti *et al.*, 2008). While cutaneous injuries and bone fractures are often neglected, the pain insensitive phenotype is not global with, for example, lower back pain and occasional headaches promptly and fully perceived. Painful sensations were also noted during childbirth. Sensory phenotype assessments showed that innocuous light touch stimuli could be detected
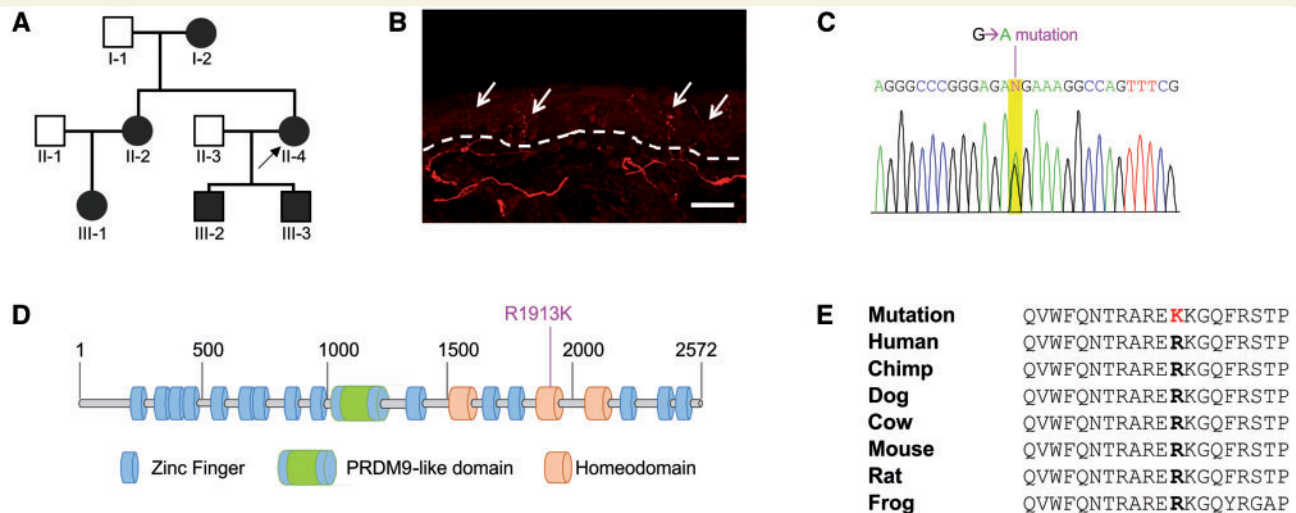
Figure 1 Missense mutation in ZFHX2 identified in pain insensitive family. (**A**) Marsili syndrome pedigree showing autosomal dominant inheritance pattern of the pain insensitive phenotype. (**B**) Microphotograph of a skin punch biopsy of the proband (Individual II-4) carrying the mutation. PGP9.5 positive profiles (in red; shown by white arrows) were counted as they crossed the dermal-epidermal junction (dotted line). Using the immunofluorescence method, 11.3 fibres/mm were counted and 6.4 fibres/mm using DAB (not shown). The intraepidermal nerve fibre density (IENFD) count was normal for age and gender. Scale bar = 50 μm. (**C**) Sanger sequencing trace showing the *ZFHX2* mutation (NM_033400:c.G5738A) that was PCR-amplified from genomic DNA isolated from the proband. All affected individuals are heterozygous for this mutation. (**D**) Schematic representation of ZFHX2 protein domain structure with the zinc finger motifs, PRDM9-like domain (aa 1033–1277) and three homeodomains (aa 1595–1657, 1857–1919 and 2065–2127) annotated. The location of the p.R1913K mutation within the second homeodomain is also indicated. See Supplementary Fig. 1 for more information. (**E**) Sequence alignment around mutation site for orthologous *Tetrapoda* ZFHX2 proteins.

normally (Supplementary Table 1). Heat pain thresholds were variable between tested individuals, with one individual particularly showing extreme insensitivity to noxious heat (Supplementary Table 1). Cold pain thresholds are also variable between individuals, ranging from hyperalgesia in one individual to a very high cold pain threshold and tolerance in another (Supplementary Table 1). The proband (Individual II-4 in Fig. 1A) reported no pain in the mechanical pain threshold detection tests and, interestingly, at high forces a sensation of pleasure was reported (Supplementary Table 1). This is consistent with intense deep pressure from massage being pleasurable, as also noted in a second affected member in the family (Individual III-3 in Fig. 1A). All affected individuals have a low sensitivity to capsaicin as shown by their ability to eat a large amount of hot pepper without any discomfort. In the capsaicin test, carried out on the forearm, the proband reported an immediate and very intense pain following capsaicin injection that, unusually, abruptly (50–60 s) disappeared (Supplementary Table 1). All patients self-report of being able to perceive odours (*SCN9A*-associated pain insensitive individuals are anosmic) although some report a higher than normal sense of smell that is associated with nausea and vomiting. All individuals have normal cognitive abilities, display no evidence of distal weakness nor joint abnormalities and exercise regularly. A skin punch biopsy of the distal leg in the proband followed by measurement of the intraepidermal nerve

fibre density showed normal fibre counts for age and gender (11.3 fibres/mm using immunofluorescence) (Provitera *et al.*, 2016), excluding the likelihood of a small fibre neuropathy in the proband (Fig. 1B).

Whole exome sequencing

The phenotype segregated amongst the six affected individuals within the family in a manner consistent with autosomal dominant inheritance (Fig. 1A). Exome sequencing was performed for all six affected members to identify the pathogenic variant. Following filtering and verification by Sanger sequencing, two novel coding variants were confirmed to co-segregate with the pain-insensitive phenotype: *SUPT3H* (NM_003599:c.G409A:p.A137T) and *ZFHX2* (NM_033400:c.G5738A:p.R1913K). The variant in *SUPT3H* is annotated as benign by both the M-CAP and PolyPhen-2 (HumVar) tools and is also predicted to not alter splicing (NNSPLICE). In contrast, the point mutation in *ZFHX2* (Fig. 1C) was indicated to be deleterious (M-CAP, PolyPhen-2 and SIFT), was absent from public SNP databases (1000 Genomes and dbSNP147) and the ExAC and Institutional (UCL) exome datasets, and so was prioritized for further analysis. *ZFHX2* encodes a large protein of 2572 amino acids (NP_207646) that comprises 17 zinc finger motifs, two of which are adjacent to either side of the central PRDM9-like domain, and three homeodomains (Fig. 1D and Supplementary Fig. 1),
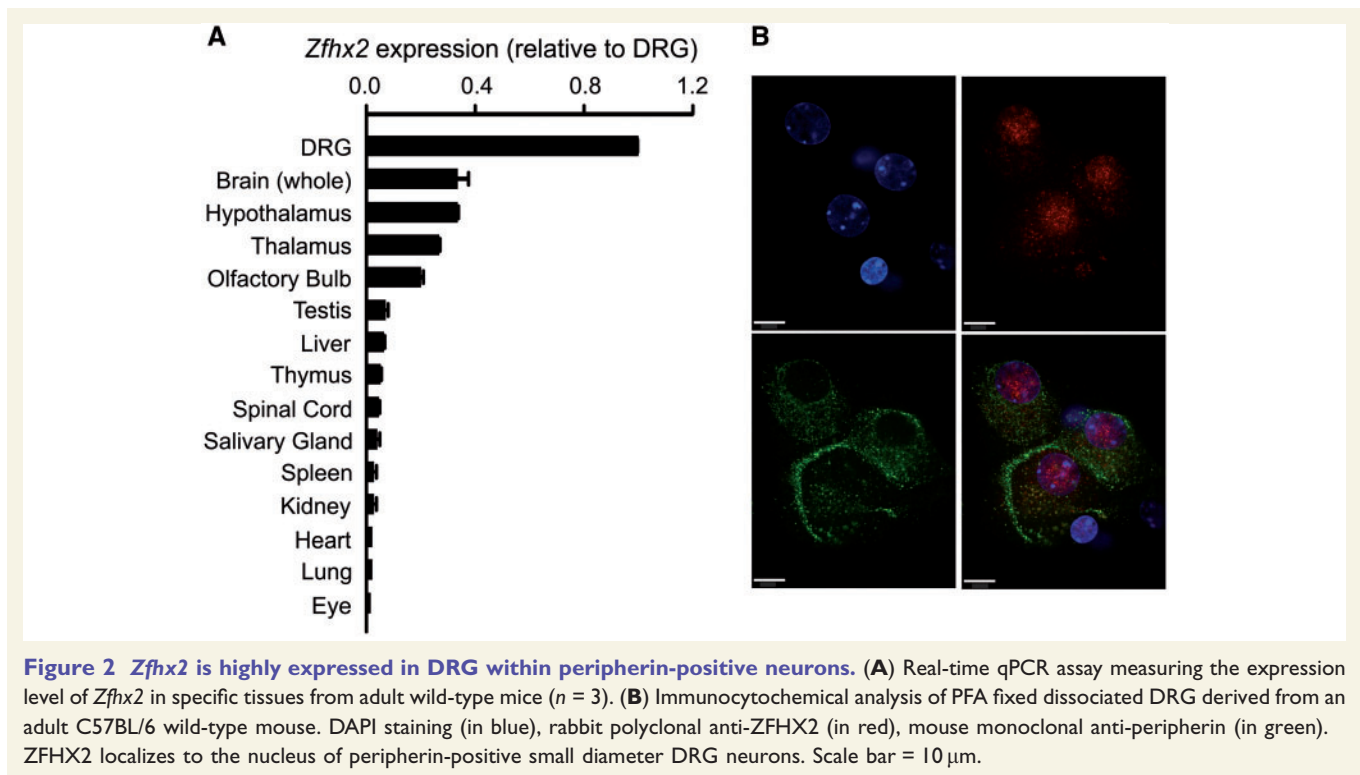
Figure 2 *Zfhx2* **is highly expressed in DRG within peripherin-positive neurons.** (**A**) Real-time qPCR assay measuring the expression level of *Zfhx2* in specific tissues from adult wild-type mice (*n* = 3). (**B**) Immunocytochemical analysis of PFA fixed dissociated DRG derived from an adult C57BL/6 wild-type mouse. DAPI staining (in blue), rabbit polyclonal anti-ZFHX2 (in red), mouse monoclonal anti-peripherin (in green). ZFHX2 localizes to the nucleus of peripherin-positive small diameter DRG neurons. Scale bar = 10 μm.

features common to transcriptional regulators (Komine *et al.*, 2006). The predicted PRDM9-like fold domain has no common active site tyrosines essential for methyl transferase activity (Wu *et al.*, 2013) but may still exhibit nucleosome binding properties. The p.R1913K mutation identified in the pain-insensitive individuals maps within the second homeodomain (Fig. 1D) and to a residue that is invariant across all known orthologous *Tetrapoda Zfhx2* genes (HomoloGene 52657) (Fig. 1E).

Zfhx2 knockout mice have altered pain thresholds

Zfhx2 was cloned in 2006 and a global knockout mouse was reported in 2012, showing several behavioural abnormalities, namely, hyperactivity, enhanced depression-like behaviours, and an aberrantly altered anxiety-like phenotype (Komine *et al.*, 2006, 2012). *Zfhx2* was shown to be highly expressed in the developing brain, including the thalamus, hypothalamus, midbrain and pontine areas, with expression persisting in adult brain. Using RT-PCR in adult wild-type mice, we found that *Zfhx2* expression is enriched within DRGs (Fig. 2A) and immunocytochemical analyses showed nuclear staining of ZFHX2 within peripherin-positive small diameter neurons (Fig. 2B). We investigated whether *Zfhx2* global knockout mice display an acute pain behavioural phenotype using a battery of assays designed to test thermal and mechanical acute pain thresholds (see 'Materials and methods' section,

Fig. 3A, B and Supplementary Fig. 2A–D). These showed that the global knockout mice, compared to their wild-type littermates, were significantly hyposensitive to noxious mechanical stimuli applied to the tail but with normal sensitivity to innocuous touch (Fig. 3A and Supplementary Fig. 2B). These data are supported by deep dorsal horn WDR neuron recordings in *Zfhx2* knockouts, which showed a significant deficit in noxious mechanical coding compared to littermate controls but no differences in response to dynamic low threshold stimuli (brush) (Fig. 3C). Interestingly, in the hot-plate test the *Zfhx2* knockout animals were significantly hypersensitive to noxious heat (Fig. 3B), highlighting the importance of the nociceptor-expressed *Zfhx2* gene in regulating both mechanical and thermal acute pain thresholds.

ZFHX2 p.R1907K transgenic mice are hyposensitive to noxious heat

To investigate the effects of the p.R1913K ZFHX2 missense mutation we cloned the full-length coding sequence of the human gene (GenBank KY781180) and expressed the wild-type (R1913) and the mutant (K1913) versions in AD293 cells (Supplementary material). Both the wild-type and mutant ZFHX2 proteins localized to the nucleus in transiently transfected cells, indicating that the phenotype was unlikely to be caused by a subcellular trafficking defect (Supplementary Fig. 3). Next, a BAC transgenic mouse model was generated in which arginine-1907, the
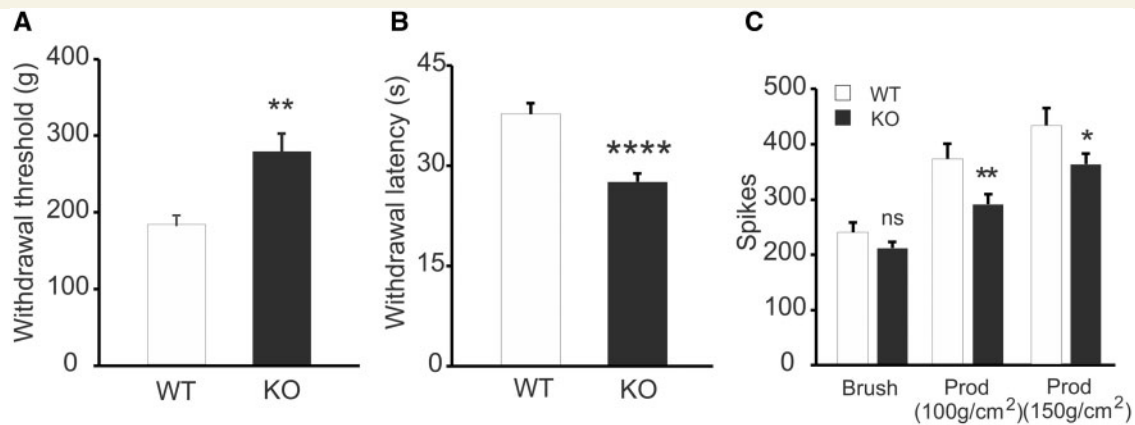
Figure 3 Zfhx2 knockout mice have altered acute mechanical and thermal pain thresholds. (**A**) Randall Selitto test measuring withdrawal thresholds in the tail to noxious mechanical stimuli in knockout (KO; $n = 15$) and wild-type (WT) littermates ($n = 13$). Knockout mice are significantly hyposensitive compared to controls ($P = 0.0017$). (**B**) Hot plate test measuring withdrawal latency to noxious thermal (50°C) stimuli in knockout ($n = 31$) and wild-type littermate ($n = 31$) controls. Knockout mice are significantly hypersensitive compared to controls ($P = 0.000008$). (**C**) ZFHX2 knockout deep dorsal horn WDR neurons show a deficit in noxious mechanical coding compared to littermate controls but no differences in response to dynamic low threshold stimuli. Brush (wild-type $n = 44$, knockout $n = 61$, $P = 0.176$); Prod 100 g/cm^2 (wild-type $n = 43$, knockout $n = 61$, $P = 0.01$); Prod 150 g/cm^2 (wild-type $n = 43$, knockout $n = 61$, $P = 0.044$). All data analysed by t-test. Results are presented as mean ± standard error of the mean (SEM); ns (not significant) $P > 0.05$; $^*P \leqslant 0.05$; $^{**}P \leqslant 0.01$; $^{****}P \leqslant 0.0001$.

orthologous amino acid to arginine-1913 in human ZFHX2, was mutated to lysine. Acute pain behaviour assays (Fig. 4 and Supplementary Fig. 4) showed that transgenic mice expressing the ZFHX2 p.R1907K mutant protein had significant deficits in sensitivity to noxious heat. Strikingly, the noxious heat pain thresholds were significantly higher in mice with the highest genomic BAC copy number (four to five genomic copies) (Fig. 4B and D). Furthermore, calcium imaging experiments conducted on cultured DRG neurons from these mice showed that they had a reduced response to capsaicin (1 µM) compared to wild-type neurons (Fig. 4E–G). Immunohistochemical analysis of lumbar (L4) DRGs isolated from adult BAC transgenic mice showed no significant differences in the number of peripherin-positive neurons compared to wild-type controls, indicating that overexpression of mutant ZFHX2 was not associated with a loss of small diameter nociceptive neurons (Supplementary Fig. 5).

Significant gene expression deregulation in dorsal root ganglion neurons from mutant mice

ZFHX2 is a putative transcriptional regulator and so we studied the effects of the p.R1907K mutation on gene expression profiles in mice bearing four genomic copies of the mutant Zfhx2 gene. Lumbar DRGs (L1–L6) were isolated from mutant and wild-type controls and RNA analysed using microarrays (Fig. 5 and Supplementary Table 2). Using an ANOVA P-value cut-off of $\leqslant 0.01$, six genes were upregulated more than 1.7-fold in mutant DRGs versus controls. Sixteen genes were downregulated

more than 1.7-fold in mutant DRGs versus controls (Supplementary Table 2). Interestingly a number of genes in this list such as Gal, Sst, Gfra3, Ptgir and others are known for their connection to pain signalling. To explore whether the genes deregulated in DRGs as a result of mutant Zfhx2 expression share any DNA sequence motifs in common we performed a phylogenetic shadowing-based approach (Bailey and Elkan, 1994) using promoter region sequences from genes which showed at least a 1.2-fold expression level change with ANOVA $P \leqslant 0.01$ (Supplementary material and Supplementary Table 2). Analysis of these genes yielded four common AG-rich DNA sequence motifs (Supplementary Fig. 6B) present in ~60% of 119 analysed genes. To verify that these AG-rich motifs are present in ZFHX2 DNA-binding regions we used human neuroblastoma SH-SY5Y cells expressing V5-tagged mutant ZFHX2 for ChIP-seq analysis (Supplementary material). Forty-five genes of those 119 being shown to be significantly deregulated in the microarray screen showed ChIP-seq peaks within their immediate promoter regions, which were different to the negative controls (IgG ChIP) and had AG-rich motifs present within immunoprecipitated DNA sequences (Supplementary Table 3 and Supplementary Fig. 6C). Among those genes were Gfra3, Gal and Ptgir (Fig. 5B). One AG-rich motif from those sequences (Supplementary Fig. 6B) was aligned with four earlier identified AG-rich motifs from genes deregulated in microarray experiments to generate the AG-rich consensus motif with STAMP software (Fig. 5A and Supplementary Fig. 6A). The gene ontology search for the resulting AG-rich motif showed its presence in gene families functionally engaged in signal
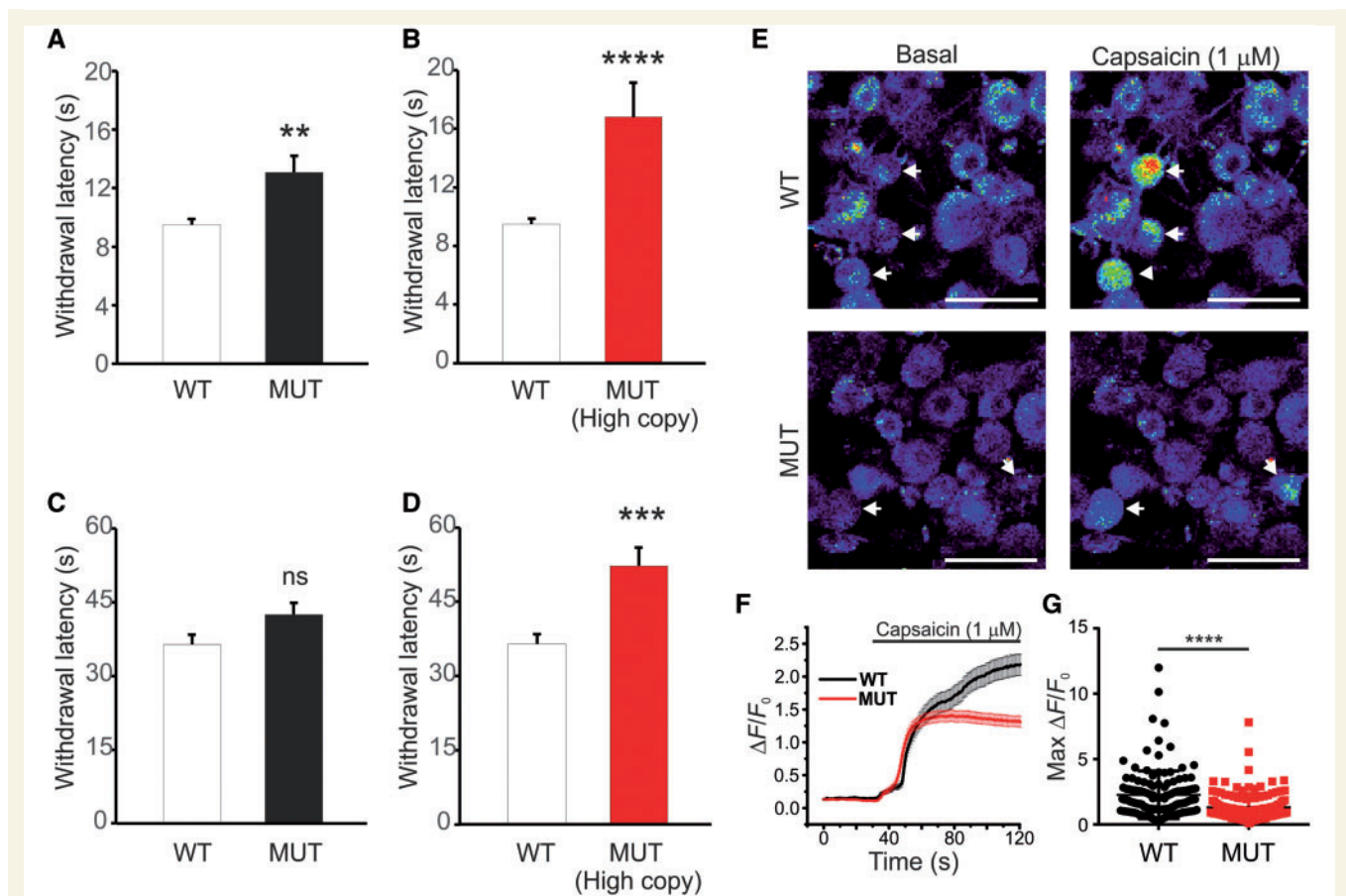
Figure 4 ZFHX2 p.R1907K BAC transgenic mice are hyposensitive to noxious heat and DRG neurons have reduced responses to capsaicin. (**A**) Hargreaves' test measuring paw withdrawal latency to noxious thermal stimuli. Wild-type (WT) $n = 16$, mutant (MUT) $n = 16$ (genomic BAC copy number 1–5), $P = 0.0048$. (**B**) Mice with the highest genomic BAC copy number (four to five copies) have a high pain threshold to noxious heat. Wild-type $n = 16$, mutant $n = 5$, $P = 0.000058$. (**C**) Hot-plate test measuring withdrawal latency to noxious thermal ($50°C$) stimuli in BAC transgenic mice (mutant $n = 16$) and wild-type littermate ($n = 16$) controls. $P = 0.058$. (**D**) Similar to the Hargreaves' test, mice with the highest genomic BAC copy number (four to five copies) have a high pain threshold to noxious heat. Wild-type $n = 16$, mutant $n = 5$, $P = 0.00095$. (**E**) Example confocal images from cultured wild-type and mutant mouse DRG neurons before and after the application of capsaicin (1 μM). Scale bar = 50 μm. (**F**) Averaged response of all wild-type ($n = 129$) and mutant ($n = 138$) mouse DRG neurons to capsaicin (1 μM) application. (**G**) Maximal relative fluorescence from baseline for wild-type and mutant mouse DRG neurons following capsaicin (1 μM) application. $P = 0.0000002$. All data analysed by t-test. Results are presented as mean ± SEM; ns $P > 0.05$; **$P \leqslant 0.01$; ***$P \leqslant 0.001$; ****$P \leqslant 0.0001$.

transduction, neuropeptide signalling and voltage-gated cation channel activity (Fig. 5A and Supplementary Table 4). Interestingly, the motif was also present in genes engaged in regulation of olfactory receptor activity and sensory perception of smell. The differentially expressed genes highlighted here, either alone or in combination, potentially contribute to the pain insensitive phenotype.

Discussion

Chronic pain remains a severe clinical problem affecting billions of people worldwide and despite the intense efforts of the pharmaceutical industry, it is still poorly treated in a significant number of patients (Nahin, 2015). The study of families with monogenic pain insensitivity disorders

remains a powerful route to identify novel analgesic drug targets (Goldberg et al., 2012). For example, since the discovery of the first SCN9A loss of function mutations in 2006, significant progress has been made to help understand why loss of function of Na$_v$1.7 leads to complete analgesia (Minett et al., 2015). This work is informing drug development strategies on how to better reproduce this phenotype pharmacologically, such as through the combination of Na$_v$1.7 channel blockers with low dose opioids or enkephalinase inhibitors (Minett et al., 2015; Deuis et al., 2017). NGF and TRK-A, previously shown to be essential for the development of nociceptors, have also since been realized to be useful analgesic targets with anti-NGF drugs already showing great promise in clinical trials (Holmes, 2012). The analgesic action of anti-NGFs is related to the post-developmental importance of NGF in
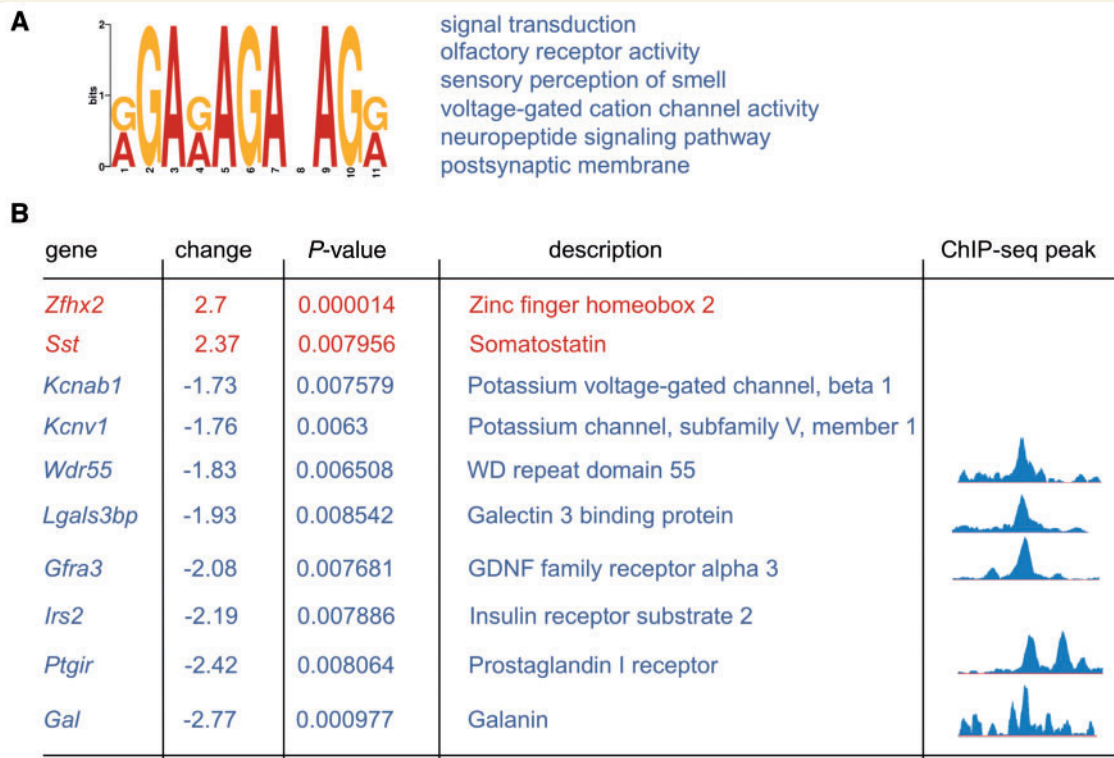
Figure 5 Potential transcriptional targets of ZFHX2. (**A**) The consensus AG-rich motif derived from promoter regions of deregulated genes in the microarray screen. The motif has been constructed from five common motifs highly represented in 1000-bp upstream regions (Supplementary Fig. 6). (**B**) The top six GO terms for genes that contain the AG-rich motif. For more information see Supplementary Table 4. The genes with the biggest change in their expression levels ($P < 0.01$). Zfhx2 expression level is shown as a positive control as it is expected to rise after introducing extra copies of the Zfhx2^{mut} gene. Some of these genes have shown an enrichment of ZFHX2 binding at their regulatory upstream regions (as indicated in *right* column) as analysed by ChIP-seq analysis.

sensitizing nociceptors and thereby increasing the response to noxious stimuli (Hirose *et al.*, 2016).

Here we have studied a family with six members affected with a pain insensitive phenotype, characterized by multiple painless bone fractures and frequent painless lesions caused by burning stimuli. Notwithstanding these injuries, all subjects carried out a normal life and only occasionally had the faint perception that something was different. It was called Marsili syndrome, from the name of the family. Using exome sequencing, we identified a novel coding mutation in the *ZFHX2* gene, which alters a strictly conserved arginine to a lysine residue within the second homeodomain. The full-length ZFHX2 protein contains three homeodomains, DNA-binding regions typically 60 amino acids long, in addition to 17 zinc-finger motifs and a PRDM9-like domain, which is probably involved in nucleosome/histone binding, indicating that ZFHX2 is likely to be a potent transcriptional regulator. The mutated arginine is located at position 57 within the homeodomain. In the consensus homeodomain sequence, lysine-57 contacts with the DNA backbone (Gehring *et al.*, 1994; D'Elia *et al.*, 2001). Although position 57 is often interchangeable between arginine and lysine in different homeodomain-containing proteins, arginine-1913 in ZFHX2 is evolutionarily conserved in every sequenced

orthologue on the UCSC genome browser, highlighting the likely functional importance of this residue. How this mutation alters the function of ZFHX2 is still to be clarified, but potentially it alters DNA binding affinity and/or transcriptional specificity of mutant ZFHX2, which could involve a post-translational modification at the mutation site and/or altered protein-protein interactions with transcriptional partners (Bobola and Merabet, 2017).

We have shown that the missense mutation in ZFHX2 causes a pain insensitive phenotype in humans and in the BAC transgenic mouse model, with both displaying deficits in responses to acute noxious heat. Furthermore, the affected family members are hyposensitive to capsaicin (Supplementary Table 1), which is consistent with the reduced responses recorded by calcium imaging in DRG neurons isolated from BAC transgenic mice (Fig. 4E–G). Interestingly, the *Zfhx2* null mouse is hypersensitive to noxious heat and shows a deficit in the Randall-Selitto test for noxious mechanical pain, linking the expression of the transcription factor in sensory neurons with altered nociceptive processing. However, the BAC transgenic mouse failed to exhibit deficits in the noxious mechanical pain test or in the cold plantar assay for noxious cold, indicating that the human phenotype is not fully

recapitulated by this particular mouse model. Furthermore, the human individuals have additional symptoms that we have yet to confirm in the transgenic mutant mice, such as painless bone fractures, reduced sweating and pleasure upon intense mechanical pressure. The differences in the human and mouse phenotypes could be related to man–mouse differences in ZFHX2 functions. Another explanation is that in the transgenic mouse, two wild-type alleles still exist that could be reducing the effect of expressing the mutant ZFHX2 protein. This is a likely possibility since we observed that the heat-insensitive phenotype in the Hargreaves' and hot-plate tests is enhanced in animals with more genomic copies of the mutant gene (Fig. 4B and D). However, we cannot exclude the possibility that the observed phenotype in the BAC transgenic line is due to overexpression of ZFHX2. Generation and analysis of a ZFHX2 p.R1907K knockin mouse model and further behaviour tests should help to clarify the full extent of the mouse phenotype. This will include understanding the variability in severity of symptoms, a feature noted in the human family and which is not uncommon in other dominantly inherited disorders.

ZFHX2 has enriched expression within DRGs, particularly within the peripherin positive population of neurons, and so we investigated if the pain insensitive phenotype was due to a peripheral neuropathy. However, the intraepidermal nerve fibre density in a punch skin biopsy from the proband and DRG cell counts in the BAC transgenic mice were within normal ranges. Given the role of ZFHX2 as a putative transcriptional regulator, we therefore assessed the gene expression profiles in whole dorsal root ganglia of BAC transgenic and wild-type animals to see if critical genes within nociceptive neurons were affected by the mutation. Several genes previously implicated in peripheral pain mechanisms were differentially expressed (Fig. 5 and Supplementary Table 2). For example, somatostatin, which is upregulated >2-fold in the DRGs from the mutant mice, has proven anti-nociceptive and anti-inflammatory effects in experimental animals and can relieve pain in humans (Mollenholt *et al.*, 1994; Carlton *et al.*, 2001; Helyes *et al.*, 2004; Pinter *et al.*, 2006). Likewise, prostacyclin is an important mediator of inflammation and pain (Bley *et al.*, 1998) and the mutant *Zfhx2* mice have a 2.4-fold downregulation of the prostacyclin receptor, PTGIR. Antagonism of this receptor and work in PTGIR-deficient mice have shown reduced pain and inflammation in various rodent models of acute and inflammatory pain (Murata *et al.*, 1997; Pulichino *et al.*, 2006). Another gene significantly downregulated in mutant DRG is *Gfra3* (GDNF receptor alpha 3), a gene that when knocked out in mice, results in hyposensitivity to noxious thermal stimuli in the Hargreaves' and tail-flick tests (Murota *et al.*, 2012). Galanin (*Gal*), the gene most downregulated in mutant DRGs, plays a complex role in pain signalling, with both facilitatory and inhibitory effects on nociceptive processing (Holmes *et al.*, 2003). Which of the above genes or any of the other less characterized DRG-expressed genes (e.g. *Fam89a*) are principally responsible for the pain-insensitive phenotype remains to be determined. As the microarrays reflect an average snapshot of multiple types of neurons within DRG, some genes may be deregulated more significantly in specific types of neurons. Thus, although we see strong changes for a group of genes we cannot exclude that some other interesting and important genes also contribute to the phenotype despite low fold changes in the current analysis of the whole DRG. Gene expression analyses in whole DRG and specific neuron populations within the DRG, and perhaps in brain regions such as the thalamus, in a knockin mouse model should help us focus on potential downstream analgesic drug targets. It remains possible that the pain insensitivity results from a combined effect of deregulating several genes, and in this scenario the mutant *ZFHX2* gene itself, perhaps via intrathecal AAV delivery, could offer a potential route for providing pain relief.

The microarray analyses were complemented by ChIP-seq experiments in human neuroblastoma cells stably expressing the mutant ZFHX2 protein. These experiments identified a likely consensus genomic binding motif for ZFHX2 that was present upstream of several of the deregulated genes identified in the DRG microarray (including *Ptgir*, *Gal* and *Gfra3*). Interestingly, gene ontology searches showed this AG-rich motif was present in gene families functionally engaged in neuropeptide signalling. Similarly, a dominant point mutation in the homologous *Zfhx3* gene was also shown to alter neuropeptide gene expression, in the suprachiasmatic nucleus, in a mouse model with accelerated circadian locomotor rhythms (Parsons *et al.*, 2015). Furthermore, the gene ontology searches for the ZFHX2 AG-rich motif also identified genes engaged in regulation of olfactory receptor activity and sensory perception of smell. Given this and the known expression of *Zfhx2* in the olfactory bulb (Fig. 2A and Allen Brain Atlas), together with the heightened sense of smell reported in some members of the human family, it is likely that mutant ZFHX2 may be important for olfaction as well as nociceptive processing. An analogy here is $Na_v1.7$, which has a critical role in nociceptive and olfactory signalling with recessive loss of function mutations causing pain insensitivity and anosmia (Cox *et al.*, 2006; Weiss *et al.*, 2011). Importantly, there is no apparent link between other genes implicated in heritable loss of pain such as *NTRK1*/TRK-A, *NGF* or *SCN9A* and the deregulated genes found in the *ZFHX2* microarray analysis. This suggests an entirely novel mechanism is involved in conferring a pain-insensitive phenotype in the family studied here.

In summary, genetic analysis of a human family with Marsili syndrome, a rare and perhaps unique inherited pain insensitive phenotype, and mouse modelling have shown *ZFHX2* as a critical gene for normal pain perception. Further work will resolve how the deregulated DRG-expressed genes contribute to the hypoalgesic phenotype and will help to determine which ones are feasible analgesic drug targets that could lead to better treatments for chronic pain.

Acknowledgements

Funding

Supplementary material

Supplementary material is available at *Brain* online.

References

Bailey TL, Elkan C. Fitting a mixture model by expectation maximization to discover motifs in biopolymers. Proc Int Conf Intell Syst Mol Biol 1994; 2: 28–36.

Bley KR, Hunter JC, Eglen RM, Smith JA. The role of IP prostanoid receptors in inflammatory pain. Trends Pharmacol Sci 1998; 19: 141–7.

Bobola N, Merabet S. Homeodomain proteins in action: similar DNA binding preferences, highly variable connectivity. Curr Opin Genet Dev 2017; 43: 1–8.

Brenner DS, Golden JP, Gereau RW IV. A novel behavioral assay for measuring cold sensation in mice. PLoS One 2012; 7: e39765.

Carlton SM, Du J, Zhou S, Coggeshall RE. Tonic control of peripheral cutaneous nociceptors by somatostatin receptors. J Neurosci 2001; 21: 4042–9.

Carvalho OP, Thornton GK, Hertecant J, Houlden H, Nicholas AK, Cox JJ, et al. A novel NGF mutation clarifies the molecular mechanism and extends the phenotypic spectrum of the HSAN5 neuropathy. J Med Genet 2011; 48: 131–5.

Chaplan SR, Bach FW, Pogrel JW, Chung JM, Yaksh TL. Quantitative assessment of tactile allodynia in the rat paw. J Neurosci Methods 1994; 53: 55–63.

Chen YC, Auer-Grumbach M, Matsukawa S, Zitzelsberger M, Themistocleous AC, Strom TM, et al. Transcriptional regulator PRDM12 is essential for human pain perception. Nat Genet 2015; 47: 803–8.

Cox JJ, Reimann F, Nicholas AK, Thornton G, Roberts E, Springell K, et al. An SCN9A channelopathy causes congenital inability to experience pain. Nature 2006; 444: 894–8.

D'Elia AV, Tell G, Paron I, Pellizzari L, Lonigro R, Damante G. Missense mutations of human homeoboxes: a review. Hum Mutat 2001; 18: 361–74.

DePristo MA, Banks E, Poplin R, Garimella KV, Maguire JR, Hartl C, et al. A framework for variation discovery and genotyping using next-generation DNA sequencing data. Nat Genet 2011; 43: 491–8.

Deuis JR, Dekan Z, Wingerd JS, Smith JJ, Munasinghe NR, Bhola RF, et al. Pharmacological characterisation of the highly NaV1.7 selective spider venom peptide Pn3a. Sci Rep 2017; 7: 40883.

Eddy NB, Leimbach D. Synthetic analgesics. II. Dithienylbutenyl- and dithienylbutylamines. J Pharmacol Exp Ther 1953; 107: 385–93.

Einarsdottir E, Carlsson A, Minde J, Toolanen G, Svensson O, Solders G, et al. A mutation in the nerve growth factor beta gene (NGFB) causes loss of pain perception. Hum Mol Genet 2004; 13: 799–805.

Emery EC, Luiz AP, Sikandar S, Magnusdottir R, Dong X, Wood JN. *In vivo* characterization of distinct modality-specific subsets of somatosensory neurons using GCaMP. Sci Adv 2016; 2: e1600990.

Gehring WJ, Qian YQ, Billeter M, Furukubo-Tokunaga K, Schier AF, Resendez-Perez D, et al. Homeodomain-DNA recognition. Cell 1994; 78: 211–23.

Goldberg YP, Pimstone SN, Namdari R, Price N, Cohen C, Sherrington RP, et al. Human Mendelian pain disorders: a key to discovery and validation of novel analgesics. Clin Genet 2012; 82: 367–73.

Habib AM, Wood JN, Cox JJ. Sodium channels and pain. Handb Exp Pharmacol 2015; 227: 39–56.

Hargreaves K, Dubner R, Brown F, Flores C, Joris J. A new and sensitive method for measuring thermal nociception in cutaneous hyperalgesia. Pain 1988; 32: 77–88.

Helyes Z, Szabo A, Nemeth J, Jakab B, Pinter E, Banvolgyi A, et al. Antiinflammatory and analgesic effects of somatostatin released from capsaicin-sensitive sensory nerve terminals in a Freund's adjuvant-induced chronic arthritis model in the rat. Arthritis Rheum 2004; 50: 1677–85.

Hirose M, Kuroda Y, Murata E. NGF/TrkA signaling as a therapeutic target for pain. Pain Pract 2016; 16: 175–82.

Holmes D. Anti-NGF painkillers back on track? Nat Rev Drug Discov 2012; 11: 337–8.

Holmes FE, Bacon A, Pope RJ, Vanderplank PA, Kerr NC, Sukumaran M, et al. Transgenic overexpression of galanin in the dorsal root ganglia modulates pain-related behavior. Proc Natl Acad Sci USA 2003; 100: 6180–5.

Indo Y, Tsuruta M, Hayashida Y, Karim MA, Ohta K, Kawano T, et al. Mutations in the TRKA/NGF receptor gene in patients with congenital insensitivity to pain with anhidrosis. Nat Genet 1996; 13: 485–8.

Komine Y, Nakamura K, Katsuki M, Yamamori T. Novel transcription factor zfh-5 is negatively regulated by its own antisense RNA in mouse brain. Mol Cell Neurosci 2006; 31: 273–83.

Komine Y, Takao K, Miyakawa T, Yamamori T. Behavioral abnormalities observed in Zfhx2-deficient mice. PLoS One 2012; 7: e53114.

Lauria G, Hsieh ST, Johansson O, Kennedy WR, Leger JM, Mellgren SI, et al. European Federation of Neurological Societies/Peripheral Nerve Society Guideline on the use of skin biopsy in the diagnosis of small fiber neuropathy. Report of a joint task force of the European Federation of Neurological Societies and the Peripheral Nerve Society. Eur J Neurol 2010; 17: 903–12, e44–9.

Leipold E, Liebmann L, Korenke GC, Heinrich T, Giesselmann S, Baets J, et al. A *de novo* gain-of-function mutation in SCN11A causes loss of pain perception. Nat Genet 2013; 45: 1399–404.

Li H, Durbin R. Fast and accurate short read alignment with Burrows-Wheeler transform. Bioinformatics 2009; 25: 1754–60.

McKenna A, Hanna M, Banks E, Sivachenko A, Cibulskis K, Kernytsky A, et al. The genome analysis toolkit: a MapReduce

framework for analyzing next-generation DNA sequencing data. Genome Res 2010; 20: 1297–303.

Minett MS, Pereira V, Sikandar S, Matsuyama A, Lolignier S, Kanellopoulos AH, et al. Endogenous opioids contribute to insensitivity to pain in humans and mice lacking sodium channel Na(v)1.7. Nat Commun 2015; 6: 8967.

Minett MS, Quick K, Wood JN. Behavioral measures of pain thresholds. Curr Protoc Mouse Biol 2011; 1: 383–412.

Mollenholt P, Rawal N, Gordh T Jr, Olsson Y. Intrathecal and epidural somatostatin for patients with cancer. Analgesic effects and postmortem neuropathologic investigations of spinal cord and nerve roots. Anesthesiology 1994; 81: 534–42.

Murata T, Ushikubi F, Matsuoka T, Hirata M, Yamasaki A, Sugimoto Y, et al. Altered pain perception and inflammatory response in mice lacking prostacyclin receptor. Nature 1997; 388: 678–82.

Murota H, Izumi M, Abd El-Latif MI, Nishioka M, Terao M, Tani M, et al. Artemin causes hypersensitivity to warm sensation, mimicking warmth-provoked pruritus in atopic dermatitis. J Allergy Clin Immunol 2012; 130: 671–82.e4.

Nahin RL. Estimates of pain prevalence and severity in adults: United States, 2012. J Pain 2015; 16: 769–80.

Nahorski MS, Chen YC, Woods CG. New Mendelian disorders of painlessness. Trends Neurosci 2015; 38: 712–24.

Parsons MJ, Brancaccio M, Sethi S, Maywood ES, Satija R, Edwards JK, et al. The regulatory factor ZFHX3 modifies circadian function in SCN via an AT Motif-Driven Axis. Cell 2015; 162: 607–21.

Phatarakijnirund V, Mumm S, McAlister WH, Novack DV, Wenkert D, Clements KL, et al. Congenital insensitivity to pain: fracturing without apparent skeletal pathobiology caused by an autosomal dominant, second mutation in SCN11A encoding voltage-gated sodium channel 1.9. Bone 2016; 84: 289–98.

Pinter E, Helyes Z, Szolcsanyi J. Inhibitory effect of somatostatin on inflammation and nociception. Pharmacol Ther 2006; 112: 440–56.

Provitera V, Gibbons CH, Wendelschafer-Crabb G, Donadio V, Vitale DF, Stancanelli A, et al. A multi-center, multinational age- and gender-adjusted normative dataset for immunofluorescent intraepidermal nerve fiber density at the distal leg. Eur J Neurol 2016; 23: 333–8.

Pulichino AM, Rowland S, Wu T, Clark P, Xu D, Mathieu MC, et al. Prostacyclin antagonism reduces pain and inflammation in rodent models of hyperalgesia and chronic arthritis. J Pharmacol Exp Ther 2006; 319: 1043–50.

Randall LO, Selitto JJ. A method for measurement of analgesic activity on inflamed tissue. Arch Int Pharmacodyn Ther 1957; 111: 409–19.

Rolke R, Baron R, Maier C, Tolle TR, Treede RD, Beyer A, et al. Quantitative sensory testing in the German Research Network on Neuropathic Pain (DFNS): standardized protocol and reference values. Pain 2006; 123: 231–43.

Rotthier A, Baets J, Timmerman V, Janssens K. Mechanisms of disease in hereditary sensory and autonomic neuropathies. Nat Rev Neurol 2012; 8: 73–85.

Spinsanti G, Zannolli R, Panti C, Ceccarelli I, Marsili L, Bachiocco V, et al. Quantitative real-time PCR detection of TRPV1-4 gene expression in human leukocytes from healthy and hyposensitive subjects. Mol Pain 2008; 4: 51.

Stirling LC, Forlani G, Baker MD, Wood JN, Matthews EA, Dickenson AH, et al. Nociceptor-specific gene deletion using heterozygous NaV1.8-Cre recombinase mice. Pain 2005; 113: 27–36.

Weiss J, Pyrski M, Jacobi E, Bufe B, Willnecker V, Schick B, et al. Loss-of-function mutations in sodium channel Nav1.7 cause anosmia. Nature 2011; 472: 186–90.

Wolf S, Hardy JD. Studies on pain. Observations on pain due to local cooling and on factors involved in the "cold pressor" effect. J Clin Invest 1941; 20: 521–33.

Wolfe F, Smythe HA, Yunus MB, Bennett RM, Bombardier C, Goldenberg DL, et al. The American College of Rheumatology 1990 criteria for the classification of fibromyalgia. Report of the Multicenter Criteria Committee. Arthritis Rheum 1990; 33: 160–72.

Woods CG, Babiker MO, Horrocks I, Tolmie J, Kurth I. The phenotype of congenital insensitivity to pain due to the NaV1.9 variant p.L811P. Eur J Hum Genet 2015; 23: 561–3.

Wu H, Mathioudakis N, Diagouraga B, Dong A, Dombrovski L, Baudat F, et al. Molecular basis for the regulation of the H3K4 methyltransferase activity of PRDM9. Cell Rep 2013; 5: 13–20.